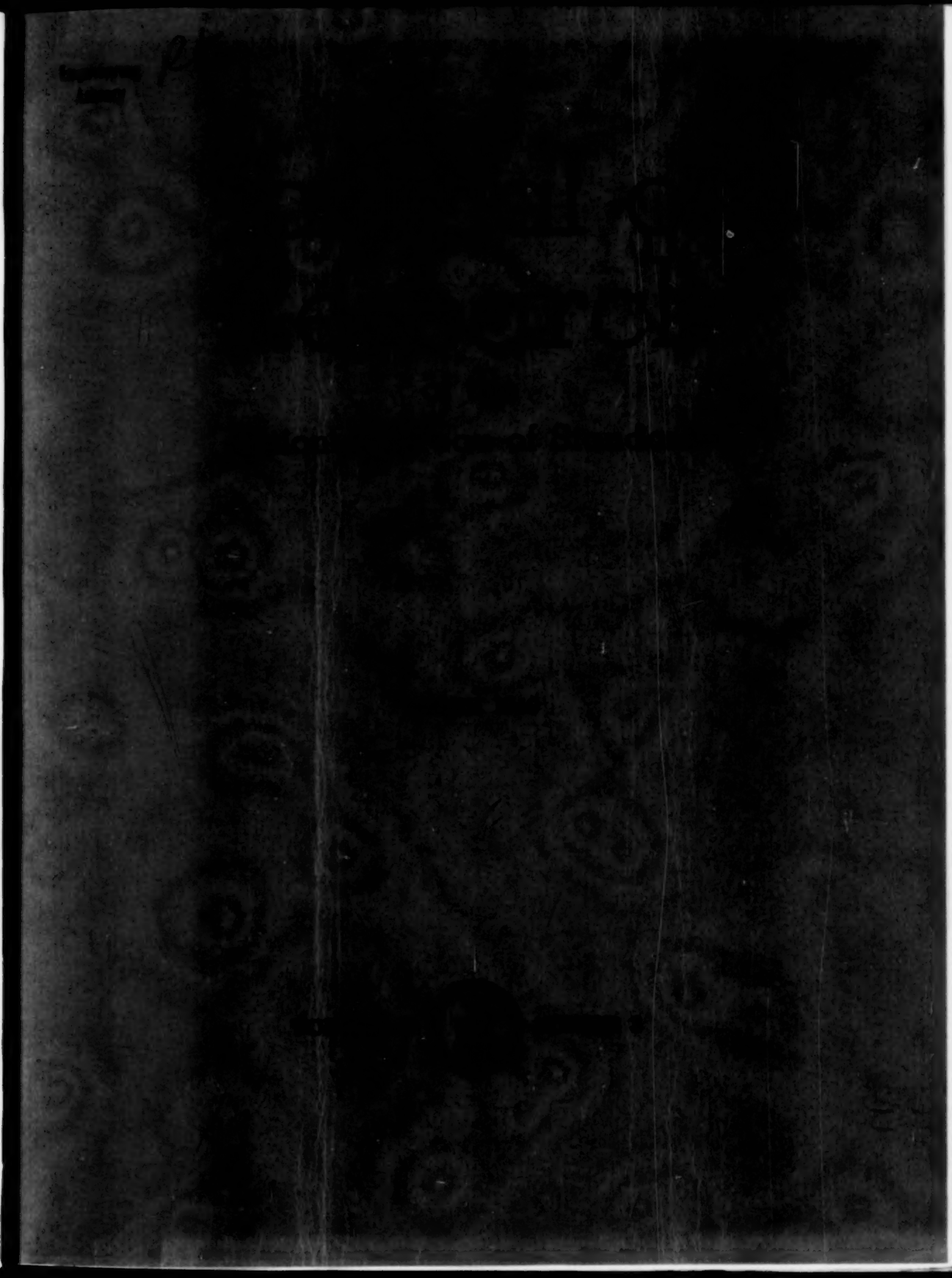

U. S. DEPARTMENT OF COMMERCE
Charles Sawyer, Secretary
NATIONAL BUREAU OF STANDARDS
E. U. Condon, Director

MARCH 1949
VOLUME • 42
NUMBER 3

JOURNAL OF RESEARCH

of the

NATIONAL BUREAU OF STANDARDS

Contents

RP		Page
1962	The international temperature scale of 1948. H. F. Stimson. (Price 10 cents)	209
1963	Absorption by sound-absorbent spheres. Richard K. Cook and Peter Chrzanowski. (Price 10 cents)	219
1964	Heats, equilibrium constants, and free energies of formation of the C_3 to C_5 diolefins, styrene, and the methylstyrenes. John E. Kilpatrick, Charles W. Beckett, Edward J. Prosen, Kenneth S. Pitzer, and Frederick D. Rossini. (Price 10 cents)	225
1965	Accurate determination of the deadtime and recovery characteristics of Geiger-Müller counters. Louis Costrell. (Price 10 cents)	241
1966	Heats of combustion and isomerization of the six C_7H_{14} alkylcyclopentanes. Walter H. Johnson, Edward J. Prosen, and Frederick D. Rossini. (Price 10 cents)	251
1967	Surface available to nitrogen in hydrated portland cements. Raymond L. Blaine and Harold J. Valis. (Price 10 cents)	257
1968	Heat of isomerization of the two butadienes. Edward J. Prosen, Frances W. Maron, and Frederick D. Rossini. (Price 10 cents)	269
1969	Optical glass of interferometer and schlieren quality for wind-tunnel optics. Leroy W. Tilton. (Price 10 cents)	279
1970	A standard of small capacitance. Chester Snow. (Price 15 cents)	287
1971	Properties of aqueous solutions of perchloric acid. Langhorne H. Brickwedde. (Price 15 cents)	309

For sale by the Superintendent of Documents, U. S. Government Printing Office, Washington 25, D. C. Price .60¢
$4.50 per year on subscription

UNITED STATES GOVERNMENT PRINTING OFFICE, WASHINGTON : 1949

U. S. Department of Commerce
National Bureau of Standards

Research Paper RP1962
Volume 42, March 1949

Part of the Journal of Research of the National Bureau of Standards

The International Temperature Scale of 1948

By H. F. Stimson

The International Temperature Scale is based upon six fixed and reproducible equilibrium temperatures to which numerical values have been assigned and upon specified interpolation formulas relating temperature to the indications of specified measuring instruments. This is the first revision of the scale adopted in 1927. It is designed to conform as nearly as practicable to the thermodynamic centigrade scale as now known, while incorporating certain refinements based on experience to make the scale more uniform and reproducible than its predecessor. A new value for the temperature of the silver point and the use of Planck's law with a new value for the radiation constant, c_2, are the only changes which produce significant effects on numerical values assigned to temperatures.

The first International Temperature Scale was adopted by the Seventh General Conference on Weights and Measures in 1927, and is now known as the International Temperature Scale of 1927.[1] The General Conference on Weights and Measures is the diplomatic body, representing 33 participating nations, which has power to adopt recommendations concerning standards of weights and measures for international use. The recommendations are made by the International Committee on Weights and Measures which nominally consists of 18 scientists (not more than one from any nation) elected by the General Conference. The General Conference is scheduled to meet at intervals of 6 years and the International Committee at intervals of 2 years.

The Seventh General Conference recommended that international thermometric conferences be called by the International Committee to revise the temperature scale as occasion required. The Eighth General Conference, in 1933, made official provision for these conferences. In June 1937 the International Committee approved the creation of an Advisory Committee on Thermometry, subject to the sanction of the Ninth General Conference.

A meeting of the Advisory Committee was first called in July 1939. It approved a revision of the text of the scale of 1927 for proposal to the International Committee, but no action was taken because World War II began before the date originally scheduled for the Ninth General Conference. At the call of the International Committee, the Advisory Committee met again in May 1948. At this meeting three resolutions and a new text for the International Temperature Scale were approved.

Both the International Committee and the Ninth General Conference met in October 1948. On the recommendation of the International Committee, the General Conference sanctioned the creation of this Advisory Committee, which is to be known as the "Advisory Committee on Thermometry and Calorimetry". The General Conference then examined and adopted the resolutions which had been proposed by the Advisory Committee and had been transmitted by the International Committee with minor modifications.

The first of these resolutions concerns the International Temperature Scale directly and is as follows:

> "1. With the present-day technique, the triple point of water is susceptible of being a more precise thermometric reference point than the 'melting point of ice'.
>
> "The Advisory Committee considers, there-

[1] Comptes Rendus des Séances de la Septième Conférence Générale des Poids et Mesures, p. 94 (1927); also in Travaux et Mémoires du Bureau international des Poids et Mesures **18** (1930); also George K. Burgess, J. S. J. Research **1**, 635 (1928) RP22.

fore, that the zero of the thermodynamic centigrade scale should be defined as being the temperature 0.0100 degree below that of the triple point of pure water."

The Conference also adopted the International Temperature Scale of 1948 as proposed by the Advisory Committee on Thermometry and Calorimetry; and, on this occasion, decided to give to the degree of temperature the designation of degree Celsius in place of degree centigrade or centesimal. Before the end of 1948 the official text of the scale was approved for publication in the Procès-Verbaux des Séances du Comité international des Poids et Mesures, t. XXI, 1948.

The National Bureau of Standards, therefore, in common with other national laboratories, began using the definitions of the International Temperature Scale of 1948 on January 1, 1949, both in its own scientific work and for calibrating instruments for other scientific and industrial purposes. It is recommended that scientists and industrial workers elsewhere conform to the definitions of the revised scale as set forth in the text.

A translation of the official text follows.

Text of The International Temperature Scale of 1948

Part I. Introduction

The Kelvin scale, on which temperatures are designated as ° K and denoted by the symbol T, is recognized as the fundamental thermodynamic scale to which all temperature measurements should ultimately be referable. On this scale the interval from the ice point, T_0, to the steam point, T_{100}, is 100 degrees. The Kelvin scale and the thermodynamic centigrade[2] scale, on which the temperature is $T-T_0$, are hereby adopted, in principle, by the Ninth General Conference on Weights and Measures. Any temperature interval expressed on one of these scales will have the same numerical value as when expressed on the other.

The experimental difficulties inherent in the measurement of temperature on the thermodynamic scale led to the adoption in 1927, by the Seventh General Conference on Weights and Measures, of a practical scale which was designated as the International Temperature Scale. This scale was intended to be as nearly identical with the thermodynamic centigrade scale as was possible with the knowledge then available. It was designed to be conveniently and accurately reproducible and to provide means for specifying any temperature on the International Scale within much narrower limits than was possible on the thermodynamic scale.

The scale herein defined represents the first revision of the scale adopted in 1927 and is designed to conform as nearly as practicable to the thermodynamic centigrade scale as now known, while incorporating certain refinements, based on experience, to make the scale more uniform and reproducible than its predecessor.

The experimental procedures by which the scale is to be realized are substantially unchanged. Only two of the revisions in the definition of the scale result in appreciable changes in the numerical values assigned to measured temperatures. The change in the value for the silver point from 960.5° to 960.8° C changes temperatures measured with the standard thermocouple. The adoption of a different value for the radiation constant, c_2, changes all temperatures above the gold point, while the use of the Planck radiation formula instead of the Wien formula affects the very high temperatures. The Planck formula is consistent with the thermodynamic scale and consequently removes the upper limit which was imposed by Wien's law in the 1927 scale.

Other important modifications, which cause little or no change in the numerical values of temperatures, but serve to make the scale more definite and reproducible are (a) the termination of one part of the scale at the oxygen point instead of at −190° C, (b) the division of the scale at the freezing point of antimony (about 630° C) instead of at 660° C, (c) the requirements for higher purity of the platinum of the standard resistance thermometer and standard thermocouple, and for smaller permissible limits for the electromotive force of the standard thermocouple at the gold point.

The scale defined by the resistance thermometer remains substantially identical with the 1927 scale. In the range between 630° and 1063° C, numerical values of temperature on the 1948 scale are higher than on the 1927 scale, the maximum difference being about 0.4 degree near 800° C.

[2] The General Conference, held in October 1948, decided to discontinue the use of the words "centesimal" and "centigrade" and to replace them by "Celsius".

Temperatures on the International Temperature Scale of 1927 were designated as ° C or ° C (Int.). Inasmuch as the designation "C" is retained in this revision, it should be applied in the future to temperatures on the last scale adopted previous to the time at which the designation is used. Where any doubt might arise, the designation should be specified as ° C (Int. 1927) or ° C (Int. 1948).

Part II. Definition of The International Temperature Scale of 1948

1. Temperatures on the International Temperature Scale of 1948 will be designated as "° C" or "° C (Int. 1948)" and denoted by the symbol, t.

2. The scale is based upon a number of fixed and reproducible equilibrium temperatures (fixed points) to which numerical values are assigned, and upon specified formulas for the relations between temperature and the indications of the instruments calibrated at these fixed points.

3. The fixed points and the numerical values assigned to them are given in Table I. These values, in each case, define the equilibrium temperature corresponding to a pressure of 1 standard atmosphere, defined as 1,013,250 dynes/cm^2. The last decimal place given for each of the values of the primary fixed points only represents the degree of reproducibility of that fixed point.

TABLE I.—*Fundamental and primary fixed points under the standard pressure of 1,013,250 dynes/cm^2*

	Temperature ° C
(a) Temperature of equilibrium between liquid oxygen and its vapor (oxygen point)	−182. 970
(b) Temperature of equilibrium between ice and air saturated water (ice point) (*Fundamental fixed point*)	0
(c) Temperature of equilibrium between liquid water and its vapor (steam point) (*Fundamental fixed point*)	100
(d) Temperature of equilibrium between liquid sulfur and its vapor (sulfur point)	444. 600
(e) Temperature of equilibrium between solid and liquid silver (silver point)	960. 8
(f) Temperature of equilibrium between solid and liquid gold (gold point)	1063. 0

4. The means available for interpolation lead to a division of the scale into four parts.

(a) From 0° C to the freezing point of antimony the temperature, t, is defined by the formula

$$R_t = R_0(1 + At + Bt^2),$$

where R_t is the resistance, at temperature, t, of the platinum resistor between the branch points formed by the junctions of the current and potential leads of a standard resistance thermometer. The constant, R_0, is the resistance at 0° C, and the constants, A and B, are to be determined from measured values of R_t at the steam and sulfur points. The platinum in a standard resistance thermometer shall be annealed, and of such purity that R_{100}/R_0 is greater than 1.3910.

(b) From the oxygen point to 0° C, the temperature, t, is defined by the formula

$$R_t = R_0[1 + At + Bt^2 + C(t-100)t^3],$$

where R_t, R_0, A, and B are determined in the same manner as in (a) above, and the constant, C, is calculated from the measured value of R_t at the oxygen point.

(c) From the freezing point of antimony to the gold point, the temperature, t, is defined by the formula

$$E = a + bt + ct^2,$$

where E is the electromotive force of a standard thermocouple of platinum and platinum-rhodium alloy when one junction is at 0° C and the other is at the temperature, t. The constants, a, b, and c, are to be calculated from measured values of E at the freezing point of antimony and at the silver and gold points. The antimony used in determining these constants shall be such that its freezing temperature, determined with a standard resistance thermometer, is not lower than 630.3° C. Alternatively the thermocouple may be calibrated by direct comparison with a standard resistance thermometer in a bath at any uniform temperature between 630.3° and 630.7° C.

The platinum wire of the standard thermocouple shall be annealed and of such purity that the ratio R_{100}/R_0 is greater than 1.3910. The alloy wire shall consist nominally of 90 percent platinum and 10 percent rhodium by weight. When one junction is at 0° C, and the other at the freezing point of antimony (630.5° C), silver, or gold, the completed thermocouple shall have electromotive forces, in microvolts, such that

$$E_{Au} = 10{,}300 \pm 50\ \mu v$$

$$E_{Au} - E_{Ag} = 1185 + 0.158(E_{Au} - 10{,}310) \pm 3\ \mu v$$

$$E_{Au} - E_{Sb} = 4776 + 0.631(E_{Au} - 10{,}310) \pm 5\ \mu v$$

(d) Above the gold point the temperature, t, is defined by the formula

$$\frac{J_t}{J_{Au}} = \frac{e^{\frac{c_2}{\lambda(t_{Au}+T_0)}}-1}{e^{\frac{c_2}{\lambda(t+T_0)}}-1},$$

in which

J_t and J_{Au} are the radiant energies per unit wavelength interval at wavelength, λ, emitted per unit time by unit area of a black body at the temperature, t, and at the gold point, t_{Au}, respectively.

c_2 is 1.438 cm degrees.

T_0 is the temperature of the ice point in ° K.

λ is a wavelength of the visible spectrum.

e is the base of Naperian logarithms.

Part III. Recommendations

The recommendations in the following sections are advisory rather than mandatory. The apparatus, methods, and procedures recommended represent good practice at this time, but there is no intention of retarding the development and use of improvements and refinements. Experience has shown these recommendations to be in the interest of uniformity and reproducibility in the realization of the temperature scale defined in part II.

1. Standard Resistance Thermometer

A standard resistance thermometer should be so designed and constructed that the wire of the platinum resistor is as nearly strain-free as practicable and will remain so during continued use. The most suitable platinum wire is that drawn from a fused ingot, not from forged sponge.

Satisfactory thermometers have been made with wire as small as 0.05 mm and as large as 0.5 mm in diameter, a short portion of each lead adjacent to the resistor being made of platinum and continuing with gold wire through the region of temperature gradient. The completed resistor of the thermometer should be annealed in air at a temperature not lower than about 450° C, or if it is to be used at temperatures above 450° C, at a temperature higher than the highest temperature at which it is to be used. It is recommended that the tube protecting the completed resistor be filled with gas containing some oxygen.

A useful criterion, which serves as a safeguard against inferior construction of the completed thermometer and against errors in the calibrations at the fixed points, is that $(R_S - R_0)/(R_{100} - R_0)$ (where R_S is the resistance at the sulfur point) should be between 4.2165 and 4.2180. Similarly, if the thermometer is calibrated for use in the range below 0° C, the ratio, $(R_a - R_{O_2})/(R_{100} - R_0)$ (where R_{O_2} is the resistance at the oxygen point) should be between 6.143 and 6.144. The constancy of resistance at a reference point, such as the triple point of water (or the ice point), before and after use at other temperatures, is also a valuable criterion of the adequacy of the annealing and the reliability of the thermometer in service.

2. Standard Thermocouple

Satisfactory standard thermocouples have been made of wires not less than 0.35 mm and not more than 0.65 mm in diameter. Before calibration, the wires of the couple should be annealed in air for an hour at about 1100° C. The wire of the thermocouple should be mounted so as to avoid all mechanical constraints in the region where steep temperature gradients are likely to occur.

3. Pressure

Each of the fixed points is given as a temperature of equilibrium at a pressure of 1,013,250 dynes/cm^2. This pressure corresponds to the pressure exerted by a column of mercury 760 mm high, having a density of 13.5951 g/cm^3 and subject to a gravitational attraction of 980.665 dynes/g. Except for work of the highest precision, pure ordinary (commercial) mercury may be taken as having a mean density of 13.5951 g/cm^3 at 0° C in such a mercury column.

In the following sections concerning fixed points, the formulas giving the relation between the pressure, p_t, at the midpoint of the platinum resistor and the corresponding equilibrium temperature, t_p, are given in two forms. The polynomial is a convenient form when the pressure is near 1 standard atmosphere, whereas the logarithmic form is applicable, as is well known, over a much larger range. Both of these forms are given as functions of the ratio of p to p_0 (standard atmospheric pressure) and, consequently, are equally applicable whether p and p_0 are expressed in dynes/cm^2 or in mm of mercury at 0° C and under a gravitational attraction of 980.665 dynes/g.

4. Zero Point of the Scale

The temperature 0° C may be realized experimentally well enough for nearly all purposes by the use of a mixture of finely divided ice and water saturated with air at 0° C in a well-insulated container such as a Dewar flask. It is recommended, however, that for work of the highest precision the zero point be realized by means of the triple point of water, a point to which the temperature +0.0100° C has been assigned.

This value agrees with all existing experimental determinations up to the present time within about 0.0002 degree.

(a) Triple Point of Water

The temperature of equilibrium between ice, liquid water, and water vapor has been realized in glass cells from 4 to 7 cm in diameter, which have an axial reentrant well for thermometers and contain only water of high purity. The amount of water should be such as to permit adequate immersion of the thermometer and to ensure the existence of the three phases during measurements. Such cells, when properly prepared for use and kept entirely immersed in an ordinary ice bath, have been found to be capable of maintaining a temperature constant to 0.0001 degree for several days.

Cells have been prepared for use by cooling the entire contents until small crystals are present throughout the liquid. A preferred method is to freeze a thick mantle of ice around the well by rapid cooling from within. With this method, the water ahead of the forming ice contains most of the impurities initially in the water frozen. This will result in an appreciable lowering of the temperature at the outside of the mantle unless the initial purity of the water is sufficiently high. If a thin layer of the pure ice next to the well is then melted, a very pure water-ice interface immediately surrounding the well is obtained, and this fixes a temperature that is constant and reproducible to better than 0.0001 degree, provided the initial outside temperature is not more than 0.001 degree lower than the temperature produced on the interior after melting the thin layer of ice.

The equilibrium temperature, t, corresponding to the depth, H (in mm), below the vapor-liquid surface, may be calculated from the formula

$$t=0.0100-0.7\times10^{-6}H.$$

(b) Ice Point

By observing precautions in regard to purity of ice and water, the saturation of the water at 0° C with uncontaminated air, and the effect of pressure, a temperature reproducible within a few tenthousandths of a degree may be realized.

The effect of pressure may be calculated from the formula[3]

$$t=0.0099\left(1-\frac{p}{p_0}\right)-0.7\times10^{-6}H,$$

where t is the equilibrium temperature, p is the prevailing atmospheric pressure at which the water is saturated with air, and H is the depth (in mm) below the surface of the mixture of water and ice.

5. Oxygen Point

The temperature of equilibrium between liquid oxygen and its vapor is usually realized experimentally by the static method. The platinum resistor of the standard thermometer and the free surface of the liquid oxygen in its container are brought to the same temperature in a suitable cryostat, such as a metal block in a well-stirred bath of liquid oxygen. The tube which connects the space containing the pure liquid oxygen to the manometer used for the measurement of the vapor pressure should be protected against temperatures lower than the temperature of the pure liquid oxygen at the location of the resistor of the standard resistance thermometer.

The equilibrium temperature, t_p, corresponding to a pressure, p, may be found to an accuracy of a few thousandths of a degree over the range from $p=660$ to $p=860$ mm, by means of the formula

$$t_p=-182.970+9.530\left(\frac{p}{p_0}-1\right)-3.72\left(\frac{p}{p_0}-1\right)^2+2.2\left(\frac{p}{p_0}-1\right)^3,$$

or to the same accuracy but over a wider range by the formula

$$t_p=-182.970+\frac{21.94\log_{10}\frac{p}{p_0}}{1-0.261\log_{10}\frac{p}{p_0}}.$$

[3] Author's note. In this formula the value, 0.0099, which appears in the official text, should be 0.010. Ordinarily the incorrect value will not lead to a significant error.

6. Steam Point

The temperature of equilibrium between liquid water and its vapor has been realized by the dynamic method with the thermometer in the saturated vapor, using apparatus of various designs, some closed and others open to the atmosphere. Closed systems, in which a steam-point apparatus and manometer are connected to a manostat of large volume filled with helium are preferable for precise calibrations at the steam point.

The design of the steam-point apparatus should be such as to avoid any superheating of the water vapor around the thermometer, contamination with air or other impurities, and radiation effects. A criterion that the equilibrium temperature has been attained is that the observed temperature corrected to a constant pressure is independent of elapsed time, of variations in the heat supply to the liquid, of variations in the heat loss from the walls, and of the depth of immersion of the thermometer.

The equilibrium temperature, t_p, corresponding to the pressure, p, may be found to an accuracy within 0.001 degree over the range from $p=660$ to $p=860$ mm by means of the formula

$$t_p=100+28.012\left(\frac{p}{p_0}-1\right)-11.64\left(\frac{p}{p_0}-1\right)^2+7.1\left(\frac{p}{p_0}-1\right)^3,$$

or to the same accuracy over a wider range by the formula

$$t_p=100+\frac{64.500\log_{10}\frac{p}{p_0}}{1-0.1979\log_{10}\frac{p}{p_0}}.$$

7. Sulfur Point

The sulfur used in a sulfur boiling-point apparatus should not contain more than 0.005 percent of impurities. Selenium and arsenic are the impurities that have been found most likely to be present in quantities sufficient to affect the temperature of equilibrium to a significant extent.

In the conventional type of sulfur boiling-point apparatus which has proved satisfactory for an accuracy of 0.01 to 0.02 degree, the sulfur is contained in a tube of glass, fused silica, or similar material with an internal diameter of 4 to 5 cm. The length of the tube is determined by the consideration that the vapor column must be long enough to accommodate a radiation shield and to permit the necessary depth of immersion of the resistance thermometer. Electric heating is preferable. Above the source of heat the tube is surrounded by heat-insulating material.

In a recent work in which an accuracy of about 0.001 degree was desired, the thermometer was not immersed directly in the sulfur vapor, but in an aluminum thermometer well, thus adapting the apparatus for use with a closed system. The thermometer well was provided with one or more radiation shields so designed that the interior of the shield approximated a black body, but with ample openings for circulation of sulfur vapor throughout the interior. An electric heater was provided to control the heat loss from the walls.

A criterion that equilibrium temperatures have been attained is that the observed temperatures corrected to a constant pressure should be independent of elapsed time, of variations in the heat supply to the liquid, of variations in the heat loss from the walls, and of the depth of immersion of the thermometer.

The equilibrium temperature, t_p, corresponding to a pressure, p, may be found to an accuracy of about 0.001 degree over the range from $p=660$ to $p=800$ mm by means of the formula

$$t_p=444.6+69.010\left(\frac{p}{p_0}-1\right)-27.48\left(\frac{p}{p_0}-1\right)^2+19.14\left(\frac{p}{p_0}-1\right)^3,$$

or, over a wider range, by the formula

$$t_p=444.6+\frac{158.92\log_{10}\frac{p}{p_0}}{1-0.234\log_{10}\frac{p}{p_0}}.$$

8. Silver and Gold Points

Data on the effect of the impurities most likely to be present in carefully purified silver or gold indicate that the addition of 0.01 percent by weight of metallic impurities to pure silver, or of 0.005 percent to pure gold will probably not change the freezing point in either case by more than 0.1 degree.

For calibrating a thermocouple, the metal is contained in a crucible of pure graphite or other

refractory material which will not contaminate the metal. Crucibles of artifical graphite about 3 cm inside diameter and 15 cm deep with a wall about 1 cm thick have been found very satisfactory. The amount of metal required in such a crucible is about 1600 g of gold or about 900g of silver. Silver must be protected from oxygen while hot.

The crucible and metal are placed in a furnace capable of heating the contents to a uniform temperature. The metal is melted and brought to a uniform temperature a few degrees above its melting point, then allowed to cool slowly. The thermocouple, mounted in a porcelain tube with porcelain insulators separating the two wires, is immersed in the molten metal through a hole in the center of the crucible cover. The depth of immersion should be such that the observed electromotive force of the thermocouple is not changed by more than 1 microvolt when the immersion is increased or decreased by 1 cm. During freezing, the electromotive force should remain constant within 1 microvolt for a period of at least 5 minutes.

9. Freezing Point of Antimony

The procedure in using the freezing point of antimony as a calibration temperature is substantially the same as outlined above for the silver and gold points. Antimony has a marked tendency to undercool before freezing. The undercooling will not be excessive if the metal is heated only a few degrees above its melting point and if the liquid metal is stirred. During freezing, the electromotive force should remain constant within 1 microvolt for a period of at least 5 minutes.

10. Temperature of the Ice Point on the Kelvin Scale

For the sake of uniformity, it is recommended that the temperature of the ice point on the Kelvin scale be taken as 273.15° K.[4] [5]

Part IV. Supplementary Information

1. Resistance-Temperature Formulas

The interpolation formula, for the range 0° C to the freezing point of antimony, as given in the definition of the scale,

$$R_t = R_0(1 + At + Bt^2),$$

may be written in the Callendar form

$$t = \frac{1}{\alpha}\left(\frac{R_t}{R_0} - 1\right) + \delta\left(\frac{t}{100} - 1\right)\left(\frac{t}{100}\right),$$

where

$$\alpha = \frac{1}{100}\left(\frac{R_{100}}{R_0} - 1\right).$$

The relations between the coefficients are

$$A = \alpha\left(1 + \frac{\delta}{100}\right), \qquad \alpha = A + 100B,$$

$$B = -\frac{\alpha\delta}{100^2}, \qquad \delta = -\frac{100^2 B}{A + 100B}.$$

The condition that R_{100}/R_0 shall be greater than 1.3910 is equivalent to requiring that α shall be greater than 0.003910. The condition that $(R_s - R_0)/(R_{100} - R_0)$ shall be between 4.2165 and 4.2180 is equivalent to requiring that δ shall be between 1.488 and 1.498.

Similarly, the interpolation formula, for the range 0° C to the oxygen point, as given in the definition of the scale,

$$R_t = R_0[1 + At + Bt^2 + C(t - 100)t^3],$$

may be written in the Callendar-Van Dusen form

$$t = \frac{1}{\alpha}\left(\frac{R_t}{R_0} - 1\right) + \delta\left(\frac{t}{100} - 1\right)\frac{t}{100} + \beta\left(\frac{t}{100} - 1\right)\left(\frac{t}{100}\right)^3.$$

---

[4] This value 273.15° K was not ratified by either the International Committee or the General Conference. The choice of the last decimal figure was postponed.

[5] *Author's note.* The value 273.15° K±.02 for the temperature of the ice point was originally proposed by the Advisory Committee on Thermometry in 1939; and, in 1948, the Committee did not consider that enough new knowledge had been gained to change this value. That some uncertainty was felt about this action is indicated by a clause in Resolution 2, which already had been approved by the Advisory Committee, and was later adopted by the General Conference. This resolution resulted from a proposal the committee had received to define an absolute thermodynamic temperature scale by assigning a value to the temperature of a single fixed point.

"Resolution 2. The Advisory Committee recognizes the principle of an absolute thermodynamic scale requiring only one fundamental fixed point, which would now be the triple point of pure water, for which the absolute temperature will be chosen later.

"The introduction of this new scale in no way affects the International Scale which continues to be the recommended practical scale."

This resolution defers the establishment of a precise value for the temperature of the ice point. Inasmuch as it is definitely stated at the beginning of Part III of this text that "The recommendations in the following sections are advisory rather than mandatory", many scientists will not consider it mandatory to accept this recommended value for the ice point. In the United States of America the value, 273.16° K, for the temperature of the ice point has been so generally accepted that its use now prevails in scientific publications, and this value will probably continue to be used until a more accurate one has been agreed upon.

The relations between A, B and α, δ are as given above and the other relations are

$$C=-\frac{\alpha\beta}{100^4}, \text{ and } \beta=-\frac{100^4C}{A+100B}.$$

The condition that $(R_S-R_{O_2})/(R_{100}-R_0)$ shall be between 6.143 and 6.144 is equivalent to requiring that $0.5852\delta-\beta$ shall be between 0.7656 and 0.7598.

2. Secondary Fixed Points

In addition to the six fundamental and primary fixed points, certain other fixed points are available and may be useful for various purposes. Some of the more constant and reproducible of these fixed points and their temperatures on the International Temperature Scale of 1948 are given in Table II. The temperatures given are those corresponding to a pressure of 1 standard atmosphere, except for the triple points of water and of benzoic acid. The formulas for the variation of temperature with pressure are intended for use over the range from $p=680$ to $p=780$ mm of mercury.

TABLE II. *Secondary Fixed Points under the pressure of 1 standard atmosphere (except for the triple points)*

	Temperature °C (Int. 1948)
Temperature of equilibrium between solid carbon dioxide and its vapor	−78.5

$$t_p=-78.5+12.12\left(\frac{p}{p_0}-1\right)-6.4\left(\frac{p}{p_0}-1\right)^2$$

Temperature of freezing mercury	−38.87
Temperature of equilibrium between ice, water and its vapor (Triple Point)	+0.0100
Temperature of transition of sodium sulphate decahydrate	32.38
Temperature of triple point of benzoic acid	122.36
Temperature of equilibrium between naphthalene and its vapor	218.0

$$t_p=218.0+44.4\left(\frac{p}{p_0}-1\right)-19\left(\frac{p}{p_0}-1\right)^2$$

Temperature of freezing tin	231.9
Temperature of equilibrium between benzophenone and its vapor	305.9

$$t_p=305.9+48.8\left(\frac{p}{p_0}-1\right)-21\left(\frac{p}{p_0}-1\right)^2$$

Temperature of freezing cadmium	320.9

TABLE II. *Secondary Fixed Points under the pressure of 1 standard atmosphere*—Continued

	Temperature °C (Int. 1948)
Temperature of freezing lead	327.3
Temperature of equilibrium between mercury and its vapor	356.58

$$t_p=356.58+55.552\left(\frac{p}{p_0}-1\right)-23.03\left(\frac{p}{p_0}-1\right)^2+14.0\left(\frac{p}{p_0}-1\right)^3$$

Temperature of freezing zinc	419.5
Temperature of freezing antimony	630.5
Temperature of freezing aluminum	660.1
Temperature of freezing copper in a reducing atmosphere	1083
Temperature of freezing nickel	1453
Temperature of freezing cobalt	1492
Temperature of freezing palladium	1552
Temperature of freezing platinum	1769
Temperature of freezing rhodium	1960
Temperature of freezing iridium	2443
Temperature of melting tungsten	3380

3. Relation Between the International Temperature Scale of 1948 and the Thermodynamic Centigrade Scale

At the time of the adoption of the International Temperature Scale of 1927, the evidence available was insufficient to establish definite differences between that scale and the thermodynamic centigrade scale. The earlier investigations, such as those published in 1911 by the Physikalisch-Technische Reichsanstalt, indicated no differences exceeding 0.05 degree in the range 0° C to the sulfur point.

Recent investigations at the Massachusetts Institute of Technology indicate larger differences between 200° C and the sulfur point. Intercomparisons of two nitrogen gas thermometers with platinum resistance thermometers were made at 0°, 25°, 50°, 75°, 100°, 150°, 200°, 250°, 300°, 350° C, the mercury boiling point, 400° C and the sulfur point. The differences found between t(thermodynamic scale) and t(International Scale) have been formulated as follows:

$$t\ (\text{therm})-t\ (\text{Int})=\frac{t}{100}\left(\frac{t}{100}-1\right)(0.04217-7.481\times10^{-5}t).$$

The sulfur point on the thermodynamic scale was found to be 444.74° C, the results obtained with the two gas thermometers differing by about 0.05 degree.

In the range from 0° C to the oxygen point, intercomparisons published by the Physikalisch-Technische Reichsanstalt in 1932 and by the Leiden Laboratory in 1935 indicate that the differences between the International and thermodynamic scales are less than 0.05 degree. Agreement is lacking as to the sign of some of the reported differences, which are of the order of magnitude of the possible uncertainties in the gas thermometer measurements.

In the range extending below the oxygen point, there is evidence that temperatures on the International Temperature Scale of 1927 are progressively higher than those on the thermodynamic scale, amounting to several hundredths of a degree at −190° C. For this reason, and also because it is advantageous to terminate the various parts of the scale at calibration points, the International Temperature Scale of 1948 extends only to the oxygen point.

In the range from the freezing point of antimony to the gold point, there is little evidence relative to the sign or magnitude of departures of the International from the thermodynamic scale. The value 1063.0° C for the gold point has been accepted as a conventional definition and will doubtless remain so until the appearance of new and more accurate basic data. The change from 960.5° to 960.8° C is well within the uncertainty of the location of the silver point on the thermodynamic scale. This change makes the thermocouple scale join more smoothly, not only with the resistance thermometer scale at the freezing point of antimony, but also with the optical pyrometer scale at the gold point when $c_2 = 1.438$ cm degrees.

It is of interest to note that, granting the validity of Planck's formula, temperatures above the gold point on the International Temperature Scale of 1948 will differ from those on the thermodynamic centigrade scale only to the extent caused by errors in the constants, c_2, t_{Au}, and T_0, used in the formula.

WASHINGTON, January 14, 1949.

U. S. Department of Commerce
National Bureau of Standards

Research Paper RP1963
Volume 42, March 1949

Part of the Journal of Research of the National Bureau of Standards

Absorption by Sound-Absorbent Spheres

By Richard K. Cook and Peter Chrzanowski

The absorption of a plane wave of sound by a sphere is computed. The calculations are based on the assumption that the complex ratio of sound pressure at a point on the sphere's surface to the normal component of particle velocity is a constant independent of the direction of incidence ("normal impedance assumption"). Absorption measurements were made on hair-felt covered spheres placed in a reverberation room, and were compared with the computed absorption by means of the reverberation room statistics appropriate for spheres. The theory and measurements both show that absorbent spheres can have absorption coefficients greater than unity. The discrepancies between theoretical and experimental coefficients seem to indicate that the normal impedance assumption is not valid for the hair felt used in the experiments.

I. Introduction

In an earlier paper [1],[1] the authors gave the results of a combined theoretical and experimental investigation of the absorption of sound by long circular cylinders having a known normal acoustic impedance. An expression was derived for the absorption coefficient of a cylinder on which is incident a plane wave of sound, having a single frequency, traveling in a direction perpendicular to the axis of the cylinder. The derivation was based on the assumption that the complex ratio of sound pressure at a point on the cylinder's surface to the normal component of particle velocity was a constant independent of the direction of incidence. The ratio was therefore equal to the acoustic impedance of the surface for perpendicularly incidence sound. This will be referred to hereafter as the "normal impedance assumption."

A comparison of the measured and theoretical absorption coefficients for random incidence seemed to indicate, however, that the normal impedance assumption was not satisfied for the hair felt. In other words, it seemed that sound was propagated also through the absorbent covering (hair felt) of the cylinders in directions other than normal to the surface. Similar conclusions were reached more recently by Scott [2] in his study of propagation of sound between walls and through ducts lined with mineral wool.

It was pointed out in the previous paper [1] that a comparison of theoretical and experimental absorption coefficients for sound absorbent spheres would give more definite information on the validity of the normal impedance assumption for hair felt. Consequently, an investigation was carried out on spheres covered with the same type of hair felt as was used for covering the cylinders.

The theoretical calculations on spheres may be divided into two parts: (1) The absorption by a sphere, calculated on the basis of the normal impedance assumption, when a plane wave of sound is incident on it, (2) a statistical calculation of the absorption by a sphere for sound waves having random incidence, the results of which have already been given in reference [1]. The measurements of the acoustic impedance of the hair felt are given in the same reference and are required here for the first part of the calculations. The calculated absorptions for random incidence are compared with measurements made in a reverberation room.

[1] Figures in brackets indicate the literature references at the end of this paper.

II. Scattering by an Absorbent Sphere

A sphere of sound-absorbent material is placed in a plane sound wave of a single frequency whose direction of propagation is parallel to the x-axis (see fig. 1). The scattering and absorption by the

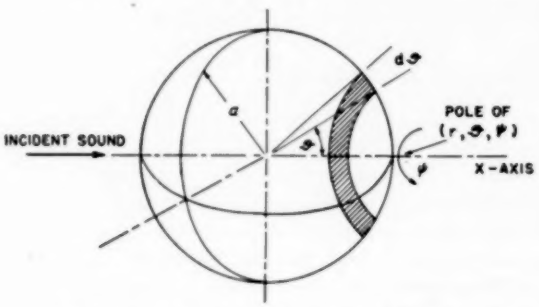

FIGURE 1. *Representation of absorbent sphere.*

sphere are to be computed. The normal impedance assumption is supposed to be valid at all points on the surface of the sphere.

The velocity potential of the incident plane wave is

$$\Phi_i=\phi_0 e^{i(\omega t-kx)}=\phi_0 e^{i(\omega t-kr\cos\vartheta)}$$
$$=\phi_0\left\{\sum_{\mu=0}^{\infty}(2\mu+1)\,(-i)^{\mu}P_{\mu}\,(\cos\vartheta)j_{\mu}(kr)\right\}e^{i\omega t}, \quad (1)$$

and for simplicity it is assumed that $\phi_0=1$. In this equation $\omega=2\pi\times$frequency of the incident wave and k is the generalized wave number. This expansion of the velocity potential in an infinite series of Legendre polynomials P_{μ} (cos ϑ) and spherical Bessel functions $j_{\mu}(kr)$ in the spherical polar coordinates r, ϑ, ψ, is introduced in order to facilitate satisfaction of the boundary conditions at the surface of the absorbent sphere. It is clear from considerations of symmetry that the velocity potential will be independent of the azimuthal angle, ψ.

The wave scattered by the sphere can be represented by

$$\Phi_s=\sum_{\mu=0}^{\infty}b_{\mu}(j_{\mu}-in_{\mu})P_{\mu}(\cos\vartheta)e^{i\omega t}, \quad (2)$$

in which it is understood that j_{μ} and n_{μ} are functions of kr. The function n_{μ} is a spherical Neumann function. Each term in this expression represents an outgoing wave, as can be seen from the asymptotic expansion of $j_{\mu}-in_{\mu}$ for large r. The b's are constants to be determined by the boundary conditions at the surface of the sphere.

The total velocity potential is $\Phi=\Phi_i+\Phi_s$. The sound pressure at any point is $p=-\rho(\partial\Phi/\partial t)$ (ρ=density of air), and the radial velocity component, which is normal to the surface of the sphere, is $v_r=(\partial\Phi/\partial r)$. Since the normal impedance assumption is supposed to be valid, the boundary condition at the surface of the sphere is

$$p=-Zv_r, \ (r=a) \quad (3)$$

where $Z=|Z|e^{i\theta}$ is the acoustic impedance. The negative sign is used because the positive direction of v_r is *out* of the absorbent surface, whereas Z is customarily measured with the positive direction for particle velocity *into* the absorbent surface. Calculation of p and v_r from Φ and substitution into eq 3 will yield equations for determination of the b_{μ}'s.

III. Absorption Coefficient

The total time-averaged acoustic power, P, absorbed by the sphere can be computed by a technique similar to that used in the earlier paper [1] for cylinders. Since the calculation is not basically different, the details will not be given here.

A definition of absorption coefficient is needed. Let the time-averaged acoustic power transmitted through unit area by the incident plane wave be P_0. The power absorbed per unit peripheral area of the sphere is $P/4\pi a^2$. The absorption coefficient α_s for a plane wave is defined here by

$$\alpha_s=\frac{P}{4\pi a^2 P_0}. \quad (4)$$

It is shown in the earlier paper that the random incidence effective absorption coefficient for a sphere measured in a reverberation room is greater than α_s by a factor of 4 if the Sabine reverberation formula is used to compute absorption coefficient from measured decay times. The reverberation-room absorption coefficient α_t is defined by

$$\alpha_t=4\alpha_s=\frac{P}{\pi a^2 P_0}. \quad (5)$$

Both α_s and α_t are expressed in sabins per unit peripheral area.

The final expression for the reverberation-room absorption coefficient in terms of the acoustic impedance is

$$\alpha_t = \frac{4}{(ka)^4}\left|\frac{Z}{\rho c}\right| \cos\delta \sum_{\mu=0}^{\infty} \frac{2\mu+1}{\left|-\frac{Z}{\rho c}(j'_\mu - in'_\mu) + i(j_\mu - in_\mu)\right|^2}. \tag{6}$$

The quantity c in this expression is the velocity of sound in air, and j'_μ, n'_μ are the derivatives of j_μ, n_μ.

IV. Experimental Results and Discussion

1. Description of Spheres

The spheres consisted of solid plaster-of-paris cores covered with a layer of cattle-hair felt. Two pieces of the felt, cut to an interlocking pattern, were sewed together over the spherical core like a cover is sewed on a baseball. The contact edges of the pieces were not cut vertically but on a slant to insure minimum distortion of the hair felt. The average diameter of the cores was 5.02 in. and the average diameter of the finished spheres was 6.33 in.

The felt, nominally ⅞ in. thick and weighing 0.60 lb/ft^2, was of the same type and was manufactured by the same concern as that used in the experiments on cylinders.

2. Impedance of Felt

The results of acoustic impedance measurements on the hair felt with rigid backing, and the method for measuring impedance, were given in the earlier paper (see fig. 5 of [1]).

3. Absorption Measurements

The reverberation room measurements were made on 68 of the felt-covered spheres. In figure 2 are shown some of the spheres suspended from wires in the reverberation room. Except for the volume swept out by a set of rotating vanes in the center of the room, the spheres were hung at least 54 in. apart in a rhombohedral lattice. Ten of the spheres were at a distance of about 24 in. from a wall and the remainder at not less than 36 in. from a wall. Descriptions of the reverberation room and the technique for measurement of decay times were given in reference [1].

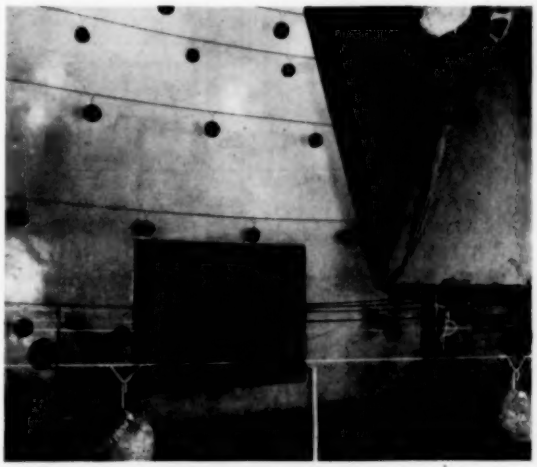

FIGURE 2. *Felt-covered spheres suspended in the reverberation room.*

Results of the reverberation room measurements of the absorption coefficient α_t (defined by eq 5) are plotted in figure 3. The theoretical values of α_t are plotted in the same figure, and were computed from the measured impedances (given in fig. 5 of [1]) by means of eq 6. The measured absorption coefficients for one layer of hair felt laid flat on the floor of the reverberation room are also plotted in figure 3. Comparison of the measured values for the large flat layer with the corresponding measured coefficients for the absorbent spheres shows that a given area of felt has considerably greater absorption, at higher frequencies, when wrapped on a sphere than when applied to a large flat surface. A similar fact was noted in the earlier measurements on absorbent cylinders.

Figure 3 shows that the spheres have absorption coefficients greater than unity at frequencies above 1,200 c/s. This latter frequency corresponds to $ka \simeq 2$. However, the maximum theoretical coefficient for the spheres is somewhat greater than the maximum measured value. This was also true in the case of the absorbent cylinders.

There is general agreement between the theoretical and measured absorption curves, but the differences at some frequencies are too great to be ascribed to experimental uncertainty. The theoretical coefficients are too low at low frequencies, too high at frequencies near $ka=2$, but are in fairly good agreement with the measured coefficients at high frequencies. The differences

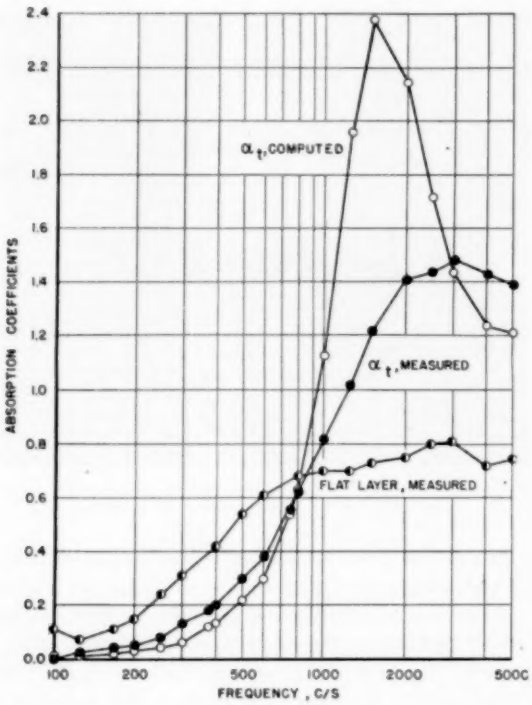

FIGURE 3. *Absorption coefficients for spheres covered with hair felt.*

○, Theoretical values of the absorption coefficient α_t computed by means of equation 6; ●, values of α_t measured in a reverberation room; ◐, absorption coefficients for a flat single layer of hair felt measured in a reverberation room.

between the theoretical and measured values of α_t can only be explained, it seems, on the grounds that the normal impedance assumption is not valid for the hair felt used in the experiments. This implies that sound waves are propagated through the felt in directions other than normal to the surface.

V. Technique of Calculation

Spherical Bessel and Neumann functions of high order and their derivatives were required for calculation of α_t (eq 6). These functions are algebraic combinations of sinusoidal functions and polynomials. At the time these calculations were made (more than 2 years ago), it seemed that the Tables of Circular and Hyperbolic Sines and Cosines [3] prepared by the Mathematical Tables Project of the National Bureau of Standards would readily yield results of the requisite accuracy, and therefore these tables were used. Recently published tables [4, 5] of amplitudes and phase angles for scattering by absorbent spheres and cylinders would probably yield the desired results more expeditiously.

Enough terms in the infinite series of eq 6 were used so that the estimated sum of the remainder terms amounted to less than 0.1 percent of the whole sum. It is estimated that the final computed values of the absorption coefficients α_t have errors (arising from the sequence of calculations) of less than 0.01.

VI. Summary and Proposals

A wave theory has been applied to the absorption of sound by an absorbent sphere. An exact expression, including the effects of diffraction, has been obtained for the absorption coefficient of a sphere on which is incident a plane wave of sound. The derivation of the expression for the absorption coefficient was based on the normal impedance assumption. This assumption is that the complex ratio of sound pressure at a point on the surface of the sphere to the normal component of particle velocity, is a constant independent of the direction of incidence. The ratio is therefore equal to the acoustic impedance of the surface for perpendicularly incident sound. The theoretical coefficients were computed for spheres covered with hair felt by using directly measured acoustic impedances.

The theoretical coefficients were compared with values obtained experimentally for spheres placed in a reverberation room. In order to effect the comparison, it was necessary to use the statistics (developed in an earlier paper) for the absorption by a sphere located in a random wave field. The theory predicts, and measurements confirm, that absorbent spheres can have absorption coefficients appreciably greater than unity. The discrepancies between theoretical and experimental coefficients seem to force the conclusion that wave propagation takes place through the absorbent material in directions other than normal to the surface, which is equivalent to saying that the normal impedance assumption is not valid for hair felt. This confirms the conclusion reached tentatively in an earlier investigation on cylinders covered with the same type of hair felt [1].

Further experiments should be made on the random incidence absorption of sound by isotrop-

ically porous spheres. The material of the spheres should absorb sound by viscous damping of the motion of air in the pores. From measurements of the velocity and attenuation (propagation constants) of waves within the porous material, and from measurements of the acoustic impedance, it should be possible to deduce the absorption when the sphere is placed in a plane wave field, and hence the absorption in a reverberation room.

The authors thank Henry J. Leinbach, Jr. and Richard P. DeAgro for their assistance in the calculations and laboratory measurements.

VII. References

[1] R. K. Cook and P. Chrzanowski, J. Research NBS **36,** 393 (1946) RP1709; J. Acous. Soc. Am. **17,** 315 (1946).

[2] R. A. Scott, Proc. Phys. Soc. **58,** 165, 253, 358 (1946).

[3] Tables of circular and hyperbolic sines and cosines (sponsored by the National Bureau of Standards), published by the Works Project Administration of the Federal Works Agency, New York (1939).

[4] A. N. Lowan, P. M. Morse, H. Feshbach, and M. Lax, Scattering and radiation from circular cylinders and spheres, published by the National Bureau of Standards and the MIT Underwater Sound Laboratory (Feb. 1945).

[5] M. Lax and H. Feshbach, J. Acous. Soc. Am. **20,** 108 (1948).

WASHINGTON, November 2, 1948.

U. S. Department of Commerce
National Bureau of Standards

Research Paper RP1964
Volume 42, March 1949

Part of the Journal of Research of the National Bureau of Standards

Heats, Equilibrium Constants, and Free Energies of Formation of the C_3 to C_5 Diolefins, Styrene, and the Methylstyrenes[1]

By John E. Kilpatrick,[2] Charles W. Beckett,[3] Edward J. Prosen, Kenneth S. Pitzer,[4] and Frederick D. Rossini[5]

For the C_3 to C_5 diolefins, styrene, and the methylstyrenes, values are presented for the following thermodynamic properties to 1,500° K: Heat-content function, free-energy function, entropy, heat content, heat capacity, heat of formation from the elements, free energy of formation from the elements, and logarithm of the equilibrium constant of formation from the elements. Equilibrium constants and concentrations are given in tabular and graphical form for some reactions of isomerization and dehydrogenation.

I. Introduction

As part of the work of the American Petroleum Institute Research Project 44 at the National Bureau of Standards and the University of California, values have been compiled for the thermodynamic properties, in the gaseous state to 1,500° K, of the heat-content function, free-energy function, entropy, heat content, heat capacity, heat of formation, free energy of formation, and logarithm of the equilibrium constant of formation for the C_3 to C_5 diolefins, styrene, and the methylstyrenes. Calculations have also been made of the free energies and equilibrium constants of a number of reactions involving isomerization and hydrogenation of these compounds.

II. Constants

The values of the constants used in the present calculations are as follows [1, 2]:[6] The calorie used is the conventional thermochemical calorie defined as 4.1840 absolute joules; the absolute temperature of the ice point is 273.160±0.010° K; the value of the radiation constant, hc/k, is 1.43847 ±0.00045 cm deg; the gas constant is 1.98719 ±0.00013 cal/deg mole. Values of other constants related to these are given in references [1, 2].

III. Heat-Content Function, Free-Energy Function, Entropy, Heat Content, and Heat Capacity

1. C_3 to C_5 Diolefins

For propadiene (allene), the thermodynamic functions were computed by using the following: The assignment of frequencies given by Thompson and Harris [3], which differs slightly from previous assignments [4, 5], two equal moments of inertia (9.82×10^{-39} g cm^2) recalculated from the spectral data on the rotational fine structure [6], a third moment of inertia (0.575×10^{-39} g cm^2) assumed to be equal to that of ethylene [7], and a symmetry number of four. The foregoing moments of inertia correspond to the following dimensions of the molecule of propadiene, which agree well with those obtained from measurements of electron diffraction [8]: C=C, 1.34 A; C−H, 1.07 A; H−C−H angle, 120°. The uncertainty in the

[1] This investigation was performed as a part of the work of the American Petroleum Institute Research Project 44 at the National Bureau of Standards and the University of California.

[2] Research Associate on the American Petroleum Institute Research Project 44 at the National Bureau of Standards.

[3] Research Associate on the American Petroleum Institute Research Project 44 at the University of California.

[4] Associate Director of the American Petroleum Institute Research Project 44; Professor Chemistry at the University of California, Berkeley, California.

[5] Director of the American Petroleum Institute Research Project 44 at the National Bureau of Standards.

[6] Figures in brackets indicate the literature references at the end of this paper.

calculated values of the thermodynamic functions is estimated to be about 0.2 cal/deg mole at the lower temperatures and somewhat greater at the higher temperatures because of the neglect of vibrational anharmonicities. The values of heat capacity calculated for propadiene in the present investigation agree very well with the experimental data that have been reported [4, 9, 10]. Some values of entropy previously calculated for propadiene by other workers [11, 12], however, differ markedly, for some unknown cause, from those given in the present report.

For 1,2-butadiene, the thermodynamic functions were computed by using the following: The assignment of frequencies given by Szasz, McCartney, and Rank [13]; moments of inertia based on the same corresponding dimensions as for propadiene, together with additional dimensions of 1.54 A for C−C and 1.09 A for H−CCH_3, giving $I_1=2.819\times10^{-39}$, $I_2=20.31\times10^{-39}$, and $I_3=22.03\times10^{-39}$ g cm^2; a reduced moment of inertia for the methyl rotation of 4.78×10^{-40} g cm^2 corresponding to $I_{CH_3}=5.30\times10^{-40}$ g cm^2; and a potential barrier restricting internal rotation of 1,800 cal/mole, which was selected to fit the experimental value of entropy of gaseous 1,2-butadiene at 273.25° K reported by Aston and Szasz [14], including a calorimetrically measured entropy of vaporization. The potential barrier from the present calculations is slightly different from that reported by Aston and Szasz [14] because of the difference in the molecular dimensions used in the respective calculations. As might be expected, the potential barrier for 1,2-butadiene is about the same as that for propylene. The assignment of vibrational frequencies made by Szasz, McCartney, and Rank [13] was tested by calculating approximate product ratios for methyl substitutions of the type used by Pitzer and Scott [15], in which calculations the values of the product ratios for 1,2-butadiene agree very well with those for the methylbenzenes. This agreement offers considerable confirmation of the assignment of frequencies for 1,2-butadiene.

For 1,3-butadiene, the available spectroscopic and other molecular data appear to be satisfactorily represented by the values of the thermodynamic functions calculated by Aston, Szasz, Wooley, and Brickwedde [16], and their values for the heat-content function, free-energy function, and heat capacity were used in the present calculations. However, it should be noted that the available spectroscopic and other molecular data are not sufficient to confirm the correctness of the details of their molecular model of 1,3-butadiene.

For the pentadienes, the available thermal, spectroscopic, and other molecular data are either insufficient or too uncertain to permit a satisfactory statistical treatment at the present time. However, by taking advantage of regularities in the properties of related compounds, thermodynamic functions for the pentadienes may be calculated by suitable combination of the thermodynamic functions for other compounds for which the appropriate values have already been calculated [15, 17, 18, 19]. For such calculations by the method of increments, the following equations were used to evaluate the thermodynamic functions for the seven pentadienes:

$$G(\text{1,2-pentadiene}) = G(\text{1-butene}) + G(\text{1,2-butadiene}) - G(\text{propylene}). \quad (1)$$

$$G(\text{2,3-pentadiene}) = 2G(\text{1,2-butadiene}) - G(\text{propadiene}) - R \ln 8. \quad (2)$$

$$G(\text{3-methyl-1,2-butadiene}) = G(\text{isobutene}) + G(\text{1,2-butadiene}) - G(\text{propylene}). \quad (3)$$

$$G(\textit{cis}\text{-1,3-pentadiene}) = G(\textit{cis}\text{-2-butene}) + G(\text{1,3-butadiene}) - G(\text{propylene}) + R \ln 4. \quad (4)$$

$$G(\textit{trans}\text{-1,3-pentadiene}) = G(\textit{trans}\text{-2-butene}) + G(\text{1,3-butadiene}) - G(\text{propylene}) + R \ln 4. \quad (5)$$

$$G(\text{2-methyl-1,3-butadiene}) = G(\text{isobutene}) + G(\text{1,3-butadiene}) - G(\text{propylene} + R \ln 4 - 0.3. \quad (6)$$

$$G(\text{1,4-pentadiene}) = 2G(\text{1-butene}) - G(\text{propane}) - \text{R ln 4}. \quad (7)$$

In the foregoing equations, G represents the heat content function, the negative of the free energy function, or the heat capacity. The constant terms, R ln 8, etc., appearing, respectively, in eq 2, 4, 5, 6, and 7, are corrections for the symmetry number and are to be used for the negative of the free-energy function, $-(F^\circ - H_0^\circ)/T$, but not for the heat-content function or the heat capacity. The values of the thermodynamic functions used for the calculations represented by eq 1 to 7, inclusive, are from the following: Propane [18]; propylene, 1-butene, *cis*-2-butene, *trans*-2-butene, and isobutene [19].

There are now available a number of checks on the accuracy of the increment method for calculating thermodynamic functions, as illustrated by eq 1 to 7, inclusive. Some confirmation of the increment method has already been reported for certain alkylbenzenes [15, 20] and for certain alkylcyclohexanes [17, 21].

In 1946, values of the thermodynamic functions for 2-methyl-2-butene were calculated [22] by means of the relation

$$G(\text{2-methyl-2-butene}) = 2/3\ G(\textit{cis}\text{-2-butene} + \textit{trans}\text{-2-butene} + \text{isobutene}) - G(\text{propylene}) + R \ln 4. \quad (8)$$

This yielded 80.90 cal/deg mole for the standard entropy in the gaseous state at 25° C, which is to be compared with the value 80.92 subsequently available from the experimental work of Todd, Oliver, and Huffman [22], and Huffman and Scott [23]. The calculated value for the heat capacity of gaseous 2-methyl-2-butene is about 1 percent higher than the experiment value that has recently become available [23].

Before the recent experimental work on 1,2-butadiene became available [14], the authors had calculated the thermodynamic functions of 1,2-butadiene by the method of increments with what now appear to be excellent results, using the equation

$$G(\text{1,2-butadiene}) = G(\text{allene}) + G(\text{propylene}) - G(\text{ethylene}). \quad (9)$$

The standard entropy of gaseous 1,2-butadiene at 25° C was calculated by the method of increments to be 69.7 cal/deg mole, which is to be compared with the new calculated value of 70.03 ± 0.20 cal/deg mole.

There is an experimental entropy available for comparison with our result for 2-methyl-1,3-butadiene (isoprene). The experimental value, 75.2 ± 0.3, [24, 25] is 0.5 cal/deg mole lower than the value given by the increment equation without the term -0.3. Although this difference is well within the expected uncertainties of the method, the additional constant term (-0.3) was added to the increment equation, in order to have better agreement with the isoprene experimental value at 298.16° K. Presumably, this change gives better extrapolated values at higher temperatures.

In connection with the calculation of the thermodynamic functions of the pentadienes by the method of increments, it is estimated that the over-all uncertainty is about 1 cal/deg mole at room temperature and greater at higher temperatures, the values for 1,4-pentadiene being particularly uncertain. However, the differences between values of the thermodynamic functions at given temperatures are more significant than the over-all uncertainties.

The resulting values of the thermodynamic functions for the diolefins, C_3 to C_5, are given in tables 1 to 5, inclusive, which give values of the following properties, respectively, from 0° to 1,500° K: Heat-content function, free-energy function, entropy, heat content, and heat capacity. The value of the entropy is obtained as the value of the heat-content function less the value of the free-energy function, and the value of the heat content is obtained by multiplying the value of the heat-content function by the temperature.

TABLE 1. *Values of the heat-content function, for the ideal gaseous state, to 1,500° K, for the C_3 to C_5 diolefins*

Compound (gas)	Formula	Temperature in ° K														
		0	298.16	300	400	500	600	700	800	900	1,000	1,100	1,200	1,300	1,400	1,500
		Heat-content function, $(H°-H\text{3})/T$, in cal/deg mole														
Propadiene (allene)	C_3H_4	0	10.12	10.15	11.54	12.94	14.28	15.51	16.66	17.71	18.68	19.57	20.40	21.17	21.88	22.54
1,2-Butadiene	C_4H_6	0	12.92	12.96	15.07	17.16	19.15	21.01	22.74	24.34	25.82	27.18	28.44	29.62	30.70	31.70
1,3-Butadiene	C_4H_6	0	12.16	12.20	14.59	16.97	19.18	21.19	23.01	24.66	26.16	27.54	28.80	29.96	31.03	32.02
1,2-Pentadiene	C_5H_8	0	16.2	16.3	19.3	22.3	25.0	27.6	29.9	32.0	34.0	35.8	37.4	39.0	40.4	41.7
cis-1,3-Pentadiene (*cis*-piperylene)	C_5H_8	0	14.5	14.6	17.5	20.5	23.4	26.0	28.5	30.7	32.7	34.6	36.3	37.9	39.4	40.7
trans-1,3-Pentadiene (*trans*-piperylene)	C_5H_8	0	15.3	15.4	18.6	21.7	24.5	27.1	29.5	31.7	33.7	35.5	37.2	38.7	40.1	41.4
1,4-Pentadiene	C_5H_8	0	16.5	16.6	19.6	22.4	25.2	27.7	29.9	32.0	34.0	35.8	37.4	39.0	40.4	41.7
2,3-Pentadiene	C_5H_8	0	15.7	15.8	18.6	21.4	24.0	26.5	28.8	31.0	33.0	34.8	36.5	38.1	39.5	40.9
3-Methyl-1,2-butadiene	C_5H_8	0	15.8	15.8	18.9	21.8	24.6	27.1	29.4	31.5	33.5	35.3	37.0	38.6	40.0	41.3
2-Methyl-1,3-butadiene (isoprene)	C_5H_8	0	15.0	15.1	18.4	21.7	24.6	27.3	29.7	31.9	33.8	35.7	37.4	38.9	40.3	41.6

TABLE 2. *Values of the free-energy function, for the ideal gaseous state, to 1,500° K, for the C_3 to C_5 diolefins*

Compound (gas)	Formula	Temperature in ° K														
		0	298.16	300	400	500	600	700	800	900	1,000	1,100	1,200	1,300	1,400	1,500
		Free-energy function, $(F°-H_0^\circ)/T$, in cal/deg mole														
Propadiene (allene)	C_3H_4	0	−48.18	−48.24	−51.35	−54.08	−56.55	−58.85	−61.00	−63.02	−64.94	−66.76	−68.50	−70.16	−71.76	−73.29
1,2-Butadiene	C_4H_6	0	−57.11	−57.19	−61.21	−64.79	−68.10	−71.19	−74.11	−76.88	−79.52	−82.04	−84.47	−86.80	−89.02	−91.18
1,3-Butadiene	C_4H_6	0	−54.46	−54.54	−58.38	−61.89	−65.18	−68.29	−71.24	−74.05	−76.72	−79.28	−81.73	−84.09	−86.35	−88.52
1,2-Pentadiene	C_5H_8	0	−63.5	−63.6	−68.7	−73.3	−77.6	−81.7	−85.5	−89.1	−92.6	−95.9	−99.1	−102.2	−105.1	−108.0
cis-1,3-Pentadiene (*cis*-piperylene)	C_5H_8	0	−62.9	−63.0	−67.6	−71.8	−75.8	−79.6	−83.3	−86.7	−90.1	−93.3	−96.4	−99.3	−102.2	−105.0
trans-1,3-Pentadiene (*trans*-piperylene)	C_5H_8	0	−61.1	−61.2	−66.1	−70.5	−74.7	−78.7	−82.5	−86.1	−89.5	−92.8	−96.0	−99.0	−101.9	−104.8
1,4-Pentadiene	C_5H_8	0	−63.2	−63.3	−68.5	−73.1	−77.4	−81.5	−85.4	−89.0	−92.5	−95.8	−99.0	−102.0	−105.0	−107.8
2,3-Pentadiene	C_5H_8	0	−61.9	−62.0	−66.9	−71.4	−75.5	−79.4	−83.1	−86.6	−90.0	−93.2	−96.3	−99.3	−102.2	−104.9
3-Methyl-1,2-butadiene	C_5H_8	0	−60.6	−60.7	−65.7	−70.2	−74.5	−78.5	−82.2	−85.8	−89.2	−92.5	−95.7	−98.7	−101.6	−104.4
2-Methyl-1,3-butadiene (isoprene)	C_5H_8	0	−60.4	−60.5	−65.3	−69.8	−74.0	−78.0	−81.8	−85.4	−88.9	−92.2	−95.4	−98.4	−101.4	−104.2

TABLE 3. *Values of the entropy, for the ideal gaseous state, to 1,500° K, for the C_3 to C_5 diolefins*

Compound (gas)	Formula	Temperature in ° K														
		0	298.16	300	400	500	600	700	800	900	1,000	1,100	1,200	1,300	1,400	1,500
		Entropy, $S°$, in cal/deg mole														
Propadiene (allene)	C_3H_4	0	58.30	58.39	62.89	67.02	70.83	74.36	77.65	80.73	83.61	86.33	88.90	91.33	93.64	95.83
1,2-Butadiene	C_4H_6	0	70.03	70.15	76.28	81.95	87.25	92.20	96.85	101.22	105.34	109.22	112.91	116.42	119.72	122.88
1,3-Butadiene	C_4H_6	0	66.62	66.74	72.97	78.86	84.36	89.48	94.25	98.71	102.88	106.82	110.53	114.05	117.38	120.54
1,2-Pentadiene	C_5H_8	0	79.7	79.9	88.0	95.6	102.6	109.3	115.4	121.1	126.6	131.7	136.5	141.2	145.5	149.7
cis-1,3-Pentadiene (*cis*-piperylene)	C_5H_8	0	77.5	77.6	85.1	92.3	99.2	105.7	111.7	117.4	122.18	127.9	132.7	137.2	141.6	145.7
trans-1,3-Pentadiene (*trans*-piperylene)	C_5H_8	0	76.4	76.8	84.6	92.2	99.2	105.8	112.0	117.8	123.2	128.3	133.1	137.7	142.1	146.2
1,4-Pentadiene	C_5H_8	0	79.7	79.9	88.1	95.5	102.6	109.2	115.3	121.0	126.5	131.6	136.4	141.0	145.3	149.5
2,3-Pentadiene	C_5H_8	0	77.6	77.8	85.5	92.8	99.5	105.9	111.9	117.6	123.0	128.0	132.8	137.4	141.7	145.8
3-Methyl-1,2-butadiene	C_5H_8	0	76.4	76.5	84.6	92.0	99.1	105.6	111.6	117.3	122.7	127.8	132.7	137.3	141.6	145.7
2-Methyl-1,3-butadiene (isoprene)	C_5H_8	0	75.4	75.6	83.7	91.4	98.6	105.3	111.5	117.3	122.7	127.9	132.7	137.3	141.7	145.8

TABLE 4. *Values of the heat content, for the ideal gaseous state, to 1,500° K, for the C_3 to C_5 diolefins*

Compound (gas)	Formula	Temperature in ° K														
		0	298.16	300	400	500	600	700	800	900	1,000	1,100	1,200	1,300	1,400	1,500
		Heat content, $(H°-H_0^\circ)$, in cal/mole														
Propadiene (allene)	C_3H_4	0	3017.4	3045.0	4616.0	6470.0	8568.0	10857.0	13328.0	15939.0	18680.0	21527.0	24480.0	27521.0	30632.0	33810.0
1,2-Butadiene	C_4H_6	0	3852.2	3888.0	6028.0	8580.0	11490.0	14707.0	18192.0	21906.0	25820.0	29898.0	34128.0	38506.0	42980.0	47550.0
1,3-Butadiene	C_4H_6	0	3625.6	3660.0	5836.0	8485.0	11508.0	14833.0	18408.0	22194.0	26160.0	30294.0	34560.0	38948.0	43442.0	48030.0
1,2-Pentadiene	C_5H_8	0	4830	4890	7720	11150	15000	19320	23920	28800	34000	39380	44880	50700	56560	62550
cis-1,3-Pentadiene (*cis*-piperylene)	C_5H_8	0	4323	4380	7000	10250	14040	18200	22800	27630	32700	38060	43560	49270	55160	61050
trans-1,3-Pentadiene (*trans*-piperylene)	C_5H_8	0	4562	4620	7440	10850	14700	18970	23600	28530	33700	39050	44640	50310	56140	62100
1,4-Pentadiene	C_5H_8	0	4920	4980	7840	11200	15120	19390	23920	28800	34000	39380	44880	50700	56560	62550
2,3-Pentadiene	C_5H_8	0	4681	4740	7440	10700	14400	18550	23040	27900	33000	38280	43800	49530	55300	61350
3-Methyl-1,2-butadiene	C_5H_8	0	4711	4740	7560	10900	14760	18970	23520	28350	33500	38830	44400	50180	56000	61950
2-Methyl-1,3-butadiene (isoprene)	C_5H_8	0	4472	4530	7360	10850	14760	19110	23760	28710	33800	39270	44880	50570	56420	62400

TABLE 5. *Values of the heat capacity, for the ideal gaseous state, to 1,500° K, for the C_3 to C_5 diolefins*

Compound (gas)	Formula	Temperature in ° K														
		0	298.16	300	400	500	600	700	800	900	1,000	1,100	1,200	1,300	1,400	1,500
		Heat capacity, C_p°, cal/deg mole														
Propadiene (allene)	C_3H_4	0	14.10	14.16	17.21	19.82	22.00	23.84	25.42	26.80	28.00	29.04	29.96	30.75	31.45	32.06
1,2-Butadiene	C_4H_6	0	19.15	19.23	23.54	27.39	30.72	33.54	36.01	38.16	40.02	41.62	43.02	44.23	45.29	46.20
1,3-Butadiene	C_4H_6	0	19.01	19.11	24.29	28.52	31.84	34.55	36.84	38.81	40.52	42.02	43.32	44.47	45.47	46.34
1,2-Pentadiene	C_5H_8	0	25.2	25.3	31.4	36.5	40.8	44.5	47.7	50.4	52.8	54.9	56.7	58.2	59.6	60.7
cis-1,3-Pentadiene (*cis*-piperylene)	C_5H_8	0	22.6	22.7	29.5	35.3	39.9	43.8	47.0	49.8	52.2	54.3	56.1	57.7	59.1	60.3
trans-1,3-Pentadiene (*trans*-piperylene)	C_5H_8	0	24.7	24.9	31.2	38.6	40.9	44.6	47.7	50.3	52.6	54.7	56.4	58.0	59.3	60.5
1,4-Pentadiene	C_5H_8	0	25.1	25.2	31.3	36.5	40.8	44.4	47.6	50.3	52.7	54.7	56.5	58.1	59.4	60.6
2,3-Pentadiene	C_5H_8	0	24.2	24.3	29.9	35.0	39.4	43.2	46.6	49.5	52.0	54.2	56.1	57.7	59.1	60.3
3-Methyl-1,2-butadiene	C_5H_8	0	25.2	25.3	31.0	36.0	40.3	44.0	47.2	50.0	52.4	54.5	56.3	57.9	59.3	60.5
2-Methyl-1,3-butadiene (isoprene)	C_5H_8	0	25.0	25.2	31.8	37.1	41.4	45.0	48.0	50.6	52.9	54.9	56.6	58.2	59.5	60.6

2. Styrene and the Methylstyrenes

For styrene and the several methylstyrenes, the values of the heat-content function, free-energy function, and heat capacity were taken from reference [26]. As usual, the value of the entropy is given by the value of the heat-content function less the value of the free-energy function, and the heat content is obtained by multiplying the value of the heat-content function by the temperature.

The resulting values of the thermodynamic functions for styrene and the methylstyrenes are given in tables 6 to 10, inclusive, which give values of the following properties, respectively, from 0° to 1,500° K: Heat-content function, free-energy function, entropy, heat content, and heat capacity.

TABLE 6. *Values of the heat-content function, for the ideal gaseous state, to 1,500° K, for styrene, C_8, and the methylstyrenes, C_9*

Compound (gas)	Formula	Temperature in ° K														
		0	298.16	300	400	500	600	700	800	900	1,000	1,100	1,200	1,300	1,400	1,500
		Heat-content function, $(H^\circ - H_0^\circ)/T$, in cal/deg mole														
Ethenylbenzene (styrene; vinylbenzene; Phenylethylene)	C_8H_8	0	16.72	16.79	21.07	25.32	29.28	32.92	36.22	39.22	41.95	44.44	46.70	48.77	50.67	52.42
Isopropenylbenzene (α-methylstyrene; 2-phenyl-1-propene)	C_9H_{10}	0	20.3	20.3	25.2	30.0	34.6	38.8	42.6	46.1	49.3	52.2	54.9	57.3	59.6	61.6
cis-1-Propenylbenzene (*cis*-β-methylstyrene; *cis*-1-phenyl-1-propene)	C_9H_{10}	0	20.3	20.3	25.2	30.0	34.6	38.8	42.6	46.1	49.3	52.2	54.9	57.3	59.6	61.6
trans-1-propenylbenzene (*trans*-β-methylstyrene; *trans*-1-phenyl-1-propene)	C_9H_{10}	0	19.9	20.0	25.1	30.0	34.6	38.9	42.7	46.2	49.5	52.4	55.1	57.5	59.8	61.8
1-Methyl-2-ethenylbenzene (o-methylstyrene)	C_9H_{10}	0	20.3	20.3	25.2	30.0	34.6	38.8	42.6	46.1	49.3	52.2	54.9	57.3	59.6	61.6
1-Methyl-3-ethenylbenzene (m-methylstyrene)	C_9H_{10}	0	20.3	20.3	25.2	30.0	34.6	38.8	42.6	46.1	49.3	52.2	54.9	57.3	59.6	61.6
1-Methyl-4-ethenylbenzene (p-methylstyrene)	C_9H_{10}	0	20.3	20.3	25.2	30.0	34.6	38.8	42.6	46.1	49.3	52.2	54.9	57.3	59.6	61.6

TABLE 7. *Values of the free-energy function, for the ideal gaseous state, to 1,500° K, for styrene, C_8, and the methylstyrenes, C_9*

Compound (gas)	Formula	Temperature in ° K														
		0	298.16	300	400	500	600	700	800	900	1,000	1,100	1,200	1,300	1,400	1,500
		Free-energy function, $(F°-H_0°)/T$, in cal/deg mole														
Ethenylbenzene (styrene; vinylbenzene; phenylethylene)	C_8H_8	0	−65.76	−65.86	−71.28	−76.44	−81.42	−86.21	−90.82	−95.26	−99.54	−103.66	−107.61	−111.44	−115.13	−118.68
Isopropenylbenzene (*α*-methylstyrene; 2-phenyl-1-propene)	C_9H_{10}	0	−71.4	−71.5	−78.1	−84.2	−90.1	−95.8	−101.2	−106.4	−111.4	−116.3	−120.9	−125.4	−129.7	−133.9
cis-1-Propenylbenzene (*cis*-*β*-methylstyrene; *cis*-1-phenyl-1-propene)	C_9H_{10}	0	−71.4	−71.5	−78.1	−84.2	−90.1	−95.8	−101.2	−106.4	−111.4	−116.3	−120.9	−125.4	−129.7	−133.9
trans-1-Propenylbenzene (*trans*-*β*-methylstyrene; *trans*-1-phenyl-1-propene)	C_9H_{10}	0	−71.0	−71.1	−77.6	−83.7	−89.6	−95.3	−100.7	−105.9	−111.0	−115.8	−120.5	−125.0	−129.4	−133.5
1-Methyl-2-ethenylbenzene (*o*-methylstyrene)	C_9H_{10}	0	−71.4	−71.5	−78.1	−84.2	−90.1	−95.8	−101.2	−106.4	−111.4	−116.3	−120.9	−125.4	−129.7	−133.9
1-Methyl-3-ethenylbenzene (*m*-methylstyrene)	C_9H_{10}	0	−72.8	−72.9	−79.5	−85.6	−91.5	−97.2	−102.6	−107.8	−112.8	−117.7	−122.3	−126.8	−131.1	−135.3
1-Methyl-4-ethenylbenzene (*p*-methylstyrene)	C_9H_{10}	0	−71.4	−71.5	−78.1	−84.2	−90.1	−95.8	−101.2	−106.4	−111.4	−116.3	−120.9	−125.4	−129.7	−133.9

TABLE 8. *Values of the entropy, for the ideal gaseous state, to 1,500° K, for styrene, C_8, and the methylstyrenes, C_9*

Compound (gas)	Formula	Temperature in ° K														
		0	298.16	300	400	500	600	700	800	900	1,000	1,100	1,200	1,300	1,400	1,500
		Entropy, $S°$, in cal/deg mole														
Ethenylbenzene (styrene; vinylbenzene; phenylethylene)	C_8H_8	0	82.48	82.65	92.35	101.76	110.70	119.13	127.04	134.48	141.49	148.10	154.31	160.21	165.80	171.10
Isopropenylbenzene (*α*-methylstyrene; 2-phenyl-1-propene)	C_9H_{10}	0	91.7	91.8	103.3	114.2	124.7	134.6	143.8	152.5	160.7	168.5	175.8	182.7	189.3	195.5
cis-1-Propenylbenzene (*cis*-*β*-methylstyrene; *cis*-1-phenyl-1-propene)	C_9H_{10}	0	91.7	91.8	103.3	114.2	124.7	134.6	143.8	152.5	160.7	167.5	175.8	182.7	189.3	195.5
trans-1-Propenylbenzene (*trans*-*β*-methylstyrene; *trans*-1-phenyl-1-propene)	C_9H_{10}	0	90.9	91.1	102.7	113.7	124.2	134.2	143.4	152.1	160.5	168.2	175.6	182.5	189.2	195.3
1-Methyl-2-ethenylbenzene (*o*-methylstyrene)	C_9H_{10}	0	91.7	91.8	103.3	114.2	124.7	134.6	143.8	152.5	160.7	168.5	175.8	182.7	189.3	195.5
1-Methyl-3-ethenylbenzene (*m*-methylstyrene)	C_9H_{10}	0	93.1	93.2	104.7	115.6	126.1	136.0	145.2	153.9	162.1	169.9	177.2	184.1	190.7	196.7
1-Methyl-4-ethenylbenzene (*p*-methylstyrene)	C_9H_{10}	0	91.7	91.8	103.3	114.2	124.7	134.6	143.8	152.5	160.7	168.5	175.8	182.7	189.3	195.5

TABLE 9. *Values of the heat content, for the ideal gaseous state, to 1,500° K, for styrene, C_8, and the methyl-styrenes, C_9*

Compound (gas)	Formula	Temperature in ° K														
		0	298.16	300	400	500	600	700	800	900	1,000	1,100	1,200	1,300	1,400	1,500
		Heat content ($H°-H°_0$), in cal/mole														
Ethenylbenzene (styrene; vinylbenzene; phenylethylene)	C_8H_8	0	4,985	5,037	8,428	12,690	17,568	23,044	28,976	35,298	41,950	48,880	56,040	63,400	70,940	78,630
Isopropenylbenzene (α-methylstyrene; 2-phenyl-1-propene)	C_9H_{10}	0	6,050	6,090	10,080	15,000	20,760	27,160	34,080	41,490	49,300	57,400	65,900	74,500	83,400	92,400
cis-1-Propenylbenzene (*cis*-β-methylstyrene; *cis*-1-phenyl-1-propene)	C_9H_{10}	0	6,050	6,090	10,080	15,000	20,760	27,160	34,080	41,490	49,300	57,400	65,900	74,500	83,400	92,400
trans-1-Propenylbenzene (*trans*-β-methylstyrene; *trans*-1-phenyl-1-propene)	C_9H_{10}	0	5,930	6,000	10,040	15,000	20,760	27,230	34,160	41,580	49,500	57,600	66,100	74,800	83,700	92,700
1-Methyl-2-ethenylbenzene (*o*-methylstyrene)	C_9H_{10}	0	6,050	6,090	10,080	15,000	20,760	27,160	34,080	41,490	49,300	57,400	65,900	74,500	83,400	92,400
1-Methyl-3-ethenylbenzene (*m*-methylstyrene)	C_9H_{10}	0	6,050	6,090	10,080	15,000	20,760	27,160	34,080	41,490	49,300	57,400	65,900	74,500	83,400	92,400
1-Methyl-4-ethenylbenzene (*p*-methylstyrene)	C_9H_{10}	0	6,050	6,090	10,080	15,000	20,760	27,160	34,080	41,490	49,300	57,400	65,900	74,500	83,400	92,400

TABLE 10. *Values of the heat capacity, for the ideal gaseous state, to 1,500° K, for styrene, C_8, and the methylstyrenes, C_9*

Compound (gas)	Formula	Temperature in ° K														
		0	298.16	300	400	500	600	700	800	900	1,000	1,100	1,200	1,300	1,400	1,500
		Heat capacity, $C°_p$, in cal/deg mole														
Ethenylbenzene (styrene; vinylbenzene; phenylethylene)	C_8H_8	0	29.18	29.35	38.32	45.94	52.14	57.21	61.40	64.93	67.92	70.48	72.66	74.54	76.16	77.57
Isopropenylbenzene (α-methylstyrene; 2-phenyl-1-propene)	C_9H_{10}	0	34.7	34.9	44.8	53.5	60.7	66.8	71.8	76.1	79.8	82.9	85.6	87.9	89.9	91.6
cis-1-Propenylbenzene (*cis*-β-methylstyrene; *cis*-1-phenyl-1-propene)	C_9H_{10}	0	34.7	34.9	44.8	53.5	60.7	66.8	71.8	76.1	79.8	82.9	85.6	87.9	89.9	91.6
trans-1-Propenylbenzene (*trans*-β-methylstyrene; *trans*-1-phenyl-1-propene)	C_9H_{10}	0	34.9	35.1	45.2	54.0	61.2	67.2	72.2	76.4	80.0	83.1	85.8	88.1	90.0	91.7
1-Methyl-2-ethenylbenzene (*o*-methylstyrene)	C_9H_{10}	0	34.7	34.9	44.8	53.5	60.7	66.8	71.8	76.1	79.8	82.9	85.6	87.9	89.9	91.6
1-Methyl-3-ethenylbenzene (*m*-methylstyrene)	C_9H_{10}	0	34.7	34.9	44.8	53.5	60.7	66.8	71.8	76.1	79.8	82.9	85.6	87.9	89.9	91.6
1-Methyl-4-ethenylbenzene (*p*-methylstyrene)	C_9H_{10}	0	34.7	34.9	44.8	53.5	60.7	66.8	71.8	76.1	79.8	82.9	85.6	87.9	89.9	91.6

IV. Heat of Formation, Free Energy of Formation, and Equilibrium Constant of Formation

For the standard heat of formation from the elements at 25° C, values for the diolefins, C_3 to C_5, were obtained as follows: 1,3-Butadiene, from reference [27]; 1,2-butadiene, from reference [28]; propadiene, *cis*- and *trans*-1,3-pentadiene, and 1,4-pentadiene, from combination of the data on heats of hydrogenation from references [36, 37] with the values for the heats of formation of the corresponding paraffin hydrocarbons from reference [29]; by calculation, using the relations between energy content and molecular structure given in references [29, 30, 31, 32, 33]. The values so calculated are believed to be uncertain by not more than about ± 0.75 kcal/mole.

For the standard heat of formation from the elements at 25° C, values for styrene and the methylstyrenes were obtained as follows:

Ethenylbenzene (styrene, vinylbenzene, or phenylethylene), from reference [28]; isopropenylbenzene (α-methylstyrene or 2-phenyl-1-propene), from reference [34]; *cis*-1-propenylbenzene (*cis*-β-methylstyrene or *cis*-1-phenyl-1-propene), *trans*-1-propenylbenzene (*trans*-β-methylstyrene or trans-1-phenyl-1-propene), 1-methyl-2-ethenylbenzene (*o*-methylstyrene), 1-methyl-3-ethenylbenzene, (*m*-methylstyrene), and 1-methyl-4-ethenylbenzene (*p*-methylstyrene) by calculation, using the relations between energy content and molecular structure given in references [29, 30, 31, 32, 33]. The values so calculated are believed to be uncertain by not more than about ± 0.75 kcal/mole.

The method of calculating values of the standard heat of formation, the standard free energy of formation, and the logarithm of the equilibrium constant of formation for the different temperatures in the range 0° to 1,500° K, is the same as that described in section IV, 1, of reference [35].

The resulting values for the formation of the given hydrocarbon in the gaseous state, from the elements carbon (solid, graphite) and hydrogen (gaseous), each in its thermodynamic standard state, are presented in tables 11 to 16, inclusive, which give values of the following properties, for the C_3 to C_5 diolefins, styrene, and the methylstyrenes, to 1,500° K: Heat of formation, free energy of formation, and logarithm of the equilibrium constant of formation. It should be noted that the uncertainties in the values for the pentadienes and the methylstyrenes are such as to make the values of the logarithm (to the base 10) of the equilibrium constants of formation for these compounds uncertain by as much as 0.3 to 0.5, which is equivalent to a factor of 2 to 3 in the value of the equilibrium constant itself.

TABLE 11. *Values of the heat of formation, for the ideal gaseous state, to 1,500° K, for the C_3 to C_5 diolefins*

Compound (gas)	Formula	Temperature in ° K														
		0	298.16	300	400	500	600	700	800	900	1,000	1,100	1,200	1,300	1,400	1,500
		Heat of formation, $\Delta Hf°$ in kcal/mole														
Propadiene (allene)	C_3H_4	47.70	45.92	45.91	45.35	44.85	44.42	44.03	43.71	43.44	43.23	43.06	42.94	42.84	42.75	42.68
1,2-Butadiene	C_4H_6	42.78	39.55	39.53	38.56	37.78	37.09	36.50	36.03	35.66	35.40	35.21	35.10	35.04	35.00	34.99
1,3-Butadiene	C_4H_6	30.20	26.75	25.83	25.80	25.12	24.53	24.05	23.67	23.37	23.17	23.04	22.96	22.91	22.89	22.89
1,2-Pentadiene	C_5H_8	39.32	34.80	34.79	33.61	32.72	31.82	31.21	30.68	30.28	30.09	29.96	29.84	29.93	29.96	30.03
cis-1,3-Pentadiene (*cis*-piperylene)	C_5H_8	23.73	18.70	18.69	17.29	16.16	15.27	14.49	13.97	13.52	13.19	13.04	12.93	12.91	12.97	12.93
trans-1,3-Pentadiene (*trans*-piperylene)	C_5H_8	23.39	18.60	18.59	17.39	16.42	15.59	14.92	14.43	14.08	13.85	13.69	13.67	13.61	13.61	13.64
1,4-Pentadiene	C_5H_8	29.63	25.20	25.19	24.04	23.01	22.25	21.59	21.00	20.59	20.40	20.27	20.15	20.24	20.27	20.34
2,3-Pentadiene	C_5H_8	37.77	33.10	33.09	31.78	30.65	29.67	28.76	28.25	27.83	27.54	27.30	27.21	27.21	27.15	27.28
3-Methyl-1,2-butadiene	C_5H_8	35.64	31.00	30.96	29.76	28.72	27.90	27.18	26.60	26.15	25.91	25.72	25.68	25.73	25.72	25.74
2-Methyl-1,2-butadiene (isoprene)	C_5H_8	22.98	18.10	18.09	16.90	16.01	15.24	14.66	14.18	13.85	13.54	13.50	13.50	13.46	13.48	13.53

TABLE 12. *Values of the free energy of formation, for the ideal gaseous state, to 1,500° K, for the C_3 to C_5 diolefins*

Compound (gas)	Formula	Temperature in ° K														
		0	298.16	300	400	500	600	700	800	900	1,000	1,100	1,200	1,300	1,400	1,500
		Free energy of formation, $\Delta Ff°$ in kcal/mole														
Propadiene (allene)	C_3H_4	47.70	48.37	48.38	49.29	50.33	51.48	52.68	53.93	55.23	56.50	57.86	59.25	60.62	61.98	63.35
1,2-Butadiene	C_4H_6	42.78	48.21	48.26	51.32	54.60	58.03	61.57	65.18	68.85	72.55	76.26	80.01	83.75	87.50	91.25
1,3-Butadiene	C_4H_6	30.20	36.43	36.49	39.88	43.47	47.20	51.02	54.90	58.82	62.78	66.74	70.72	74.70	78.67	82.66
1,2-Pentadiene	C_5H_8	39.32	50.29	50.38	55.77	61.44	67.28	73.21	79.27	85.41	91.53	97.70	103.85	109.96	116.16	122.22
cis-1,3-Pentadiene (*cis*-piperylene)	C_5H_8	23.73	34.88	34.97	40.61	46.60	52.77	59.09	65.44	71.98	78.44	84.97	91.50	98.14	104.77	111.13
trans-1,3-Pentadiene (*trans*-piperylene)	C_5H_8	23.39	35.07	35.17	40.87	46.91	53.09	59.38	65.74	72.18	78.70	85.18	91.64	98.19	104.71	111.09
1,4-Pentadiene	C_5H_8	29.63	40.69	40.78	46.16	51.85	57.71	63.66	69.66	75.81	81.94	88.12	94.28	100.53	106.61	112.83
2,3-Pentadiene	C_5H_8	37.77	49.22	49.31	54.94	60.84	66.99	73.27	79.64	86.11	92.58	99.12	105.66	112.18	118.67	125.32
3-Methyl-1,2-butadiene	C_5H_8	35.64	47.47	47.57	53.29	59.31	65.46	71.77	78.23	84.70	91.25	97.76	104.25	110.83	117.38	123.94
2-Methyl-1,3-butadiene (isoprene)	C_5H_8	22.98	34.87	34.97	40.78	46.85	53.10	59.46	65.89	72.40	78.89	85.43	91.95	98.56	105.00	111.58

TABLE 13. *Values of the logarithm of the equilibrium constant of formation, for the ideal gaseous state, to 1,500° K, for the C_2 to C_5 diolefins*

Compound (gas)	Formula	Temperature in ° K														
		0	298.16	300	400	500	600	700	800	900	1,000	1,100	1,200	1,300	1,400	1,500
		Logarithm of equilibrium constant of formation, $\log_{10} Kf$														
Propadiene (allene)	C_3H_4	Infinite	−35.4519	−35.2462	−26.9316	−22.0008	−18.7503	−16.4479	−14.7338	−13.4123	−12.3488	−11.5024	−10.7904	−10.1907	−9.6747	−9.2306
1,2-Butadiene	C_4H_6	do	−35.3377	−35.1597	−28.0379	−23.8644	−21.1356	−19.2218	−17.8050	−16.7181	−15.8564	−15.1512	−14.5710	−14.0790	−13.6600	−13.2943
1,3-Butadiene	C_4H_6	do	−26.7004	−26.5796	−21.7868	−19.0023	−17.1941	−15.9302	−14.9974	−14.2834	−13.7205	−13.2602	−12.8799	−12.5573	−12.2809	−12.8070
1,2-Pentadiene	C_5H_8	do	−36.861	−36.705	−30.409	−26.854	−24.507	−22.857	−21.655	−20.741	−20.004	−19.412	−18.913	−18.486	−18.134	−17.044
cis-1,3-Pentadiene(*cis*-piperylene)	C_5H_8	do	−25.563	−25.477	−22.100	−20.367	−19.221	−18.448	−17.877	−17.479	−17.142	−16.882	−16.664	−16.499	−16.355	−16.191
trans-1,3-Pentadiene (*trans*-piperylene)	C_5H_8	do	−25.707	−25.624	−22.332	−20.502	−19.337	−18.538	−17.959	−17.528	−17.199	−16.924	−16.689	−16.507	−16.346	−16.185
1,4-Pentadiene	C_5H_8	do	−29.824	−29.712	−25.219	−22.663	−21.021	−19.875	−19.030	−18.410	−17.908	−17.508	−17.171	−16.901	−16.643	−16.439
2,3-Pentadiene	C_5H_8	do	−36.074	−35.925	−30.017	−26.592	−24.401	−22.875	−21.756	−20.910	−20.233	−19.693	−19.243	−18.859	−18.526	−18.259
3-Methyl-1,2-butadiene	C_5H_8	do	−34.797	−34.657	−29.114	−25.923	−23.843	−22.407	−21.371	−20.568	−19.942	−19.423	−18.986	−18.632	−18.324	−18.058
2-Methyl-1,3-butadiene(isoprene)	C_5H_8	do	−25.560	−25.477	−22.284	−20.476	−19.341	−18.563	−18.000	−17.581	−17.241	−16.973	−16.746	−16.569	−16.392	−16.257

TABLE 14. *Values of the heat of formation, for the ideal gaseous state, to 1,500° K, for styrene, C_8, and the methylstyrenes, C_9.*

Compound (gas)	Formula	Temperature in ° K														
		0	298.16	300	400	500	600	700	800	900	1,000	1,100	1,200	1,300	1,400	1,500
		Heat of formation, $\Delta Hf°$ in kcal/mole														
Ethenylbenzene (styrene; vinylbenzene; phenylethylene)	C_8H_8	40.34	35.22	35.19	33.83	32.72	31.81	31.08	30.51	30.09	29.83	29.69	29.63	29.61	29.63	29.68
Isopropenylbenzene (α-methylstyrene; 2-phenyl-1-propene)	C_9H_{10}	33.33	27.00	26.94	25.23	23.80	22.66	21.73	20.99	20.45	20.13	19.93	19.90	19.83	19.95	19.93
cis-1-Propenylbenzene (*cis*-β-Methylstyrene; *cis*-1-phenyl-1-propene)	C_9H_{10}	35.33	29.00	28.94	27.23	25.80	24.66	23.73	22.99	22.45	22.13	21.93	21.90	21.83	21.95	21.93
trans-1-Propenylbenzene (*trans*-β-methylstyrene; *trans*-1-phenyl-1-propene)	C_9H_{10}	34.45	28.00	27.97	26.31	24.92	23.78	22.92	22.19	21.66	21.45	21.27	21.26	21.21	21.35	21.35
1-Methyl-2-ethenylbenzene) (o-methylstyrene	C_9H_{10}	34.63	28.30	28.24	26.53	25.10	23.96	23.03	22.29	21.75	21.43	21.23	21.20	21.13	21.25	21.23
1-Methyl-3-ethenylbenzene (*m*-methylstyrene)	C_9H_{10}	33.93	27.60	27.54	25.83	24.40	23.26	22.33	21.59	21.05	20.73	20.53	20.50	20.43	20.55	20.53
1-Methyl-4-ethenylbenzene (*p*-methylstyrene)	C_9H_{10}	33.73	27.40	27.34	25.63	24.20	23.06	22.13	21.39	20.85	20.53	20.33	20.30	20.23	20.35	20.33

TABLE 15. *Values of the free energy of formation, for the ideal gaseous state, to 1,500° K, for styrene, C_8, and the methylstyrenes, C_9*

Compound (gas)	Formula	Temperature in ° K														
		0	298.16	300	400	500	600	700	800	900	1,000	1,100	1,200	1,300	1,400	1,500
		Free energy of formation, $\Delta Ff°$ in kcal/mole														
Ethenylbenzene (styrene; vinylbenzene; phenylethylene)	C_8H_8	40.34	51.10	51.20	56.74	62.61	68.67	74.87	81.16	87.53	93.92	100.33	106.77	113.19	119.60	126.03
Isopropenylbenzene (α-methylstyrene; 2-phenyl-1-propene)	C_9H_{10}	33.33	49.84	49.99	57.90	66.26	74.85	83.60	92.51	101.51	110.56	119.53	128.66	137.72	146.82	155.85
cis-1-Propenylbenzene (*cis*-β-methylstyrene; *cis*-1-phenyl-1-propene)	C_9H_{10}	35.33	51.84	51.99	59.90	68.26	76.85	85.60	94.51	103.51	112.56	121.53	130.66	139.72	148.82	157.85
trans-1-Propenylbenzene (*trans*-β-methylstyrene; *trans*-1-phenyl-1-propene)	C_9H_{10}	34.45	51.08	51.23	59.22	67.63	76.27	85.07	94.03	103.08	112.08	121.20	130.26	139.36	148.36	157.57
1-Methyl-2-ethenylbenzene (o-methylstyrene)	C_9H_{10}	34.63	51.14	51.29	59.20	67.56	76.15	84.90	93.81	102.81	111.86	120.83	129.96	139.02	148.12	157.15
1-Methyl-3-ethenylbenzene (m-methylstyrene)	C_9H_{10}	33.93	50.02	50.17	57.94	66.16	74.61	83.22	91.99	100.85	109.76	118.59	127.58	136.50	145.46	154.35
1-Methyl-4-ethenylbenzene (p-methylstyrene)	C_9H_{10}	33.73	50.24	50.39	58.30	66.66	75.25	84.00	92.91	101.91	110.96	119.93	129.06	138.12	147.22	156.25

TABLE 16. *Values of the logarithm of the equilibrium constant of formation, for the ideal gaseous state, to 1,500° K, for styrene, C_8, and the methylstyrenes, C_9*

Compound (gas)	Formula	Temperature in ° K														
		0	298.16	300	400	500	600	700	800	900	1,000	1,100	1,200	1,300	1,400	1,500
		Logarithm of equilibrium constant of formation, $\log_{10} Kf$														
Ethenylbenzene (styrene; vinylbenzene; phenylethylene)	C_8H_8	Infinite	−37.4532	−37.2963	−31.0030	−27.3649	−25.0117	−23.3762	−22.1729	−21.2543	−20.5264	−19.9330	−19.4456	−19.0295	−18.6705	−18.3630
Isopropenylbenzene (α-methylstyrene; 2-phenyl-1-propene)	C_9H_{10}	do	−36.531	−36.416	−31.636	−28.963	−27.266	−26.101	−25.272	−24.649	−24.162	−23.749	−23.433	−23.153	−22.919	−22.707
cis-1-Propenylbenzene (cis-β-methylstyrene; cis-1-phenyl-1-propene)	C_9H_{10}	do	−37.998	−37.874	−32.729	−29.837	−27.994	−26.726	−25.818	−25.134	−24.600	−24.146	−23.797	−23.490	−23.231	−22.998
trans-1-Propenylbenzene (trans-β-methylstyrene; trans-1-phenyl-1-propene)	C_9H_{10}	do	−37.440	−37.320	−32.357	−29.562	−27.783	−26.560	−25.687	−25.030	−24.495	−24.081	−23.724	−23.429	−23.159	−22.958
1-Methyl-2-ethenylbenzene (o-methylstyrene)	C_9H_{10}	do	−37.484	−37.364	−32.346	−29.531	−27.739	−26.560	−25.627	−24.965	−24.446	−24.007	−23.670	−23.352	−23.122	−22.896
1-Methyl-3-ethenylbenzene (m-methylstyrene)	C_9H_{10}	do	−36.665	−36.548	−31.658	−28.919	−27.178	−25.982	−25.130	−24.488	−23.988	−23.562	−23.236	−22.948	−22.706	−22.488
1-Methyl-4-ethenylbenzene (p-methylstyrene)	C_9H_{10}	do	−36.825	−36.708	−31.855	−29.138	−27.411	−26.226	−25.381	−24.746	−24.250	−23.828	−23.506	−23.220	−22.981	−22.765

V. Free Energies and Equilibria of Some Reactions of Isomerization and Dehydrogenation

In figure 1 are plotted, as a function of temperature, for the two butadienes, the amounts, in mole fraction, of each of the isomers present at equilibrium with the other isomer in the gaseous state. The corresponding numerical values are given in table 17.

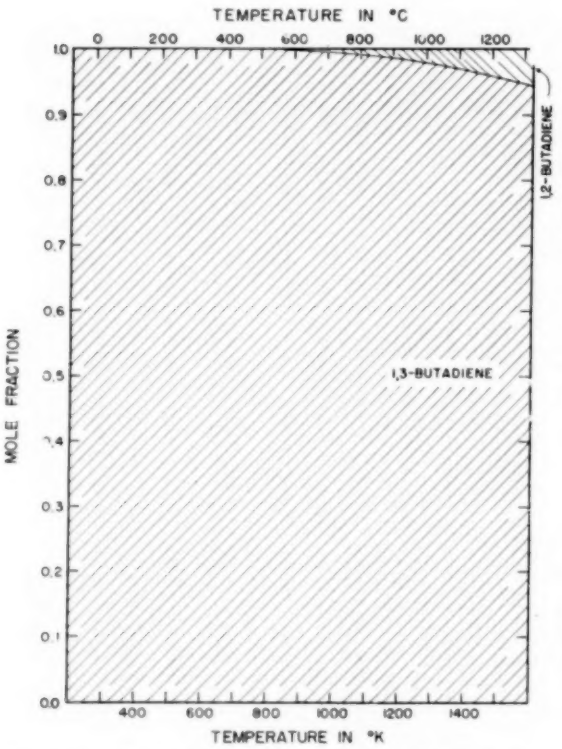

FIGURE 1. *Equilibrium concentrations of the two butadienes.*

The scale of ordinates measures the amount in mole fraction, and the scale of abscissas gives the temperature in degrees Kelvin and degrees Centigrade. The vertical width of a band at a given temperature measures the mole fraction of the given isomer present at equilibrium with all of its other isomers in the gaseous state.

In figure 2 are plotted, as a function of temperature, for the seven pentadienes, the amounts, in mole fraction, of each of the isomers present at equilibrium with the other isomers in the gaseous state. The corresponding numerical values are given in table 18.

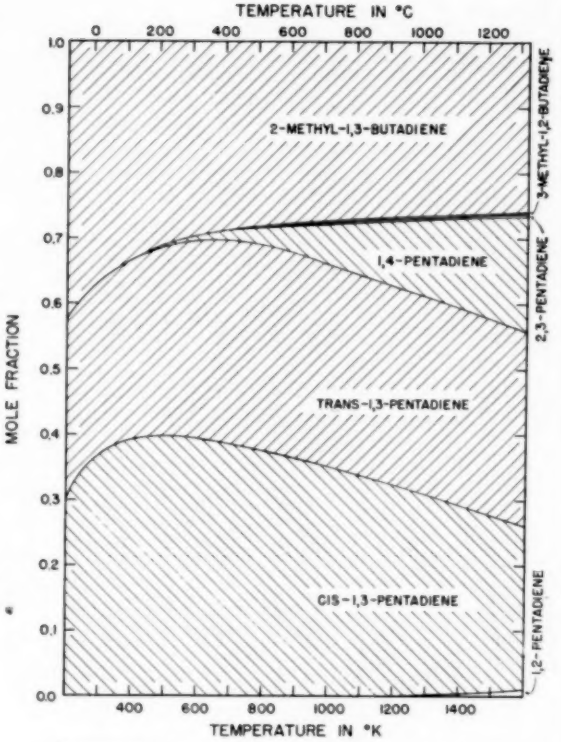

FIGURE 2. *Equilibrium concentrations of the seven pentadienes.*

The scale of ordinates measures the amount in mole fraction, and the scale of abscissas gives the temperature in degrees Kelvin and degrees Centigrade. The vertical width of a band at a given temperature measures the mole fraction of the given isomer present at equilibrium with all of its other isomers in the gaseous state.

TABLE 17. *Equilibrium concentrations of the two butadienes in the ideal gaseous state to 1,500° K*

Temperature	Composition, in mole fraction of the mixture of isomers at at equilibrium	
	1,2-Butadiene	1,3-Butadiene
°K		
298.16	0.000	1.000
300	.000	1.000
400	.000	1.000
500	.000	1.000
600	.000	1.000
700	.001	.999
800	.002	.998
900	.004	.996
1,000	.007	.993
1,100	.013	.987
1,200	.020	.980
1,300	.029	.971
1,400	.040	.960
1,500	.053	.947

TABLE 18. *Equilibrium concentrations of the seven pentadienes in the ideal gaseous state to 1,500° K*

Temperature	Composition, in mole fraction, of the mixture of isomers at equilibrium						
	1,2-Pentadiene	*cis*-1,3-Pentadiene	*trans*-1,3-Pentadiene	1,4-Pentadiene	2,3-Pentadiene	3-Methyl-1,2-butadiene	2-Methyl-1,3-butadiene
°K							
298.16	0.000	0.367	0.263	0.000	0.000	0.000	0.370
300	.000	.369	.262	.000	.000	.000	.369
400	.000	.396	.285	.000	.000	.000	.319
500	.000	.398	.291	.002	.000	.000	.309
600	.000	.394	.301	.006	.000	.000	.299
700	.000	.382	.311	.014	.000	.000	.293
800	.000	.377	.312	.027	.000	.000	.284
900	.000	.357	.319	.042	.000	.000	.282
1000	.000	.351	.308	.060	.000	.001	.280
1100	.001	.338	.306	.080	.001	.001	.274
1200	.002	.323	.305	.100	.001	.002	.267
1300	.003	.308	.302	.122	.001	.002	.262
1400	.005	.286	.293	.148	.002	.003	.263
1500	.007	.287	.291	.162	.0035	.004	.246

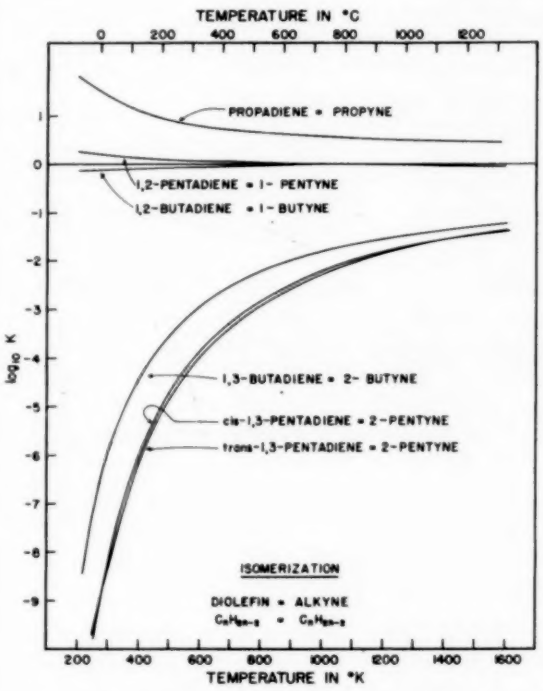
TEMPERATURE IN °C
0 200 400 600 800 1000 1200
PROPADIENE = PROPYNE
1,2-PENTADIENE = 1- PENTYNE
1,2-BUTADIENE = 1- BUTYNE
1,3-BUTADIENE = 2- BUTYNE
cis-1,3-PENTADIENE = 2-PENTYNE
trans-1,3-PENTADIENE = 2-PENTYNE
ISOMERIZATION
DIOLEFIN = ALKYNE
log10 K
1 0 -1 -2 -3 -4 -5 -6 -7 -8 -9
200 400 600 800 1000 1200 1400 1600
TEMPERATURE IN °K

FIGURE 3. *Dehydrogenation of monoolefins to diolefins.*

The scale of ordinates gives the value of the logarithm (to the base 10) o the equilibrium constant for the reaction of dehydrogenating a given monoole fin to a given diolefin, in the gaseous state. The scale of abscissas gives the temperature in degrees Kelvin. The several curves refer to the following reactions in the gaseous state: A, Propylene=propadiene+hydrogen; B, 1-butene=1,3-butadiene+hydrogen; C, *cis*-2-butene=1,3-butadiene+hydrogen; D, *trans*-2-butene=1,3-butadiene+hydrogen; E, isobutene=1,3-butadiene+hydrogen.

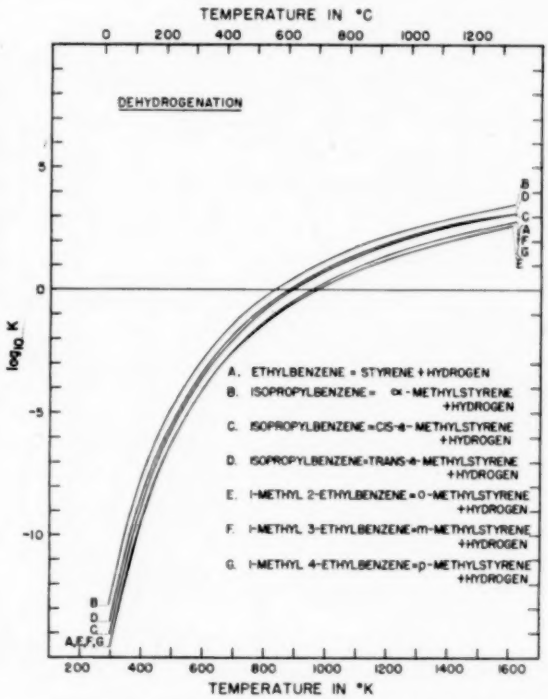
TEMPERATURE IN °C
0 200 400 600 800 1000 1200
DEHYDROGENATION
B
D
C
A,F,G
E
log10 K
5 0 -5 -10
A. ETHYLBENZENE = STYRENE + HYDROGEN
B. ISOPROPYLBENZENE = α - METHYLSTYRENE + HYDROGEN
C. ISOPROPYLBENZENE = CIS-β- METHYLSTYRENE + HYDROGEN
D. ISOPROPYLBENZENE = TRANS-β- METHYLSTYRENE + HYDROGEN
E. I-METHYL 2-ETHYLBENZENE = o - METHYLSTYRENE + HYDROGEN
F. I-METHYL 3-ETHYLBENZENE = m - METHYLSTYRENE + HYDROGEN
G. I-METHYL 4-ETHYLBENZENE = p - METHYLSTYRENE + HYDROGEN
B
D
C
A,E,F,G
200 400 600 800 1000 1200 1400 1600
TEMPERATURE IN °K

FIGURE 4. *Isomerization of diolefins to acetylenes.*

The scale of ordinates gives the value of the logarithm (to the base 10) of the equilibrium constant for the reaction of isomerization of a given diolefin to a given acetylene hydrocarbon, in the gaseous state. The scale of abscissas gives the temperature in degrees Kelvin. The several curves are for the following reactions in the gaseous state, as indicated: Propadiene=propyne; 1,2-butadiene=1-butyne; 1,2-pentadiene=1-pentyne; 1,3-butadiene=2-butyne; *cis*-1,3-pentadiene=2-pentyne; *trans*-1,3-pentadiene=2-pentyne.

TABLE 19. *Equilibrium concentrations of the six methylstyrenes in the ideal gaseous state to 1,500° K*

Temperature	Composition, in mole fraction, of the mixture of isomers, at equilibrium					
	α-Methylstyrene	cis-β-Methylstyrene	trans-β-Methylstyrene	o-Methylstyrene	m-Methylstyrene	p-Methylstyrene
°K						
298.16	0.414	0.014	0.051	0.046	0.265	0.210
300	.396	.014	.049	.045	.293	.203
400	.329	.027	.062	.064	.319	.199
500	.292	.039	.073	.079	.322	.195
600	.265	.050	.081	.089	.325	.190
700	.247	.059	.086	.097	.325	.186
800	.234	.066	.090	.103	.325	.182
900	.224	.073	.093	.108	.323	.180
1,000	.215	.079	.096	.112	.322	.176
1,100	.208	.083	.100	.115	.320	.174
1,200	.202	.088	.103	.117	.319	.171
1,300	.198	.091	.105	.120	.318	.168
1,400	.192	.093	.110	.120	.319	.166
1,500	.191	.097	.107	.123	.315	.167

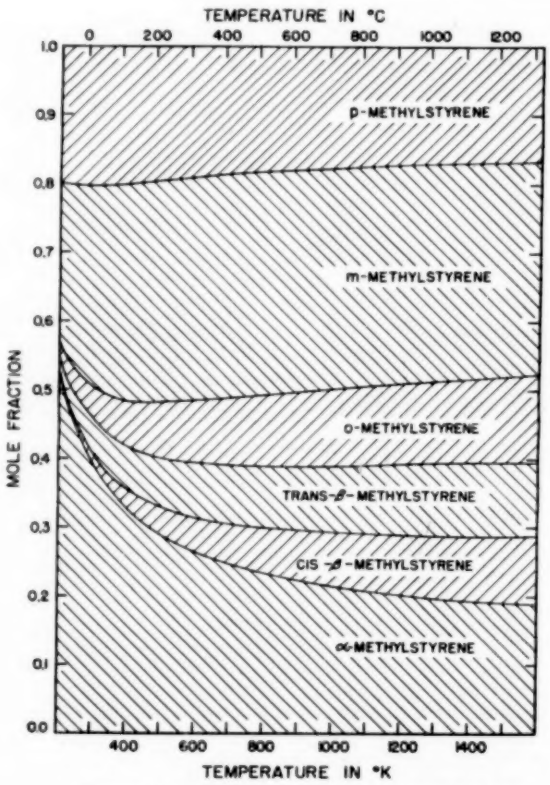

FIGURE 5.—*Equilibrium concentrations of the six methylstyrenes.*

The scale of ordinates measures the amount in mole fraction, and the scale of abscissas gives the temperature in degrees Kelvin and degrees Centigrade. The vertical width of a band at a given temperature measures the mole fraction of the given isomer present at equilibrium with all of its other isomers in the gaseous state.

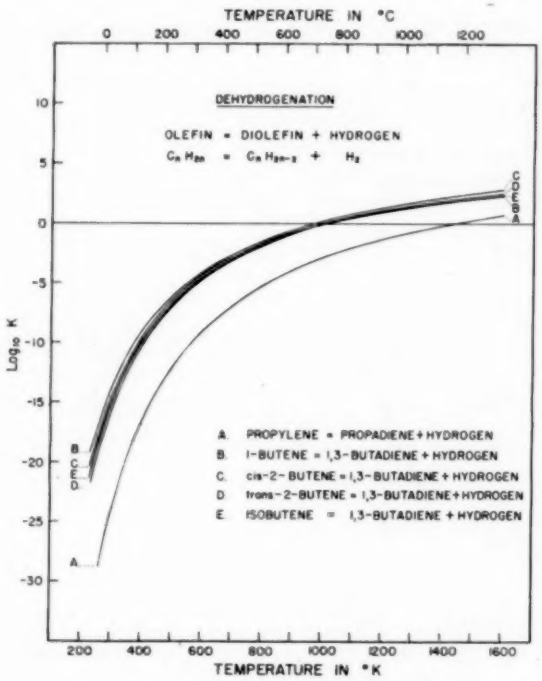

FIGURE 6. *Dehydrogenation of alkylbenzenes to corresponding styrenes.*

The scale of ordinates gives the value of the logarithm (to the base 10) of the equilibrium constant for the reaction of dehydrogenating a given alkylbenzene to a corresponding styrene, in the gaseous state. The scale of abscissas gives the temperature in degrees Kelvin. The several curves refer to the following reactions in the gaseous state: A, Ethylbenzene=styrene+hydrogen; B, isopropylbenzene=α-methylstyrene+hydrogen; C, isopropylbenzene=*cis*-β-methylstyrene+hydrogen; D, isopropylbenzene=*trans*-β-methylstyrene+hydrogen; E, 1-methyl-2-ethylbenzene=*o*-methylstyrene+hydrogen; F, 1-methyl-3-ethylbenzene=*m*-methylstyrene+hydrogen; G, 1-methyl-4-ethylbenzene=*p*-methylstyrene+hydrogen.

In figure 3 are plotted, as a function of temperature, values of the logarithm of the equilibrium constant for the reactions of dehydrogenation of propylene to propadiene and of each of the four butenes to 1,3-butadiene.

In figure 4 are plotted, as a function of temperature, values of the logarithm of the equilibrium constant for the reactions of isomerization of propadiene to propyne, 1,2-butadiene to 1-butyne, 1,2-pentadiene to 1-pentyne, 1,3-butadiene to 2-butyne, *cis*-1,3-pentadiene to 2-pentyne, and *trans*-1,3-pentadiene to 2-pentyne.

In figure 5 are plotted, as a function of temperature, for the six methylstyrenes, the amounts, in mole fraction, of each of the isomers present at equilibrium with the other isomers in the gaseous state. The corresponding numerical values are given in table 19.

In figure 6 are plotted, as a function of temperature, values of the logarithm of the equilibrium constant for the reactions of dehydrogenation of ethylbenzene to styrene, isopropylbenzene to α-methylstyrene, isopropylbenzene to *cis*-β-methylstyrene, isopropylbenzene to *trans*-β-methylstyrene, 1-methyl-2-ethylbenzene to *o*-methylstyrene, 1-methyl-3-ethylbenzene to *m*-methylstyrene, and 1-methyl-4-ethylbenzene to *p*-methylstyrene.

Acknowledgment is gratefully made to William Weltner for assistance in the calculations of the thermodynamic functions of the allene-type C_4 and C_5 diolefins, and also to Helene G. Werner, Rita Braun, and Mary Frances Helm for assistance in other calculations.

VI. References

[1] Selected values of chemical thermodynamic properties (December 31, 1947). National Bureau of Standards.

[2] Selected values of properties of hydrocarbons. Table α. (December 31, 1947). American Petroleum Institute Research Project 44. National Bureau of Standards.

[3] H. W. Thompson and G. P. Harris, Trans. Faraday Soc. **40,** 295 (1944).

[4] J. W. Linnett and W. H. Avery, J. Chem. Phys. **6,** 686 (1938).

[5] G. Herzberg, Infrared and Raman spectra of polyatomic molecules (D. Van Nostrand Co., New York, N. Y., 1945).

[6] E. H. Eyster, J. Chem. Phys. **6,** 580 (1938).

[7] W. S. Gallaway and E. F. Barker, J. Chem. Phys. **10,** 88 (1942).

[8] L. Pauling and L. O. Brockway, J. Am. Chem. Soc. **59,** 1223 (1937).

[9] G. B. Kistiakowsky and W. W. Rice. J. Chem. Phys. **8,** 610 (1940).

[10] G. B. Kistiakowsky, J. P. Lacher, and W. W. Ransom J. Chem. Phys. **8,** 970 (1940).

[11] D. A. Frank-Kamenetskii and V. G. Markovich, Acta Physicochim. USSR **17,** 308 (1942).

[12] D. A. Frank-Kamenetskii and V. G. Markovich, J. Gen. Chem. USSR **12,** 619 (1942).

[13] G. J. Szasz, J. S. McCartney, and D. H. Rank, J. Am. Chem. Soc. **69,** 3150 (1947).

[14] J. G. Aston and G. J. Szasz. J. Am. Chem. Soc. **69,** 3108 (1947).

[15] K. S. Pitzer and D. W. Scott. J. Am. Chem. Soc. **65,** 803 (1943).

[16] J. G. Aston, G. J. Szasz, H. W. Wooley, and F. G. Brickwedde, J. Chem. Phys. **14,** 67 (1946).

[17] C. W. Beckett, K. S. Pitzer, and R. Spitzer, J. Am. Chem. Soc. **69,** 248 (1947).

[18] K. S. Pitzer. Ind. Eng. Chem. **36,** 829 (1944).

[19] J. E. Kilpatrick and K. S. Pitzer, J. Research NBS **37,** 163 (1946).

[20] W. J. Taylor, D. D. Wagman, M. G. Williams, K. S. Pitzer, and F. D. Rossini, J. Research NBS **37,** 95 (1946).

[21] J. E. Kilpatrick, H. G. Werner, C. W. Beckett, K. S. Pitzer, and F. D. Rossini, J. Research NBS **39,** 523 (1947).

[22] S. S. Todd, G. D. Oliver, and H. M. Huffman, J. Am. Chem. Soc. **69,** 1519 (1947).

[23] H. M. Huffman and D. W. Scott, U. S. Bureau of Mines, Bartlesville, Okla. Private communication.

[24] N. P. Bekkedahl and L. A. Wood, J. Research NBS **19,** 55 (1937).

[25] American Petroleum Institute Research Project 44. National Bureau of Standards. Unpublished.

[26] C. W. Beckett and K. S. Pitzer, J. Am. Chem. Soc. **68,** 2213 (1946).

[27] E. J. Prosen and F. D. Rossini, J. Research NBS **34,** 59 (1945).

[28] E. J. Prosen, F. W. Maron, and F. D. Rossini, National Bureau of Standards. Unpublished.

[29] E. J. Prosen and F. D. Rossini, J. Research NBS **34,** 255 (1945).

822521—49—— 3

[30] E. J. Prosen and F. D. Rossini. J. Research NBS **36,** 269 (1946).
[31] E. J. Prosen, W. H. Johnson, and F. D. Rossini, J. Research NBS **36,** 455 (1946), RP1714.
[32] E. J. Prosen, W. H. Johnson, and F. D. Rossini, J. Research NBS **37,** 51 (1946), RP1728.
[33] E. J. Prosen and F. D. Rossini, National Bureau of Standards. Unpublished.
[34] W. H. Johnson, E. J. Prosen, and F. D. Rossini, National Bureau of Standards. Unpublished.
[35] D. D. Wagman, J. E. Kilpatrick, W. J. Taylor, K. S. Pitzer, and F. D. Rossini, J. Research NBS **34,** 143 (1945) RP1634.
[36] G. B. Kistiakowsky, J. R. Ruhoff, H. A. Smith, and W. E. Vaughan, J. Am. Chem. Soc. **58,** 146 (1936).
[37] M. A. Dolliver, T. L. Gresham, G. B. Kistiakowsky, and W. E. Vaughan, J. Am. Chem. Soc. **59,** 831 (1937).

WASHINGTON, October 29, 1948.

U. S. Department of Commerce
National Bureau of Standards

Research Paper RP1965
Volume 42, March 1949

Part of the Journal of Research of the National Bureau of Standards

Accurate Determination of the Deadtime and Recovery Characteristics of Geiger-Müller Counters

By Louis Costrell

A brief description of the theory of operation of Geiger-Müller counters is presented, with special emphasis on the deadtime and recovery characteristics. An electronic gating instrument is described that has been developed for the determination of deadtime and recovery characteristics to an accuracy of 1 percent or 2 microseconds. Experimental data are presented showing variation of deadtime and recovery time with counter pressure and overvoltage.

I. Introduction

Geiger-Müller counters are extensively used in the measurement of radiation from atomic nuclei. A knowledge of their characteristics is, therefore, essential in interpreting the data obtained. The deadtime and the recovery characteristics of Geiger counters are of interest not only because they are important factors in determining the errors that occur, but also because they are intimately associated with the discharge mechanism. An electronic instrument has been designed and constructed for the accurate determination of the deadtime and recovery characteristics of Geiger counters. The pulses initiate "gates" that can be set to predetermined durations so as to permit registering of pulses that follow the initiating pulses within the time that the gate is open. A few instruments,[1,2,3,4] quite different in design, though somewhat similar in function, have been developed for determination of spurious pulses and resolving time. The instrument described herein uses no relays or gas tubes, hard vacuum tubes being used exclusively. The instrument has been designed specifically for the determination of the deadtime and recovery characteristics of Geiger counters and has high accuracy when used for this purpose. An accuracy of 1 percent or 2 microseconds (whichever gives the larger error) is obtained.

II. Deadtime, Recovery Time, and Resolving Time

When an ionizing event occurs in a Geiger-Müller counter, the negative electrons are attracted to the positive wire. Since the electric field in the vicinity of the wire is extremely high, the electrons released in the initial ionization acquire sufficient velocity to release additional electrons from neutral atoms that lie in their paths. The electrons so released dislodge additional electrons as they travel toward the wire. This cumulative ionization is known as a Townsend avalanche. The electrons that reach the wire contribute a negative electric charge to the wire. This charge is responsible for the negative voltage pulses obtained from the counter.

The electrons, being light and therefore highly mobile, reach the wire within a fraction of a microsecond after the ionization has occurred. The positive ions proceed at the same time toward the negative cylinder. However, being

[1] R. L. Driscoll, M. W. Hodge, and A. E. Ruark, Rev. Sci. Inst. **11**, 241 (1940). The instrument described is suitable only for intervals greater than 0.1 sec.

[2] Arthur Roberts, Rev. Sci. Inst. **12**, 71 (1941). The instrument described has a range of 10^{-4} to 0.3 sec. It utilizes gas tubes preceding a pulse lengthener and a Rossi coincidence circuit. Counter characteristics and resolving time have been investigated with this instrument. Counters giving even a small percentage of multiple pulses are apparently readily detected.

[3] F. L. Davis and L. F. Curtiss, J. Research NBS **29**, 405 (1942) RP1509. The instrument described has a range of 3×10^{-5} to 0.2 sec. and is used primarily for testing for multiple pulses in alcohol-argon counters. The data obtained permit determination of the resolving time.

[4] S. C. Curran and E. R. Rae, Rev. Sci. Instr. **18**, 871 (1947). The instrument described is a modification of the Roberts instrument. A variable time delay is included that permits accurate determination of the number of spurious counts that occur.

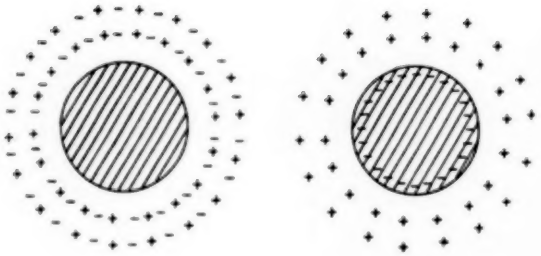

FIGURE 1. *Sheath of electrons and positive ions about positive wire of Geiger counter.*

a, Immediately after avalanche; b, a fraction of a microsecond later.

heavy particles, they proceed at a slow rate compared to the fast-moving electrons. In addition, they have a further handicap in that they have a considerably longer distance to travel than do the electrons. This is the case since practically all of the secondary electrons are produced in the high field region very close to the wire. Figure 1, a, shows a simplified version of the region very close to the wire immediately after the avalanche has occurred. A fraction of a microsecond later the electrons have reached the wire, whereas the positive ions are still stranded about the wire, as shown in figure 1, b. This sheath of positive ions forms a shield about the wire, thus reducing the field intensity to less than the value necessary for Geiger action. A particle entering the counter at this time is thus unable to produce an avalanche. This sheath of positive ions moves slowly outward, finally traveling far enough from the wire so that the electric field about the wire increases to a value sufficient to permit Geiger action to resume.[5] However, since the positive ion sheath is still unneutralized within the counter, its shielding effect does not permit the normal electric field intensity to exist about the wire. Therefore, pulses of reduced size will result from particles entering the counter very shortly after the positive ions have moved an amount sufficient to permit the resumption of Geiger action. As the ions move toward the cylinder, the electric field intensity near the wire increases, finally reaching its full value when the ions have reached the cylinder. Thus, full size pulses cannot occur until the positive ions have reached the cylinder. The action of polyatomic gas molecules in quenching the discharge also plays an important part in the counter operation, though this action will not be discussed here.

Physically, the deadtime is the time required for the positive ions to travel far enough from the wire to permit the resumption of Geiger action, and the recovery time is the time required for the positive ions to reach the counter wall. Functionally, the deadtime and recovery time can be defined as follows:

Deadtime: The time interval after a pulse has occurred during which the counter is insensitive to further ionizing events.

Recovery time: The time interval that must elapse after a pulse has occurred before a full-size pulse can again occur.

Since a pulse of finite size is required to operate a detecting circuit, the resolving time of the counter and its accessories (amplifying and scaling circuits, etc.) exceeds the deadtime of the counter.

The resolving time can be defined as follows:

Resolving time: [6] The minimum time interval by which two pulses must be separated to be detected as separate pulses by the counter and its accessories.

Stever [7] has described a method for determining the deadtime and recovery characteristics of Geiger counters by means of a cathode ray oscilloscope. The accuracy is adequate for most purposes. For best results a time exposure photograph should be taken of the oscilloscope screen pattern, though the deadtime and the recovery curve can be observed visually, especially if a high counting rate and persistent screen are used. This method will be described as it gives an excellent picture of the deadtime and recovery phenomena. The pulses from the counter are applied to the *Y*-axis amplifier of the oscilloscope and also made to trigger the sweeps. (Some oscilloscopes, such as the DuMont type 248, have driven sweep circuits that can be triggered externally and are well suited for this purpose. The 1,000-microsecond sweep on the DuMont type 248 oscilloscope gives good results.) Consider counter pulses applied to an oscilloscope in this manner

[5] The theory of the action of the positive ion sheath in this manner is due to C. G. and D. D. Montgomery, J. Franklin Inst. **231**, 509 (1941).

[6] Resolving time has been a loosely used term, frequently being applied to a counter. Actually, the resolving time is a function of the input sensitivity of the scaler, as well as of the deadtime and recovery characteristic of the counter.

[7] H. G. Stever, Phys. Rev. **61**, 38 (1942).

with a sweep of 1,000-microseconds duration. If the counting rate is 100 counts per second, the average spacing between pulses will be 10,000 microseconds. Thus, after a sweep has been initiated by a pulse, there is a probability of approximately one out of 10 that another pulse will appear on the screen. Such a pulse is shown as pulse P1 in figure 2, a. During some other sweep a pulse, P2, as shown in figure 2, b, will appear. On still another sweep, a pulse P3 of figure 2, c, will appear on the screen. If a time exposure photograph is taken of the screen, random pulses appearing at various instances will be recorded on the film, giving the pattern shown in figure 2, d. The deadtime, recovery time, and resolving time are indicated in figure 2, d.

III. Resolving Time Errors

Since nuclear disintegrations occur in a random manner, there is a finite probability of two disintegrations occurring within any given time interval. Since the counter is dead for a short period after a pulse has occurred, some of the disintegrations will not be detected. This will introduce a discrepancy between the number of particles entering the counter and the number of counts recorded. The resulting error can be calculated as follows:

The counter is insensitive for a time, t_r, after each pulse, where t_r is the resolving time of the counter in seconds. On the average, the counter is sensitive for a period $(1/a-t_r)$ after each pulse, where a represents the true number of particles detected per second. For values of $t_r<<1/a$, the sensitive time is, therefore, approximately $1/a$. Therefore,

$$\frac{\text{insensitive time}}{\text{sensitive time}}=\frac{t_r}{1/a}=at_r.$$

For values of $at_r<<1/a$, n (the observed number of particles detected per second) is approximately equal to a. Therefore,

$$\text{Percentage error}=100nt_r. \qquad (1)$$

It is readily seen that a counting rate of 100 counts per second, using a counter with a resolving time of 300 microseconds, will result in a resolving time error of 3 percent, whereas the same counting rate with a counter with a 1,000-microsecond resolving time will result in a resolving time error of approximately 10 percent. If the counter is calibrated against a source of the same intensity as the test sample, the resolving time error will be automatically compensated for. However, this is not the case when the calibrating standard and the test sample vary appreciably in intensity. Corrections can, however, be made for the resolving time error by the use of eq 1.

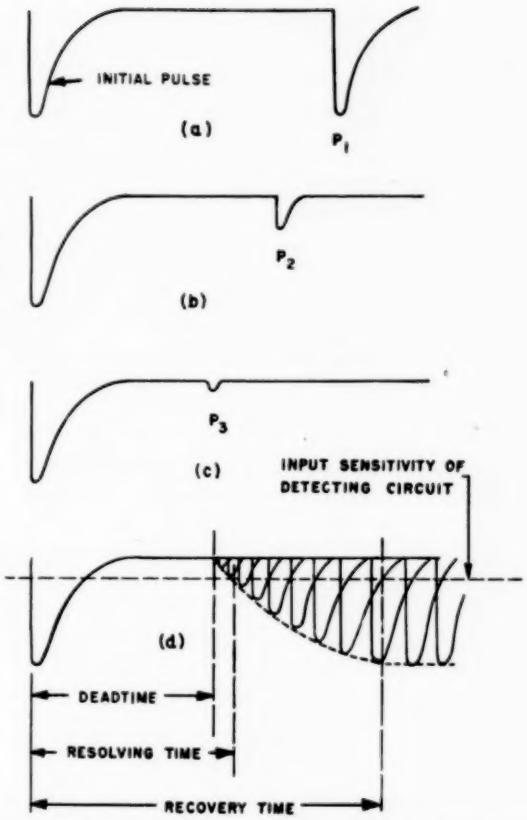

FIGURE 2. *Deadtime, recovery time, and resolving time.* P1, P2, and P3 are random pulses.

IV. Statistical Analysis

Determination of the deadtime and recovery characteristics of Geiger counters by consideration of the number of pulses falling within given time intervals necessitates analysis of the statistical behavior of random events. Let

N=Accepted counts per second (particles detected per second that occur within given time intervals after preceding detected particles).

a=True particles detected per second.

n=Observed particles detected per second (true particles detected per second minus coincidence loss).

t=time in seconds.

t_d=deadtime in seconds.

t_g=gating time in seconds.

t_{80}, t_{50}, t_{20}, etc.=time in seconds to recover to 80, 50, 20 percent, etc.

The instrument described later accepts only pulses occurring between the end of the deadtime and the end of the gating period. The instrument is thus sensitive only during the time interval (t_g-t_d). The probability that no countable particle will appear during this time interval is $e^{-a(t_g-t_d)}$. For values of $a(t_g-t_d)$ much less than unity, the average number of counts per second that will occur in the time interval (t_g-t_d) is given by eq 2.

$$N=a[1-e^{-a(t_g-t_d)}]. \quad (2)$$

Figure 3 is a plot of eq 2. The time-axis intercept of the curve gives the deadtime.

Equation 2 can be simplified as follows:
Expanding eq 2

$$N=a[1-1+a(t_g-t_d)-\frac{a^2(t_g-t_d)^2}{2!}+\ldots]$$

Ignoring terms higher than first order,

$$N=a^2(t_g-t_d).$$

Since n is approximately equal to a,

$$N=n^2(t_g-t_d). \quad (3)$$

Rearranging,

$$t_d=t_g-\frac{N}{n^2} \quad (4)$$

Best results are obtained by determining a few points on the straight-line portion of the curve of figure 3 and extrapolating the curve to give the deadtime. If only pulses above a certain size are accepted by the instrument, a curve similar to figure 3, but displaced somewhat to the right, will

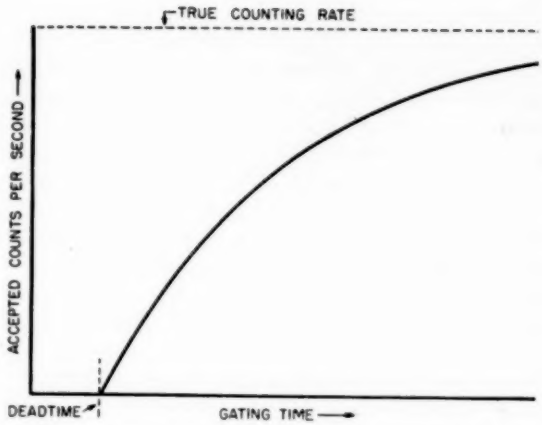

FIGURE 3. *Accepted counts per second versus gating time.*

be obtained. The time axis intercepts of each of these curves represents the time for recovery to the minimum pulse size accepted. Figure 4 shows such curves for various minimum pulse sizes. The data from figure 4 can be replotted to give the complete recovery curve of the counter, as shown in figure 5.

V. Description of Instrument

The instrument developed for the determination of the deadtime and recovery characteristics of Geiger counters is shown in block form in figure 6. Figure 7 is a schematic diagram of the circuit.

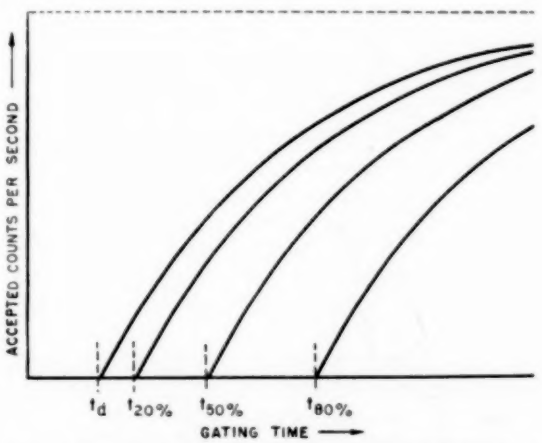

FIGURE 4. *Accepted counts per second versus gating time for various degrees of recovery.*

t_d, Deadtime; $t_{20\%}$, time to recover to 20 percent; $t_{50\%}$, time to recover to 50 percent; $t_{80\%}$, time to recover to 80 percent.

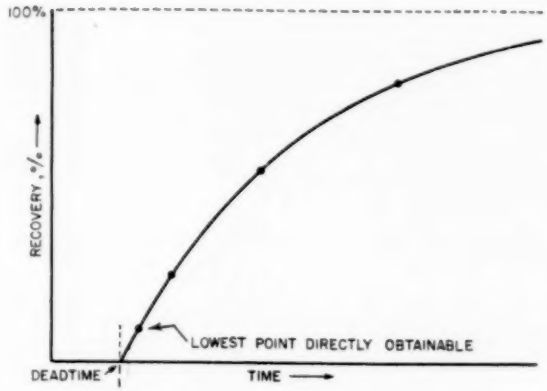

FIGURE 5. *Recovery curve of Geiger counter.*

The random pulses from the Geiger counter are fed into a pulse amplifier, then into a pulse height selector, then through pulse shaping circuits to give sharp negative pulses of uniform height. These sharp negative pulses then follow two paths; one by the way of an amplifier stage to a heavily biased amplifier, the output of which connects to the input of a conventional scaler, and the other through a 15-microsecond delay circuit to a "one-shot" gating multivibrator. Figure 8 is a schematic diagram of the delay circuit and gating multivibrator. The gating multivibrator controls the bias on the biased amplifier so as to permit pulses that follow other pulses by less than the gating time to go through the biased amplifier and actuate the scaling and recording circuits.

The gate is delayed 15 microseconds with respect to the initiating pulse, so that the pulse initiating the gate will be completed before the gate opens. Thus a pulse cannot pass through the gate that it initiates, though succeeding pulses that follow within the gating time are accepted. In the pulse height selector stage the bias is varied so as to discriminate against pulses of less than a given height. This permits determination of the recovery curve of the counter. A simple visual pulse-size indicator, as shown in figure 9, is incorporated in the instrument to permit ready adjustment of the input potentiometer.

The counter pulses are applied through potentiometers R_2 and R_3 (fig. 7) to the control grid of tube T1 which is a conventional class A resistance coupled amplifier. The output of this stage is then applied to the pulse size indicator and to the control grid of the pulse height selector. The pulse height selector, tube T2, is a sharp cut-off amplifier in which the control grid bias is adjusted by means of potentiometer R_9 to obtain the desired pulse size discrimination. (A biased diode would also be satisfactory for this application.) This permits determination of the recovery curve, as shown in figure 5. The bias voltage is indicated on the voltmeter shown in the grid circuit of tube T2. The output pulses of the pulse height selector vary considerably in size. The pulses are, therefore, amplified by tube T3a and T3b, and then clipped by tube T4a so that the pulses at the clipper output are of uni-

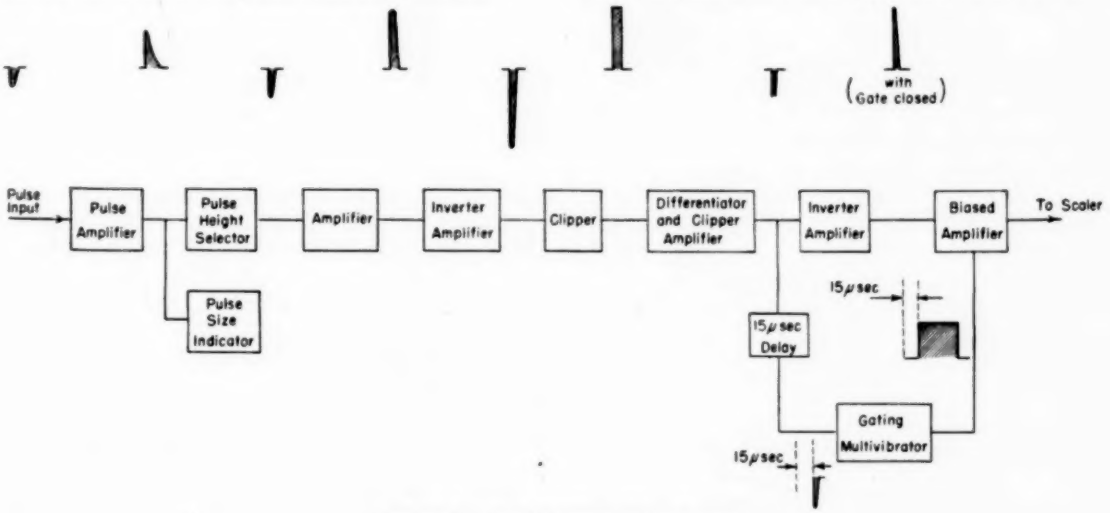

FIGURE 6.—*Block diagram of instrument.*

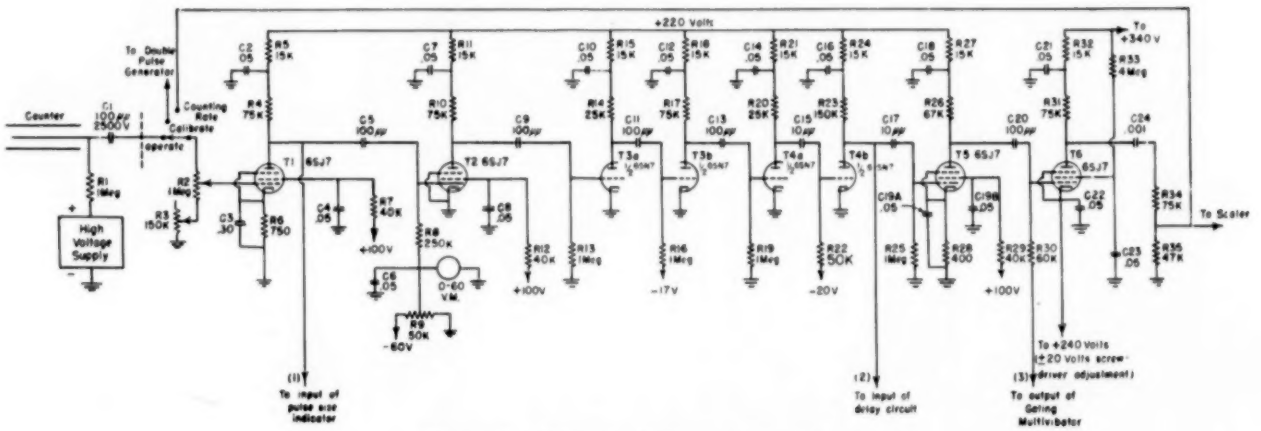

FIGURE 7. *Schematic diagram of instrument.*

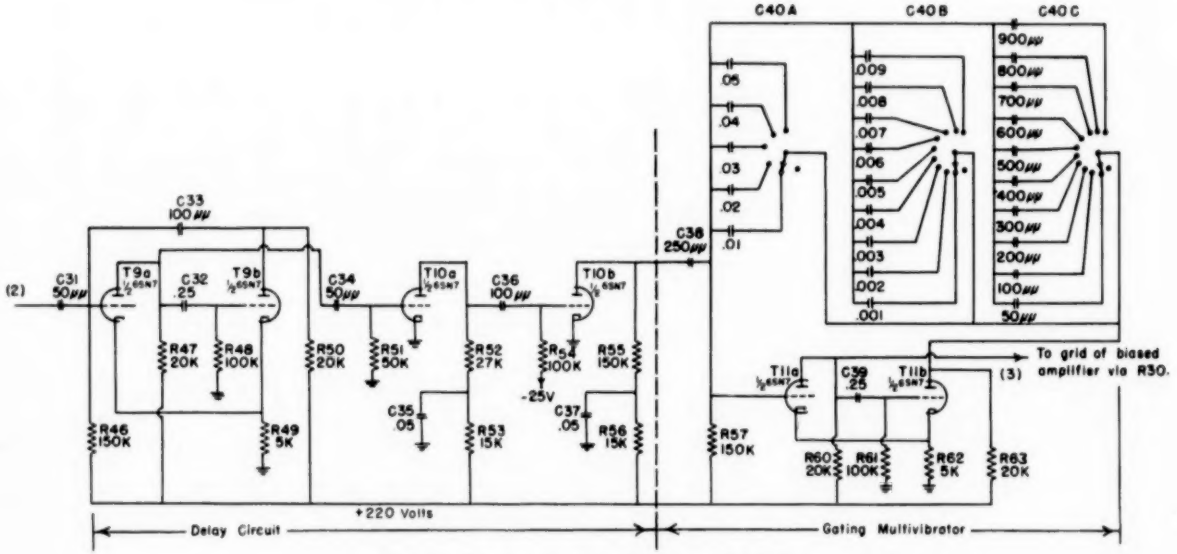

FIGURE 8. *Delay circuit and gating multivibrator.*

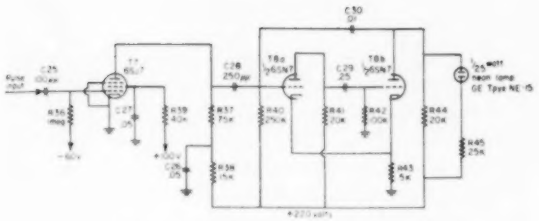

FIGURE 9. *Pulse size indicator.*

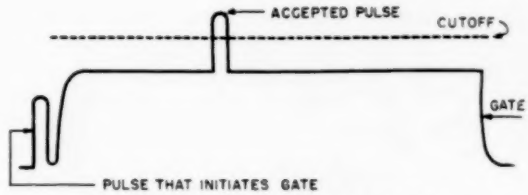

FIGURE 10. *Voltage on grid of biased amplifier.*

form height. The positive output pulses of the clipper are differentiated by the RC network in the grid circuit of tube T4b. The trailing edge pulse is clipped by means of the grid bias, whereas the leading edge is retained. The sharp negative pulses at the output of *T4b* trigger the delay circuit, that in turn triggers the gating multivibrator. The pulses from *T4b* are also inverted and amplified by T5 to produce large positive output pulses for application to the biased amplifier T6.

The biased amplifier, T6, has a high negative bias so as to block the positive pulses from T5. Since the control grid of T6 is connected to the plate of the normally conducting half of the gating multivibrator, it is at a positive potential of approximately 80 v with respect to ground. Therefore, the negative bias of approximately 120 v is obtained by maintaining the cathode at approximately 200 v positive. When the gating multivibrator "opens the gate", the bias is reduced sufficiently to permit the acceptance of the positive pulses from the output of T5, as shown in figure 10. The pulses at the output of the biased amplifier T6 are then applied to the scaling circuit, where they register as accepted counts.

The negative pulses at the output of T4b trigger the one-shot multivibrator, tube T9a and T9b of figure 8, producing rectangular pulses of approximately 15-microseconds duration. These rectangular pulses are differentiated, amplified, and then clipped. The pulse resulting from the leading edge of the 15-microsecond pulse is eliminated in the clipping operation, while the trailing edge pulse is retained. The pulse retained is thus delayed approximately 15 microseconds with respect to the initiating pulse and is used to trigger the gating multivibrator.[8]

[8] It is planned to replace the 15-microsecond delay circuit by a variable time delay circuit in order to increase the versatility of the instrument.

The gating multivibrator, tube T11a and T11b of figure 8, is a one-shot multivibrator with a plateau adjustable between approximately 30- and approximately 5,000-microsecond duration. T11a is normally conducting. It is rendered nonconducting by a negative pulse and remains nonconducting for a time determined by the values of capacitors C40 and resistor R57. When T11a becomes nonconducting, its plate voltage rises and assumes the value of the supply voltage. Thus, a rectangular positive pulse appears at the output of the gating multivibrator, when triggered. This rectangular pulse is applied to the grid of the biased amplifier T6, opening the gate by decreasing the bias to such a value that pulses from T5 that occur while the gate is open, are accepted by the biased amplifier and, therefore, actuate the scaling circuit. It will be noted from figure 10 that the gate begins approximately 15 microseconds after the initiating pulse, so that a pulse cannot pass through the gate that it initiates. Since the 15 microseconds is considerably shorter than the deadtime of Geiger counters of the types now in general use, none of the pulses that should register are blocked because of the delay.

The pulse size, indicator, figure 9, consists simply of a biased amplifier and a one-shot multivibrator with a neon lamp across the load resistor of the normally nonconducting triode. When the input pulses are of sufficient amplitude to overcome the bias on the biased amplifier T7 and trigger the multivibrator T8a and T8b, the voltage across the load resistor R44 rises to approximately 100 v for approximately 2,500 microseconds. Since the neon lamp starts conducting at approximately 70 v, this causes the lamp to conduct. The lamp is essentially a constant-voltage device, maintaining a voltage of approximately 65 v while conducting. Thus, the voltage across the 25K resistor is approximately 35 v and the current through the lamp and the resistor approximately 1.4 mils. This current is drawn for approxi-

822521—49——4

mately 2,500 microseconds for each pulse, producing bright flashes. With counting rates of the order generally used (approximately 100 pulses per second) the flashes appear so frequently that the lamp appears to be on continuously when flashing. The bias of T7 is permanently adjusted so that the lamp will begin to flicker when the input pulses are of the proper size. A biased diode would also be satisfactory for this application, in lieu of the pentode used for T7.

Any accurate double pulse generator can be used to calibrate the instrument. Conventional double pulse generators utilize blocking oscillators or one-shot multivibrators. Actually, a double pulse generator utilizing a shock-excited oscillator was used. The shock-excited oscillator is sharply attenuated by means of resistance across the tuned circuit. The oscillations are then clipped to eliminate all but two half cycles, and these two are shaped to give the double pulses desired. The spacing between the two pulses comprising a pair is determined primarily by the constants in the cathode circuit of the shock-excited oscillator. The repetition frequency is the repetition frequency of the square wave generator that controls the shock-excited oscillator.

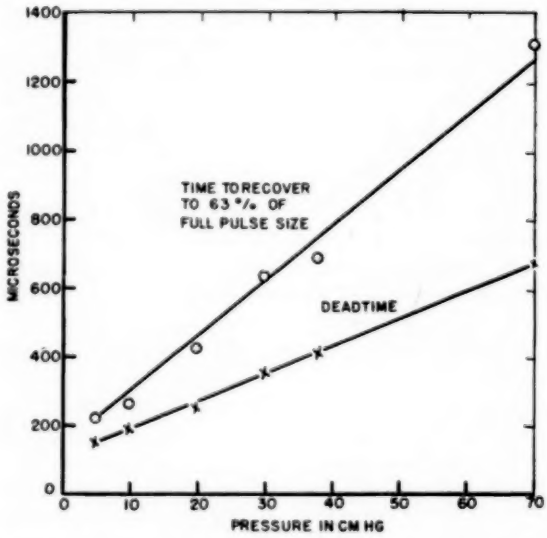

FIGURE 11. *Variation of deadtime and recovery time of mica window argon-alcohol counters with variation in total pressure.*

Counters filled with alcohol at pressure of 12 mm (hg) and remainder argon. Overvoltage=75±5v.

VI. Typical Data

The instrument is currently being used in the routine determination of the deadtime and recovery characteristics of Geiger counters.

Investigations have been made of the influence of pressure and overvoltage on deadtime and recovery time. The counters tested were of the mica window type and contained argon, to which had been added alcohol at a pressure of 12 mm of mercury. The results of these investigations are shown in figures 11 and 12. It will be noted that the curves of deadtime and recovery time versus pressure are essentially straight lines. It will also be noted that the deadtime and recovery time both decrease with over-voltage. Figure 12 includes a curve of resolving time versus overvoltage for which it is assumed that the detecting circuit responds only to pulses larger than 30

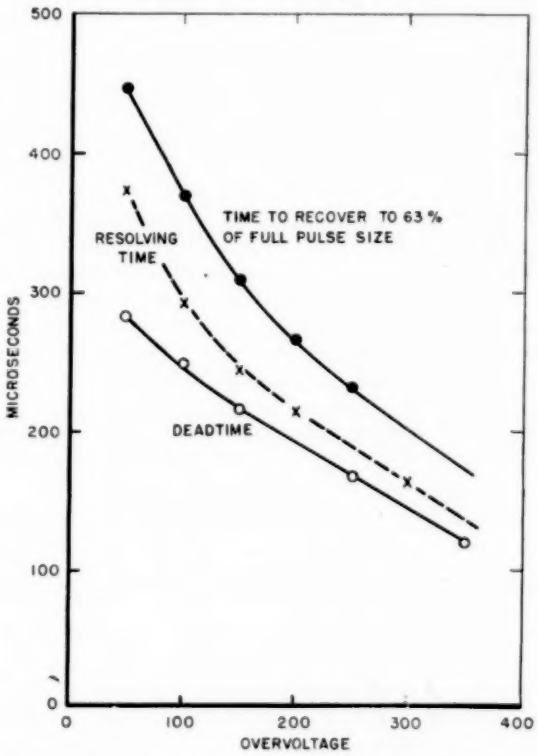

FIGURE 12. *Variation of deadtime, resolving time, and recovery time of typical mica window argon-alcohol counter (20-cm pressure) with variation in overvoltage.*

For the resolving-time curve, it is assumed that the detecting circuit responds only to pulses greater than 30 percent of the full pulse size obtained at an overvoltage of 100 v.

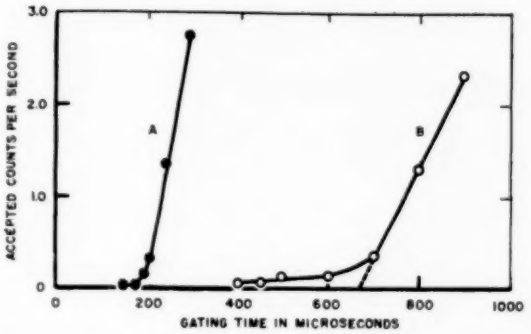

FIGURE 13. *Accepted counting rate versus gating time of two mica-window argon-alcohol counters, identical except for gas content.*

Counters filled with alcohol at a pressure of 12 mm (hg) and remainder argon. Curve A is for counter with 10-cm pressure, curve B for counter with 70-cm pressure.

percent of the normal pulse size. Since the pulse size increases with voltage, the resolving time decreases with over-voltage at a greater rate than do the deadtime and the recovery time.

Figure 13 shows curves of accepted counts per second versus gating time for two mica-window counters identical except for gas content. Curve A is for a counter with 10-cm (Hg) total pressure, whereas curve B is for a counter with 70-cm (Hg) total pressure. Since each of the counters contained alcohol at a pressure of 12-mm (Hg), the high-pressure counter (curve B) had an abnormally low percentage of alcohol. It will be noted that curve B has a pronounced "tail," whereas that of curve A is negligible. The tail is due to the fact that, after a pulse occurs, the efficiency of a counter increases gradually from zero to its full value, as reported by Curran and Rae (see footnote 4). Because of the approximately straight-line

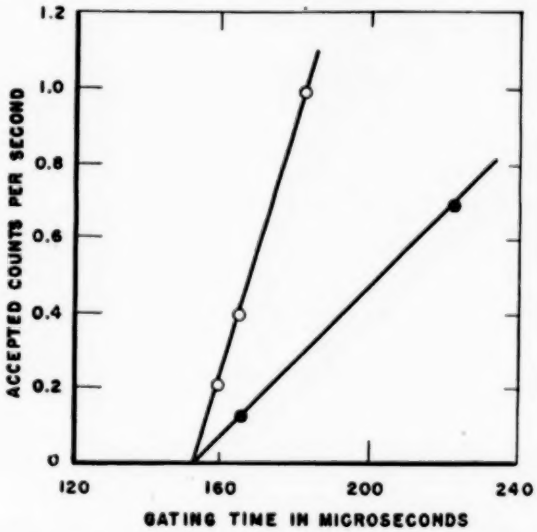

FIGURE 14. *Accepted counts per second versus gating time for 5-percent recovery taken on a single counter at two different counting rates.*

rise of efficiency, extrapolation of the straight-line portion of the curves, such as shown in figure 13, gives the same deadtime as is represented by the point at which the counter efficiency reaches half its full value.

Figure 14 shows curves of accepted counts per second versus gating time taken on a single counter at two different counting rates. The time axis intercepts give the 5-percent recovery time. Both curves give a 5-percent recovery time of 153 microseconds. This is indicative of the reproducibility obtained with the instrument.

WASHINGTON, JULY 9, 1948

U. S. Department of Commerce
National Bureau of Standards

Research Paper RP1966
Volume 42, March 1949

Journal of Research of the National Bureau of Standards

Heats of Combustion and Isomerization of the Six C_7H_{14} Alkylcyclopentanes

By Walter H. Johnson, Edward J. Prosen, and Frederick D. Rossini

The heats of isomerization of the six C_7H_{14} alkylcyclopentanes were determined by measurement of the ratios of the heats of combustion of purified samples of these compounds in the liquid state by the procedure previously described for other isomeric hydrocarbons. The data yield the following values for the heat of isomerization, $\Delta H°$, in the liquid state at 25° C, of ethylcyclopentane into each of the dimethylcyclopentanes, in kilocalories per mole: Ethylcyclopentane, 0.00; 1,1-dimethylcyclopentane, -2.06 ± 0.12; *cis*-1,2-dimethylcyclopentane, -0.44 ± 0.20; *trans*-1,2-dimethylcyclopentane, -1.86 ± 0.16; *cis*-1,3-dimethylcyclopentane, -1.11 ± 0.24; *trans*-1,3-dimethylcyclopentane, -1.60 ± 0.14. These values were combined with values for the differences in the heats of vaporization of these isomers to obtain values for the heats of isomerization in the gaseous state at 25° C.

Utilizing the values previously reported for the heats of combustion and formation of ethylcyclopentane in the liquid and gaseous states at 25° C, values were calculated for the heats of combustion and formation of the five dimethylcyclopentanes in the liquid and gaseous states at 25° C.

I. Introduction

In continuation of the program of determining the heats of combustion, formation, and isomerization of hydrocarbons of various types [1],[1] calorimetric measurements have been made that yield values for the differences in the heats of combustion, or the heats of isomerization, of the six C_7H_{14} alkylcyclopentanes in the liquid state at 25° C. These values of heats of isomerization were combined with values [2] for the differences in the heats of vaporization of these isomers at 25° C to obtain values for the heats of isomerization in the gaseous state at 25° C. Utilizing the values previously reported [3] for the heats of combustion and formation of ethylcyclopentane in the liquid and gaseous states at 25° C, corresponding values were calculated for the five dimethylcyclopentanes.

[1] Figures in brackets indicate the literature references at the end of this paper.

II. Unit of Energy, Molecular Weights, Uncertainties

The unit of energy upon which values reported in this paper are based is the absolute joule, derived from mean solar seconds and absolute ohms and volts, in terms of which certification of standard resistors and cells is made by this Bureau. For conversion to the conventional thermochemical calorie, the following relation is used [4, 5]:

1 calorie = 4.1840 absolute joules.

The molecular weight of carbon dioxide, the mass of which was used to determine the amount of reaction, was taken as 44.010, from the 1947 table of international atomic weights [6].

The uncertainties assigned to the various quantities dealt with in this paper were derived, where possible, by a method previously described [7].

Definitions of the symbols used are given in previous papers [1, 8].

III. Method and Apparatus

The same method and apparatus were used as in the investigations recently reported from this laboratory [1]. One calorimetric system, resistance bridge (No. 404), and platinum resistance thermometer (No. 373,730) were used for all the experiments reported here.

No products associated with incomplete combustion were found in any of the experiments.

IV. Materials

The compounds used in the present investigation were samples from the API–NBS series of highly purified hydrocarbons, which are being prepared through a cooperative undertaking of the American Petroleum Institute and the National Bureau of Standards.

These samples of API–NBS hydrocarbons have been made available by the American Petroleum Institute and the National Bureau of Standards through the API Research Project 44 on the "Collection, analysis, calculation, and compilation of data on the properties of hydrocarbons." The samples were purified at the National Bureau of Standards by the API Research Project 6 on the "Analysis, purification, and properties of hydrocarbons," from material supplied by the following laboratories:

Ethylcyclopentane (A), *cis*-1,3-dimethylcyclopentane, and *trans*-1,3-dimethylcyclopentane (A) by the American Petroleum Institute Research Project 45 at the Ohio State University, Columbus, Ohio, under the supervision of C. E. Boord.

1,1-Dimethylcyclopentane, *cis*-1,2-dimethylcyclopentane, and *trans*-1,2-dimethylcyclopentane by Hydrocarbon Laboratory at the Pennsylvania State College, State College, Pa.

A complete description of the purification, purity, and freezing points of the six API-NBS hydrocarbons used in the present investigation is given in references [9, 10, 11], which reported the amounts of impurity in these samples, as determined from measurements of freezing points, to be as follows in mole fraction: Ethylcyclopentane (A), 0.0008 $\pm$0.0004; 1,1-dimethylcyclopentane, 0.0003 $\pm$0.0002; *cis*-1,2-dimethylcyclopentane, 0.00025 $\pm$0.00016; *trans*-1,2-dimethylcyclopentane, 0.0013 $\pm$0.0010; *cis*-1,3-dimethylcyclopentane, 0.0041 $\pm$0.0023; *trans*-1,3-dimethylcyclopentane (A) 0.0035 $\pm$0.0009.

As the manner of purification [9, 10, 11] was such as to leave substantially only close-boiling isomeric impurities in the respective compounds, it is calculated that in the extreme case the measured heat of combustion would be affected by less than 0.001 percent because of impurities.

The samples of *trans*-1,2-dimethylcyclopentane and *trans*-1,3-dimethylcyclopentane are the *racemic* mixtures of the *dextro* and *levo* forms. With regard to energy content, the *dextro* and *levo* forms are identical, and any difference between these and the *racemic* mixture would be insignificant.

V. Results

The experimental results of the present investigation are summarized in table 1, which gives for each of the six compounds the following data: The number of experiments performed; the minimum and maximum values of the mass of carbon dioxide formed in the combustion and of the calorimetric quantities, ΔR_c, Δr_t, and Δr_n [8]; the mean value of B, and its standard deviation, in ohms per gram of carbon dioxide formed, as defined by eq 4 of reference [8]. The symbols have the same significance as in reference [1].

In table 2 are given, for the six C_7H_{14} alkylcyclopentanes, values of the following: The constant B, in ohms per gram of carbon dioxide, as given in table 1; $B°$, which is the value of B corrected to the ideal bomb reaction by the method of Washburn [12] [2]; $B_i°/B_n°$, which is equal to the ratio of the heat evolved, per mole of hydrocarbon, in the ideal bomb process at 28° C for each isomer to that of ethylcyclopentane; and $(-\Delta U°)_n-(-\Delta U°)_i$, the difference, between ethylcyclopentane and each isomer, in the heat of combustion in the ideal bomb process at 28° C.

[2] The Washburn correction is the same for all these compounds as they are isomers, but account is taken of the variation of the correction with the amount of sample burned. As used here, the Washburn correction was modified to apply to 28° C (the temperature to which the measured heat of combustion is referred) and to the gases at zero pressure (instead of 1 atmosphere).

TABLE 1. *Results of the calorimetric combustion experiments*

Compound	Number of experiments	Mass of carbon dioxide formed	ΔR_f	Δr_i	Δr_n	B	
						Mean	Standard deviation of mean
		g	*Ohm*	*Ohm*	*Ohm*	*Ohm/g* CO_2	*Ohm/g* CO_2
Ethylcyclopentane	7	2.69117 to 2.86858	0.293466 to 0.312878	0.000254 to 0.000263	0.000004 to 0.000005	0.1089810	±0.0000055
1,1-Dimethylcyclopentane	5	2.61833 to 2.82697	0.285029 to 0.307731	0.000253 to 0.000262	0.000003 to 0.000003	.1087759	±.0000032
cis-1,2-Dimethylcyclopentane	7	2.76937 to 2.87510	0.301970 to 0.313576	0.000240 to 0.000259	0.000056 to 0.000066	.1089371	±.0000085
trans-1,2-Dimethylcyclopentane	7	2.68335 to 2.86133	0.292203 to 0.311521	0.000253 to 0.000263	0.000006 to 0.000065	.1087961	±.0000058
cis-1,3-Dimethylcyclopentane	5	2.46454 to 2.69782	0.268433 to 0.293808	0.000259 to 0.000271	0.000065 to 0.000075	.1088694	±.0000106
trans-1,3-Dimethylcyclopentane	5	2.73538 to 2.81293	0.297897 to 0.306325	0.000253 to 0.000255	0.000006 to 0.000006	.1088215	±.0000045

TABLE 2. *Heats of isomerization in the liquid state*

Compound	B at 28° C	B° at 28° C	Ratio of the heats of combustion in the ideal bomb process, B_i°/B_n°, at 28.00° C	Difference in the heats of combustion in the ideal bomb process, $(-\Delta U^\circ)_n-(-\Delta U^\circ)_i$, at 28.00° C	
				kj/mole	*kcal/mole*
	Ohm/g CO_2	*Ohm/g* CO_2			
Ethylcyclopentane	0.1089810±.0000110	0.1089503±.0000108	1.000000	0.00	0.00
1,1-Dimethylcyclopentane	.1087759±.0000064	.1087453±.0000062	0.998118±.000114	8.62±0.52	2.06±.12
cis-1,2-Dimethylcyclopentane	.1089371±.0000170	.1089063±.0000170	.999596±.000185	1.85±0.85	0.44±.20
trans-1,2-Dimethylcyclopentane	.1087961±.0000116	.1087655±.0000116	.998304±.000146	7.77±0.67	1.86±.16
cis-1,3-Dimethylcyclopentane	.1088694±.0000212	.1088394±.0000212	.998982±.000219	4.66±1.00	1.11±.24
trans-1,3-Dimethylcyclopentane	.1088215±.0000090	.1087908±.0000090	.998536±.000129	6.71±0.59	1.60±.14

The values of the differences in the heats of combustion in the ideal bomb process, $(-\Delta U^\circ)_n-(-\Delta U^\circ)_i$, were obtained by means of the relation [8]

$$(-\Delta U^\circ)_n-(-\Delta U^\circ)_i=(-\Delta U^\circ)_n\left(1-\frac{B_i^\circ}{B_n^\circ}\right).$$

For this calculation, the value of $(-\Delta U^\circ)_n$ at 28°C was taken from reference [13] as 4581.5 int kj/mole or 4582.3 abs kj/mole.

In table 3 are given, for the six C_7H_{14} alkylcyclopentanes, values for the following: $H_i^\circ-H_n^\circ$, the heat of isomerization of ethylcyclopentane into each isomer at 25° C for the liquid and gaseous states; $-\Delta Hc^\circ$, the decrement in the heat content accompanying the reaction of combustion of the hydrocarbon in the liquid or gaseous state, as indicated, in gaseous oxygen to form gaseous carbon dioxide and liquid water at 25° C; and ΔHf°, the increment in heat content or enthalpy of the process of forming the given hydrocarbon in the liquid or gaseous state, as indicated, from its elements, gaseous hydrogen and solid carbon (graphite), at 25° C.

TABLE 3. *Heats of isomerization, combustion, and formation in the liquid and gaseous states*

Compound	Heat of isomerization, $H_i^\circ - H_n^\circ$, at 25° C		Heat of combustion, $-\Delta He^\circ$, at 25° C		Heat of formation, ΔHf°, at 25° C	
	Liquid	Gas	Liquid	Gas	Liquid	Gas
	kcal/mole	*kcal/mole*	*kcal/mole*	*kcal/mole*	*kcal/mole*	*kcal/mole*
Ethylcyclopentane	0.00	0.00	1097.50±.22	1106.23±.23	−39.08±.24	−30.35±.25
1,1-Dimethylcyclopentane	−2.06±.12	−2.70±.12	1095.44±.25	1103.53±.26	−41.14±.27	−33.05±.28
cis-1,2-Dimethylcyclopentane	−0.44±.20	−0.61±.20	1097.06±.30	1105.62±.30	−39.52±.31	−30.96±.32
trans-1,2-Dimethylcyclopentane	−1.86±.16	−2.32±.16	1095.64±.27	1103.91±.28	−40.94±.29	−32.67±.30
cis-1,3-Dimethylcyclopentane	−1.11±.24	−1.58±.24	1096.39±.33	1104.65±.33	−40.19±.34	−31.93±.35
trans-1,3-Dimethylcyclopentante	−1.60±.14	−2.12±.14	1095.93±.26	1104.11±.27	−40.68±.28	−32.47±.29

The heat of isomerization, $H_i^\circ - H_n^\circ$, in the liquid state at 25° C was taken as equal to the difference $(-\Delta U^\circ)_i - (-\Delta U^\circ)_n$ between each isomer and ethylcyclopentane, in the heats of combustion in the ideal bomb process at 28° C, since for these isomers the conversion to the constant-pressure process and to 25° C will be the same, well within the limits of uncertainty assigned to the values.

The heats of isomerization, $H_i^\circ - H_n^\circ$, in the gaseous state, were obtained from the values in the liquid state by use of the following values for the difference in the heat of vaporization of each isomer to that of ethylcyclopentane [2], in kcal/mole: Ethylcyclopentane, 0.00; 1,1-dimethylcyclopentane, 0.64; *cis*-1,2-dimethylcyclopentane, 0.17; *trans*-1,2-dimethylcyclopentane, 0.46; *cis*-1,3-dimethylcyclopentane, 0.47; *trans*-1,3-dimethylcyclopentane, 0.52.

The value of the heat of combustion or formation of a given isomer was obtained by appropriately combining the heat of isomerization with the heat of combustion or formation of ethylcyclopentane as given by the following values from references [13, 14, 15]:

C_7H_{14}(ethylcyclopentane, liquid)$+21/2O_2$(gas)$=7CO_2$(gas)$+7H_2O$(liquid).

$$\Delta H^\circ_{298.16} = -1097.50 \pm 0.22 \text{ kcal/mole.}$$

C_7H_{14}(ethylcyclopentane, gas)$+21/2O_2$(gas)$=7CO_2$(gas)$+7H_2O$(liquid).

$$\Delta H^\circ_{298.16} = -1106.23 \pm 0.23 \text{ kcal/mole.}$$

7C(solid, graphite)$+7H_2$(gas)$=C_7H_{14}$(ethylcyclopentane, liquid).

$$\Delta H^\circ_{298.16} = -39.08 \pm 0.24 \text{ kcal/mole.}$$

7C(solid, graphite)$+7H_2$(gas)$=C_7H_{14}$(ethylcyclopentane, gas).

$$\Delta H^\circ_{298.16} = -30.35 \pm 0.25 \text{ kcal/mole.}$$

All the uncertainties assigned to the experimental quantities in table 2 (except the heats of combustion and formation) are equal to twice the standard deviation of the mean. The uncertainties assigned to the values of the heats of combustion and formation were obtained by combining [7] the uncertainty in the values of the heats of combustion and formation of ethylcyclopentane [14], with the uncertainties in the values of the heats of isomerization. The uncertainty to be assigned to the value of the heat of isomerization of any one of the isomers into any other one may conservatively be taken as ±0.25 kcal/mole.

VI. References

[1] W. H. Johnson, E. J. Prosen, and F. D. Rossini, J. Research NBS **39,** 49 (1947) RP1812.

[2] Selected Values of Properties of Hydrocarbons. American Petroleum Institute Research Project 44 at the National Bureau of Standards. Table 6q. Cyclopentanes C_5 to C_7. Heat, free energy, and entropy of vaporization at 25° C. (October 31, 1948).

[3] E. J. Prosen, W. H. Johnson, and F. D. Rossini, J. Research NBS **37,** 51 (1946) RP1728.

[4] E. F. Mueller and F. D. Rossini, Am. J. Phys. **12,** 1 (1944).

[5] Selected Values of Chemical Thermodynamic Properties. National Bureau of Standards. Values of Constants (December 31, 1947).

[6] G. P. Baxter, M. Guichard, and R. Whytlaw-Gray, J. Am. Chem. Soc. **69,** 734 (1947).

[7] F. D. Rossini and W. E. Deming, J. Wash. Acad. Sci. **29,** 416 (1939).

[8] E. J. Prosen and F. D. Rossini, J. Research NBS **27,** 289 (1941) RP1420.

[9] A. R. Glasgow, Jr., E. T. Murphy, C. B.Willingham, and F. D. Rossini, J. Research NBS **37,** 141 (1946) RP1734.

[10] A. J. Streiff, E. T. Murphy, J. C. Cahill, H. F. Flanagan, V. A. Sedlak, C. B. Willingham, and F. D. Rossini, J. Research NBS **38,** 53 (1947) RP1760.

[11] A. J. Streiff, J. C. Zimmerman, L. F. Soule, M. T. Butt, V. A. Sedlak, C. B. Willingham, and F. D. Rossini, J. Research NBS **41,** 323 (1948) RP1929.

[12] E. W. Washburn, J. Research NBS **10,** 525 (1933) RP546.

[13] W. H. Johnson, E. J. Prosen, and F. D. Rossini, J. Research NBS **36,** 463 (1946) RP1715.

[14] E. J. Prosen, W. H. Johnson, and F. D. Rossini, J. Research NBS **37,** 51 (1946) RP1728.

[15] Selected Values of Properties of Hydrocarbons. American Petroleum Institute Research Project 44 at the National Bureau of Standards. Table 6n. Cyclopentanes C_5 to C_7. Heat of Combustion at 25° C, for liquid and gas (October 31, 1948).

WASHINGTON, November 16, 1948.

U. S. Department of Commerce
National Bureau of Standards

Research Paper RP1967
Volume 42, March 1949

Part of the Journal of Research of the National Bureau of Standards

Surface Available to Nitrogen in Hydrated Portland Cements

By Raymond L. Blaine and Harold J. Valis

Measurements were made of the adsorption of nitrogen, oxygen, and argon at or near the boiling point of the adsorbate on samples of hydrated portland cement. Surface-area values calculated on the basis of the Brunauer-Emmett-Teller theory indicated an increase in surface available to nitrogen with age of test specimens when a high water-cement ratio was used in preparing the paste but not when a low water-cement ratio was used. Temperature of storage and type of moist storage made little difference in the apparent surface available to nitrogen. Surface values calculated from the N_2, O_2, and A isotherms were much smaller than those previously reported, which were calculated from the adsorption of water vapor.

I. Introduction

The low-temperature adsorption test, in which nitrogen or another inert gas is adsorbed at or near the boiling point of the gas, has been used for a number of years as a measure of the surface areas of particulate materials [1].[1] It is also used to measure the internal surface of porous materials, that is, the surface of pores large enough for the gas molecule to enter [2]. Hydrated portland cement paste is a porous solid, as evidenced by water permeability and water absorption measurements [3]. However, different cements and different quantities of mixing water used in making the neat paste, as well as different curing conditions, result in different pore structures in the hydrated specimens [4]. Furthermore, there is evidence that changes take place in the pore structure and crystal form as a cement continues to hydrate [5].

Powers and Brownyard [6] made studies of the internal surface areas of hydrated portland cement pastes by using water vapor as the adsorbate. In the present study it seemed desirable to use a gas that would be less reactive with the cement constituents, in order to measure the internal surface areas of the partially hydrated portland cement pastes.

The purpose of this study was to determine some of the variables of the nitrogen adsorption method, the applicability of the low-temperature adsorption method to the study of hydrated cements, and the precision of the test method. It was also desired to determine the effect of various factors such as storage, age, and water-cement ratio of hydrated paste on the surface areas available to nitrogen.

II. Scope

In the low-temperature adsorption test it is necessary to evacuate the sample in order to clear the surfaces of adsorbed or absorbed molecules. Ordinarily this is done at a temperature of 200° to 400° C. However, compounds having water of crystallization, such as are found in hydrated portland cement, may lose this water at such temperatures. It was necessary, therefore, to evacuate the samples at various temperatures in order to determine the effect of the temperature of evacuation on the calculated surface values. Thermal analyses were also made of the granulated pastes evacuated at different temperatures. In the preliminary tests the effect of size upon

[1] Figures in brackets indicate the literature references at the end of this paper.

apparent surface area was investigated to determine whether the ½ by 2-in. specimens could be tested whole or had to be broken up into granules, and what size of granules would be required.

It was not practicable to make duplicate determinations in all cases. However, determinations were made on five specimens prepared on different days, in which an attempt was made to keep all variables constant in order to obtain data on the reproducibility of the surface values obtained.

Although the surface area calculations are based on the portion of the adsorption curve between partial pressures of 0.05 and 0.30, the nature of the entire adsorption and desorption curve is of importance in interpreting some of the results. The complete adsorption isotherm was determined for only one sample in this series. This isotherm was similar to others previously determined for cement pastes in this laboratory; hence most isotherms were determined only to a partial pressure of 0.5. Most of the determinations were made by using nitrogen as the adsorbate; a few tests were made using argon and oxygen.

Measurements were made to determine the effect of the water-cement ratio used in preparing the neat paste, the type of storage (moist air or water), and the temperature and time of storage on the surface area available to nitrogen. Most of the tests were made by using one cement; a few were made with other cements.

III. Materials and Methods of Test

The portland cement used for the majority of the tests in this investigation met the requirements for Type I cement of Federal Specification SS–C–191b. A few surface area determinations were also made on specimens of the high-early strength and type II cements used in the ASTM, C–1 cooperative investigation (1948).

Cement pastes were made by using water-cement ratios of 0.25, 0.40, and 0.55 by weight. The cement and water were mixed in a beaker for 5 min by means of a spatula. The paste was then poured into paraffin-lined brass molds, ½ in. in diameter and 2 in. deep. The brass mold was sealed to a brass plate with rosin-paraffin mixture previous to filling with the paste. The mold with paste was stored in moist air for the first 24 hrs. For the 21° C. storage, the 90-percent relative humidity moist cabinet ordinarily used in cement testing was used. For the 5° C. storage, the mold containing the specimens was stored in a tight jar containing a small quantity of distilled water, which was immersed in a constant-temperature bath maintained at 5.0°±0.5° C.

A similar procedure was used for the 38° C storage, except that the jar with mold was placed in an oven maintained at 38° ±1° C. After 24 hrs, the specimens were removed from the molds, stripped of any adhering paraffin and stored either at 5°, 21°, or 38° C over distilled water in closed containers or in water in the regular cement-specimen storage tank maintained at 21° ±1° C.

Twenty-four hours after casting, some specimens were broken to granules in a mortar. These granules were sieved, the 10–20 mesh material being saved for some specimens. For others, the 20–50 mesh or the 50–100 mesh materials were saved for test. Additional specimens were broken into granules and sieved after specified periods of storage immediately before test.

Specimens were sealed into sample holders at 1, 3, 7, 28, and 84 days after casting. The

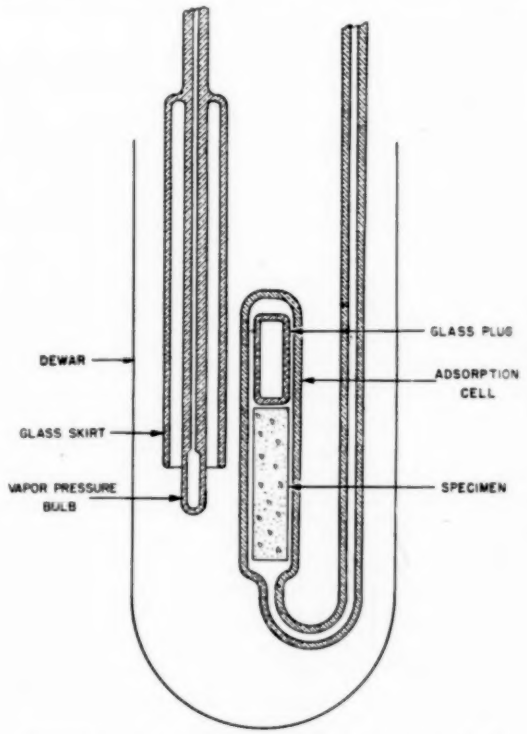

FIGURE 1. *Specimen holder and vapor-pressure bulb.*

samples were immediately evacuated, and the adsorption tests were made the following day. The coating formed on water-stored specimens was scraped off before test.

A piece of closed-off glass tubing was placed between the specimen and the top seal to prevent drying of the specimen in the sealing operation (see fig. 1). The sample was then evacuated to less than 1 mm Hg at room temperature for approximately 6 hrs by means of a mechanical vacuum pump. The specimen holder was then attached to the adsorption apparatus and evacuated by means of a mercury diffusion pump for a period of approximately 16 hr. The vacuum attained in the system was of the order of 1×10^{-6} mm of mercury as measured by means of a McLeod gage. An oven was placed around the sample container after attaching it to the apparatus for the tests in which the sample was evacuated at 100° to 110° C or 200° to 210° C.

Specimens were weighed before sealing into the sample containers. In order to determine the loss of water, the sealed specimen holder with sample was weighed before evacuation and again immediately after the adsorption test. The original weight of the sample minus the loss during evacuation was taken as the basis for computing the surface area per gram and also for computing the loss of water in evacuation. Ordinarily the specimen tested had a dry weight of 7 to 10 g depending, in part at least, on the water-cement ratio used in the original paste.

The apparatus used for determining the adsorption isotherm was of the volumetric type, which has previously been described [1]. The volume of the sample bulb not occupied by the solid portion of the sample was determined by means of helium, which had been passed over activated charcoal in a liquid nitrogen bath just before admission to the adsorption apparatus. The volume of helium admitted was determined from four pressure-volume measurements. Four additional pressure-volume measurements were made with the helium to determine the volume of the sample bulb not occupied by the solid. This calibration was made with the sample bulb immersed in liquid nitrogen or oxygen, depending on the gas to be adsorbed. After the helium calibration, the sample was evacuated for 2 hrs at room temperature.

Water-pumped tank nitrogen purified by passage over magnesium perchlorate, chabasite, copper turnings at 400° C and then through magnesium perchlorate immediately before admission to the apparatus was used for the adsorption measurements with most samples. The nitrogen entering the adsorption apparatus was allowed to come to room temperature, and its volume was determined after which the nitrogen was admitted to the sample bulb. After equilibrium had been attained (usually in about 20 min but at times longer than 1 hr), the volume of nitrogen not adsorbed was determined. Additional nitrogen was then added either from the burette system or from the tank, and the above process was repeated. All volumes were calculated on the basis of the volume at 0° C and 760 mm mercury pressure. Corrections were made for density of the mercury in the manometers, the changes in scales with temperature, and for the "nonideal" behavior of the gas in the dead space around the sample.

Five or more values at partial pressures between 0.05 and 0.35 on the adsorption isotherm were determined for each of the samples. Additional values were obtained up to partial pressures of 0.5 to 0.7 on most of the samples, and on one sample the adsorption curve was obtained to above 0.9 partial pressure, after which desorption values were obtained.

The vapor pressure of the adsorbate was determined from the condensed adsorbate in a vapor pressure bulb in the bath alongside the sample (see fig. 1). The glass tube leading from the bulb to the manometer was jacketed with a larger tube in order to measure the vapor pressure near the adsorption bulb rather than at the surface of the bath, which may be slightly cooler than the sample.

Oxygen gas was used as the adsorbate on one sample, using a liquid oxygen bath. Argon was used as the adsorbate on one sample using a liquid oxygen bath and on another sample using a liquid nitrogen bath.

Surface areas of all samples were evaluated by means of the BET equation [7] as follows:

$$\frac{P}{V(P_0-P)}=\frac{1}{V_mC}+\frac{(C-1)P}{V_mCP_0},$$

where

P = pressure of adsorbate,

P_0 = vapor pressure of adsorbate at temperature of bath,

V=volume of gas adsorbed (standard temperature and pressure) at pressure P,

V_m=volume of gas required for monolayer,

$C=ke$ exponential $(E_1-E_L)/RT$,

k=a constant,

E_1=heat of adsorption,

E_L=heat of liquefaction,

R=gas constant,

T=absolute temperature.

$P/V(P_0-P)$ was plotted against the partial pressure P/P_0. The slope and intercept of a line drawn through the points on the graph between partial pressures of 0.05 and 0.30 were used to evaluate V_m and C. The area on the surface occupied by each molecule corresponds with those calculated by Emmett [1] from the liquid or solid density, molecular weight, and Avogadro's number. The values for area occupied by each molecule as used for the surface area calculations were as follows: N_2, 16.2 sq A; O_2, 14.1 sq A; argon at liquid-nitrogen temperature, 12.8 sq A and at liquid-oxygen temperature, 14.4 sq A.

In order to study the pore diameters of the hydrated specimens, isotherms were calculated on the basis of the V_m and C values obtained for the particular samples [7]. Various values of n were substituted in the following equation and these calculated isotherms were superimposed on the adsorption isotherm.

$$V=\frac{V_mCx}{1-x}\frac{1-(n+1)x^n+nx^{(n+1)}}{1+(c-1)x-cx^{(n+1)}},$$

where

n=maximum number of layers that can be adsorbed on the walls of the capillary,

$x=P/P_0$,

V, C, and V_m are the same as in the previous equation.

The values reported are the results of single determinations. In order to determine the precision of the test results, five determinations were made in which the water-cement ratio, curing conditions, age, and temperature of evacuation were nominally constant. These five determinations were made on different days over a period of about 3 months during the period when most of the other tests were made.

IV. Results of Tests

1. Effect of Temperature of Evacuation

The effect of the temperature of evacuation on the apparent surface was determined on both the ½- by 2-in. specimens and on the 10–20 mesh granules. A water-cement ratio of 0.55 was used in preparing the pastes. The granules were prepared at 24 hr, and the granules and whole specimens were stored in moist air at 21° C until tested at 7 days. The values of surface areas available to nitrogen, calculated on the basis of the weight of the evacuated specimens, are presented in the tabulation below. Presented also are the amounts of water removed from the specimens expressed as a percentage of the weight of the evacuated sample.

½- by 2-in. specimens			10–20 mesh granules	
Temperature of evacuation	Surface	Water loss	Surface	Water loss
°C	m^2/g	%	m^2/g	%
25	14.5	20.9	20.3	25.4
100	[a] 25.9	[a] 30.7	33.2	30.0
200	27.9	32.9	35.7	33.8

[a] Average of 5 determinations.

It is apparent from this table that the higher the temperature of evacuation the greater is the amount of surface available to nitrogen. The amount of water removed from the specimens also increased with increased temperature of evacuation. Inasmuch as the surface area values were calculated on the basis of the weight of the specimens after evacuation, these values are not on a comparable basis as far as the actual cement content of the specimens is concerned. A better basis of comparison would probably have been the actual cement content or the ignited weight of the samples tested. This was not apparent at the time of test, but is suggested for further studies. Although the values determined after evacuation at 200° C were greater by a significant amount than the values determined after evacuation at 100° C, the difference was small as compared to the difference between the 25° and 100° C evacuations. Because of this, the remaining samples were evacuated at 100° to 110° C after the pre-

liminary evacuation at room temperature to take out most of the water. Evacuation at 100° C is, however, quite arbitrary, and different surface area values are obtained at different temperatures of evacuation.

Thermal analyses made of granulated samples evacuated at approximately 25°, 100°, and 200° C indicated a loss of water of crystallization with samples evacuated at both 100° and 200° C. Nearly as much loss of water occurred during the 100° C evacuation as during the 200° C evacuation.

2. Effect of Size of Test Specimens

It may be noted in the tabulation on page 260 that the 10–20 mesh granules had greater higher values for surface area than the whole specimens (solid cylinders) at each of the temperatures of evacuation. By using the same water-cement ratio and storage as in the previous tests, 20–50 and 50–100 mesh granules were prepared at 1 day and tested at 7 days to determine the effect of size of specimens. The samples were evacuated at 100° to 110° C. The values obtained for surface area available to nitrogen and the quantity of water removed in evacuation are presented in the tabulation below. Also included in this table are the results obtained with the ½- by 2-in. specimens and ½- by 2-in. specimens made with a ⅛-in. core, which was removed at the time of initial set, leaving a hollow cylinder.

Type of specimen	Surface	Water loss
	m^2/g	%
Solid cylinder	[a] 25. 9	[a] 32. 7
Hollow cylinder	[b] 26. 0	[b] 30. 4
Crushed to 10–20 mesh	33. 2	30. 0
Crushed to 20–50 mesh	29. 0	26. 2
Crushed to 50–100 mesh	20. 4	17. 3

[a] Average of 5 determinations.
[b] Average of 2 determinations.

One would expect that breaking the specimens into granules would not only make the interior surface more readily available but would also create new surface in those instances where crystals are fractured. The 10–20 and 20–50 mesh granulated materials had higher surface area values than did the whole specimens but there was an apparent decrease in surface with decrease in size of granules. The relation of the apparent surface area to the percentage of water loss of the different size granules is presented in figure 2. Presented also in this figure are the data from the tabulation on page 260 showing the relation of the surface area of the whole specimens, evacuated at different temperatures, to the water loss. Other tests made on granulated samples are reported under the section on autogenous healing.

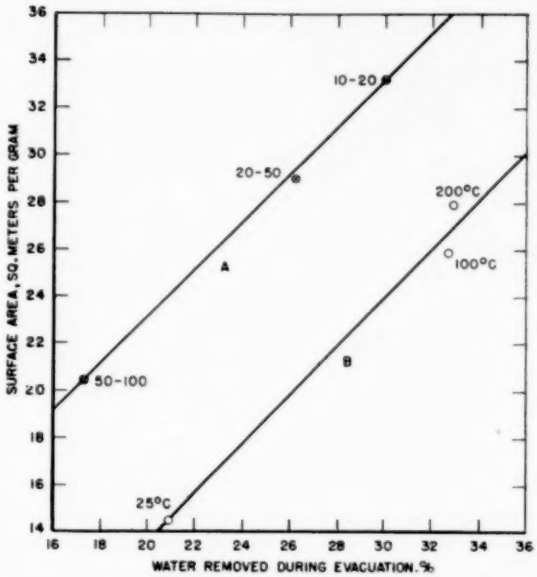

FIGURE 2. *Relation of surface area to water removed during evacuation at various temperatures.*

Whole specimens and granules were made by using a water-cement ratio of 0.55 and were moist-air cured for 7 days. A, Granules evacuated at 100° C; B, whole specimen.

There was no great difference observed in the rate of adsorption of the granulated and the whole specimens. Inasmuch as the whole specimens appeared satisfactory from the standpoint of testing procedure and breaking the specimens to granules added another variable (that of the size of the granules), the remaining tests were made on whole specimens.

3. Reproducibility

Five ½- by 2-in. specimens were made on different days using a water-cement ratio of 0.55 and stored in moist air at 21° C. The age of the specimens at the start of the test was 7 days in each case, and the specimens were all evacuated

at 100° to 110° C. The surface areas determined for the specimens were as follows:

Test specimen number	Surface	Water loss
	m^2/g	%
1	26. 24	34. 0
2	25. 51	29. 6
3	25. 58	32. 7
4	26. 20	32. 9
5	26. 20	34. 5
Average	25. 94	32. 7
Standard deviation	0. 33	1. 9
Coefficient of variation, %	1. 3	5. 8

The observed differences may be caused by variations in water-cement ratio, mixing of paste, storage of specimens, and evacuation of the specimens, as well as by errors in the testing procedure. Differences in surface-area values of less than 1 m^2/g (3 times the standard deviation) cannot therefore be considered significant for single determinations. The coefficient of variation of the percentage of water loss was 5.8 percent as compared to 1.3 percent for the surface values. A part of this variation may have been caused by the amount of evaporation occurring during the sealing operation.

4. Adsorption Isotherm

An isotherm obtained for the adsorption of nitrogen on hydrated cement at the boiling temperature of liquid nitrogen is illustrated in figure 3. This isotherm was obtained on a ½- by 2-in. specimen, 0.55 water-cement ratio, hydrated 7 days in moist air and evacuated at 100° C. The adsorption curve is a type 2 isotherm as classified by Brunauer-Emmett-Teller (BET) [7]. The desorption portion of the curve indicates a slight hysteresis, as is commonly found with porous adsorbents. The hysteresis loop was closed at a partial pressure of slightly above 0.4, below which the adsorption and desorption curves coincide. Also presented in this figure are the calculated values of the number of layers that would correspond with the V_m and C values for this particular isotherm. It may be noted that the adsorption isotherm corresponds with a porous material permitting five layers of molecules up to a partial pressure of 0.5, after which the adsorption curve crosses the lines corresponding to six, seven, eight, and nine layers. Assuming 3.15 A as the diameter of the nitrogen molecule, the average pore diameter is of the order of 30 A, which corresponds very well with the 20 to 40 A reported by Powers and Brownyard, who used water vapor as adsorbate.

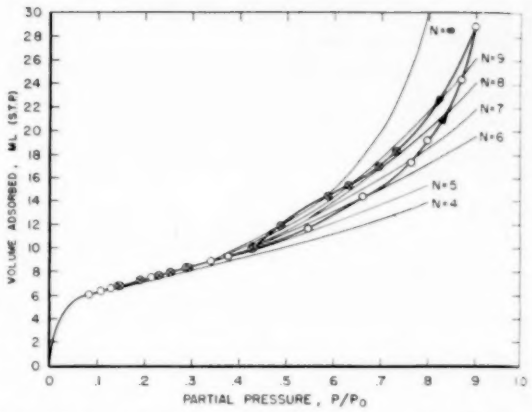

FIGURE 3. *Adsorption and desorption isotherms obtained on whole specimen made with 0.55 water-cement ratio and moist-air cured for 7 days.*

Included are the calculated isotherms assuming various values for the number of molecular layers (N) that could be accommodated. ○, Adsorption; ⊗, desorption.

5. Use of Different Gases as Adsorbate

The surface area calculated from the nitrogen isotherm on the cement paste hydrated for 7 days is only about 26 m^2/g, whereas Powers and Brownyard reported values on the order of 100 m^2/g when using water vapor as the adsorbate. Because of this difference, it seemed desirable to determine the surface area as measured by different gases. Oxygen gas was adsorbed at liquid oxygen temperature, and argon gas was adsorbed at liquid oxygen and liquid-nitrogen temperatures. Adsorption tests were made on 0.55 water-cement ratio, 7-day, 21° C, moist-air-cured whole specimens evacuated at 100° to 110° C. The surface

area values calculated from the adsorption isotherms are presented in the tabulation below.

Adsorbate	Temperature	Area/molecule	Surface area
	° C	sq Å	m^2/g
N_2	−195	16. 2	25. 9
O_2	−183	14. 1	20. 8
A	−195	14. 4	19. 4
A	−183	12. 8	20. 7

Although the values for surface area obtained with the use of oxygen and argon are somewhat lower than those obtained with the use of nitrogen, they are of the same order. The values are, however, much lower than those obtained with water vapor.

6. Effect of Water-Cement Ratio and Age of Test Specimens

Specimens were made with water-cement ratios of 0.55, 0.40, and 0.25 and stored in moist air at 21° C. The specimens were tested at 1, 3, 7, 28, and 84 days. All of these specimens were evacuated at 100° to 110° C. The results of these tests are presented in figure 4. Whereas the more porous paste (highest water-cement ratio) indicates an increase in the surface available to nitrogen with age, the paste having the lowest water-cement ratio indicated a trend toward a decrease in surface available to nitrogen with age. The paste with an intermediate water-cement ratio had an apparent increase in surface up to 7 days, after which no significant increase was obtained up to 84 days.

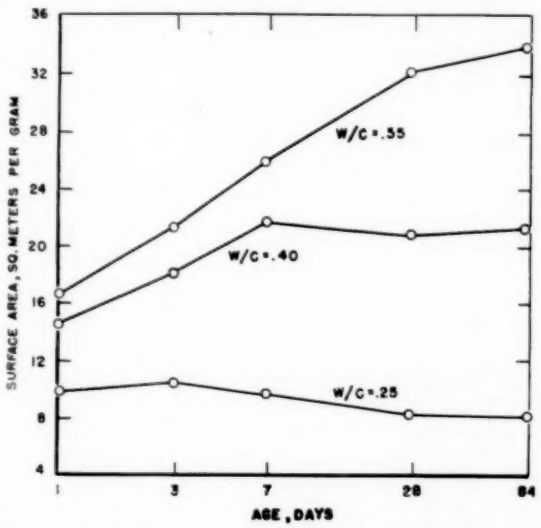

FIGURE 4. *Surface area available to nitrogen of ½- by 2-in. specimens made with different water-cement ratios, cured in moist air at 21° C for different periods of time and tested at various ages.*

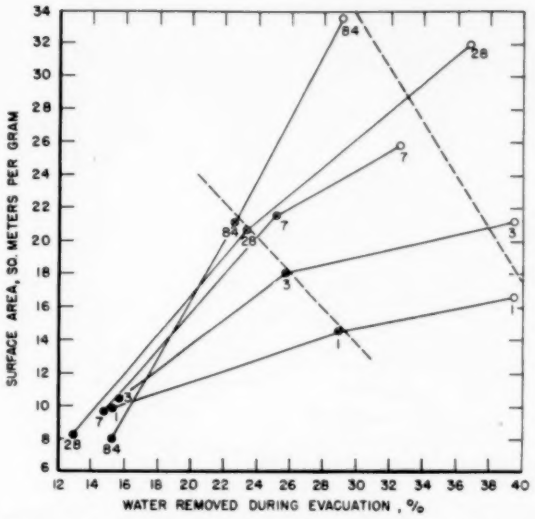

FIGURE 5. *Surface area available to nitrogen versus percentage of water removed in evacuation of ½- by 2-in. specimens made with different water-cement ratios, moist-air cured and tested at various ages.*

○, w/c=0.55; ⊗, w/c=0.40; ●, w/c=0.25.

The relation between the surface areas of these specimens and the percentage of water lost in evacuation is presented in figure 5. The pastes made of the 0.40 and 0.55 water-cement ratios indicated a trend of higher surface areas with lower percentages of water removed, as indicated by the dashed lines. Specimens tested at the same age are connected by lines and indicate different slopes at the different ages.

7. Effect of Temperature of Hydration and Age

Cement pastes of 0.55 water-cement ratio were allowed to hydrate in moist air at 5° and 38° C for comparison with the specimens stored at 21° C. Tests were made at 1, 3, 7, 28, and 84 days. All specimens were evacuated at 100° to 110° C. The results of tests are presented in figure 6. Although the specimens stored at 5° C were so soft that difficulty was encountered in removing them from

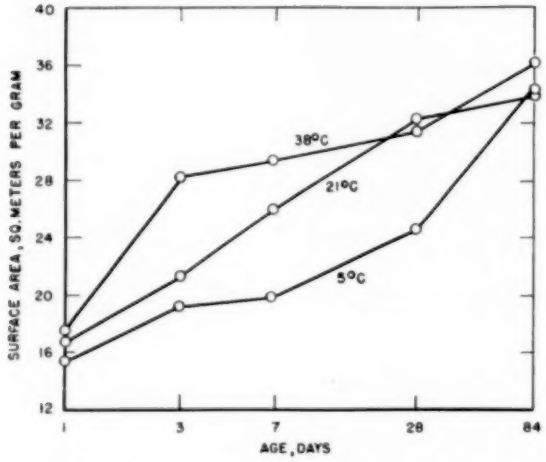

FIGURE 6. *Effect of curing temperature and age on surface area available to nitrogen of ½- by 2-in. specimens made with a water-cement ratio of 0.55 and cured in moist air.*

the molds, the surface was only slightly less at 1 day than that of the specimens stored at 21° or 38° C. The specimens stored at 38° C indicated only a slight increase in surface after 3 days, whereas the specimens stored at 5° and 21° C continued to increase in surface with age. The surface area vs percentage of water loss is shown in figure 11.

8. Effect of Water and Moist Air Storage on Different Cements

The ½- by 2-in. specimens of the type I cement made with 0.55 water-cement ratio were stored in water at 21° C after 24 hours in the moist cabinet, for comparison with the specimens stored continuously in moist air. Specimens were also made of a type II and a type III cement and stored in water and in moist air. Coatings formed on the water-stored specimens were scraped off before they were sealed in the specimen holders. All specimens were evacuated at 100° to 110° C after the preliminary evacuation at room temperature. A comparison of the values obtained for the different cements and storage conditions is presented in figures 7 and 8. At 28 and 84 days the water-cured specimens of the type I cement had appreciably greater surface areas available to nitrogen than did the respective moist-air stored specimens.

The neat pastes made of the type II and the type III cement with a water-cement ratio of 0.55 and stored in moist air had greater surface area

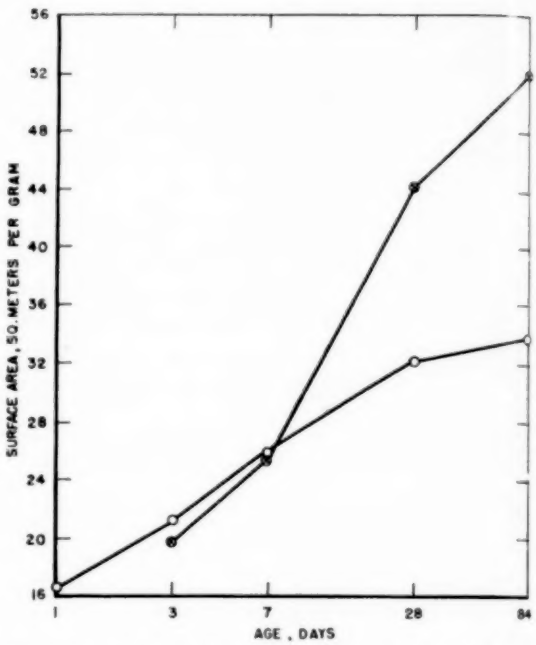

FIGURE 7. *Surface area available to nitrogen of ½- by 2-in. specimens of type I cement made with 0.55 water-cement ratio and cured in moist air or in water for various ages.*

○, Moist-air storage; ⊗, water storage.

values at the respective ages than did the corresponding specimens made of the type I cement. The apparent surface of the 28-day, water-stored specimens of type II and type III cements was less than the respective moist-air stored specimens; however, the water-stored specimens of the type I cement had greater surface than did the moist-air cured specimens, at 28 days.

9. Autogenous Healing

In some tests made previous to the present study, normal and high-early-strength cement pastes of normal consistency (water-cement ratio approximately 0.23) were broken to 10–40 mesh at 24 hours and stored in moist air at 21° C. Surface area values were determined at various ages after evacuation at 200° C and are based on the weight of the evacuated granules. The results of tests are presented in figure 9. Although the results are somewhat erratic, there appears to be a definite decrease in surface available to nitrogen with age. This was believed to be caused by the autogenous healing of cracks or crevices in the

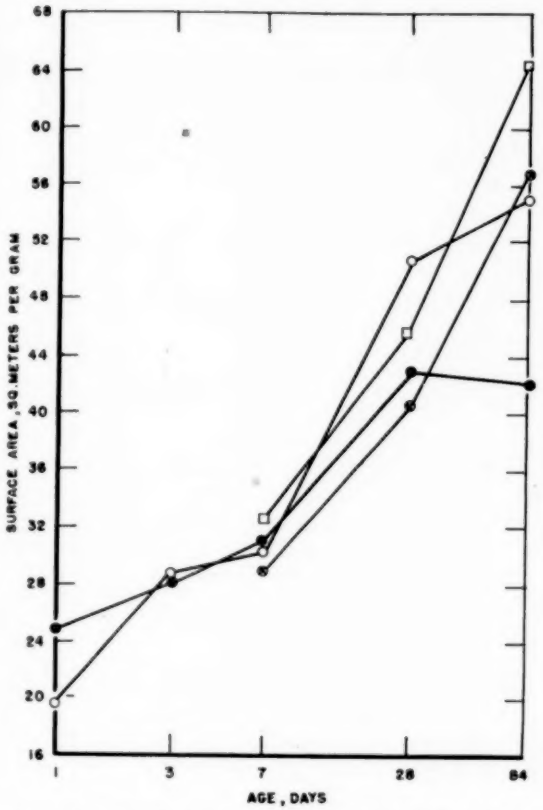

FIGURE 8. *Surface area available to nitrogen of ½- by 2-in. specimens of types II and III cements made with 0.55 water-cement ratio and cured in moist air or in water for various ages.*

○, Type II, moist-air storage; □, type II, water storage; ●, type III, moist-air storage; ⊗, type III, water storage.

granules. However, in the present series of tests where specimens were broken at 1 day and tested at various ages and comparative specimens were granulated just previous to testing, there was no conclusive proof of autogenous healing with the higher water-cement ratio pastes. The results presented in figure 10 indicated that at two of the three ages the surface values obtained were not affected appreciably by the age at which the specimens were broken. A second set of tests of 28-day specimens indicated the same values (within experimental error) as obtained with the first set of 28-day specimens.

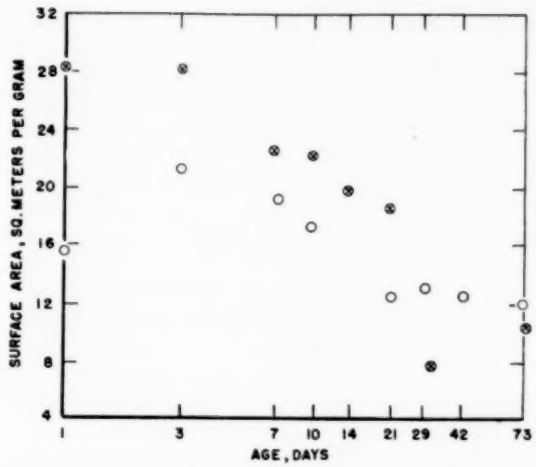

FIGURE 9. *Effect of time of storage on surface available to nitrogen of granules of a normal portland a high-early-strength cement paste made with 0.23 water-cement ratio.*

The neat cement past was broken to granules at 1 day and stored in moist air at 21° C until tested. ○, Normal portland; ⊗, high-early-strength portland.

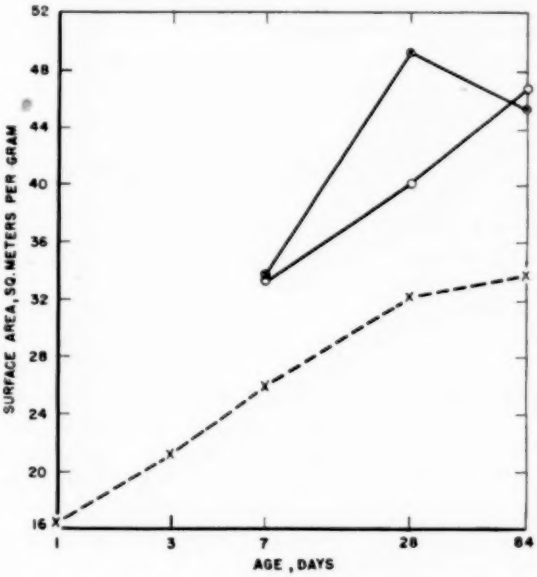

FIGURE 10. *Effect of age at which the specimens were granulated on the surface available to nitrogen.*

The neat pastes were made with a water-cement ratio of 0.55, and all specimens were stored in moist air at 21° C until tested. ○, Broken at 1 day; ⊗, broken at age of test; ×, whole specimens.

V. Discussion

The surface area of hydrated neat cement as measured by adsorption of nitrogen, oxygen, or argon was much lower than that reported by Powers and Brownyard [6], who used water vapor. Also, the desorption curve obtained with nitrogen did not have as large an hysteresis loop as did the curves obtained by Powers and Brownyard using water vapor. The water molecule is slightly smaller than the nitrogen molecule, hence the additional surface as measured by the water molecules may have consisted of intercrystalline spaces or pores too small for the nitrogen molecule to enter. Similar results have been obtained with montmorillonite [8], where the water molecule could apparently enter the space between the layers of mineral, whereas the larger molecules could not enter. The oxygen and argon molecules, which are smaller than the nitrogen molecule but larger than the water molecule, indicated less surface available to oxygen and argon than to nitrogen in the hydrated paste. Certain organic materials, such as paper [2] and textile fibers [9], also have greater surface areas available to water than to nitrogen. The apparent surface of paper and textile fibers available to nitrogen decreased with increased temperature of evacuation, whereas the hydrated cements showed the opposite effect.

Loss of water of crystallization is usually accompanied by an increase of surface area [10]. Certain of the compounds in hydrated portland cements may be expected to lose a portion of the water of crystallization on evacuation at 100° or 200° C, as carried out in this study. Although this evacuation was more severe than that used by Powers and Brownyard, the surface-area values were lower. There was more surface available to nitrogen also a greater loss of water when the samples were evacuated at the higher temperatures. The additional water that was removed may have been water of crystallization.

It appears then that the greater portion of the surface available to water vapor in hydrated cement pastes must consist essentially of pores smaller than 3.15 A, the diameter of the nitrogen molecule.

Figure 11 indicates no consistent relation between the percentage of water loss on evacuation and the surface available to nitrogen of pastes made with the same water-cement ratio and cured at different temperatures. However, when different water-cement ratios were used in preparing the paste, as previously indicated in figure 5, or testing different cements of the same water-cement ratio, different values were obtained.

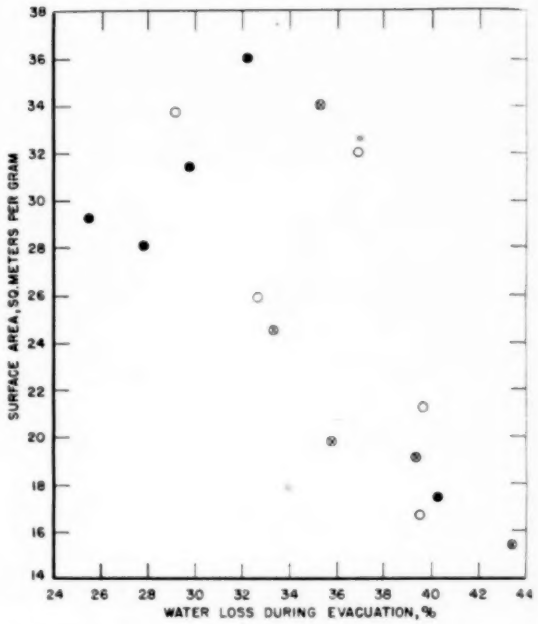

FIGURE 11. *Surface area available to nitrogen versus percentage of water loss during evacuation of ½- by 2-in. specimens made of type I cement with 0.55 water-cement ratio and stored in moist air at different temperatures until tested.*

⊗, 5° C storage; ○, 21° C storage; ●, 38° C storage.

VI. Summary

Measurements of the internal surface of hydrated portland cement neat pastes, computed on the basis of the BET theory from the amount of nitrogen adsorbed at the temperature of liquid nitrogen, indicate that:

1. Higher surface values were obtained on specimens evacuated at the higher temperatures.
2. The hydrated cement ground to pass a No. 10 sieve and retained on a No. 20 sieve had higher surface values than did the whole specimens.
3. The surface values of granulated specimens were lower for the smaller granules.

4. The surface values obtained by use of nitrogen at liquid nitrogen temperature were of the same order as those obtained with oxygen at liquid oxygen temperature, and argon at liquid oxygen or liquid nitrogen temperatures.

5. The surface available to nitrogen was much less than that previously reported as available to water molecules.

6. The surface values increased with age for specimens made with high water-cement ratio but not when made with a low water-cement ratio.

7. The surface values of specimens stored in moist air at 38° C were higher than those of specimens stored at 21° C up to 28 days.

8. The surface values of specimens stored in moist air at 5° C were approximately the same at 1 day as were those stored at 21° or 38° C, but increased more slowly with age than did those stored at the higher temperatures.

9. The surface values of a type I cement were higher at 28 days and 84 days after storage in water than after storage in moist air.

10. The surface values of pastes made of a type II and a type III cement were higher than those obtained with the type I cement neat paste at all ages of moist air storage.

11. The surface values of the type II and the type III cements were approximately the same when stored in water as when stored in moist air, except at 84 days when the water-stored specimens had greater surface values.

12. The pore diameter of the hydrated pastes was of the order of 30 angstroms.

VII. References

[1] P. H. Emmett, Symposium on new methods for particle size determination in the subsieve range, Am. Soc. Testing Materials (1941).

[2] P. H. Emmett and T. De Witt, Ind., & Eng. Chem. (Anal. Ed.) **13,** 28 (1941).

[3] W. M. Dunagan, Proc. Am. Soc. Testing Materials **39,** 866 (1939).

[4] L. S. Brown and R. W. Carlson, Proc. Am. Soc. Testing Materials **36,** 332 (1936).

[5] R. H. Bogue, The chemistry of portland cement, p. 454 (Reinhold Publishing Corp., New York, N. Y., 1947).

[6] T. C. Powers and T. L. Brownyard, J. Am. Concr. Inst. **18,** 469 (1946).

[7] S. Brunauer, The adsorption of gases and vapors, p. 153 (Princeton University Press, Princeton, N. J., 1945).

[8] S. B. Hendricks, R. A. Nelson, and L. T. Alexander, J. Am. Chem. Soc. **62,** 1457 (1940).

[9] J. W. Rowen and R. L. Blaine, J. Research NBS **39,** 479 (1947) RP1842.

[10] S. Brunauer and P. H. Emmett, J. Am. Chem. Soc. **59,** 2682 (1937).

Washington, November 8, 1948.

U. S. Department of Commerce
National Bureau of Standards

Research Paper RP1968
Volume 42, March 1949

Part of the Journal of Research of the National Bureau of Standards

Heat of Isomerization of the Two Butadienes

By Edward J. Prosen, Frances W. Maron, and Frederick D. Rossini

The heat of isomerization of 1,3-butadiene to 1,2-butadiene, in the gaseous state at 25° C was determined by measurement of the ratio of their heats of combustion in oxygen to form carbon dioxide and water. The combustion of the gaseous hydrocarbon occurred in a flame at constant pressure in a glass calorimetric reaction vessel of improved design. A complete description of the new calorimetric reaction vessel is given.

The following experimental value is reported for the reaction of isomerization:

1,3-butadiene(gas) = 1,2-butadiene(gas), $\Delta H°$ at 25° C = 12.78 ± 0.16 kcal/mole.

Using the value for the heat of formation of 1,3-butadiene previously reported, the following calculated values are given for the reactions of formation and combustion of 1,2-butadiene:

$4C(\text{solid, graphite}) + 3H_2(\text{gas}) = C_4H_6(\text{1,2-butadiene, gas})$, $\Delta H°$ at 25° C = 39.53 ± 0.28 kcal/mole.

$C_4H_6(\text{1,2-butadiene, gas}) + 5\frac{1}{2}\ O_2(\text{gas}) = 4CO_2(\text{gas}) + 3H_2O(\text{liquid})$, $\Delta H°$ at 25° C = −620.69 ± 0.28 kcal/mole.

I. Introduction

This work, sponsored by the Office of Rubber Reserve, is part of a thermochemical investigation of monomeric compounds of importance in the national synthetic rubber program, and is also a part of the work of the thermochemical laboratory of this Bureau on the determination of the heats of formation of compounds of importance to industry and science.

Calorimetric measurements have been made that yield a value for the difference in the heats of combustion at constant pressure of 1,3-butadiene and 1,2-butadiene in the gaseous state at 25° C. Combination of this value, which is the heat of isomerization in the gaseous state at 25° C, with the previously reported value for the heat of formation of 1,3-butadiene [1],[1] yields values for the heats of formation and combustion of 1,2-butadiene.

II. Unit of Energy, Molecular Weights, Uncertainties

The unit of energy upon which values reported in this paper are based is the absolute joule, derived from mean solar seconds, and absolute ohms and volts, in terms of which certification of standard resistances and standard cells is made by this Bureau. For conversion to the conventional thermochemical calorie, the following relation [2,3] is used:

1 calorie = 4.1840 absolute joules.

The atomic weights were taken as O = 16.0000, H = 1.0080, and C = 12.010 from the 1947 table of international atomic weights [4].

The uncertainties assigned to the various quantities dealt with in this paper were dervied, where possible, by the method previously described [5].

III. Method

The aim of this investigation was to determine as precisely as possible the heat of isomerization of 1,3-butadiene (gas) to 1,2-butadiene (gas) at constant pressure and 25° C. This was done by determining the ratio of the heats of combustion of these isomers [6]. The value of the difference between this ratio and unity, multiplied by an accepted value for the heat of combustion of 1,3-butadiene, gives the heat of isomerization of 1,3-butadiene to 1,2-butadiene. In principle, the

[1] Figures in brackets indicate the literature references at the end of this paper.

ratio of the heats of combustion of these isomers was determined as the inverse ratio of the masses of carbon dioxide, whose formation in the combustion of the respective isomers produced identical increases in temperature in the standard calorimeter system, measured as increases in resistance of the platinum resistance thermometer as determined on the given resistance bridge. With this procedure, the energy equivalent of the calorimeter system or the heat of combustion of one of the isomers need be known only approximately, and other systematic errors tend to cancel out.

The method of reducing the experimental observations was as follows: Let

ΔR_c = the corrected increase in temperature of the calorimeter system, expressed as the increase in resistance in ohms of the given platinum thermometer at a mean temperature of 25° C, as measured with the given resistance bridge;

m_{CO_2} = the mass of carbon dioxide formed in the combustion of the hydrocarbon, in grams;

E_s = the energy equivalent, over the "standard" interval of temperature, of the "standard" calorimeter system, obtained as the ratio of a given quantity of electric energy to the value of ΔR_c produced by it, expressed as joules per ohm;

q_i = the energy introduced into the calorimeter in the "ignition" process, consisting of sparking, igniting the flame, and extinguishing the flame, but not including any part of the heat of combustion, expressed in joules;

q_g = the energy introduced into the calorimeter by gases entering or leaving at a temperature different from 25° C.

q_v = the energy (negative) introduced into the calorimeter by the process of evaporating such water as leaves or remains in the calorimeter in the gaseous state.

q_c = the energy introduced into the calorimeter by the "standard calorimetric process" of combustion.

The total energy, q, introduced into the calorimeter by the actual combustion process in an experiment is

$$q = E_s \Delta R_c = q_c + q_g + q_v + q_i. \quad (1)$$

Letting

$$B = \frac{q_c}{E_s m_{CO_2}}, \quad (2)$$

we obtain the following relation from which B is calculated for any given experiment:

$$B = \left(\frac{\Delta R_c}{m_{CO_2}}\right)\left[1 - \frac{(q_g + q_v + q_i)}{E_s \Delta R_c}\right]. \quad (3)$$

For any two isomers, the ratio of the heats evolved per gram of carbon dioxide is equal to the ratio of their heats of combustion per mole. If the subscripts a and b refer to 1,3-butadiene and 1,2-butadiene, respectively, and $-\Delta Hc°$ is the heat evolved in the standard combustion of one mole of the hydrocarbon, then

$$B_b/B_a = (-\Delta Hc°)_b/(-\Delta Hc°)_a, \quad (4)$$

and

$$(-\Delta Hc°)_a - (-\Delta Hc°)_b = (-\Delta Hc°)_a(1 - B_b/B_a). \quad (5)$$

For the reaction of isomerization,

$$1,3\text{-butadiene (gas)} = 1,2\text{-butadiene (gas)}, \quad (6)$$

the standard heat of isomerization is

$$\Delta H°(\text{isomerization}) = -(-\Delta Hc°)_a(1 - B_b/B_a). \quad (7)$$

It may be seen from eq 3 and 7 that the heat of isomerization derived by this procedure is not sensitive to the value of E_s or of $(-\Delta Hc°)_a$. The total amount of energy in one experiment is about 60,000 j, and the largest variation in the value of $q_v + q_g + q_i$ is about 150 j. Therefore, an error of 1 percent in the value of E_s, used in eq 3, would cause an error of not more than 0.002 percent in the value of B_b/B_a. This corresponds to an error of 0.01 kcal/mole in the value of $\Delta H°$ (isomerization). Similarly, an error of 0.1 percent in the value of $(-\Delta Hc°)_a$ used in eq 5 would cause an error of 0.01 kcal/mole in the value of $\Delta H°$ (isomerization).

IV. Apparatus

1. Calorimeter Assembly and Thermometric System

The calorimeter assembly used in this investigation was similar to that used in other investiga-

tions in this laboratory [6, 7], with some improvements added. The jacket of the calorimeter was maintained near 27.00° C, at a temperature constant within ±0.002° C, by means of an automatic regulator. In all experiments, the calorimeter uniformly contained 3627.56 ±0.02 g of water, together with the stirrer, platinum resistance thermometer, calorimeter heater, and the glass reaction vessel with its metal support. The stirrer was operated at a substantially constant speed of 276 rpm with a belt drive from a synchronous motor.

The calorimeter heater consisted of about 65 ohms of enameled constantan resistance wire, No. 30 AWG, wound on a Pizein-coated, thin, copper cylinder, the whole covered with Pizein [7].

The thermometer system consisted of a platinum resistance thermometer No. 262,214 and Mueller resistance bridge No. 404 [8].

2. Reaction Vessel

An improved glass reaction vessel was designed and made for this and subsequent investigations involving combustions in a flame at constant pressure. The new reaction vessel is shown in figure 1.

In the combustion of hydrocarbons other than methane and ethane in a flame in a glass reaction vessel, it is necessary to mix some "primary" oxygen with the combustible gas before it reaches the flame, in order to prevent deposition of unburned carbon in the burner tube. For a given rate of flow of the combustible gas, the flame velocity is required to be such that the flame will neither flash back inside the burner tube, nor blow off from the burner tip. For a given combustible gas burning in an atmosphere of oxygen, the position of the flame at the burner tip is determined largely by the amount of "primary" oxygen mixed with the combustible gas. In the previous design of reaction vessel [7], the admixture of primary oxygen was determined largely by the size of the Bunsen openings at the base of the burner tip. The size of the Bunsen openings could be changed only by cutting the reaction vessel apart. As changes were always required for different types of hydrocarbons, this was a cumbersome arrangement. In the new design, the primary oxygen is introduced through a sep-

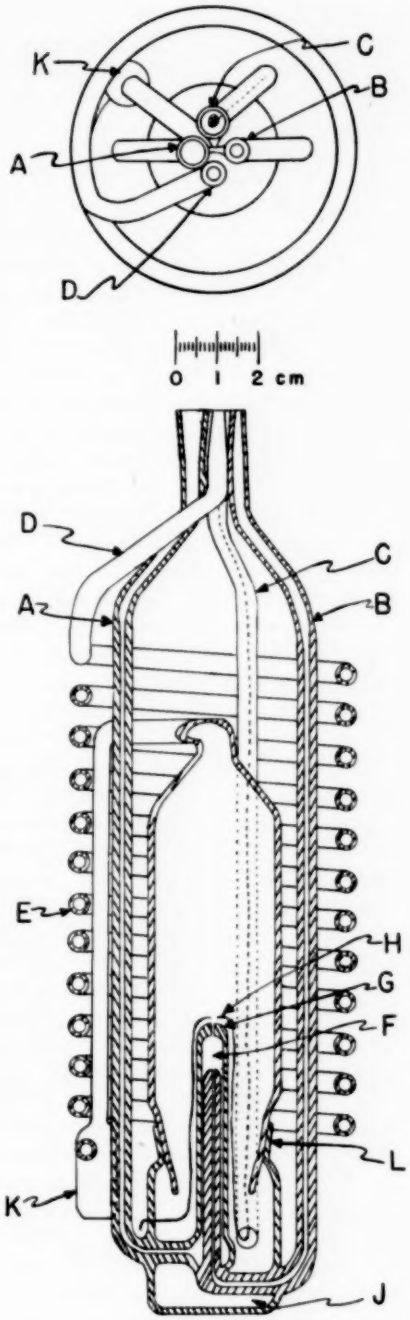

FIGURE 1. *Diagram of the reaction vessel.*

arate line, and the fraction of primary oxygen in the combustible mixture reaching the flame at the burner tip is easily controlled by regulating separately the rate of flow of the combustible gas and of the oxygen.

In the present investigation, a rate of flow of butadiene equal to 29 ml/min (or 0.0012 mole/min) was found to be satisfactory. The primary oxygen was adjusted to produce a blue flame with a sharp inner cone. The primary oxygen supplied about 30 percent of the oxygen requried for complete combustion of the hydrocarbon. The total oxygen (primary plus secondary) was about 150 percent of that required for complete combustion. (In order to avoid possible damage to the glass reaction vessel, preliminary tests of the amount of primary oxygen required for the satisfactory combustion of a given hydrocarbon, at given rates of flow, were made with a similar burner tube made of brass and provided with a glass chimney.)

The method of operation of the new reaction vessel is as follows: The hydrocarbon enters through inlet tube *A*, the primary oxygen through *B*, and the secondary oxygen through *C*. The hydrocarbon and primary oxygen mix in the chamber *F* and emerge through a hole (about 0.5 mm diameter) in the quartz tip *G*. Sparking across the platinum wires *H*, above the tip, ignites the mixture, which burns in a steady flame in the atmosphere of secondary oxygen supplied through the inlet *C*. One of the platinum wires enters through the secondary oxygen inlet tube *C*; the other is grounded to the calorimeter can. The gap between the platinum wires is about 3 mm. The gaseous products of combustion leave the combustion chamber at the top, are cooled to the temperature of the calorimeter in their passage through the glass spiral *E*, and leave the calorimeter through the outlet *D*. Most of the water vapor condenses to liquid, which collects at the bottom of the vessel at *J*, or in the bulb *K*, at the bottom of the spiral. The vessel is constructed to come apart at the joint *L*, to facilitate adjusting the spark gap and cleaning the vessel.

3. Sparking System

A new sparking system was assembled for this investigation. It consisted of a high-tension coil (Delco-Remy 538-z), a condenser having a capacity of 0.2 microfarad, and breaker points operated by a hexagonal cam driven by a synchronous motor having a speed of 1,800 rpm. Four dry cells were used as a source of energy. The spark gap at the burner tip was about 3 mm, and the normal time of sparking was 15 sec.

V. Chemical Procedure

1. Source and Purity of the Butadienes

The sample of 1,3-butadiene used was from a lot of 1,3-butadiene labeled Research Grade, Phillips Petroleum Co. The purity of this material, sampled from the vapor phase, was determined by measurements of freezing points by A. R. Glasgow, Jr. to be 99.83 ± 0.06 mole percent [9].

The 1,2-butadiene used was a sample from the API–NBS series of highly purified hydrocarbons, which are being prepared through a cooperative undertaking of the American Petroleum Institute and the National Bureau of Standards. It was made available through the American Petroleum Institute Research Project 44 at the National Bureau of Standards on "Data on properties of hydrocarbons" and was purified at the National Bureau of Standards by the American Petroleum Institute Research Project 6 on the "Analysis, purification, and properties of hydrocarbons" from material supplied by the Standard Oil Development Co. through W. J. Sweeney. A complete description of the purification and purity of this compound is given by Streiff, Murphy, Zimmerman, Soule, Sedlak, Willingham, and Rossini [10], who reported the purity by measurement of freezing points, to be 99.94 ± 0.05 mole percent.

It is calculated that in the extreme case, the heat of combustion would be affected by less than the following amounts because of the impurities: 0.012 percent for impurities in 1,3-butadiene; and 0.003 percent for impurities in 1,2-butadiene.

The butadiene was withdrawn in the vapor phase from its container, passed through a tube of anhydrous calcium sulfate followed by a small amount of anhydrous magnesium perchlorate to remove traces of water, and fed directly into the reaction vessel in the calorimeter for the combustion.

2. Purification of the Oxygen Used for Combustion

The oxygen used for combustion, including both the primary and secondary streams, was commer-

cial oxygen that was freed of combustible impurities by passage through copper oxide at about 550° C. The oxygen in both lines was freed of carbon dioxide and water before entering the calorimeter by passage through tubes containing, successively, ascarite, magnesium perchlorate, and phosphorus pentoxide.

3. Purity of the Reaction of Combustion

As a check on the purity of the reaction of combustion, both the water and carbon dioxide formed in the combustion were collected and the masses determined for each experiment. In eight combustion experiments with 1,3-butadiene, the mean value of the ratio, r, of one-fourth of the number of moles of carbon dioxide to one-third of the number of moles of water, was found to be 1.00024, with a standard deviation of ± 0.00022. Similarly for six experiments with 1,2-butadiene, the mean value of r was found to be 0.99994, with a standard deviation of ± 0.00019.

Samples of the products of combustion were analyzed for carbon monoxide by the Gas Chemistry Section of this Bureau [11]. In no case was the total amount of carbon monoxide greater than 0.004 percent of the amount of carbon dioxide formed in the combustion.

The effect of any possible incomplete combustion during the ignition or extinction of the flame was eliminated by the procedure, described below, of determining the "ignition" energy in separate experiments in which the flame was allowed to burn only long enough to produce a steady flame, and then was extinguished. With this procedure, the heat of combustion was in reality determined from the portion of the combustion when the flame was in a steady state, any constant errors associated with the ignition and extinction of the flame cancelling out.

4. Determination of the Amount of Reaction

For each calorimetric combustion experiment, the amount of reaction was determined from the mass of carbon dioxide formed, taking 1 mole or 44.010 g of carbon dioxide as equivalent to one-fourth mole of butadiene.

VI. Calorimetric Procedure

1. Calorimetric Combustion Experiments

The following procedure was followed in preparing the calorimeter for all experiments: The calorimeter jacket was brought to temperature, near 27.00° C, where it was automatically maintained constant, within about ± 0.002° C, throughout the whole experiment. The standard mass of water, 3627.56 ± 0.02 g, was weighed into the calorimeter can on the pan of a 5-kg balance, having a sensitivity at this load of 0.008 g per scale division, using the same weights in all experiments. The calorimeter can was placed in the calorimeter jacket, the dry reaction vessel with the heater around it was lowered into the can, the cover was placed on the can, the jacket was covered, the stirrer was connected, and the platinum resistance thermometer inserted into the calorimeter can through the hole in the jacket cover. The hydrocarbon and primary and secondary oxygen lines were connected to the reaction vessel through flexible glass spirals. The weighed absorption tubes for water and carbon dioxide, a guard tube containing magnesium perchlorate and ascarite, a sampling bulb, and a flowmeter were connected to the outlet side of the reaction vessel through a three-way stopcock near the vessel. This stopcock permitted oxygen to bypass the reaction vessel at the end of a combustion to flush any water and carbon dioxide in the lines into the absorption tubes. The calorimeter was brought to near the starting temperature by electrical heating, and a period of about 20 min was allowed for equilibrium to be established. The calorimetric observations were begun when the calorimeter reached the selected starting temperature. The standard temperature rise was about 4 degrees for the combustion experiments, and the final temperature was slightly below the jacket temperature.

The calorimetric observations during an experiment consisted of: (a) a fore period of 20 min during which the reaction vessel, containing oxygen at atmospheric pressure, remained closed, and readings of the resistance of the platinum thermometer were taken every 2 min; (b) a "reaction" period during which the reaction took place, with a period allowed for equilibrium to be reestablished in the calorimeter, and during which readings of the resistance of the platinum thermometer were taken about every 15 sec or every minute, depending on the shape of the time-temperature curve; and (c) an after period of 20 min during which the reaction vessel remained closed, the calorimeter temperature was slightly

below the jacket temperature, and readings of the resistance of the platinum thermometer were taken every 2 min.

The manipulation of the apparatus controlling the reaction during a combustion experiment was as follows: Before the calorimetric experiment, the two absorption tubes for water and carbon dioxide were flushed with hydrogen and weighed by a method previously described [12, 13, 14]. The hydrocarbon inlet tube was flushed with helium to remove oxygen from this line and the rest of the reaction vessel then flushed and left filled with oxygen at atmospheric pressure. During the fore period, the rates of flow of the primary and secondary oxygen and gaseous hydrocarbon were regulated through bypass flowmeters. At the end of the fore period, the three-way stopcock outlet on the reaction vessel was opened to the absorption tubes, the primary and secondary streams of oxygen were turned into the vessel, the spark was turned on, and the hydrocarbon was then turned into the vessel. The sparking was continued for 15 sec, or until the flame was started, as indicated by the flowmeter at the end of the line. The flame was allowed to burn until a final temperature slightly below the jacket temperature was reached, when the flame was extinguished by turning off the hydrocarbon. The time of combustion was usually about 22 min. The primary and secondary streams of oxygen were left on for an additional 10 min and then cut off. The reaction vessel was closed by setting the three-way stopcock at the outlet such that the oxygen would bypass the reaction vessel but would flow through the absorption tubes. Thus, all the water vapor not in the calorimetric reaction vessel was swept into the absorption tube. An additional period of about 6 min was allowed for equilibrium to be established before starting the after period. After the experiment, the absorption tube for water was flushed with hydrogen and weighed to obtain the amount of water carried out of the calorimeter as vapor. The absorption tubes were replaced on the train and the reaction vessel flushed with oxygen overnight to carry all the water and carbon dixoide into the absorption tubes. Both tubes were then flushed with hydrogen and weighed. The mass of carbon dioxide produced was used to determine the amount of reaction, and the stoichiometric ratio of the masses of carbon dixoide and water was used to check the purity of the reaction of combustion.

The corrected increase in temperature of the calorimeter system, ΔRc, expressed as the increase in resistance in ohms of the given platinum thermometer at a mean temperature of 25° C, was taken as the difference in the resistance of the thermometer between the beginning of the after period and the end of the fore period, corrected for heat of stirring and thermal leakage [15].

2. Determination of the "Ignition" Energy

Experiments to determine the energy associated with the ignition and extinction of the flame ("ignition" energy experiments) were performed in the same manner as the regular combustion experiments, except that the flame was allowed to burn only long enough to be sure a steady flame was attained. The flame was usually left burning for about 40 seconds. The initial temperature in these experiments was a fraction of a degree below the jacket temperature, and the rise of temperature was about 0.1 deg. Experiments were also performed in which only sparking energy was added to the calorimeter.

The mean value for the "ignition" energy, which is the energy associated with the process of ignition and extinction of the flame, but not including any part of the heat of combustion, obtained from seven experiments with 1,3-butadiene and two experiments with 1,2-butadiene, with an average of 0.0005 mole of butadiene burned in each experiment, was found to be 33.1 j, with a standard deviation of ± 2.8 j. In separate experiments in which no hydrocarbon was burned and sparking alone for the standard time occurred, the sparking energy was found to be 31.1 j with a standard deviation of ± 0.8 j. In making these calculations, the value of E_s, the standard energy equivalent, was taken as 154,446 abs j/ohm.

For the present experiments, the ignition energy for the standard time (15 sec) of sparking was taken as the weighted mean of the foregoing values, 31.3 j with a standard deviation of 0.8 j.

3. Reduction to the Standard Calorimetric Process

The process that actually takes place in the calorimetric reaction vessel during a combustion experiment is the following:

$$n\mathrm{C_4H_6}(\mathrm{gas},\ 1\ \mathrm{atm}, t_r)+(m_1+m_2+m_3)\mathrm{O_2}\ (\mathrm{gas},\ 1\ \mathrm{atm}, t_r)=[r\mathrm{CO_2}+m_2\mathrm{O_2}+b\mathrm{H_2O}]\ (\mathrm{gas},\ 1\ \mathrm{atm}, t_m)+[m_3\mathrm{O_2}+c\mathrm{H_2O}](\mathrm{gas},\ 1\ \mathrm{atm}, t_f)+(a-b-c)\mathrm{H_2O}(\mathrm{liq},\ 1\ \mathrm{atm}, t_f). \quad (8)$$

The energy evolved in this reaction and including the ignition energy is $q=E_s\Delta R_c$. In the foregoing equation, t_r is the temperature of the room; t_m and t_f are the mean and final temperatures, respectively, of the calorimeter; n is the number of moles of hydrocarbon entering the calorimeter; $(m_1+m_2+m_3)$ is the number of moles of oxygen entering the calorimeter; $m_1=\frac{11}{2}n$ is the number of moles entering during the actual combustion period and being used in the combustion; m_2 is the excess number of moles entering during the actual combustion period and leaving the calorimeter as a mixture with $r=4n$ moles of carbon dioxide and b moles of water vapor; m_3 is the number of moles of oxygen entering the calorimeter during the flushing immediately following the actual combustion period and leaving the calorimeter as a mixture with c moles of water vapor; $(a\text{-}b\text{-}c)$ is the number of moles of water left in the calorimeter in the liquid state; and $a=3n$ is the total number of moles of water formed in the combustion. The quantity c also includes a very small amount of water left in the calorimeter in the gaseous state.

It is desirable to correct the results of each calorimetric experiment to a common basis for comparison. This can be done by adjusting all results to the basis of a "standard calorimetric process" defined by the equation

$$n\mathrm{C_4H_6}(\mathrm{gas},\ 1\ \mathrm{atm},\ t_{25})+(m_1+m_2)\mathrm{O_2}\ (\mathrm{gas},\ 1\ \mathrm{atm},\ t_{25})=[r\mathrm{CO_2}+m_2\mathrm{O_2}](\mathrm{gas},\ 1\ \mathrm{atm},\ t_{25})+a\mathrm{H_2O}(\mathrm{liq},\ 1\ \mathrm{atm},\ t_{25}) \quad (9)$$

The energy evolved in this reaction is q_c.

For the present experiments the various quantities have the values

$$m_1=\frac{11}{2}n,\ m_2=\frac{11}{4}n,\ r=4n, \text{ and } a=3n.$$

The difference between the energy, q_c, evolved in the standard calorimetric process expressed by eq 9, and that evolved in the actual calorimetric process expressed by eq 8, but including the energy of ignition, is $q_c-q=-(q_s+q_r+q_i)$.

The energy associated with the adjustment of the composition of the carbon dioxide-oxygen mixture issuing from the calorimeter in the individual experiments to the average composition as expressed in the "standard calorimetric process" is negligible. The quantities q_s and q_r were evaluated by the relations:

$$q_s=\mathrm{C_1}[n(t_r-t_{25})]+\mathrm{C_2}[m_1(t_r-t_{25})+m_2(t_r-t_m)+m_3(t_r-t_f)]+\mathrm{C_3}[b(t_{25}-t_m)+c(t_{25}-t_f)]+\mathrm{C_4}[(a-b-c)(t_{25}-t_f)]+\mathrm{C_5}[r(t_{25}-t_m)],$$

$$q_r=-(b+c)[\Delta Hv];$$

where $\mathrm{C_1}=80.1$, $\mathrm{C_2}=29.4$, $\mathrm{C_3}=33.6$, $\mathrm{C_4}=75.3$, and $\mathrm{C_5}=37.1$ are the approximate heat capacities of butadiene(gas), oxygen(gas), $\mathrm{H_2O}$(gas), $\mathrm{H_2O}$(liq), and $\mathrm{CO_2}$(gas), respectively, in j/deg mole, and $\Delta Hv=43{,}992$ abs j/mole is the heat of vaporization of water at 25° C and saturation pressure.

To obtain the values of the standard heat of reaction, $\Delta H°$, from the standard calorimetric process indicated by eq 9, it is only necessary to take account of the change in heat content with pressure at constant temperature for each gas from its given pressure to zero pressure, so that each substance will have the heat content of the thermodynamic standard state. Since this correction will not be significantly different for the two isomers, the ratio of the values of ΔH for the standard calorimetric process will also be the ratio of the values of $\Delta H°$ for the standard thermodynamic process.

VII. Results of the Present Investigation

The results of the calorimetric combustion experiments for 1,3-butadiene and 1,2-butadiene are given in tables 1 and 2, respectively. For these calculations, the value of E_s, the energy equivalent, was taken as approximately 154,446 j/ohm. The value of B were calculated from eq 3.

TABLE 1. *Results of calorimetric combustion experiments on 1,3-butadiene*

Experiment	ΔR_c	Mass of carbon dioxide	q_2	q_3	q_4	B	Deviation from mean
	Ohms	*g*	*j*	*j*	*j*	*Ohms/g* CO_2	*Ohms/g* CO_2
1	0.388048	4.17091	+16.5	−342.3	31.3	0.0934941	−0.0000514
2	.381756	4.10179	−2.4	−331.2	31.3	.0935478	+.0000023
3	.381025	4.09487	+0.1	−360.3	31.3	.0935695	+.0000240
4	.397671	4.27289	−2.8	−355.4	31.3	.0935637	+.0000182
5	.384888	4.13689	−16.8	−352.2	31.3	.0935695	+.0000240
6	.390584	4.19985	−18.6	−362.7	31.3	.0935390	−.0000065
7	.391438	4.20192	−23.9	−236.5	31.3	.0935099	−.0000356
8	.378484	4.07076	−17.2	−389.7	31.3	.0935735	+.0000280
Mean						0.0935455	
Standard deviation of the mean						±.0000104	

TABLE 2. *Results of calorimetric combustion experiments on 1,2-butadiene*

Experiment	ΔR_c	Mass of carbon dioxide	q_2	q_3	q_4	B	Deviation from mean
	Ohms	*g*	*j*	*j*	*j*	*Ohms/g* CO_2	*Ohms/g* CO_2
1	0.384743	4.04783	−13.2	−304.9	31.3	0.0955079	−0.0000048
2	.380613	4.00684	−5.5	−345.8	31.3	.0955080	−.0000047
3	.388498	4.09171	−10.1	−368.8	31.3	.0954977	−.0000150
4	.395315	4.16322	−7.7	−383.4	31.3	.0955137	+.0000010
5	.397521	4.18337	−10.8	−352.4	31.3	.0955377	+.0000250
6	.388279	4.08829	−16.6	−354.3	31.3	.0955112	−.0000015
Mean						0.0955127	
Standard deviation of the mean						±.0000055	

From these data, the ratio of the heat of combustion of 1,2-butadiene to that of 1,3-butadiene is

$$(-\Delta Hc^\circ)_b/(-\Delta Hc^\circ)_a = B_b/B_a = 1.021029 \pm 0.000256. \quad (14)$$

The values previously reported [1] for the heats of combustion and formation of 1,3-butadiene (gas) are

$$C_4H_6(1,3\text{-butadiene, gas}) + \frac{11}{2}O_2(\text{gas}) =$$
$$4CO_2(\text{gas}) + 3H_2O(\text{liquid}), \quad (15)$$
$$-\Delta Hc^\circ_{298.16} = 607.91 \pm 0.23 \text{ kcal/mole.}$$

$$4C(c, \text{graphite}) + 3H_2(\text{gas}) =$$
$$C_4H_6(1,3\text{-butadiene, gas}),$$
$$\Delta Hf^\circ_{298.16} = 26.75 \pm 0.23 \text{ kcal/mole.} \quad (16)$$

The heat of isomerization at 25° C thus becomes (from eq 7):

$$1,3\text{-butadiene (gas)} = 1,2\text{-butadiene (gas)} \quad (17)$$
$$\Delta H^\circ \text{ (isomerization)} = 12.78 \pm 0.16 \text{ kcal/mole.}$$

The heats of combustion and formation of 1,2-butadiene become:

$$C_4H_6(1,2\text{-butadiene, gas}) + \frac{11}{2}O_2(\text{gas}) =$$
$$4CO_2(\text{gas}) + 3H_2O(\text{liquid}), \quad (18)$$
$$-\Delta Hc^\circ_{298.16} = 620.69 = 0.28 \text{ kcal/mole.}$$

$$4C\ (c, \text{graphite}) + 3H_2(\text{gas}) =$$
$$C_4H_6(1,2\text{-butadiene, gas}),$$
$$\Delta Hf^\circ_{298.16} = 39.53 \pm 0.28 \text{ kcal/mole.} \quad (19)$$

VIII. References

[1] E. J. Prosen and F. D. Rossini, J. Research NBS **34,** 59 (1945) RP1628.

[2] E. F. Mueller and F. D. Rossini, Am. J. Phys. **12,** 1 (1944).

[3] Selected Values of Chemical Thermodynamic Properties. National Bureau Standards. Values of Constants. (December 31, 1947.)

[4] G. P. Baxter, M. Guichard, and R. Whytlaw-Gray, J. Am. Chem. Soc. **69,** 734 (1947).

[5] F. D. Rossini and W. E. Deming, J. Wash. Acad. Sci. **29,** 416 (1939).

[6] E. J. Prosen and F. D. Rossini, J. Research NBS **27,** 289 (1941) RP1420.

[7] F. D. Rossini, BS J. Research **12,** 735 (1934) RP686.

[8] F. D. Rossini and J. W. Knowlton, J. Research NBS **19,** 249 (1937) RP1024.

[9] A. R. Glasgow, Jr., N. C. Krouskop, J. Beadle, G. D. Axilrod, and F. D. Rossini, Anal. Chem. **20,** 410 (1948).

[10] A. J. Streiff, E. T. Murphy, J. C. Zimmerman, L. F. Soule, V. A. Sedlak, C. B. Willingham, and F. D. Rossini, J. Research NBS **39,** 321 (1947) RP1833.

[11] M. Shepherd, Anal. Chem. **19,** 77 (1947).

[12] E. J. Prosen and F. D. Rossini, J. Research NBS **33,** 255 (1944) RP1607.

[13] F. D. Rossini, BS J. Research **6,** 1 (1931) RP259.

[14] F. D. Rossini, BS J. Research **6,** 37 (1931) RP260.

[15] J. R. Eckman and F. D. Rossini, BS J. Research **3,** 597 (1929) RP111.

WASHINGTON, October 29, 1948.

U. S. Department of Commerce
National Bureau of Standards

Research Paper RP1969
Volume 42, March 1949

Part of the Journal of Research of the National Bureau of Standards

Optical Glass of Interferometer and Schlieren Quality for Wind-Tunnel Optics

By Leroy W. Tilton

Large disks for wind tunnels should be uniform in optical thickness within $\pm 1/16\ \lambda$ if highest accuracy in measurements by interference fringes is to be insured. This means that heterogeneities in the glass shall be less than $\pm 5 \times 10^{-7}$ in refractive index for thicknesses of 3 or 4 centimeters. Evidence is cited to show that differences in chemical composition in good glass may not prevent realization of the desired uniformity, and that stress birefringence cannot be an important preventing factor. The remaining source of nonuniformity in glass is the existence of temperature gradients during annealing that can cause changes in structure, and it has been found that these can be reduced within required limits simply by encasing the glass, during annealings, in a sufficient number of concentric boxes composed of alternately heat-conducting and insulating layers.

I. Introduction

Demands for large interferometer plates (beam splitters) and large windows for schlieren apparatus have occasioned renewed interest in the existing degree of uniformity of optical glass and in possible improvements. Because of imperfections in glass, the figuring of optical surfaces has often been employed, especially when linear apertures are to be large as in the larger astronomical objectives, and when the optical path in the glass must be long as is the case in some large prisms. Figuring procedures were sometimes found necessary, because the optical performance was otherwise poor and unacceptable.

Figuring, or local repolishing, of optical surfaces is done only by expert artisans, perhaps artists in a way, and as we progress in modern methods of the design and construction of optical systems, it becomes increasingly difficult to find experienced men who can undertake figuring with confidence. Consequently the glass makers have been and are improving the quality of their product, but they cannot be expected to do so in advance of widespread demands for glass of better quality.

The quality of optical glass is commonly judged by its freedom from color, seeds, stones, feather, striae, and other plainly visible defects and also by its freedom from internal stresses as indicated by tests for birefringence. Usually, glass that is rated high in these respects has been found by the tests of actual use to be satisfactory in many precise optical instruments, and it has been generally believed that exceptions were caused by inherent nonuniformity in chemical composition. The work of Tool [1][1] and his associates at this Bureau has shown, however, that glass may be physically inhomogeneous, because of temperature gradients that existed during heat treatment, and still show little or no stress birefringence and be quite uniform in chemical composition. As a result some previous failures can be explained, it is possible to successfully retreat and recondition some elements that have failed in optical performance, and best of all steps can be indicated that will lead to much better uniformity in the refractivity of glass.

For some purposes, refractive uniformity may be desirable for a given type of glass that is produced over long periods, as the successive pots are made, or it may be necessary merely that many small pieces from a given pot of glass shall be equally refractive. In these cases, there is no problem in testing the degree of the existing uniformity that is attained. In single large pieces of

[1] Figures in brackets indicate the literature references at the end of this paper.

822521—49——6

glass, however, we have no completely satisfactory way of knowing just what degree of refractive uniformity exists. Optical homogeneity is not assured by freedom from birefringence and visible defects. Interference methods of investigating homogeneity become very difficult when the thickness of glass exceeds 2 or 2½ in., because the fringes formed by reflections from the surfaces involve such a large difference in equivalent air path, namely $2nt$, that they are indistinct and have seldom or never been accurately and quantitatively observed. Prism methods of measuring the differences in refractivity require depletion or destruction of the blanks, or else yield merely some sort of an average value for long paths in the glass.

II. Permissible Phase Differences

Strict tolerances in uniformity of optical glass become progressively more important as activities in the optical industry become less a matter of individual skill and thus approach the American ideal of standardization for mass production. In general, the designers' tolerances, whether concerned with the usual instruments for taking precision observations or with the exacting requirements of certain fixed-focus instruments, are comparatively liberal. They relate chiefly to intermelt and interblank uniformity rather than to the intrablank homogeneity that is of importance in wind-tunnel optics.

In setting tolerances in optical uniformity, it is generally assumed that heterogeneity of refracting media of optical systems can be tolerated unless a noticeable amount of aberration is introduced, that is, an amount which results in something short of "best definition" as judged, usually, by the observation of the diffraction pattern of a "point" source. For this limiting condition, Rayleigh [2] placed the limiting departure from true sphericity of wave front at 1/4-λ phase difference. At this limit the "aberration begins to be decidedly prejudicial." But Rayleigh considered only certain types of aberration, and it is possible that other types might necessitate a less liberal tolerance. Very little is known precisely concerning the actual defects in imagery that may be produced by irregular refractivity in lens systems.

Chalmers [3] found that in practice the figuring of small objectives is employed to reduce path differences to 1/5 λ (±1/10 λ from the mean) or less to meet the requirements of definition. As a result of an experimental study of the distribution of intensities near a focus, Martin [4] concludes that "to secure the placing of the full amount of light into its correct place in the image such phase residuals should be brought within 1/6 λ at the best visual focus". This is fairly in accord with the suggestion of Conrady [5] that "for instruments of the highest quality the limits should be reduced to 1/6 or even 1/8 of a wave-length", because with the classical Rayleigh limit, "there is in every case a decided loss of contrast in the image of an extended object". Elsewhere [6] the same author has considered the requirements for depth of focus and focal range without serious loss of definition. He concludes that it is desirable to keep the residuals of aberration well below the limit set by the requirements of definition and contrast at any one definite focus. For maximum focal range, zero phase difference would be required, but values of 1/8 and 1/16 λ are mentioned by Conrady as limits of phase difference at which the discrepancies between maximum and realized focal range are "unimportant" and "quite insensible", respectively. This is of importance in microscopy with high numerical apertures, especially for projection and photographic methods.

So far, only resolution and contrast have been implicitly considered in relation to definition. Wadsworth, [7] however, has emphasized the importance of accuracy as an element of good definition (using the latter term in the broad sense), which is often of more importance than either resolution or contrast. He finds the requirements for "metrological power" more exacting than those for either resolving or delineating power. For instruments intended for *maximum accuracy of measurement*, he concludes that the differential distortion of those wave fronts that form simultaneous or successive images on which settings are to be made must not exceed one-fourth of that which would affect good optical definition according to Rayleigh. That is, Wadsworth places the phase difference limit at 1/16 λ instead of 1/4 λ as did Rayleigh. It is owing to slight shifts of the distribution of energy in the diffraction pattern that error can arise from such small aberration, and if the effect is constant between successive measurements, then a *difference* of such measurements, which

frequently is all that is desired, is of course free from such error. But after an examination of the conditions under which such small aberrations are constant, Wadsworth decides that it is impossible in all cases to secure such conditions and that the only entirely safe procedure is to reduce the phase differences themselves to the small value of 1/16 λ. This, probably, is the desirable phase tolerance in some applications of wind-tunnel optics.

III. Effects of the Distribution of Heterogeneity

In order to decide upon the degree of heterogeneity permissible without violation of a given degree of phase uniformity, it is necessary to consider the distribution of the departure from the average optical density of the refracting media. Some useful ideas, directly applicable to a consideration of wind-tunnel optics, are obtained from an examination of a few simple cases:

(1) For any optical component having plane surfaces (i. e., producing zero effect on the vergence of transmitted light), a small uniform transverse optical density gradient will introduce no appreciable aberration but merely a deviation in the direction of propagation of the wave.

(2) For any optical component, a more or less concentric and systematically progressive index gradient from center to periphery may produce chiefly longitudinal and symmetrical aberration that can usually be partially eliminated by refocusing of the viewing system.

(3) If the distribution of abnormal density is somewhat irregular it is quite possible that, of the total aperture, certain moderately large [2] areas are covered with glass of different average index from that of other large areas. In some such cases the result can be almost entirely one of asymmetrical aberration, the amount being the maximum that can result from the index deviations present.

Even in case (3), however, it may happen that some hypothetical regular transverse index gradient from center to edge can approximate the existing nonuniformities and thus permit amelioration of the irregular effects by simple orientation and refocusing.

IV. An Index-Heterogeneity Tolerance

In any event, it is useful to establish the index-heterogeneity tolerance corresponding to the residual effects referred to under case (3). If two rays traverse paths of equal length, a, through glasses of indices n' and n'', respectively, the numbers of wavelengths are

$$N' = \frac{an'}{\lambda},$$

and

$$N'' = \frac{an''}{\lambda},$$

whence the optical path difference is

$$(N'' - N') = \frac{a(n'' - n')}{\lambda},$$

where λ is the wave length in air. If $(n'' - n')$ be expressed as $2\Delta n$, n being the average index of the glasses, and $(N'' - N')$ be expressed as $2\Delta N$, where $\pm\Delta n$ and $\pm\Delta N$ are deviations from the mean values of n and N, then for any given tolerance in phase, $2\Delta N$ (maximum phase difference), the corresponding tolerance in index (departure from the mean) is expressible as

$$\Delta n = \pm\frac{\Delta N \lambda}{a}.$$

For a glass thickness of 1 cm, table 1 shows the corresponding values of Δn computed according to the Rayleigh and also to the Wadsworth limit for a few frequently used wavelengths.

TABLE 1. *Suggested maximum permissible phase differences and corresponding homogeneity tolerances in Δn for 1-cm glass path*

Phase difference, $2\Delta N$	Tolerances in refractive index, Δn				
	C 6,563 *A*	*D* 5,893 *A*	*F* 4,861 *A*	*g* 4,358 *A*	*h* 4,047 *A*
¼	±0.000008	±0.000007	±0.000006	±0.000005	±0.000005
1/16	±.0000021	±.0000018	±.0000015	±.0000014	±.0000013

Considering, on one hand, the smallness of these index differences in comparison with those known to exist in many glasses, and, on the other, the known degree of perfection attained in many optical systems, sharp disparity appears, but

[2] It is necessary to distinguish this case from that which usually obtains when striae or other local abrupt changes in density are present. (See A. Arnulf, Rev. D'Optique **6**, 2 (1927). In glass of good quality these can affect only small proportions of the total apertures, unless the latter are themselves small, as in microscope objectives. Consequently, the intensity of the out-of-phase light due to striae is in general so small a proportion of the total that the noticeable effects are of a much smaller order than those to be referred to in this discussion.

several considerations may be mentioned to show that no inconsistency necessarily exists.

In the first place the tolerances correspond only to case (3), that of the most unfavorable of the possible distributions of index heterogeneity. Secondly, excellence of performance is quite frequently judged by the relatively easily attained standard of theoretical resolving power, based on ¼-λ phase difference. Even a phase difference as large as ½ λ does not always entirely prevent resolution [8]. Furthermore, the really exacting tests, involving the accuracy of measurements carried out under conditions requiring constancy of aberration are seldom made. Wadsworth treated some cases of this kind in detail. The heliometer and the spectrograph are examples where varying portions of the apertures of the optical components come into use for the different measurements. Varying angular presentation of the wave front to the optical surfaces is one of the most commonly encountered conditions of a nature giving opportunity for exact tests. This occurs whenever the telescope is used for measurements on images having considerable angular separation in the field of view and in the use of cameras for airplane mapping. But in most such cases, even the errors of design are not reduced to negligible proportions, and exact tests are not made because the calibration is relied upon to include also the errors of material and workmanship, or because null methods are used to eliminate all error, as in the test for the Einstein effect.

Another matter to be mentioned in this connection is the part played by the skilled craftsman in the use of imperfect materials, as already referred to in the introduction to this paper. This consideration is probably of greater importance than those already named and indeed, in itself, may be a sufficient explanation of the bridging of the gap between the required and the attained degree of optical homogeneity of refracting media.

V. Causes of Nonuniformity in Refractivity of Glass

A priori, variations in chemical composition would seem to be the causes of nonuniform index in "well annealed" optical glass, and such views predominated until it was shown [9] conclusively that the index differences in good annealed optical glass can be greatly reduced by reannealings in which more care is taken to have uniformity of temperature in the glass during the annealing processes. In short, it was discovered that thermally induced inhomogeneity could be present without appreciable accompanying birefringence. Assuming that the chemical composition varies in glass so as to produce somewhat vaguely delimited regions (relatively very large as compared to striae) having different indices, then a blank made from such glass can pass all usual tests and be regarded as homogeneous, unless prism tests of index are made from several peripheral portions of the blank.

A similar condition of potentially dangerous and vaguely delimited inhomogeneity can occur because of temperature gradients that exist in the furnace during annealing. Prior to demands for large components for wind-tunnel optics, there appeared no necessity for using extreme care to eliminate these small temperature gradients. Consequently, it is impossible to say to what further extent the uniformity of glass may be improved, or to what extent a residual variation in chemical composition may exist. The part that is thermal in origin can be erased by still greater care in heat treatment, but that of chemical nature probably presents more serious problems. Reports made on the degree of homogeneity of glass without quantitative appreciation of the direct effects of nonuniform heat treatment are of little value for estimating the attainable degree of uniformity.

VI. Stress Birefringence

The subject of strain still plays such a prominent part in discussions of annealing that it is necessary, especially in view of the high standards of homogeneity that seem really desirable, to determine some quantitative measures of its contribution to optical heterogeneity. The birefringence that it causes is a commonly used measure of the internal stress producing the strain, and it would seem desirable if possible to continue to use the same indicator as a measure of the lack of homogeneity [3] thus occasioned.

[3] For the sake of clearness it seems necessary to observe that it is of course true that any piece of glass in which strain exists is as a whole a balanced system involving both compressions and tensions so that in a certain sense the index changes produced, being of opposite sign, offset each other. But portions of the glass showing definite birefringence of a given sign experience a corresponding change in index, and such portions of the medium may be legitimately considered to the exclusion of other portions, because such procedure enables us to arrive at an estimate of the lack of homogeneity arising or existing *in situ* in a large optical component.

The use of Neumann's [10] equations is so well known through the work of Pockels [11], that it is unnecessary to give details of the derivation of the equation for expressing the absolute birefringence, $(n_y - n_z)$, in terms of the unidirectional thrust, P, and certain constants of the glass. As written by Adams and Williamson [12], it is

$$(n_y - n_z) = \frac{nP}{E}(1+\sigma)\left(\frac{q}{r} - \frac{p}{v}\right), \tag{1}$$

where the constants of the glass are, E, Young's modulus; σ, Poisson's ratio; n, the index of refraction of the unstrained medium in which the velocity of light is r; whereas p and q are coefficients determined experimentally. The subscripts y and z appended to the symbol n represent the indices of the medium for light vibrating in planes parallel and perpendicular, respectively, to the direction of the thrust. This equation was obtained by subtraction, from the equations

$$(n_y - n) = \frac{nP}{E}\left(-2\sigma\frac{p}{r} + \frac{q}{r}\right), \tag{2}$$

and

$$(n_z - n) = \frac{nP}{E}\left[(1-\sigma)\frac{p}{r} - \sigma\frac{q}{r}\right]. \tag{3}$$

From eq 1 it is evident that when $p=q$ (which, as Pockels showed, occurs with a flint glass containing about 74% of PbO), no amount of unidirectional pressure is sufficient to produce birefringence. But eq 2 and 3 indicate that in such cases there are, nevertheless, certain index changes (unless $\sigma=0.50$ as for an incompressible fluid, or unless $p=q=0$). Thus it might seem that Pockels' work should be extended before it can safely be assumed that no other glasses exist that are exceptional in this respect. Certainly it seems evident that birefringence is not in general a thoroughly reliable quantitative measure of index changes produced, either by external pressure or internal stress, the sensitivity of such a test decreasing as it is used on glasses whose compositions approach that of a glass having the exceptional property described.

On the other hand, the measurements of birefringence that have been made by Pockels, Filon [13], and Adams and Williamson [14] on a combined total of 24 optical glasses, show a small and regular variation giving little or no indication of the existence of other compositions having the remarkable properties referred to in the case of the 74-percent-PbO glass. Circumstances thus seem to warrant a continuation of the use of birefringence as a qualitative measure of strain in all of the usual types of glass, except high-index flints included within the approximate limits of index 1.8 to 1.9, and also its extension to the qualitative measurement of the change in index so produced.

By the use of eq 2 and 3, and assuming reasonable upper limits of tensile strength, it is possible to arrive at some idea concerning the order of magnitude of the index changes that internal stresses may cause. In this way, it can be shown that strain could never have produced more than a fraction of the lack of homogeneity, which has been commonly attributed thereto. Also, it may be seen that the present practice of annealing to reduce birefringence to 5 or 10 mμ/cm is ample [15] (with possible exception of indices 1.8 to 1.9) for the elimination of strain effects on index to a degree consistent with the most exacting of previous requirements of optical uniformity. On the other hand, in the absence of extensive tests on the character and magnitude of surface deformation that may result from the presence and gradual release of strain, it cannot definitely be said that the present standards of stress removal are unnecessarily high.

VII. Chemical Heterogeneity

After publication of Eckert's work [16], it appeared that the intrinsic heterogeneities in optical glass were not necessarily as large as previously supposed. Briefly, the result bearing on the present question of intrabland homogeneity was his intramelt spread of only 2×10^{-5} in refractive index within each of three melts. This was soon confirmed, for glass of European origin, by the reannealing of certain lens blanks at this Bureau [9]. According to this report, the chemical intramelt index variations among six random samples from a single melt were confined to a few units of the sixth decimal place. Such a high degree of chemical homogeneity, if found in all types of optical glass, will mean that with proper heat treatment the ideal of homogeneous refracting media of standardized index is attainable.

Some interesting evidence bearing on this subject is to be obtained from use of the interference method of testing a glass melt for uniformity as described by Dalladay and Twyman [17]. Their

procedure is in reality a test of the chemical heterogeneity only because, as pointed out by Lebedeff [18], the reannealing of the composite block insures the canceling of physiochemical effects. Consequently the high degree of homogeneity that these investigators found is also encouraging evidence of possible chemical uniformity.

Precise data on the index uniformity of samples taken from pots of optical glass were determined at this Bureau [19] on six types of optical glass. In each case 10 prisms were cut after recording their relative positions and linear separations in two or three dimensions. After precise index measurements by the method of minimum deviation, it was possible to compute approximate index gradients in the original larger pieces of each type of glass from which the individual prisms were taken. These gradients ranged in value from 6 to 49 x 10^{-6} per decimeter but, in general, it was found that the gradients were roughly proportional to the changes that can be produced in the refractive indices of these glasses by heat treatment. Moreover, in each case, as might be inferred from the facts as stated, two prisms of each melt having maximum difference in index were annealed together in the same furnace, and their index differences were thereby very materially reduced. Since the original differences were themselves in the fifth decimal place, it was indicated that the chemically caused variations must indeed be small in the sixth decimal over distances of a decimeter in the glass.

Recently, 10 2-in. cubes of borosilicate glass were annealed at this Bureau and, for each of the three orthogonal directions, the "average" index along each of 24 paths through 2 in. of glass was compared with that for a similar average central path through the face centers. This was done on a Twyman-Green interferometer by the method that Twyman [20] has recommended for thin plates. The surfaces are very good but need not be perfect, and the near parallelism is adjusted to give a convenient number of fringes. By transmitted light each fringe delineates the path corresponding to constancy of $2(n-1)t$ whereas, by shielding both mirrors, one can see fringes of constancy of $2nt$. In other words, in these two cases the fringes are different functions of n, the average index of refraction of the glass along the glass path that is traveled. If a cube of homogeneous glass ($\Delta n=0$ from path to path through a perfect cube) is slightly thicker at one edge, then the number of fringes seen by reflection and by transmission must be in the ratio $n/n-1$. Any other value of this ratio shows at once that the glass is inhomogeneous. Both Δt and Δn may be evaluated and the corresponding contours plotted with respect to any arbitrarily selected path. The index differences found for each of the three faces of one of the cubes were ± 2.5, ± 3, and $\pm 4 \times 10^{-6}$, but the average for 27 faces of the 9 other cubes was only $\pm 1 \times 10^{-6}$.

VIII. Temperature Gradients in Annealing Furances

The desirability of uniformity of heat conditions in annealing was stressed at this Bureau even before the true nature of the thermal effects was fully realized [21]. For the annealing of optical components for use in wind tunnels, the necessity of uniform temperature conditions must now be stressed with multiple emphasis. At the same time there is one fortunate alleviating feature. Whereas, when thinking in terms of strain alone, relatively slight fluctuations were considered important, especially during cooling through certain temperature ranges, now [22], it is plain that, considering temperatures in the annealing range, only an *integrated effect* is of highest importance for optical uniformity. Consequently it is suggested that the best way of investigating effective deleterious furnace gradients is by measurement of the index heterogeneity actually impressed on small prismatic samples of the glass, which can be located at various places in the furnace while annealings are in progress.

It is by means of this method that it is sometimes possible to analyze index data, post mortem, and get useful information concerning the effective temperature gradients that existed in the annealing furnaces that were used. For example, from the data that Eckert published it is possible to infer that furnace temperature differences during his fine annealings were as large as 1 or 3° C over the unknown linear distances that may have been involved. Temperature differences of this order, or greater, over distances of 10 to 30 cm have probably existed during almost all of the best annealings until very recently. Their possible maximum effects can easily be estimated

from the list of equilibrium temperature coefficients of refractivity that have been determined at this Bureau for 21 optical glasses. They range from 20 to 60×10^{-6} for various silica glasses, depending roughly on the mole fractions of non-silica oxides that are used in their composition. The full sensitivity of glasses to annealing temperature is thus about 10 times as great as their sensitivity to room temperature changes.

Considering borosilicate glass, which is the type most often used for large windows and interferometer plates, equilibrium temperature coefficients of 38, 38, 50, and 53×10^{-6} per deg C have been found on samples differing somewhat in chemical composition. If the full potential effects of temperature gradients in glass during the holding period of an annealing should be realized, it is obvious that the steady *systematic* furnace gradients must, in general, be reduced to a very few hundredths of 1 degree over the linear dimensions of an optical component, if optical glass is to be homogeneous to 1×10^{-6} in index. Fortunately, in practice, the full effects are not realized. If the holding temperature is high enough to permit equilibrium during the short holding periods, then it is likely that further changes during the early stages of cooling will ameliorate the inhomogeneity. If the holding temperature is low, the holding time may not be long enough for attainment of the full inhomogeneity corresponding to the temperature gradient. However, very large pieces must be annealed at low holding temperatures, and the period must be long for the proper relaxation of stresses. Thus they will probably experience a larger proportion of the full equilibrium changes in index than is the case for smaller components with which the glass makers have had more experience.

At this Bureau the temperature gradients in annealing furnaces have progressively and successfully been reduced by placing the glass in a closely fitting metal box, which is inclosed in another box or boxes, that is by inserting more and more metal in the furnace between the glass and the heating coils. Large disks or other large components of glass are symmetrically placed with respect to this added metal and with respect to the furnace walls. Alternate layers of conducting and non-conducting materials are particularly advantageous. Copper as a conductor is objectionable because of excessive oxidation. Aluminum has been found very satisfactory but, for some glasses, care must be exercised to keep preheating below the melting point of this metal. The temperature range can be satisfactorily extended by use of certain alloys of aluminum.

The importance of uniform annealing temperature is so great in the successful production of wind-tunnel optics that it may be necessary to provide for slow continuous rotations of the glass or of the furnace in which it is contained. Possibly simultaneous or successive rotations about two axes may be desirable. Certainly a very high degree of temperature uniformity will be necessary if we are to determine just what degree of residual inhomogeneity is chemical in nature. At present we seem to be safe in saying that in much of our properly selected best optical glass the maximum inhomogeneities are small in the sixth-decimal place over distances of several inches.

IX. References

[1] A. Q. Tool and E. E. Hill, Trans. Soc. Glass Tech. **9**, 185 (1925).

[2] Lord Rayleigh, Phil. Mag. **8**, 409 (1879).

[3] S. Chalmers, Trans. Opt. Soc. (London) **18**, 192 (1917).

[4] L. C. Martin, Trans. Opt. Soc. (London) **23**, 88 (1921).

[5] A. E. Conrady, Mon. Notices Roy. Astr. Soc. **79**, 591 (1919).

[6] Dictionary of Applied Physics IV, 222 (Macmillan and Co., Ltd., London, 1923).

[7] F. L. O. Wadsworth, Astro. Phys. J. **16**, 267 (1902); **17**, 1 (1903).

[8] A. E. Conrady, Mon. Notices Roy. Astr. Soc. **79**, 582 (1919).

[9] L. W. Tilton, A. N. Finn, and A. Q. Tool, BS Sci. Pap. **22**, 719 (1928) S572.

[10] F. Neumann, Ann. Physik **54**, 449 (1841).

[11] F. Pockels, Ann. Physik [4] **7**, 745 (1902); **9**, 221 (1902); **11**, 652 (1903).

[12] L. H. Adams and F. D. Williamson, J. Wash. Acad. Sci. **9**, No. 20, 618 (1919).

[13] L. N. G. Filon, Cambridge Phil. Soc. Proc. **11**, 478 (1902); **12**, 55 (1903).

[14] L. H. Adams and F. D. Williams, J. Opt. Soc. Am. **4**, 217 (1920).

[15] L. W. Tilton, J. Research NBS **14,** 413 (1935) RP776.
[16] Fritz Eckert, Z. Tech. Phys. **7,** 282 to 287 (1926).
[17] A. Dalladay and F. Twyman, Jr., Soc. Glass Tech. **5,** 325 (1921).
[18] A. A. Lebedeff, Die Glas Industrie **35,** 9 (1929).
[19] L. W. Tilton, J. Wash. Acad. Sci. **20,** 121 (1929).
[20] F. Twyman, Prism and lens making, p. 136 (Adam Hilger, London).
[21] A. Q. Tool and J. Valasek, BS Sci. Pap. **15,** 562 (1920) S358.
[22] A. Q. Tool, L. W. Tilton, and J. B. Saunders, J. Research NBS **38,** 519 (1947) RP1793.

WASHINGTON, September 3, 1948.

U. S. Department of Commerce
National Bureau of Standards

Research Paper RP1970
Volume 42, March 1949

Part of the Journal of Research of the National Bureau of Standards

A Standard of Small Capacitance

By Chester Snow

A formula is derived for computing the electrical capacitance of an absolute standard that is a modification of the ordinary parallel-plate condenser with coplanar guard. The modification consists in placing the circular face of the electrode at the bottom of a cylindrical hole in the guard. The analogous two-dimensional arrangement is also considered. The two cases are formulated as special cases of a more general one, in such a manner as to show that certain approximate formulas have errors of the same order of magnitude in each case. The magnitude of the error is then determined by comparison with an exact formula obtained for the two-dimensional case by conformal transformation. With certain restrictions, easily made in practice, this error seems to be less than one part in two thousand.

I. Introduction

To meet the demand for a standard of very small electrical capacitance that may be computed from its dimensions, the ordinary parallel-plate type with coplanar guard has been modified by placing one electrode at the bottom of a cylindrical hole (or well) in the guard as shown in figure 1, a. A formula is required for computing the coefficient of capacitance C between the conductor on the left and the rod that snugly fits the cylindrical hole.

For the mathematical formulation of the problem it has been idealized in two ways. Further restrictions are made, but these are easy to meet in practice.

If the radius of the disk on the left in figure 1, a, is sufficiently large compared to its distance from the guard, there will be a region between them where the electrostatic field is nearly uniform. If it were perfectly uniform, the distribution of charge at the edge of the hole, in the cavity, and on the piston would be the same as if the radius of the left-hand conductor and guard were infinite. This is the first simplification in passing from figure 1, a, to the diagram in figure 1, b. In the latter it is sufficient to show only the half of a meridian section, since the potential has axial symmetry. The most sensitive experimental tests show that when the radius in figure 1, a (corresponding to A_2A_0 in fig. 1, b) is five times the

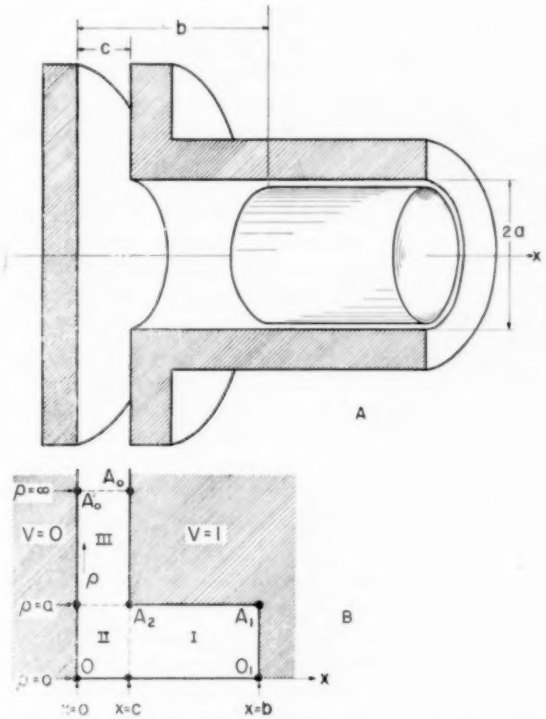

FIGURE 1. *The dielectric volume is generated by rotation around the x-axis of the plane region I+II+III.*

A, Isometric drawing of capacitor; B, meridian section in the half-plane of the cylindrical coordinates (X, ρ).

separation, c, there is no detectable change in capacitance by further increase in this ratio.

The second assumption, as shown in figure 1, b, is that the clearance between the piston and its guard may be ignored. The two are kept at the same potential but insulated from each other. Condensers of this type have been constructed in which this insulation is several hundred megohms, although the clearance is almost invisible to the naked eye. If the hole were very shallow, the edge A_1 being close to A_2, a correction for clearance would be more important, but if the depth of the hole were of the order of magnitude of its radius, both being large compared to the clearance, such a correction appears to be unimportant. With no clearance, the electric field vanishes at the edge A_1. There is another reason for making the hole relatively deep, say greater than its radius or one-half of its radius. This arises out of purely mathematical difficulties.

After adopting these two simplifications and formulating the potential, on the basis indicated in figure 1, b, a formula for the capacitance C was obtained in terms of known functions and an infinite set of positive constants x_s ($s=1, 2, 3. \ldots \infty$), which are the solutions of an infinite system of linear equations. The formulation as an integral equation is given in the appendix. It suggested the proof, which is given, that the solution by the method of successive substitutions would be convergent for all positive real values of the depth-ratio, $\beta=(b-c)/a$, and of the spacing-ratio, $\gamma=c/a$. The computation of the iterated series, which give the constants x_s, seems to be very laborious in general. To obtain a simple, explicit formula for each x_s (and therefore for capacitance C) it was assumed that $0\leq\gamma\leq 1/5$ and $1\leq\beta\leq\infty$, or roughly of this order. The shallow hole is again excluded, and the restriction on γ is such as must be made in practice even for the coplanar case.

These restrictions do not prevent the extension of the range of standard capacitance down to the lowest desirable values. Since there are three adjustable lengths a, b, and c, it is also practicable to make a capacitor to which our formula applies, whose value C is as large as that of a coplanar type with smaller radius a. Each capacitance could be computed and they could be compared experimentally, so there is a possibility of experimental check on the restricted formula for C that is given here. (We have no practicable formula of precision for the case of a relatively shallow hole.)

It is not desirable to construct a set of standards of very low values, whose capacitance must be found experimentally by stepping down from the parallel-plate type. Hence the estimate of the order of magnitude of error in the restricted formula for C (eq 35) should be based on mathematical considerations if possible. Such an estimate is made here by what amounts to a mathematical experiment.

To make this we consider the corresponding two-dimensional arrangement, which may also be represented by the half-plane of figure 1, b, viewing it as a cross section of endless conductors, x and ρ now being rectangular coordinates instead of the cylindrical coordinates used before when the x axis was the axis of symmetry. On this figure the two-dimensional potential has the same boundary values as before, but instead of the axially symmetric potential equation

$$\left(D_x^2+D_\rho^2+\frac{1}{\rho}D_\rho\right)V=0,$$

we now have

$$(D_x^2+D_\rho^2)\ V=0.$$

The formulation of this problem in every step is analogous to that used before. A parallel treatment of the two cases, which was first used, was later abandoned in favor of the combined treatment given here, the two potential equations now being special cases of a more general one. The analogue of C/a is formally $\pi C'$, where C' is the capacitance per unit length of slot (the analogue of the cylindrical hole of diameter $2a$, being the endless slot of width $2a$). The general formula gives C/a (eq 25 below) as the same function of β and γ and the roots α_s of $J_0(\alpha)=0$, that $\pi C'$ is of β and γ and the roots α_s' of $\cos\alpha=0$. The same is true of the restricted formulas 35 and 35a. The combined formulation of the two cases makes it evident that the error is of the same order of magnitude in both cases for the restricted formulas 35 and 35a.

But it is known that the two-dimensional problem may be solved by conformal transformation with integrals of elliptic functions, and this leads to a formula by which $\pi C'$ may be computed with any desired precision. From this it appears that

the restricted formula 35a (and hence eq 35) is in error by not more than one part in two thousand $\left(\text{when } 0<\gamma\leq\frac{1}{5} \text{ and } 1<\beta<\infty\right)$.

Capacitors that approximate to each of the two types here considered have been constructed by C. Moon, and their coefficients C and C' measured by comparison with the parallel-plate type. The values agree with those computed by the restricted formulas given here, the experimental error being estimated as one part in a thousand. The longish, two-dimensional type is more difficult to construct with precision.

II. Combined Formulation of the Two Potential Problems

The potential $V(x, \rho)$ must satisfy the boundary conditions

$$\begin{aligned} V(o, \rho)&=0 \qquad \text{for } o\leq\rho\leq\infty \\ V(b, \rho)&=1 \qquad \text{for } o\leq\rho\leq a \\ V(x, a)&=1 \qquad \text{for } c\leq x\leq b \\ V(c, \rho)&=1 \qquad \text{for } a\leq\rho\leq\infty \end{aligned}$$

$D_\rho V=0$ when $\rho=0$, and $V\to x/c$ when $\rho\to\infty$.

In the dielectric region the axially symmetric potential V satisfies the partial differential equation

$$(D_x^2+D^2)V+\frac{1}{\rho}D_\rho V=0.$$

The two-dimensional potential has the same boundary conditions but satisfies the equation

$$(D_x^2+D_\rho^2)V=0.$$

They may be considered as special cases, $\nu=0$ and $\nu=-1/2$ of $V(x, \rho)$, which has the same boundary conditions and is a solution of

$$(D_x^2+D_\rho^2)V+\frac{1+2\nu}{\rho}D_\rho V=0.$$

As far as the formulation of the problem is concerned, it is only necessary to assume that the constant parameter ν is real and greater than -1.

With this restriction let α_s denote the s^{th} positive root of $J_\nu(\alpha)=0$. It is known that for the interval $0<\xi<1$, the set of normal functions (with weighting factor ξ)

$$\phi_s(\xi)\equiv\sqrt{2}\,\frac{J_\nu(\alpha_s\xi)}{J_{\nu+1}(\alpha_s)} \quad (s=1, 2, 3, \ldots \infty),$$

form a closed set, and they are normalized, for

$$\int_0^1 \xi\phi_s(\xi)\phi_n(\xi)d\xi=\delta_{ns}=1 \text{ if } n=s, =0 \text{ if } n\neq s.$$

Another independent closed set, associated with the same constants is

$$\psi_s(\xi)\equiv\sqrt{2}\,\frac{J_{\nu+1}(\alpha_s\xi)}{J_{\nu+1}(\alpha_s)}.$$

We use $J_\nu(t)$ and $H_\nu(t)$ to denote Bessel's cylinder function of t and the first kind of Hankel's function, and assume that the t-plane is cut along its negative real axis. Between these two functions and their derivatives, there is the identical relation in t,

$$\frac{J_\nu'(t)}{J_\nu(t)}-\frac{H_\nu'(t)}{H_\nu(t)}=\frac{2}{i\pi tH_\nu(t)J_\nu(t)}. \tag{1}$$

There is also the identity in t,

$$2\sum_{s=1}^{\infty}\frac{J_{\nu+n}(\alpha_s\xi)}{\alpha_s^{n-1}(\alpha_s^2-t^2)J_{\nu+1}(\alpha_s)}=\frac{J_{\nu+n}(t\xi)}{t^nJ_\nu(t)}, \tag{2}$$

which is valid for $0\leq\xi\leq1$, if $n=1, 2, 3, \ldots$ and for $0\leq\xi<1$ in case $n=0$, which becomes

$$2\sum_{s=1}^{\infty}\frac{\alpha_s^\nu J_\nu(\alpha_s\xi)}{(\alpha_s^2-t^2)J_{\nu+1}(\alpha_s)}=\frac{J_\nu(t\xi)}{J_\nu(t)} \text{ for } 0\leq\xi<1. \tag{2a}$$

Letting $t\to0$ in this gives

$$2\sum_{s=1}^{\infty}\frac{J_\nu(\alpha_s\xi)}{\alpha_s^\nu J_{\nu+1}(\alpha_s)}=\xi^\nu \text{ for } 0\leq\xi<1. \tag{2b}$$

For brevity let $\xi=\rho/a$

$$\beta\equiv\frac{b-c}{a} \text{ and } \gamma\equiv\frac{c}{a}. \tag{3}$$

In the appendix is a formulation by contour integrals leading to an integral equation. The much shorter discussion given here contains all that is essential without reference to the appendix.

Consider the particular solutions $V_s(x,\rho)$ $(s=1, 2, 3 \ldots)$, which vanish on all the boundaries of the dielectric and are continuous throughout, but have discontinuities in $\partial V/\partial x$ at the plane $x=c$, corresponding to a surface density σ_s at this plane, where

$$4\pi\sigma_s=\left(\frac{\partial V}{\partial x}\right)_{x=c-0}-\left(\frac{\partial V}{\partial x}\right)_{x=c+0}.$$

Assume in region I it is

$$V_s(x,\rho)=\frac{\sinh\alpha_s(b-x)/a}{\alpha_s\sinh\beta\alpha_s}\cdot\frac{\xi^{-\nu}J_\nu(\alpha_s\xi)}{J_{\nu+1}(\alpha_s)}; \quad (4a)$$

then in region II it must be

$$V_s(x,\rho)=\frac{\sinh\alpha_s x/a}{\alpha_s\sinh\gamma\alpha_s}\cdot\frac{\xi^{-\nu}J_\nu(\alpha_s\xi)}{J_{\nu+1}(\alpha_s)}+\pi\gamma\xi^{-\nu}\cdot$$

$$\sum_{n=1}^{\infty}(-1)^{n+1}\sin\left(\frac{n\pi x}{c}\right)\frac{(in\pi/\gamma)H_\nu(in\pi/\gamma)J_\nu(in\pi\xi/\gamma)}{[(n\pi)^2+(\gamma\alpha_s)^2]} \quad (4b)$$

and in region III it must be

$$V_s(x,\rho)=\pi\gamma\xi^{-\nu}\cdot$$

$$\sum_{n=1}^{\infty}(-1)^{n+1}\sin\left(\frac{n\pi x}{c}\right)\frac{(in\pi/\gamma)H_\nu(in\pi\xi/\gamma)J_\nu(in\pi/\gamma)}{[(n\pi)^2+(\gamma\alpha_s)^2]} \quad (4c)$$

By use of the identities (1) and (2a), each for $t=(in\pi/\gamma)$, it may be verified that not only V_s but also $\partial V_s/\partial\rho$ is continuous at $\rho=a$. Also, since V_s is continuous at $x=c$, it is found that the surface density σ_s is given by

$$4\pi a\xi^{\nu}\sigma_s=(\coth\gamma\alpha_s+\coth\beta\alpha_s)\frac{J_\nu(\alpha_s\xi)}{J_{\nu+1}(\alpha_s)}-$$

$$\gamma^2\sum_{k=1}^{\infty}\alpha_k X_{sk}^{(1)}\frac{J_\nu(\alpha_k\xi)}{J_{\nu+1}(\alpha_k)} \quad (5)$$

where the positive real coefficients are functions of γ defined by:

$$X_{sk}^{(1)}=X_{ks}^{(1)}=\sum_{n=1}^{\infty}\frac{2n\pi^2(in\pi/\gamma)H_\nu(in\pi/\gamma)J_\nu(in\pi/\gamma)}{[(n\pi)^2+(\gamma\alpha_s)^2]\cdot[(n\pi)^2+(\gamma\alpha_k)^2]}. \quad (6)$$

The required potential V_s may be represented in the form

$$V_s(x,\rho)=\frac{x}{c}-2\sum_{s=1}^{\infty}x_sV_s(x,\rho) \text{ in II and III}=$$

$$1-2\sum_{s=1}^{\infty}x_sV_s(x,\rho) \text{ in I} \quad (7)$$

where the real constants x_s must be so chosen that $\partial V_s/\partial x$ is continuous at $x=c$, that is

$$2\sum_{s=1}^{\infty}x_s\,(4\pi a\sigma_s)=\frac{1}{\gamma} \text{ for } 0\leq\xi<1,$$

or by eq 5

$$2\sum_{s=1}^{\infty}\frac{J_\nu(\alpha_s\xi)}{J_{\nu+1}(\alpha_s)}\cdot$$

$$\left[(\coth\gamma\alpha_s+\coth\beta\alpha_s)x_s-\gamma^2\alpha_s\sum_{k=1}^{\infty}X_{sk}^{(1)}x_k\right]=$$

$$\frac{\xi^{\nu}}{\gamma}=(2/\gamma)\sum_{1}^{\infty}J_\nu(\alpha_s\xi)/[\alpha_sJ_{\nu+1}(\alpha_s)]. \text{ by (2b)}$$

If, for brevity, we place

$$A_s\equiv\frac{1}{\coth\gamma\alpha_s+\coth\beta\alpha_s}=\frac{\sinh\beta\alpha_s\sinh\gamma\alpha_s}{\sinh(\beta+\gamma)\alpha_s}, \quad (8)$$

the system of linear equations that determine the x_s may be written

$$x_s=A_s\left[\frac{1}{\gamma\alpha_s}+\gamma^2\alpha_s\sum_{k=1}^{\infty}X_{sk}^{(1)}x_k\right] \text{ for } s=1,2,3,\ldots\infty. \quad (9)$$

By "successive substitutions" this system is found to be equivalent to

$$x_s=\frac{\alpha_sA_s}{\gamma}\left[\frac{1}{\alpha_s^2}+\gamma^2\sum_{k=1}^{\infty}\frac{X_{sk}^{(1)}A_k}{\alpha_k}+\gamma^4\sum_{k=1}^{\infty}\frac{X_{sk}^{(2)}A_k}{\alpha_k}+\ldots\right.$$

$$\left.\gamma^{2(m-1)}\sum_{k=1}^{\infty}\frac{X_{sk}^{(m-1)}A_k}{\alpha_k}+\gamma^{2(m-1)}\sum_{k=1}^{\infty}X_{sk}^{(m)}x_k\right], \quad (10)$$

where m is any positive integer; in case $m=1$ this reduces to eq 9.

The iterated coefficients are positive reals, defined by

$$X_{sk}^{(m+1)}=X_{ks}^{(m+1)}=\sum_{r=1}^{\infty}\alpha_rA_rX_{rs}^{(1)}X_{rk}^{(m)}, \quad (11)$$

where $X_{sk}^{(1)}$ is defined in eq 6.

If $m\to\infty$, the second number of eq 10 becomes an infinitive series that either converges or diverges to $+\infty$ (it cannot oscillate since all the terms are positive). If the series converges it gives the solution of the system (eq 9).

To examine this question let $x_s^{(1)}, x_s^{(2)}, \ldots x_s^{(m)}$ $(s=1,2,3\ldots\infty)$ each denote an infinite set of positive constants, each being derived from its predecessor by the operation that is the second member of eq 9.

$$x_s^{(m+1)}=\frac{\alpha_sA_s}{\gamma}\left[\frac{1}{\alpha_s^2}+\gamma^2\sum_{k=1}^{\infty}X_{sk}^{(1)}x_k^{(m)}\right]. \quad (12a)$$

Starting from any bounded initial set $x_s^{(1)}$, otherwise arbitrary, say

$$0<x_s^{(1)}\leq M^{(1)},$$

the repeated application of this operation gives

$$x_s^{(m+1)}=\frac{\alpha_sA_s}{\gamma}\left[\frac{1}{\alpha_s^2}+\gamma^2\sum_{k=1}^{\infty}\frac{X_{sk}^{(1)}A_k}{\alpha_k}+\gamma^4\sum_{k=1}^{\infty}\frac{X_{sk}^{(2)}A_k}{\alpha_k}+\ldots+\right.$$

$$\gamma^{2(m-1)}\sum_{k=1}^{\infty}\frac{X_{sk}^{(m-1)}A_k}{\alpha_k}+\gamma^{2m+1}\sum_{k=1}^{\infty}X_{sk}^{(m)}x_k^{(1)}\Bigg]. \quad (12b)$$

If we take the initial set, $x_s^{(1)}\equiv 1$, this becomes the second member of eq. 10, but it is here assumed merely that $x_s^{(1)}$ is bounded.

If $\quad 0<x_s^{(m)}\leqq M^{(m)}$ for every s,

we may then prove that

$$0<x_s^{(m+1)}<M^{(m)}-1 \text{ for every } s, \text{ when } M^{(m)}>2 \quad (13a)$$

and

$$0<x_s^{(m+1)}<1 \text{ for every } s, \text{ when } M^{(m)}\leqq 2. \quad (13b)$$

This proposition will be shown to hold for every finite value of the positive constants β and γ, but in the proof we exclude the case $\beta=\gamma=0$ in which there is no problem, and also the limiting case, $\gamma\to 0$, $0<\beta<\infty$, in which the solution of eq 10 is obviously $x_s=1$ for every s.

Before attempting a detailed proof, we may notice that if eq 13a is true, it then follows that, whatever the initial set (provided it is bounded), we shall arrive at an integer m for which $M^{(m)}\leqq 2$. Proceeding to larger values of m we find that if eq 13b is true then an integer m exists such that for every larger integer m the set $x_s^{(m+1)}$ remains bounded and less than 1. Combining this with the fact that $x_s^{(m+1)}$ continually increases with increasing m, it is evident that the set $x_s^{(m+1)}$ approaches a limit and the second members of eq 12b and 10 become a convergent infinite series of positive terms that is the solution of the set of eq 9 irrespective of the arbitrary initial set with which we start. In fact, certain initial sets $x_s^{(1)}$ may be found, which make say $x_s^{(2)}$ or $x_s^{(3)}$ a closer approximation to the solution than would be obtained by starting with the initial set suggested by eq 10, namely,

$$x_s^{(1)}=\frac{A_s}{\gamma\alpha_s}.$$

It would follow that this solution must lie in the interval

$$\frac{A_s}{\gamma\alpha_s}<x_s<1 \text{ for every } s. \quad (14a)$$

This inequality shows that the remainder for a given m, (the last series in eq 10), has an upper bound

$$\gamma^{2m+1}\sum_{k=1}^{\infty}X_{sk}^{(m)}x_k<\gamma^{2m+1}\sum_{k=1}^{\infty}X_{sk}^{(m)}. \quad (14b)$$

From eq 8 and 11 it is evident that all the positive quantities $X_{sk}^{(m)}$ are functions of β and γ, except that $X_{sk}^{(1)}$ by its definition (eq 6) depends on γ only.

To prove the propositions of eq 13a and 13b we start with the inequality

$$X_s^{(m+1)}<\frac{\alpha_s A_s}{\gamma}\left[\frac{1}{\alpha_s^2}+\gamma^3 M^{(m)}\sum_{k=1}^{\infty}X_{sk}^{(1)}\right]=$$

$$\frac{A_s}{\gamma\alpha_s}+\alpha_s A_s M^{(m)}\sum_{n=1}^{\infty}$$

$$\frac{n\pi\left[\pi\left(\frac{in\pi}{\gamma}\right)H_\nu\left(\frac{in\pi}{\gamma}\right)J_\nu\left(\frac{in\pi}{\gamma}\right)\right]}{(n\pi)^2+(\gamma\alpha_s)^2}\sum_{k=1}^{\infty}\frac{2}{\alpha_k^2+(n\pi/\gamma)^2}$$

by (6)

If, in the identity (eq 2), we take $n=1$, $\xi=1$, and $t=in\pi/\gamma$, it becomes

$$\sum_{k=1}^{\infty}\frac{2}{\alpha_k^2+\left(\frac{n\pi}{\gamma}\right)^2}=\frac{J_{\nu+1}(in\pi/\gamma)}{(in\pi/\gamma)J_\nu(in\pi)\gamma}.$$

Hence, for every s,

$$x_s^{(m+1)}<\frac{\alpha_s A_s}{\gamma}\cdot$$

$$\left[\frac{1}{\alpha_s^2}+M^{(m)}\gamma^2\sum_{n=1}^{\infty}\frac{\pi(n\pi/\gamma)H_\nu(in\pi/\gamma)J_{\nu+1}(in\pi/\gamma)}{(n\pi)^2+(\gamma\alpha_s)^2}\right].$$

It will appear presently that

$$0<\pi\left(\frac{n\pi}{\gamma}\right)H_\nu\left(\frac{in\pi}{\gamma}\right)J_{\nu+1}\left(in\,\frac{\pi}{\gamma}\right)<1 \quad (15)$$

for every finite positive integer n, this positive real quantity being a monotone increasing function of $\frac{n\pi}{\gamma}$, which only reaches 1 in the limit $n\to\infty$.

Hence

$$x_s^{(m+1)}<\frac{\alpha_s A_s}{\gamma}\left[\frac{1}{\alpha_s^2}+\frac{M^{(m)}}{2\alpha_s^2}\sum_{n=1}^{\infty}\frac{2(\gamma\alpha_s)^2}{(n\pi)^2+(\gamma\alpha_s)^2}\right]$$

or since

$$\sum_{n=1}^{\infty}\frac{2(\gamma\alpha_s)^2}{(n\pi)^2+(\gamma\alpha_s)^2}=\gamma\alpha_s\coth\gamma\alpha_s-1$$

and $A_s = 1/(\coth \gamma\alpha_s + \coth \beta\alpha_s)$ by eq 8, this becomes

$$0 < x_s^{(m+1)} < \frac{1 + \frac{M^{(m)}}{2}(\gamma\alpha_s \coth \gamma\alpha_s - 1)}{\gamma\alpha_s (\coth \gamma\alpha_s + \coth \beta\alpha_s)} \quad (16)$$

for $s = 1, 2, 3, \ldots \infty$.

From this, the second part of the theorem to be proved, eq 13b, follows directly, for if $M^{(m)} \leq 2$, this becomes

$$\frac{A_s}{\gamma\alpha_s} = \frac{1}{\gamma\alpha_s (\coth \gamma\alpha_s + \coth \beta\alpha_s)} < x_s^{(m+1)} < \frac{\coth \gamma\alpha_s}{\coth \gamma\alpha_s + \coth \beta\alpha_s}$$

for every s.

To prove eq 13a, the four expressions

$$\frac{M^{(m)}}{2} - 1, M^{(m)} - 2, \gamma\alpha_s \coth \gamma\alpha_s \text{ and } \gamma\alpha_s \coth \gamma\alpha_s - 1$$

are each positive when $M^{(m)} > 2$.
Hence

$$(M^{(m)} - 1)\gamma\alpha \coth \beta\alpha + \left(\frac{M^{(m)}}{2} - 1\right)(\gamma\alpha \coth \gamma\alpha - 1) + M^{(m)} - 2 > 0.$$

Adding $\frac{M^{(m)}}{2}(\gamma\alpha \coth \gamma\alpha - 1)$ to both sides gives

$$1 + \frac{M^{(m)}}{2}(\gamma\alpha_s \coth \gamma\alpha_s - 1) < (M^{(m)} - 1)\gamma\alpha_s (\coth \gamma\alpha_s + \coth \beta\alpha_s).$$

The inequality (eq 16) then becomes eq 13a, which was to be proved.

Consequently the second member of eq 10 when $m \to \infty$ gives the solution x_s of eq 9 as a convergent infinite series of positive terms, which may be written

$$x_s = \frac{A_s}{\gamma\alpha_s}\left\{1 + (\gamma\alpha_s)^2 \sum_{k=1}^{\infty} \frac{A_k}{\alpha_k}\left[X_{sk}^{(1)} + \gamma^2 X_{sk}^{(2)} + \gamma^4 X_{sk}^{(3)} + \ldots\right]\right\}. \quad (17)$$

where A_s, $X_{sk}^{(1)}$ and $X_{sk}^{(m)}$ may be computed by eq 8, 6, and 11. The process is straightforward, the series converges for every positive β and γ and is therefore the complete solution of the general problem, but as such is practically useless in all its generality. By good luck we may restrict the problem so that only the first series of eq 17 is necessary.

Eq 2 with $n = 1$, $\xi = 1$ and $t = in\pi/\gamma$, becomes

$$2\left(\frac{in\pi}{\gamma}\right) J_\nu\left(\frac{in\pi}{\gamma}\right) \sum_{k=1}^{\infty} \frac{1}{\alpha_k^2 + \left(\frac{n\pi}{\gamma}\right)^2} = J_{\nu+1}\left(\frac{in\pi}{\gamma}\right).$$

Using this, the definition eq 6 of $X_{sk}^{(1)}$ leads to the exact equation,

$$\gamma \sum_{k=1}^{\infty} X_{sk}^{(1)} = \sum_{n=1}^{\infty} \frac{\pi(n\pi/\gamma) H_\nu(in\pi/\gamma) J_{\nu+1}(in\pi/\gamma)}{(n\pi)^2 + (\gamma\alpha_s)^2}. \quad (18)$$

To complete the proof it is necessary to show that the inequality eq 15 is satisfied in both cases, $\nu = 0$, and $\nu = -1/2$.

In the case $\nu = 0$, $J_0(\alpha_s) = 0$, the two positive real quantities have the asymptotic expansions

$$\pi\left(\frac{in\pi}{\gamma}\right) H_0\left(\frac{in\pi}{\gamma}\right) J_0\left(\frac{in\pi}{\gamma}\right) \sim 1 + \frac{1}{8}\left(\frac{\gamma}{n\pi}\right)^2 \quad (19a)$$

$$\pi\left(\frac{n\pi}{\gamma}\right) H_0\left(\frac{in\pi}{\gamma}\right) J_1\left(\frac{in\pi}{\gamma}\right) \sim 1 - \frac{1}{2}\left(\frac{\gamma}{n\pi}\right) - \frac{3}{16}\left(\frac{\gamma}{n\pi}\right)^3. \quad (19b)$$

If $\gamma \leq 1/5$ these are in error (in the most unfavorable case $n = 1$) by less than one part in 10^5.

From tables of $H_0(ix)$ and $J_1(ix)$ for $x > 0$, it may be verified that the first member of eq 19a is a monotone increasing function of $(n\pi/\gamma)$, so the inequality (eq 15) is true.

In the two-dimensional potential ($\nu = -1/2$)

$$H_{-\frac{1}{2}}(t) = iH_{\frac{1}{2}}(t) = \left(\frac{2}{\pi t}\right)^{\frac{1}{2}} e^{it}$$

and

$$H_{-\frac{1}{2}}^{(2)}(t) = -iH_{\frac{1}{2}}^{(2)}(t) = \left(\frac{2}{\pi t}\right)^{\frac{1}{2}} e^{-it},$$

$$J_{-\frac{1}{2}}(t) = \left(\frac{2}{\pi t}\right)^{\frac{1}{2}} \cos t$$

and

$$J_{\frac{1}{2}}(t) = \left(\frac{2}{\pi t}\right)^{\frac{1}{2}} \sin t,$$

so the analogues of eq 19a and 19b are

$$\pi\left(\frac{in\pi}{\gamma}\right) H_{-\frac{1}{2}}\left(\frac{in\pi}{\gamma}\right) J_{-\frac{1}{2}}\left(\frac{in\pi}{\gamma}\right) = 1 + e^{\frac{-2n\pi}{\gamma}} \quad (20a)$$

$$\pi\left(\frac{n\pi}{\gamma}\right) H_{-\frac{1}{2}}\left(\frac{in\pi}{\gamma}\right) J_{\frac{1}{2}}\left(\frac{in\pi}{\gamma}\right) = 1 - e^{\frac{-2n\pi}{\gamma}}, \quad (20b)$$

the latter being also a monotone increasing function of $n\pi/\gamma$ as in eq 15 with $+1$ as upper limit.

For small values of γ we may place the second member of eq 19a equal to 1, (as is very accurately the second member of eq (20a), which gives by eq 6 for both values of ν,

$$X_{sk}^{(1)}=\frac{2}{\pi^3}\sum_{n=1}^{\infty}\frac{n}{\left[n^2+\left(\frac{\gamma\alpha_s}{\pi}\right)^2\right]\cdot\left[n^2+\left(\frac{\gamma\alpha_k}{\pi}\right)^2\right]}$$

$$=\frac{2}{\pi^3(\alpha_k^2-\alpha_s^2)}\sum_{n=1}^{\infty}\left\{\frac{\alpha_k^2}{n\left[n^2+\left(\frac{\gamma\alpha_k}{\pi}\right)^2\right]}-\frac{\alpha_s^2}{n\left[n^2+\left(\frac{\gamma\alpha_s}{\pi}\right)^2\right]}\right\} \tag{21a}$$

$$=\frac{2}{\pi^3(\alpha_k^2-\alpha_s^2)}\left[\alpha_k^2 S\left(\frac{\gamma\alpha_k}{\pi}\right)-\alpha_s^2 S\left(\frac{\gamma\alpha_s}{\pi}\right)\right].$$

For $k=s$ this is 0/0 but is determinate,

$$X_{ss}^{(1)}=\frac{2}{\pi^3}\left[S\left(\frac{\gamma\alpha_s}{\pi}\right)-\left(\frac{\gamma\alpha_s}{\pi}\right)^2 T\left(\frac{\gamma\alpha_s}{\pi}\right)\right], \tag{21b}$$

where $S(u)$ and $T(u)$ are defined below.

The expressions (eq 21a and 21b) are, for all practical purposes, exact in the two-dimensional case $\nu=-1/2$, but as shown by eq 19a they may be in error for the case $\nu=0$ by a part in 2,000 when γ is as large as 1/5. However this corresponds to an error of 2 in 10^6 in capacitance so that eq 21a and 21b are sufficient in either case. To the same approximation, eq 18 becomes

$$\gamma\sum_{k=1}^{\infty}X_{sk}^{(1)}=\coth\gamma\alpha_s-\frac{1}{\gamma\alpha_s} \tag{21c}$$

$$S(u)\equiv\sum_{n=1}^{\infty}\frac{1}{n(n^2+u^2)}=\frac{1}{u^2}\left[0.57722+R\psi(1+iu)\right] \tag{22a}$$

$$T(u)=-D_{u^2}S(u)=\sum_{1}^{\infty}\frac{1}{n\,(n^2+u^2)^2} \tag{22b}$$

where $\psi(z)=\frac{d}{dz}\log\Gamma(z)$. From the asymptotic expansion of the psi-function it is found that when u is large $S(u)$ vanishes with the asymptotic expansion,

$$S(u)\sim\frac{1}{u^2}\left[\frac{1}{2}\log(1+u^2)+0.57722-\frac{1}{2(1+u^2)}\right]. \tag{23}$$

For value of u as small as 1 this formula is in error by less than one percent.

We have to compute $S(u)$ and $T(u)$ for values of u from u slightly greater than zero up to $u=1$ or 2. For this purpose we may get more rapidly converging series by use of the identity

$$\frac{1}{n(n^2+u^2)}=\frac{1}{n^3}-\frac{u^2}{n^5}+\frac{u^4}{n^7}-\frac{u^6}{n^9}+\frac{u^8}{n^{11}}-\frac{u^{10}}{n^{11}(n^2+u^2)}$$

Since $\sum_{n=1}^{\infty}\frac{1}{n^{2k+1}}$ is accurately known, we find

$$S(u)=1.20206-1.03693\,u^2+1.00835\,u^4-$$

$$1.00201\,u^6+1.00049\,u^8-u^{10}\sum_{n=1}^{\infty}\frac{1}{n^{11}(n^2+u^2)} \tag{24a}$$

and

$$T(u)=1.03693-2.01\;70\,u^2+3.00602\,u^4-$$

$$4u^6\sum_{n=1}^{\infty}\frac{1}{n^7(n^2+u^2)^2}-3u^8\sum_{n=1}^{\infty}\frac{1}{n^9(n^2+u^2)^2}. \tag{24b}$$

III. Application to Capacitance

The surface density of charge on the bottom of the hole or slot is a function of $\xi(=\rho/a)$, given by

$$2\pi a\sigma=\frac{a}{2}(D_z V)_{z=b}=\sum_{s=1}^{\infty}\frac{x_s\xi^{-\nu}J_\nu(\alpha_s\xi)}{\sinh\beta\alpha_s J_{\nu+1}(\alpha_s)}.$$

The charge on this circular face of radius a is

$$Q=2\pi\int_0^a\rho\sigma d\rho=a\sum_{s=1}^{\infty}\frac{x_s}{\alpha_s\sinh\beta\alpha_s}.$$

The charge on the bottom of the slot, (whose width is $2a$) and per cm length of slot, is

$$Q'=2\int_0^a\sigma d\rho=\frac{1}{\pi}\sum_{s=1}^{\infty}\frac{x_s}{\alpha_s\sinh\beta\alpha_s}.$$

The coefficient of capacitance, C, between the plane $x=0$ and the bottom of the hole is given (in cm) by

$$\frac{C}{a}=\sum_{s=1}^{\infty}\frac{x_s}{\alpha_s\sinh\beta\alpha_s}\text{ where }J_\nu(\alpha_s)=0. \tag{25}$$

In the two-dimensional case, the coefficient C' per unit length of slot is given by

$$\pi C' = \sum_{s=1}^{\infty} \frac{x_s'}{\alpha_s' \sinh \beta\alpha_s'}, \text{ where } \cos \alpha_s' = 0. \quad (25a)$$

$$\alpha_s' = \left(s - \frac{1}{2}\right)\pi$$

The coefficients, x_s, are solutions of eq 9 given by eq 17 and x_s' are similar functions of α_s'.

The two infinite, parallel planes with separation c (fig. 1), bring about a uniform electric field at points between them, which are far from the edge A_2 of the hole. To approximate this with small planes, they must be close together. Hence one restriction which, in the nature of the case, must always be made is that γ, $(=c/a)$ is small. A second restriction that may be made, and which further simplifies the computations, is that the hole is not relatively shallow. There would be no hardship in practice if these restrictions are, roughly

$$0 \leq \gamma \equiv c/a \leq 1/5 \quad (26a)$$

$$1 \leq \beta \equiv (b-c)/a < \infty. \quad (26b)$$

By reason of the first, the constants x_1, x_2, x_3 are of the order of magnitude of unity, but they are by no means of equal importance in the formula for capacitance. By reason of the second restriction, the denominators in eq 25 and 25a are such powerful convergence factors that the second term of of the series is less than 2 percent of the first, and any term is less than 4 percent of the term that precedes it. Only two or three terms of these series are required, and the accuracy depends mainly upon the precision with which the first constant x_1 is evaluated.

For this reason we retain in eq 17 only the first approximation

$$x_s = \frac{A_s}{\gamma\alpha_s} \text{ for } s > 1. \quad (27a)$$

For the important constant x_1 we retain also the first series in eq 17

$$x_1 = \frac{A_1}{\gamma\alpha_1}(1+\epsilon_1), \quad (27b)$$

where

$$\epsilon_1 = (\gamma\alpha_1)^2 \sum_{k=1}^{\infty} \frac{A_k X_{1k}^{(1)}}{\alpha_k}$$

$$= (\gamma\alpha_1)^2 \sum_{k=1}^{\infty} \frac{X_{1k}^{(1)}}{\alpha_k(\coth \gamma\alpha_k + \coth \beta\alpha_k)}$$

or by eq 21

$$\epsilon_1 = \frac{2}{\pi}\left(\frac{\gamma\alpha_1}{\pi}\right)^2 \left[\sum_{k=1}^{n} P_k + R_{n+1}\right], \quad (28)$$

where

$$R_{n+1} = \sum_{k=n+1}^{\infty} P_k$$

$$P_1 = \frac{S\left(\frac{\gamma\alpha_1}{\pi}\right) - \left(\frac{\gamma\alpha_1}{\pi}\right)^2 T\left(\frac{\gamma\alpha_1}{\pi}\right)}{\alpha_1(\coth \gamma\alpha_1 + \coth \beta\alpha_1)} \quad (29)$$

For $k > 1$

$$P_k = \frac{1}{\alpha_k(\coth \gamma\alpha_k + \coth \beta\alpha_k)} \cdot \left\{ S\left(\frac{\gamma\alpha_k}{\pi}\right) - \frac{\alpha_1^2\left[S\left(\frac{\gamma\alpha_1}{\pi}\right) - S\left(\frac{\gamma\alpha_k}{\pi}\right)\right]}{\alpha_k^2 - \alpha_1^2} \right\} \quad (30)$$

When $\beta \geq 1$ we may place $\coth \beta\alpha_k = 1$ for $k > 1$ since $\coth \alpha_2 = 1.000$. If we take n just large enough to make $\gamma\alpha_n/\pi$ as large as 1/2, then $\gamma\alpha_{n+1}$ is of the order of 3/2, so that in the series defining R_{n+1} we may neglect variations of $\coth \gamma\alpha_k$. Also the term in eq 30 with factor $\alpha_1^2/(\alpha_k^2 - \alpha_1^2)$ will then be negligible compared with the first terms so that

$$R_{n+1} = \frac{\gamma}{\pi(1+\coth \gamma\alpha_{n+1})} \sum_{k=n+1}^{\infty} \frac{S(\gamma\alpha_k/\pi)}{(\gamma\alpha_k/\pi)}.$$

We may estimate R_{n+1} by using eq 23 so

$$2\pi(1+\coth \gamma\alpha_{n+1})R_{n+1} = \gamma \sum_{k=n+1}^{\infty} f\left(\frac{\gamma\alpha_k}{\pi}\right) \quad (31)$$

$$f(x) \equiv \frac{1}{x^3}\left[\log (1+x^2) + 1.1544 - \frac{1}{1+x^2}\right], \quad (31a)$$

where $f(x)$, defined by this equation, is a positive, monotone function of x, which decreases slowly with increasing x.

At this point it becomes necessary to distinguish between the two cases.

In the three-dimensional case $(\nu = 0)$

$$\alpha_k/\pi \sim k - \frac{1}{4},$$

very approximately, so

$$2\pi(1+\coth \gamma\alpha_{n+1})R_{n+1} = \gamma \sum_{k=n+1}^{\infty} f\left(\gamma\left[k - \frac{1}{4}\right]\right),$$

in the case $\nu=0$.

Also $\alpha_k/\pi=k-\frac{1}{2}$ exactly, in the case $\nu=-\frac{1}{2}$, so that

$$2\pi(1+\coth\gamma\alpha_{n+1})\,R_{n+1}=\gamma\sum_{k=n+1}^{\infty}f\left(\gamma\left[k-\frac{1}{2}\right]\right)$$

in the case $\nu=-\frac{1}{2}$.

The numerical value of the sum of a convergent series of positive terms which continually decrease, say

$$A=\sum_{k=n+1}^{\infty}F(k),$$

represents the sum of the areas of the rectangles each of unit width and height $F(k)$.

The positive, monotone function of x,

$$y=F(x-1/2),$$

represents a smooth curve that passes through the mid-point of the top of each rectangle.

When, as in the present case, this function decreases slowly with increasing x, the area under this curve from $x=n+1$ to $x=\infty$ is a good approximation to the value A of the series, so that

$$A=\sum_{k=n+1}^{\infty}F(k)$$
$$=\int_{x=n+1}^{\infty}F\left(x-\frac{1}{2}\right)dx=\int_{x=n+\frac{1}{2}}^{\infty}F(x)dx.$$

Taking $F(k)=\gamma f\left(\frac{\gamma\alpha}{\pi}k\right)$ gives

$$\left.\begin{aligned}\gamma\sum_{k=n+1}^{\infty}f\left(\frac{\gamma\alpha}{\pi}k\right)&=\int_{\gamma\left(\frac{\alpha_n}{\pi}+\frac{1}{2}\right)}^{\infty}f(x)dx\\ \text{where}\\ \frac{\alpha_n}{\pi}+\frac{1}{2}&\sim n+\frac{1}{4}\text{ if }J_0(\alpha_k)=0\\ &=n\text{ if }\cos\alpha_k=0,\end{aligned}\right\}\qquad(32)$$

provided $f(x)$ is a positive, monotone decreasing function of x for

$$x>\gamma\left(\frac{\alpha_n}{\pi}+\frac{1}{2}\right).$$

Hence from the function $f(x)$ in eq 31 we obtain

$$R_{n+1}\sim\frac{1}{4\pi(1+\coth\gamma\alpha_{n+1})}\left\{\frac{0.1544+1}{x_n^2}(\log+x_n^2)+2\log\left(\frac{1+x_n^2}{x_n^2}\right)\right\},\qquad(33)$$

where

$$x_n=\gamma\left(\frac{\alpha_n}{\pi}+\frac{1}{2}\right).\qquad(34)$$

Equations 25 and 25a for capacitance become

$$\frac{C}{a}=\frac{1}{\gamma}\sum_{s=1}^{\infty}\frac{(1+\epsilon_s)\sinh\gamma\alpha_s}{\alpha_s^2\sinh(\beta+\gamma)\alpha_s}\text{ where }J_0(\alpha_s)=0\qquad(35)$$

$$\pi C'=\frac{1}{\gamma}\sum_{s=1}^{\infty}\frac{(1+\epsilon_s')\sinh\gamma\alpha_s'}{(\alpha_s')^2\sinh(\beta+\gamma)\alpha_s'}\text{ where }\cos\alpha_s'=0\qquad(35a)$$

ϵ_s, $\epsilon_s'=0$ if $s>1$, $\gamma\equiv c/a$ and $\beta\equiv(b-c)/a$

ϵ_1, ϵ_1' computed by eq 24, 28, 29, 30, and 33.

From an examination of the effects of retaining all terms in the second members of eq 19a and 19b it is easy to ascertain that the error in eq 35, whatever it is, must be of the same order of magnitude as that in eq 35′. The terms of eq 19a and 19b, which are neglected, are estimated to produce an alteration less than 2 in 10^5 in capacitance. The error in eq 35 and 35a increases with γ, vanishing with it, but is practically independent of β, for $1\leq\beta<\infty$. The computed capacitance will be lower than the correct value.

To estimate the error we apply eq 35a to compute $\pi C'$ for the case of a standard capacitor constructed here, which approximates to the two-dimensional type. Its dimensions are

$$\left.\begin{aligned}a&=0.8540\text{ cm}\\ c&=0.2000\text{ cm}\\ b-c&=1.8940\text{ cm}\end{aligned}\right\}\text{ so }\begin{cases}\gamma=\dfrac{c}{a}=0.23419\\ \beta=(b-c)/a=2.2178\end{cases}$$

By eq 28, taking $n=4$,

$$\epsilon_1=0.00873\left[\sum_{k=1}^{4}P_k+R_5\right]$$

$$\begin{aligned}P_1&=0.194_5\\ P_2&=0.101_5\\ P_3&=0.057_2\\ P_4&=0.034_8\\ R_5&=0.096_1\end{aligned}$$

$$0.484=\sum_{k=1}^{4}P_k+R_5$$

This gives $\epsilon_1 = 0.00423$.

It was found that with $n=10$, the sum $\left[\sum_{k=1}^{10} P_k + R_{11}\right]$ gave a value of ϵ_1 so near this as to affect the capacitance by less than two parts in a millon.

The result of computing $\pi C'$ by eq 35a is to be compared with that given by the exact equation (eq 48) to be derived below. The constant ξ_0 appearing in eq 48 is given by eq 43a, which gives $\xi_0 = \frac{2}{\pi}\tan^{-1}\gamma = 0.146454_4$.

	$\pi C'$	
	by eq 35a	by eq 48
1st term	0. 027 795	0. 027 810 8
2d term	. 000 005	. 000 003 7
3d term	. 000 000	. 000 000 00
$\pi C'$	. 027 800	. 027 814 5

Equation 35a here gives C' too low by one in 2,000.

Another computation for a shallower slot, $\beta=1$, with the same γ as above gives a coefficient of capacitance C' about seven times as large.

	$\pi C'$	
	by eq 35a	by eq 48
1st term	0. 192 142	0. 192 688
2d term	. 001 537	. 001 146
3d term	. 000 026	. 000 000
$\pi C'$	. 193 707	. 193 834

Hence we expect the pacitance in case of the cylindrical hole computed by eq 35 will also be lower than the correct value by about one in 2,000 (if $\gamma=0.2$). This is probably less than the experimental error of the comparison of such very small capacitors.

If a precision greater than one in 2,000 were required, this might be found by retaining one more series in eq 17 for x_1, that is,

$$x_1 = \frac{A_1}{\gamma\alpha_1}\left[1+(\gamma\alpha_1)^2\sum_{k=1}^{\infty}\frac{A_k X_{1k}^{(1)}}{\alpha_k}+\gamma^4\alpha_1^2\sum_{k=1}^{\infty}\frac{A_k X_{1k}^{(2)}}{\alpha_k}\right] = \frac{A_1}{\gamma\alpha_1}[1+\epsilon_1+\delta_1]$$

where

$$\delta = \gamma^4\alpha_1^2\sum_{k=1}^{\infty}\frac{A_k X_{1k}^{(2)}}{\alpha_k} = \gamma^4\alpha_1^2\sum_{k=1}^{\infty}\frac{A_k}{\alpha_k}\sum_{s=1}^{\infty}\alpha_s A_s X_{1s}^{(1)} X_{sk}^{(1)},$$

where $X_{sk}^{(1)}$ is given by eq 21a, A_k by eq 8.

For $\gamma=1/5$ eq 35 gives values of C that are too small by one in 500 neglecting both ϵ_1 and δ_1; and too small by one in 2,000 neglecting δ_1 only. From the computations given it appears that δ_1 is about 1/8 of ϵ_1. The approximate evaluation of δ_1 by this double series would require an evaluation of each remainder, as in the single series for ϵ_1. It would require much labor for small gain.

An alternative estimate would be given by making a plot of the error in eq 35a as a function of γ from $\gamma=0.1$ to 0.5 all with $\beta=1$. This could be taken as an estimate of the error in eq 35.

IV. The Two-Dimensional Potential

Let $\phi\ (x,\ \rho)$ be the two-dimensional potential that vanishes on the plane $x=0$ and has the constant value π on the guard-conductor and on the base of the slot. Its conjugate function $\psi\ (x,\ \rho)$ is zero on the x-axis. Let ψ_1 and ψ_2 denote the value of ψ_1 at the points A_1 and A_2 respectively. The capacitance C' per unit length of slot is proportional to ψ, for the surface density σ of charge on the base of the slot is given by

$$4\pi\sigma = \left[\frac{\partial\phi(x,\ \rho)}{\partial x}\right]_{x=b} = \frac{\partial}{\partial\rho}\psi(b,\ \rho),$$

so the total charge Q' upon the base of the slot, (of width $2a$), per cm length of slot is

$$Q' = \int_{-a}^{+a}\sigma(\rho)d\rho = \frac{1}{2\pi}\int_0^a \frac{\partial\psi(b,\ \rho)}{\partial\rho}\,d\rho = \frac{\psi_1}{2\pi}.$$

The coefficient of capacitance C' per cm length of slot between the plane $x=0$ and the bottom of the slot is $C' = \frac{Q'}{\pi}$ (cm) or $\pi C' = \frac{\psi_1}{2\pi}$.

To find ψ_1 we first obtain the complex potential

$$\omega = \phi + i\psi,$$

which may be considered a function $\omega\ (z)$ of the complex variable $z = x + i\rho$.

To do this, the dielectric region (D) of figure 2a is first represented conformally upon the

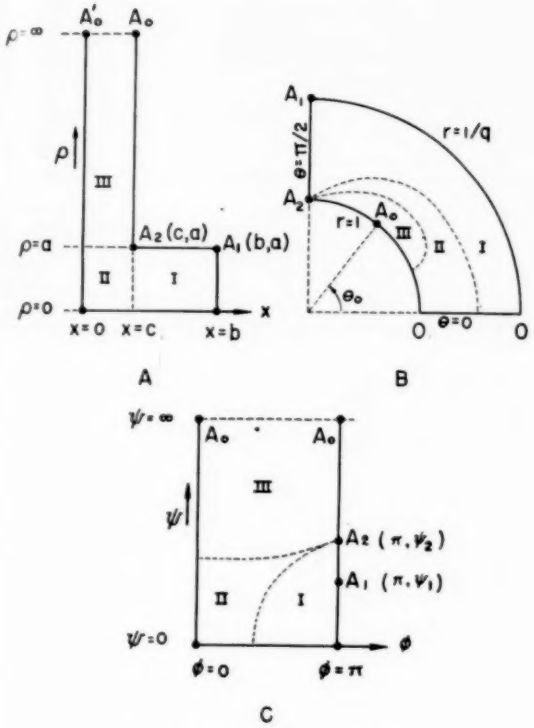

FIGURE 2. *Dielectric volume.*

A, Plane of $Z=X+iy$; B, plane of $t=re^{i\theta}$, eq 38; C, potential strip $\omega=\phi+i\psi$ (eq 47).

quarter-annulus of figure 2b defined by the plane polar coordinates

$$1<r<\frac{1}{q} \text{ and } 0<\theta<\frac{\pi}{2}.$$

The conformance is indicated by similar lettering in figures 2, a and 2, b. This region (D) may also be represented on the semi-infinite, potential-strip as shown in figure 2, c where

$$0<\phi<\pi \text{ and } 0<\psi<\infty.$$

The mapping equation we take is equivalent to

$$\frac{\pi z}{c}=\frac{4ai\zeta}{c}+i\log\frac{\vartheta_1(\zeta_0+\zeta)\vartheta_2(\zeta_0+\zeta)}{\vartheta_1(\zeta_0-\zeta)\vartheta_2(\zeta_0-\zeta)}, \tag{37}$$

and the potential is equivalent to

$$\omega=i\log\frac{\vartheta_1(\zeta_0+\zeta)\vartheta_2(\zeta_0-\zeta)}{\vartheta_1(\zeta_0-\zeta)\vartheta_2(\zeta_0+\zeta)}$$

$$=i\log\frac{sn(u_0+u)cn(u_0-u)}{cn(u_0+u)sn(u_0-u)}\left(\text{where } u=\frac{2K}{\pi}\zeta\right). \tag{37a}$$

One is led to the equation of transformation by well-known methods, but for convenience of numerical computation, it is better to use the series that are equivalent to eq 37 and 37a. By this method the discussion of the equation of transformation and of the potential may be made without any reference to, or knowledge of, theta-functions or elliptic functions.

Accordingly we take a complex variable,

$$t=re^{i\theta}=e^{2i\zeta}=e,^{i\pi u/K}$$

and start with the equation of transformation,

$$\frac{\pi}{a}(z-b)=2\log(qt)-\gamma\left\{i\log\frac{(t-e^{i\theta_0})}{(t-e^{-i\theta_0})}\frac{(t+e^{i\theta_0})}{(t+e^{-i\theta_0})}+\right.$$
$$\left.4\sum_{n=1}^{\infty}\frac{q^{4n}(t^{-2n}-t^{2n})}{2n(1-q^{4n})}\sin 2n\theta_0\right\}, \tag{38a}$$

where the positive constants, $0<q<1$, and the angle θ_0, $\left(0<\theta_0<\frac{\pi}{2}\right)$, are to be found in terms of the given constants

$$\gamma\equiv\frac{c}{a} \text{ and } \beta\equiv\frac{b-c}{a}.$$

Since $1<|t|=r<\frac{1}{q}$ in figure 2b the logarithm in eq 38a may be expanded in a series so that

$$\frac{\pi}{a}(z-b)=2\log(qt)-$$
$$4\gamma\sum_{n=1}^{\infty}\frac{q^{2n}[(qt)^{-2n}-(qt)^{2n}]}{2n(1-q^{4n})}\sin 2n\theta_0, \tag{38b}$$

which converges within and on the boundaries of the region (D) of figure 2b. Its term-by-term derivative converges within, but not on the arc $r=1$.

To obtain a series for $\frac{dz}{dt}$ convergent on the boundaries, eq 38a may be differentiated, giving

$$\left(\frac{\pi t}{2a}\right)\frac{dz}{dt}=1+\gamma\left[\frac{4t^2\sin\theta_0\cos\theta_0}{(t^2+1)^2-4t^2\cos^2\theta_0}+\right.$$
$$\left.2\sum_{n=1}^{\infty}\frac{q^{4n}(t^{-2n}+t^{2n})}{1-q^{4n}}\sin 2n\theta_0\right]. \tag{39}$$

To establish the correspondence for the point A_2 of figure 2a and figure 2b, we place $z=c+ia$ and and $t=e^{\frac{\pi}{2}}$ in eq 38a. This gives

$$q=e^{-\frac{\pi}{2}\left[\beta+\frac{2\gamma}{\pi}\theta_0\right]}. \tag{40a}$$

Also, since the point A_2 is the only point where angles are not preserved by this transformation, it is necessary that dz/dt be either zero or infinite there. Since z is continuous there, dz/dt must vanish. Hence the second member of eq 39 must vanish when $t=e^{i\pi/2}$. That is

$$\tan\theta_0+4\sum_{n=1}^{\infty}\frac{(-1)^{n+1}q^{4n}\sin 2n\theta_0}{1-q^{4n}}=\frac{1}{\gamma}. \quad (40b)$$

These two equations determine q and θ_0 as functions of β and γ.

If we write

$$\left.\begin{aligned}\frac{\pi}{2}\xi_0&=\frac{\pi}{2}-\theta_0 \text{ so } 0<\xi_0<1\\ \text{and}\qquad \gamma&=\tan\delta\end{aligned}\right\} \quad (41)$$

then, eliminating q between eq 40a and 40b gives the following equation to determine ξ_0

$$\cot\frac{\pi\xi_0}{2}+4\sum_{n=1}^{\infty}\frac{e^{-2n\pi(\beta+\gamma-\gamma\xi_0)}\sin n\pi\xi_0}{1-e^{-2n\pi(\beta+\gamma-\gamma\xi_0)}}=\cot\delta. \quad (42)$$

A very accurate solution of this for the case in which the slot is not relatively shallow (β not small) may be obtained by using a few terms of this series.

Thus it is found that

$$\frac{\pi}{2}-\theta_0=\frac{\pi\xi_0}{2}=\delta+8\sin^3\delta\cos\delta\, e^{-2\pi\left[\beta+\left(1-\frac{2\delta}{\pi}\right)\tan\delta\right]}\cdot\left\{1+3C_1e^{-2\pi\left[\beta+\left(1-\frac{2\delta}{\pi}\right)\tan\delta\right]}+C_2e^{-4\pi\left[\beta+\left(1-\frac{2\delta}{\pi}\right)\tan\delta\right]}\right\} \quad (43a)$$

where $C_1=1+4\sin^2\delta-\frac{8}{3}\sin^3\delta\cos\delta+\frac{16}{3}\sin^4\delta$.

Also $|C_2|<32$, so the term in C_2 is negligible when $\beta\geq 1$ and δ is small.

When θ_0 or ξ_0 is computed by this formula, the parameter q is then computed by

$$q=e^{-\pi(\beta+\gamma-\gamma\xi_0)/2}.$$

Since $t=re^{i\theta}$, eq 38$_b$ gives x and ρ as functions of r and θ by series that converge in (D), and on its boundaries

$$\frac{x}{a}=\frac{b}{a}+\frac{2}{\pi}\log(qr)-\frac{2\gamma}{\pi}\sum_{n=1}^{\infty}\frac{q^{2n}[(qr)^{-2n}-(qr)^{2n}]}{n(1-q^{4n})}\sin 2n\theta_0\cos 2n\theta \quad (44a)$$

$$\frac{\rho}{a}=\frac{2\theta}{\pi}+\frac{2\gamma}{\pi}\sum_{n=1}^{\infty}\frac{q^{2n}[(qr)^{-2n}+(qr)^{2n}]}{n(1-q^{4n})}\sin 2n\theta_0\sin 2n\theta \quad (44b)$$

$$\text{for } 1\leq r\leq\frac{1}{q} \text{ and } 0\leq\theta\leq\pi/2.$$

The complex potential is

$$\omega=\pi-4\sum_{n=1}^{\infty}\frac{q^{2n-1}[(qt)^{-(2n-1)}-(qt)^{2n-1}]}{(2n-1)(1-q^{4n-2})}\sin(2n-1)\theta_0, \quad (45)$$

which resolves into the two real equations

$$\phi=\pi-4\sum_{n=1}^{\infty}\frac{q^{2n-1}[(qr)^{-(2n-1)}-(qr)^{2n-1}]}{(2n-1)(1-q^{4n-2})}\sin(2n-1)\theta_0\cos(2n-1)\theta \quad (46a)$$

$$\psi=4\sum_{n=1}^{\infty}\frac{q^{2n-1}[(qr)^{-(2n-1)}+(qr)^{2n-1}]}{(2n-1)(1-q^{4n-2})}\sin(2n-1)\theta_0\sin(2n-1)\theta. \quad (46b)$$

The constant ψ_1 (at A_1) corresponds to $r=\frac{1}{q}$, $\theta=\frac{\pi}{2}$.

The constant ψ_2 (at A_2) corresponds to $r=1$, $\theta=\frac{\pi}{2}$.

If these two positive constants are determined thus, the equation that maps the region (D) of the z-plane conformally upon the semi-infinite strip of figure 2c is

$$z=\frac{c}{\pi}\int_0^{\omega}\sqrt{\frac{\cos\omega'+\cosh\psi_2}{\cos\omega'+\cosh\psi_1}}\,d\omega'. \quad (47)$$

To prove this we take the complementary modulus of the elliptic function of u in eq 37 as

$$k'=\frac{\tanh\frac{\psi_2}{2}-\tanh\frac{\psi_1}{2}}{\tanh\frac{\psi_2}{2}+\tanh\frac{\psi_1}{2}}$$

and determine the constant u_0 by

$$\frac{snu_0cnu_0}{dnu_0}=\frac{1}{2}\left(\tanh\frac{\psi_2}{2}+\tanh\frac{\psi_1}{2}\right) \text{ where } 0<u_0<\frac{K'}{2}.$$

Details are omitted as we do not make use of the relation (eq 47).

From eq 46b we obtain (placing $r=\frac{1}{q}$ and $\theta=\frac{\pi}{2}$)

$$\frac{\psi_1}{2\pi}=\frac{4}{\pi}\sum_{n=1}^{\infty}\frac{(-1)^{n+1}q^{2n-1}\sin(2n-1)\theta_0}{(2n-1)(1-q^{4n-2})}.$$

Hence the coefficient C' of capacitance per unit length of slot is given by

$$\pi C'=\frac{4}{\pi}\sum_{n=1}^{\infty}\frac{(-1)^{n+1}q^{2n-1}\sin(2n-1)\theta_0}{(2n-1)(1-q^{4n-2})}$$

Or letting $\alpha_s'=(2s-1)\frac{\pi}{2}$ this may be written

$$\pi C'=\sum_{s=1}^{\infty}\frac{\cos\alpha_s'\xi_0}{\alpha_s'\sinh\alpha_s'(\beta+\gamma-\gamma\xi_0)}, \tag{48}$$

where ξ_0 is the root of eq 42, which may be computed by eq 43a. This equation gives C' with all the precision that may be desired. This is the equation which may be used to find the error in eq 35a which would be of the same order as that in the three-dimensional formula (eq 35).

The deeper the slot, the more rapid is the convergence of the series (eq 48). Although this series converges for any slot however shallow, it becomes practically useless for computation when β is small.

To obtain a formula of complementary nature to eq 48, whose rate of convergence gets more rapid as the slot gets more shallow we may make use of a transformation, which introduces a parameter q_1, which is found to be equal to $\sqrt{q'}$.

In this case we transform the dielectric region of figure 2, a, upon the semicircular annulus of a t plane, as shown in figure 3.

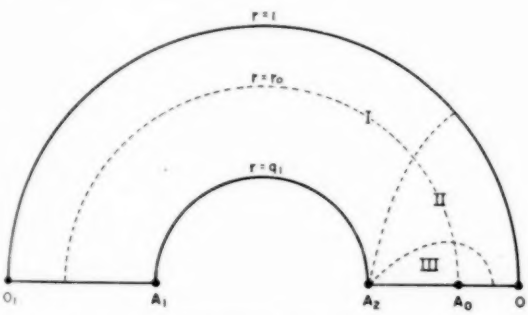

FIGURE 3. *Semicircular annulus for eq 49*

As in the preceding case r and θ are polar coordinates and

$$t=re^{i\theta},$$

but in figure 3 the range of r and θ is

$$q_1<r<1 \text{ and } 0<\theta<\pi.$$

The equation of transformation is now

$$\frac{i\pi z}{c}=\left(\frac{b-c}{c}\right)\log t+\log\left(\frac{t-r_0}{1-r_0t}\right)+\sum_{n=1}^{\infty}\frac{q_1^{2n}(r_0^{-n}-r_0^{n})(t^{-n}-t^{n})}{n(1-q_1^{2n})}. \tag{49}$$

The positive constants q_1 and r_0 where $0<q_1<r_0<1$ are determined by securing the correspondence at A_2 and the vanishing of dZ/dt at A_2 where angles are not preserved. These two equations are

$$2\sum_{n=1}^{\infty}\left(\frac{q_1}{r_0}\right)^n\cdot\left(\frac{1-r_0^{2n}}{1-q_1^{2n}}\right)=\frac{b-c}{c}=\frac{\beta}{\gamma} \tag{50a}$$

and

$$q_1^{\beta}=e^{-\pi}r_0^{-\gamma} \tag{50b}$$

$$\left.\begin{aligned}\text{Let } u_1&=\log\frac{1}{q_1} \text{ or } q_1=e^{-u_1}\\ u_0&=\log\frac{1}{r_0} \text{ or } r_0=e^{-u_0}.\end{aligned}\right\} \tag{51}$$

Then the two equations (eq 50a and 50b) may be written

$$2\sum_{n=1}^{\infty}\frac{\sinh nu_0}{\sinh nu_1}=\beta/\gamma \tag{52a}$$

and

$$u_0=\frac{\pi-\beta u_1}{\gamma}. \tag{52b}$$

Hence, eliminating u_0, the equation that determines u_1 is

$$2\sum_{n=1}^{\infty}\frac{\sinh n(\pi-\beta u_1)/\gamma}{\sinh nu_1}=\frac{\beta}{\gamma}. \tag{52c}$$

The complex potential is

$$\omega=\phi+i\psi$$

$$=-i\log\left(\frac{t-r_0}{1-r_0t}\right)+i\sum_{n=1}^{\infty}\frac{q_1^{2n}(r_0^{-n}-r_0^{n})(t^{-n}-t^{n})}{n(1+q_1^{2n})}$$

$$=\frac{\pi z}{c}+i\left(\frac{b-c}{c}\right)\log t+2i\sum_{n=1}^{\infty}\frac{q_1^{2n}(r_0^{-n}-r_0^{n})(t^{-n}-t^{n})}{n(1-q_1^{4n})}. \tag{53}$$

At the point A_1, $\frac{\pi z}{c}=\frac{\pi b}{c}+\frac{i\pi a}{c}$, $\phi=\pi$, $\psi=\psi_1$, $t=q_1e^{i\pi}$

$$=-q_1.$$

Equation 53 gives

$$\psi_1=\frac{\pi a}{c}+\left(\frac{b-c}{c}\right)\log q_1-2\sum_{n=1}^{\infty}\frac{(-1)^{n+1}q_1^n(r_0^{-n}-r_0^n)}{n(1+q_1^{2n})}$$

$$=\frac{\pi a}{c}-\frac{\beta}{\gamma}u_1-2\sum_{n=1}^{\infty}\frac{(-1)^{n+1}\sinh nu_0}{n\cosh nu_1}. \tag{54}$$

From this we obtain the following equivalent of eq 48:

$$\pi C'=\frac{a}{2c}-\frac{1}{2\pi}\left[\frac{\beta u_1}{\gamma}+2\sum_{n=1}^{\infty}\frac{(-1)^{n+1}\sinh n(\pi-\beta u_1)/\gamma}{n\cosh nu_1}\right], \tag{55}$$

where u_1 is a function of β and γ determined by eq 52c. This may also be written

$$\pi C'=\frac{a}{2c}-\frac{1}{2\pi}\left[\frac{\beta}{\gamma}\log\frac{1}{q_1}+2\sum_{n=1}^{\infty}\frac{(-1)^{n+1}q_1^n(r_0^{-n}-r_0^n)}{n(1+q_1^{2n})}\right], \tag{56}$$

where r_0 and q_1 are determined by eq 50a and 50b. For a relatively shallow slot in which β/γ is small, while π/γ is neither very small nor very large, we find to the second order inclusive in β or q_1

$$q_1=\frac{\beta}{2\gamma}\left(1-\frac{\beta}{2\gamma}\coth\frac{\pi}{\gamma}\right)\frac{r_0}{1-r_0^2}, \tag{57a}$$

where

$$\log r_0=-\left[\frac{\pi}{\gamma}+\left(\frac{\beta}{\gamma+\beta\coth\pi/\gamma}\right)\log\frac{\beta\left(1-\frac{\beta}{2\gamma}\coth\frac{\pi}{\gamma}\right)}{4\gamma\sinh\pi/\gamma}\right]. \tag{57b}$$

This applies for a slot so shallow that formula (eq 48) would be impracticable.

V. Appendix

Formulation of the potential as Contour Integrals.

The generalized potential equation (where $\nu=0$ or $\nu=-1/2$),

$$(D_x^2+D_\rho^2)V+\frac{1+2\nu}{\rho}D_\rho V=0, \tag{1}$$

has solutions of the form

$$V=\left((C_1\cosh\frac{tx}{a}+C_2\sinh\frac{tx}{a}\right)\xi^{-\nu}C_\nu(t\xi), \tag{2}$$

where $\xi=\rho/a$ and C_ν is any cylinder function of $t\xi$ with parameter ν. The constant t is arbitrary and may be complex. The two fundamental equations, which are satisfied by all cylinder functions, will be needed for reference. They are

$$\left.\begin{aligned}C_{\nu-1}(t\xi)-C_{\nu+1}(t\xi)&=2C_\nu'(t\xi)\\ C_{\nu-1}(t\xi)+C_{\nu+1}(t\xi)&=\frac{2\nu}{t\xi}C_\nu(t\xi),\end{aligned}\right\} \tag{3}$$

which are equivalent to

$$\left.\begin{aligned}D_\xi(\xi^\nu C_\nu(t\xi))&=t\xi^\nu C_{\nu-1}(t\xi)\\ D_\xi(\xi^{-\nu}C_\nu(t\xi))&=t\xi^{-\nu}C_{\nu+1}(t\xi).\end{aligned}\right\} \tag{3a}$$

The cylinder functions here used are Bessel's function $J_\nu(t)$ and the two Hankel's fanctions $H_\nu^{(1)}(t)$ and $H_\nu^{(2)}(t)$. However, the latter will only be used in passing, so that since $H_\nu^{(1)}$ occurs frequently it may be denoted by $H_\nu(t)$.

From the identity in t,

$$H_\nu(t)J_\nu'(t)-H_\nu'(t)J_\nu(t)=\frac{2}{i\pi t}, \tag{4}$$

we obtain from the fundamental equations (eq 3) for the case $t=\alpha_s$,
where $J_\nu(\alpha_s)=0$,

$$\left.\begin{aligned}J_\nu'(\alpha_s)&=-J_{\nu+1}(\alpha_s)\text{ and }i\pi\alpha_sH_\nu(\alpha_s)\\ &=-2/J_{\nu+1}(\alpha_s)\\ \frac{i\pi tH_\nu(t)}{2J_\nu'(t)}&=\frac{1}{J_\nu^2(\alpha_s)}\text{ when }t=\alpha_s.\end{aligned}\right\} \tag{4a}$$

In all that follows it is understood that the t-plane is cut along the negative real axis so that $-\pi<\arg t<\pi$.
There is the identical relation

$$2J_\nu(t)=H_\nu(t)+H_\nu^{(2)}(t). \tag{5}$$

The circuital relations around the branch-point $t=0$ are

$$H_\nu^{(2)}(te^{-i\pi})=-e^{i\nu\pi}H_\nu(t)\text{ and }J_\nu(te^{\mp i\pi})=e^{\mp i\nu\pi}J_\nu(t). \tag{6}$$

When $|t|$ is large

$$\left.\begin{aligned}H_\nu(t)&\sim\sqrt{\frac{2}{\pi t}}e^{i\left(t-\left[\nu+\frac{1}{2}\right]\frac{\pi}{2}\right)}\\ \text{and}\\ H_\nu^{(2)}(t)&\sim\sqrt{\frac{2}{\pi t}}e^{-i\left(t-\left[\nu+\frac{1}{2}\right]\frac{\pi}{2}\right)}.\end{aligned}\right\} \tag{7}$$

In certain cases the cut in the t-plane may be disregarded, for $t^{-\nu}J\nu(t)$ is an even integral function of t. Since ν is here considered real and $\nu > -1$, the zeros of $t^{-\nu}J\nu(t)=0$ are real, at $t=\pm\alpha_s (s=1, 2, 3)$. If $t^{-\sigma}F_\sigma(t)$ were another even integral function of t, where $\sigma > -1$, the ratio $t^{-\sigma}F_\sigma(t)/(J_\nu)(t)$ is an even function of t. Suppose $f(t)$ is another analytic function that may possibly have simple zeros at $t=t_n$.

If

$$\frac{t^{1+\nu-\sigma}F\sigma(t)}{f(t)J_\nu(t)} \to 0 \text{ when } t\to\infty, \tag{8a}$$

the integral around a circle of radius $|t|=r$,

$$\frac{1}{2\pi i}\int \frac{t^{\nu-\sigma}F_\sigma(t)}{f(t)J_\nu(t)}\,dt,$$

will approach zero when r increases without limit and without passing through the points $t=t_n$ or $t=\pm\alpha_s$. By Cauchy's theorem this gives (since $J'_\nu(\alpha_s)=-J_{\nu+1}(\alpha_s)$,

$$\sum_n \frac{t_n^{\nu-\sigma}F_\sigma(t_n)}{f'(t_n)J_\nu(t_n)} = \sum_{s=1}^{\infty} \frac{\alpha_s^{\nu-\sigma}F_\sigma(\alpha_s)}{J_{\nu+1}(\alpha_s)}\left[\frac{1}{f(\alpha_s)} - \frac{1}{f(-\alpha_s)}\right]. \tag{8a}$$

This would be a trivial identity $0=0$, only in the case where $f(t)$ is an even function of t.

Taking $f(t)=t-t_0$ gives the identity in t,

$$t^{-\sigma}F_\sigma(t) = 2t^{-\nu}J_\nu(t)\sum_{s=1}^{\infty}\frac{\alpha_s^{1+\nu-\sigma}F_\sigma(\alpha_s)}{(\alpha_s^2-t^2)J_{\nu+1}(\alpha_s)}, \tag{9}$$

if

$$\frac{t^{\nu-\sigma}F_\sigma(t)}{J_\nu(t)} \to 0 \text{ when } t\to\infty$$

where $t^{-\sigma}F_\sigma\ (t)$ is an even integral function of t. Equation 9 applies when ν and σ are both real and exceed -1. Replacing σ by $\nu+\sigma$ and taking $F_{\sigma+\nu}(t)=J_{\nu+\sigma}(t_s)$ gives

$$J_{\nu+\sigma}(t\xi) = 2t^\nu J_\nu(t)\sum_{s=1}^{\infty}\frac{\alpha_s^{1-\sigma}J_{\nu+\sigma}(\alpha_s\xi)}{(\alpha_s^2-t^2)J_{\nu+1}(\alpha_s)} \tag{9a}$$

for any t, when $0\leq\xi<1$ if $-1<\nu$ and $-1<\nu+\sigma$ and when $\xi=1$ if $-1<\nu$ and $0<\sigma$.

The case of this ($\xi=1$, $\sigma>0$) is a special case $\mu=0$ of the following, which is obtained by use of the even function of t,

$$t^\nu J_{\nu+\sigma}(\sqrt{t^2-\mu^2})/[(t^2-\mu^2)^{\frac{\nu+\sigma}{2}}J_\nu(t)]$$

$$\frac{t^\nu J_{\nu+\sigma}(\sqrt{t^2-\mu^2})}{(\sqrt{t^2-\mu^2})^{\nu+\sigma}} = 2J_\nu(t)\sum_{s=1}^{\infty}\frac{\alpha_s^{\nu+1}J_{\nu+\sigma}(\sqrt{\alpha_s^2-\mu^2})}{(\alpha_s^2-t^2)J_{\nu+1}(\alpha_s)(\sqrt{\alpha_s^2-\mu^2})^{\nu+\sigma}}, \tag{9b}$$

where $-1<\nu$, $0<\sigma$, t and μ arbitrary.

Another case of eq 9 with $F_\sigma(t)=G_\nu(t)$:

If $t^{-\nu}G_\nu(t)$ is an even integral function of t (10a)

and $G_\nu(t)/J_\nu(t)\to 0$ when $t\to\infty\ (t\neq\alpha_s)$ (10b)

then by eq. 9

$$G_\nu(t) = 2J_\nu(t)\sum_{s=1}^{\infty}\frac{\alpha_s G_\nu(\alpha_s)}{(\alpha_s^2-t^2)J_{\nu+1}(\alpha_s)}. \tag{10c}$$

It will be found that the infinite set of functions,

$$u_s(t) \equiv \frac{J\nu(t)}{\alpha_s^2-t^2} (\text{where } s=1, 2, 3, \ldots\infty), \tag{11a}$$

constitute an open set of normal functions for the positive real interval $0<t<\infty$. That is

$$\int_0^\infty t\left(\frac{J_\nu(t)}{\alpha_s^2-t^2}\right)\left(\frac{J_\nu(t)}{\alpha_k^2-t^2}\right)dt = \frac{1}{2\alpha_s^2} \text{ if } k=s, =0 \text{ if } k\neq s. \tag{11b}$$

Since the set is not closed, an arbitrary function could not in general be developed in a series of these functions, but eq 10c shows that such developments are possible for a function $G_\nu(t)$ satisfying the conditions of eq 10a and 10b.

A function $G_\nu(t)$ would satisfy eq 10a if defined by a series

$$G_\nu(t) \equiv 2J_\nu(t)\sum_{s=1}^{\infty}\frac{x_s}{\alpha_s^2-t^2} = 2\sum_{s=1}^{\infty}x_s u_s(t), \tag{12}$$

which would converge absolutely if $|x_s|<cs^p$ for $s>s_0$ where $p<1$. Letting $t\to\alpha_s$ shows that

$$x_s=\alpha_s G_\nu(\alpha_s)/J_{\nu+1}(\alpha_s) \text{ as in (10c).}$$

To prove the set u_s is not closed it is sufficient to find one function $f(t)$ (not a null-function) for which

$$\int_0^\infty tf(t)u_s(t)dt = 0 \text{ for every } s(=1, 2, 3, \ldots\infty.$$

A class of such functions will be found immediately; one of the simplest is $J_\nu\ (t\xi)$ where $1\leq\xi$, for it will appear that

$$\int_0^\infty tJ_\nu(t\xi)u_s(t)dt = 0 \text{ for every } s. \tag{13}$$

When eq 13 and 11b are proved, the following will be a consequence:

If $G(t)$ is defined by a series (eq 12), or having the character of eq 10a and 10b is developable in a series like eq 12, then by eq 13

$$\int_0^\infty tG_\nu(t)J_\nu(t\xi)dt=0 \text{ when } 1\leq\xi<\infty, \quad (14a)$$

but when $0\leq\xi<1$

$$\int_0^\infty tG_\nu(t)J_\nu(t\xi)dt=g_\nu(\xi)\equiv 2\sum_{s=1}^{\infty}\frac{G_\nu(\alpha_s)J_\nu(\alpha_s\xi)}{J^2_{\nu+1}(\alpha_s)}. \quad (14b)$$

These two equations show that $G_\nu(t)$ is the Hankel's transform of the function $g_\nu(\xi)$, which is zero for $\xi\geq 1$, where

$$G_\nu(t)=\int_0^1 \xi g_\nu(\xi)J_\nu(t\xi)d\xi. \quad (14c)$$

Conversely, if, with a given function $g_\nu(\xi)$, its transformation $G_\nu(t)$ were defined by this equation, the development (eq 14b) is the formula for developing $g_\nu(\xi)$ for $0\leq\xi<1$ in the series of normal functions $J_\nu(\alpha_s\xi)$.

Equation 14a also follows from eq 14c by reason of Hankel's integral representation of $g_\nu(\xi)$. Finally the identity in t of eq 10c would then be obtained by replacing $J_\nu(\xi t)$ in the integral (eq 14c) by the second member of eq 9a with $\sigma=0$.

The equivalence of eq 10c and 14c as to establishing eq 14a will be important to remember.

To derive eq 14b for the case $0\leq\xi<1$ we find by eq 9a with $\sigma=0$

$$\int_0^\infty tG_\nu(t)J_\nu(\xi t)dt=2\sum_{s=1}^{\infty}\frac{\alpha_s J_\nu(\alpha_s\xi)}{J_{\nu+1}(\alpha_s)}\int_0^\infty \frac{tJ_\nu(t)}{\alpha_s^2-t^2}G_\nu(t)dt=$$

$$2\sum_{s=1}^{\infty}\frac{\alpha_s J_\nu(\alpha_s\xi)}{J_{\nu+1}(\alpha_s)}\int_0^\infty tu_s(t)G_\nu(t)dt=$$

$$2\sum_{s=1}^{\infty}\frac{\alpha_s J_\nu(\alpha_s\xi)}{J_{\nu+1}(\alpha_s)}\sum_{k=1}^{\infty}x_k 2\int_0^\infty tu_s(t)u_k(t)dt. \quad \text{by eq (12)}$$

The use of the orthogonal relations (eq 11b) leads to eq 14b.

We require next some transformations of the integral

$$I=\int_0^\infty tG_\nu(t)J_\nu(\xi t)W(t)dt$$

assumed to be convergent. The function $W(t)$ has no singularities in the immediate neighborhood of the real axis of t and is an even function of t. $G_\nu(t)$ is defined by a series (eq 12), so that it has the same circuital relation around the branch-point $t=0$ as $J_\nu(t)$, that is $G(te^{\pm i\pi})=e^{\pm i\nu\pi}G_\nu(t)$.

As a first step displace the path of I slightly downward so that it goes from $0-i0$ to $\infty-i0$ just below the positive real axis of t. After this replace $J_\mu(\xi t)$ by

$$\frac{1}{2}[H_\mu(\xi t)+H_\nu^{(2)}(\xi t)] \text{ eq 5.}$$

Then

$$I=\frac{1}{2}\int_{0-i0}^{\infty-i0} tG_\nu(t)H_\nu(\xi t)W(t)dt+$$

$$\frac{1}{2}\int_{0-i0}^{\infty-i0} tG_\nu(t)H_\nu^{(2)}(\xi t)W(t)dt.$$

In the second integral let $t=t'e^{-i\pi}$ and take account of the branch relations (eq 6). This gives

$$I=\frac{1}{2}\int_p tG_\nu(t)H_\nu(\xi t)W(t)dt,$$

where the path p begins at $t=-\infty+i\ 0$ and continues above the cut (on negative real axis of t), crosses the axis at $t=+0$ and thence to $+\infty-i\ 0$ below the positive real axis.

For the next transformation leave $J_\nu(\xi t)$ in the integrand of I but break up $G_\nu(t)$. For this we may use temporarily the abbreviation $F(t)$ for the even function of t.

$$F(t)=\sum_{s=1}^{\infty}\frac{x_s}{\alpha_s^2-t^2}$$

so that eq 12 is $G_\nu(t)=2F(t)J_\nu(t)=F(t)[H(t)+H^{(2)}(t)]$.
Hence

$$I=\int_{0-i0}^{\infty-i0} tJ_\nu(\xi t)F(t)W(t)H_\nu(t)dt+$$

$$\int_{0-i0}^{\infty-i0} tJ_\nu(\xi t)F(t)W(t)H_\nu^{(2)}(t)dt.$$

The substitution $t=t'e^{-i\pi}$ in the second integral works out as before, giving

$$I=\int_p tJ_\nu(t\xi)F(t)W(t)H_\nu(t)dt.$$

On restoring $G_\nu(t)$ by $F(t)=G_\nu(t)/2J(t)$ this gives

$$\int_0^\infty G_\nu(t)J_\nu(\xi t)W(t)dt=\frac{1}{2}\int_p tG_\nu(t)H_\nu(t)\frac{J_\nu(\xi t)}{J_\nu(t)}W(t)dt$$

$$= \frac{1}{2}\int_p tG_\nu(t)H_\nu(\xi t)W(t)dt. \quad (15)$$

where

$$\int_p dt = \int_{-\infty+i0}^{+0+i0} dt + \int_{+0-i0}^{+\infty-i0} dt.$$

If the first integral converges, the only other assumption necessary for this transformation is that $t^{-\nu}G_\nu(t)\ W(t)$ be an even, analytic function of t in a region that includes the real axis.

Taking $W(t)=1$ and $G_\nu(t)=u_s(t)=J_\nu(t)/(\alpha_s^2-t^2)$ gives

$$\int_0^\infty tu_s(t)J_\nu(\xi t)dt = \frac{1}{2}\int_p tu_s(t)H_\nu(\xi t)dt$$

$$= \frac{1}{2\pi i}\int_p \frac{i\pi tJ_\nu(t)H_\nu(\xi t)}{\alpha_s^2-t^2}\,dt.$$

On the infinite semicircle above the real axis

$$|i\pi tJ_\nu(t)H_\nu(\xi t)| \to 0 \text{ if } 1<\xi\leq\infty$$

$$\to 1 \text{ if } \xi=1.$$

Hence, closing the path gives

$$\int_0^\infty tu_s(t)J_\nu(\xi t)dt=0 \text{ if } 1\leq\xi\leq\infty, \text{ which is eq 13.}$$

Similarly,

$$\int_0^\infty tu_s(t)u_k(t)dt = \int_0^\infty t\left[\frac{J_\nu(t)}{\alpha_s^2-t^2}\right]\cdot\left[\frac{J_\nu(t)}{\alpha_k^2-t^2}\right]dt$$

$$= \frac{1}{2\pi i}\int_p \frac{i\pi tH_\nu(t)J_\nu(t)}{(\alpha_s^2-t^2)(\alpha_k^2-t^2)}\,dt,$$

which gives the orthogonal relation (eq 11b).

The potential $V(x,\xi)$, which satisfies eq 1, vanishes in the plane $x=0$ and has the value 1 on the right hand boundary of figure 1, may be formulated in terms of its (unknown) values on the artificial boundary $x=c$, $0<\xi=\frac{\rho}{a}<1$.

Let

$$V(c,\ \xi)=1-f_\nu(\xi)=1-\xi^{-\nu}g_\nu(\xi) \text{ for } 0\leq\xi\leq 1$$

$$=1 \text{ for } 1\leq\xi\leq\infty, \quad (16)$$

where $f_\nu\ (1)=0=g_\nu\ (1)$.

Consider $g_\nu(\xi)$ the function represented by the series (eq 14b) and $G_\nu(t)$, its transform defined by eq 14c so that Hankel's integral identity is

$$\int_0^\infty tG_\nu(t)\ J_\nu(\xi t)dt = g_\nu(\xi) \text{ when } 0\leq\xi\leq 1$$

$$=0 \text{ when} 1\leq\xi\leq\infty. \quad (17)$$

Also the series (eq 10c) represents $G_\nu(t)$ for all values of t and $t^{-\nu}G_\nu(t)$ is an even integral function of t. Since $g_\nu(\xi)$ vanishes when $\xi=1$, its representation in eq 14b as a series of normal functions

$$\phi_s(\xi)=\frac{\sqrt{2}J_\nu(\alpha_s\xi)}{J_{\nu+1}(\alpha_s)} \text{ is valid for } 0\leq\xi\leq 1.$$

The related set of normal functions,

$$\psi_s(\xi)=\frac{\sqrt{2}J_{\nu+1}(\alpha_s\xi)}{J_{\nu+1}(\alpha_s)}$$

are suitable for the development of the function

$$\xi^\nu f_\nu'(\xi)=g_\nu'(\xi)-\frac{\nu}{\xi}g_\nu(\xi),$$

for it is known by the general theory of these series of Dini's type that a function that becomes infinite when $\xi\to 1$ may be so developed provided its integral converges. The formula is

$$\xi^\nu f_\nu'(\xi)=2\sum_{s=1}^{\infty}\frac{J_{\nu+1}(\alpha_s\xi)}{J_{\nu+1}^2(\alpha_s)}\int_0^1 \xi_1 J_{\nu+1}(\alpha_s\xi_1)\xi_1^\nu f_\nu'(\xi_1)d\xi_1.$$

That is,

$$g_\nu'(\xi)-\frac{\nu}{\xi}g_\nu(\xi)=$$

$$2\sum_{s=1}^{\infty}\frac{J_{\nu+1}(\alpha_s\xi)}{J_{\nu+1}^2(\alpha_s)}\int_0^1 \xi_1 J_{\nu+1}(\alpha_s\xi_1)\left[g_\nu'(\xi_1)-\frac{\nu}{\xi_1}g_\nu(\xi_1)\right]d\xi_1.$$

By integration by parts the integral is found to be

$$-\int_0^{'}[\alpha_s\xi_1 J_{\nu+1}'(\alpha_s\xi_1)+(\nu+1)J_{\nu+1}(\alpha_s\xi_1)]g_\nu(\xi_1)d\xi_1.$$

By use of eq 3 and 3a this reduces to

$$-\alpha_s\int_0^{'}\xi_1 g_\nu(\xi_1)J_\nu(\alpha_s\xi_1)d\xi_1,$$

which is $-\alpha_s G_\nu(\alpha_s)$, so that

$$\xi_\nu\frac{d}{d\xi}[\xi^{-\nu}g_\nu(\xi)]=g_\nu'(\xi)-$$

$$\frac{\nu}{\xi}g_\nu(\xi)=-2\sum_{s=1}^{\infty}\frac{\alpha_s G_\nu(\alpha_s)}{J_{\nu+1}^2(\alpha_s)}J_{\nu+1}(\alpha_s\xi), \quad (18)$$

which is valid for $0\leq\xi<1$. As $\xi\to 1$ this series converges to values that increases without limit,

822521—49——7

as it must do to represent the function on the left in which $f'_\nu(\xi)$ and $g'_\nu(\xi)$ go to $-\infty$. This method of derivation of eq 18 proves that it is permissible to make term-by-term application to eq 14a of the differentiating operator $\xi^\nu \frac{d}{d\xi}[\xi^{-\nu} g_\nu \xi]$, for this gives eq 18.

To test the convergence of series and integrals representing the potential, and to make certain transformation of these integrals, a knowledge of the principal term in the asymptotic expansion of $G_\nu(t)$ is required. These may be derived from the well-known fact that if the interior angle at A_2 in figure 1 is θ, the potential in its neighborhood must vanish like $A\ (1-\xi^2)^{\pi/\theta}$. Since θ is $3\pi/2$ in this problem, consider the comparison-funtion

$$\bar{g}_\nu(\xi)=\xi^\nu \bar{f}_\nu(\xi)=A_\nu \xi^\nu (1-\xi^2)^{2/3} \text{ where } A_\nu>0. \quad (19a)$$

Its transform is

$$\bar{G}_\nu(t)=A_\nu \int_0^1 \xi^{\nu+1}(1-\xi^2)^{2/3} J_\nu(t\xi)\,d\xi. \quad (19b)$$

Hence $\bar{g}_\nu(\xi)$ is represented by a series like eq 14b and also by eq 18

$$\bar{g}'_\nu(\xi)-\frac{\nu}{\xi}\bar{g}_\nu(\xi)=-2\sum_{s=1}^{\infty}\frac{\alpha_s \bar{G}_\nu(\alpha_s)}{J^2_{\nu+1}(\alpha_s)} J_{\nu+1}(\alpha_s \xi) \quad (19c)$$

In the actual potential in both cases $\nu=0$ and $\nu=-1/2$ the potential must vanish at A_2 so that g_ν vanishes like the comparison-function $\bar{g}_\nu(\xi)$ when $\xi\to 1$. Consequently there must be a finite limit L_ν such that when $\xi\to 1$

$$g_\nu(\xi)-\bar{g}_\nu(\xi)=\infty-\infty=L_\nu.$$

This finite constant L_ν may be positive, negative, or zero. Its value is not required, nor is that of the positive constant A.

If we subtract from eq 10c the corresponding identity,

$$\bar{G}_\nu(t)=2J_\nu(t)\sum_{s=1}^{\infty}\frac{\alpha_s \bar{G}_\nu(\alpha_s)}{(\alpha_s^2-t^2)J^{(\alpha_s)}_{\nu+1}},$$

we get, after multiplying the resulting equation by $t^2/J_\nu(t)$,

$$\frac{t^2[G_\nu(t)-\bar{G}_\nu(t)]}{J_\nu(t)}=-2\sum_{s=1}^{\infty}\frac{\alpha_s}{J^{(\alpha_s)}_{\nu+1}}\left[\frac{G_\nu(\alpha_s)-\bar{G}_\nu(\alpha_s)}{1-\frac{\alpha_s^2}{t^2}}\right].$$

Subtracting eq 19a from eq 18 we get in the limit (since $\bar{g}_\nu(\xi)\to 0$ and $g_\nu(\xi)\to 0$ when $\xi\to 1$)

$$\lim_{\xi\to 1}[g'_\nu(\xi)-\bar{g}'_\nu(\xi)]=\infty-\infty=L_\nu$$
$$=-2\sum_{s=1}^{\infty}\frac{\alpha_s}{J_{\nu+1}(\alpha_s)}[G_\nu(\alpha_s)-\bar{G}_\nu(\alpha_s)],$$

which shows that the second member of the preceding equation approaches some of finite limit L_ν when $t\to\infty$ without passing through any zero α_s of $J_\nu(t)$.

Consequently the principal term in the asymptotic expansion of $G_\nu(t)$ is contained in

$$G_\nu(t)\sim\bar{G}_\nu(t)+\frac{L_\nu}{t^2}J_\nu(t). \quad (20)$$

To see which of these two terms is the important one, we may find $\bar{G}_\nu(t)$ by application of Sonin's integral. If σ and ν are real and $\sigma>0$, $\nu>-1$, while t and μ are arbitrary, Sonin's integral is

$$(i\mu)^{1-\sigma}\int_0^{\pi/2}\cos^{\nu+1}\phi\sin^\sigma\phi J_{\sigma-1}(i\mu\sin\phi)J_\nu(t\cos\phi)\,d\phi=$$
$$(i\mu)^{1-\sigma}\int_0^1 \xi J_\nu(\xi t)\left[\xi^\nu(1-\xi^2)^{\frac{\sigma-1}{2}}J_{\sigma-1}(i\mu\sqrt{1-\xi^2})\right]d\xi=$$
$$\frac{t^\nu J_{\nu+\sigma}(\sqrt{t^2-\mu^2})}{(\sqrt{t^2-\mu^2})^{\nu+\sigma}}, \quad (21)$$

which becomes with $\mu=0$

$$\int_0^1 \xi^{\nu+1}(1-\xi^2)^{\sigma-1}J_\nu(\xi t)\,d\xi=\frac{\Gamma(\sigma)}{2}\left(\frac{2}{t}\right)^\sigma J_{\nu+\sigma}(t). \quad (22)$$

Hence taking $\sigma=5/3$, eq 19b gives

$$\bar{G}_\nu(t)=\frac{A_\nu}{2}\left(\frac{2}{t}\right)^{5/3}J_{\nu+5/3}(t).$$

When t is large this is the important term in eq 20 so the asymptotic expression for $G_\nu(t)$ may be taken in the form

$$t^{5/3}\frac{G_\nu(t)}{J_\nu(t)}\sim\text{constant when } t\to\infty\,(t\neq\alpha_s). \quad (23)$$

If the interior angle at A_2 of figure 1 were any other than $\theta=3/2$, say $\pi<\theta<2\pi$ the factor $t^{5/3}$ would be replaced by $t^{1+\pi/\theta}$.

The formulation of the potential will be implicitly in terms of $g_\nu(\xi)$ but explicitly in terms of its transforma $G_\nu(t)$.

All that is assumed as to $G_\nu(t)$ is that $t^{-\nu}G_\nu(t)$ is an even integral function of t with asymptotic expansion (eq 23).

If $\gamma=c/a$ and $\beta=(b-c)/a$, the potential in region I may be written as an integral over a path p_1, which encircles in positive direction the positive real axis of t, (all the positive zeros $t=\alpha_s$ of $J_\nu(t)=0$).

In region I

$$V(x,\xi)=1-\frac{\xi^{-\nu}}{2}\int_{p_1} tG_\nu(t)H_\nu(t)\frac{J_\nu(t\xi)\sinh(b-x)t/a}{J_\nu(t)\sinh\beta t}dt. \tag{24a}$$

In the combined region II and III

$$V(x,\xi)=\frac{x}{c}-\frac{\xi^{-\nu}}{2}\int_p tG_\nu(t)H_\nu(t)\frac{J_\nu(t\xi)\sinh xt/a}{J_\nu(t)\sinh\gamma t}dt. \tag{24b}$$

To show that this potential is everywhere continuous and satisfies the required boundary conditions, consider the first integral in eq 24a. This vanishes when $x=b$ and again when $\rho=a$, $(\xi=1)$ since the denominator $J_\nu(t)$ disappears, and the path p_1 then encloses no singular points. At the internal boundary $x=c$ the integrands in eq 24a and 24b become equal. Also, since the denominators $\sinh\beta t$ and $\sinh\gamma t$ disappear the integrands have no singularity above the real axis of t so the paths p and p_1 become equivalent. Consequently the potential is continuous at $x=c$, $0\leq\xi\leq1$.

The integral in eq 24b and the potential vanish when $x=0$. To see that the integral (eq 24b) also vanishes when $\xi\to\infty$, reference to eq 15 shows that eq 24b is equivalent to two other integrals all equally valid in the combined region II and III.

$$V(x,\xi)=\frac{x}{c}-\frac{\xi^{-\nu}}{2}\int_p tG_\nu(t)H_\nu(t\xi)\frac{\sinh xt/a}{\sinh\gamma t}dt \tag{24c}$$

and

$$V(x,\xi)=\frac{x}{c}-\xi^{-\nu}\int_0^\infty tG_\nu(t)J_\nu(t\xi)\frac{\sinh xt/a}{\sinh\gamma t}dt. \tag{24d}$$

By eq 23 the path p of eq 24c may be closed with an infinite semicircle above the real axis of t, when $\xi\geq1$. It encircles the poles at $t=in\pi/\gamma$ where $\sinh\gamma t=0$, so that
in region III $(0\leq x\leq c$ and $a\leq\rho\leq\infty)$

$$V(x,\xi)=\frac{x}{c}+\frac{\pi\xi^{-\nu}}{\gamma}\sum_{n=1}^{\infty}(-1)^n\sin\left(\frac{n\pi x}{c}\right)\left(\frac{in\pi}{\gamma}\right)H_\nu\left(\frac{in\pi}{\gamma}\xi\right)G_\nu\left(\frac{in\pi}{\gamma}\right). \tag{25}$$

In region II where $0\leq\xi<1$ it is eq 24b whose path may be closed with the same semicircle. The path then encircles two sets of poles, the set where $\sinh\gamma t=0$ and the set $t=\alpha_s$ on the positive real axis of t. Hence in region II (where $0\leq x\leq c$ and $0\leq\rho\leq a$) eq 24b is equivalent to the series

$$V(x,\xi)=\frac{x}{c}-2\xi^{-\nu}\sum_{s=1}^{\infty}\frac{G_\nu(\alpha_s)J_\nu(\alpha_s\xi)\sinh x\alpha_s/a}{J^2_{\nu+1}(\alpha_s)\sinh\gamma\alpha_s}+\frac{\pi\xi^{-\nu}}{\gamma}\sum_{n=1}^{\infty}(-1)^n\sin\left(\frac{n\pi x}{c}\right)\left(\frac{in\pi}{\gamma}\right)H_\nu\left(\frac{in\pi}{\gamma}\right)G_\nu\left(\frac{in\pi}{\gamma}\right)\frac{J_\nu(in\pi\xi/\gamma)}{J_\nu(in\pi/\gamma)}. \tag{26a}$$

Similarly in region I (where $c\leq x\leq b$ and $0\leq\rho\leq a$) eq 24a is equivalent to

$$V(x,\xi)=1-2\xi^{-\nu}\sum_{s=1}^{\infty}\frac{Gv(\alpha_s)J_\nu(\alpha_s\xi)\sinh(b-x)\alpha_s/a}{J^2_{\nu+1}(\alpha_s)\sinh\beta\alpha_s}. \tag{26b}$$

From the last two series, we get the series that states the continuity of D_xV,

$$c\xi^\nu[(D_xV)_{x=c+0}-(D_xV)_{x=c-0}]=2\sum_{s=1}^{\infty}\frac{J_\nu(\alpha_s\xi)}{\alpha_sJ_{\nu+1}(\alpha_s)}\left[\gamma\alpha_s(\coth\gamma\alpha_s+\coth\beta\alpha_s)\frac{\alpha_sG_\nu(\alpha_s)}{J_{\nu+1}(\alpha_s)}\right]-\pi\sum_{n=1}^{\infty}\left(\frac{n\pi}{\gamma}\right)\frac{J_\nu(in\pi\xi/\gamma)}{J_\nu(in\pi/\gamma}\left(\frac{in\pi}{\gamma}\right)H_\nu\left(\frac{in\pi}{\gamma}\right)G_\nu\left(\frac{in\pi}{\gamma}\right)-\xi^\nu=0, \tag{27}$$

which must be true only for $0\leq\xi<1$.

For this interval

$$\xi^\nu=2\sum_{s=1}^{\infty}\frac{J_\nu(\alpha_s\xi)}{\alpha_sJ_{\nu+1}(\alpha_s)}. \tag{28}$$

Also by eq 9a with $\sigma=0$ and $t=in\pi/\nu$

$$\frac{J_\nu(in\pi\xi/\gamma)}{J_\nu(in\pi/\gamma)}=2\sum_{s=1}^{\infty}\frac{J_\nu(\alpha_s\xi)}{\alpha_sJ_{\nu+1}(\alpha_s)}\left[\frac{\alpha_s^2}{\alpha_s^2+(n\pi/\gamma)^2}\right]. \tag{29}$$

Placing these in eq 27 gives a series $\sum_1^\infty C_sJ_0(\alpha_s\xi)=0$ so each coefficient C_s must vanish.

Hence the continuity of D_xV at $x=c$ requires that $G_\nu(t)$ be such a function as to satisfy the infinite system of linear equations, in which, for brevity,

$$A_s\equiv\frac{1}{\coth\gamma\alpha_s+\coth\beta\alpha_s}=\frac{\sinh\gamma\alpha_s\sinh\beta\alpha_s}{\sinh(\beta+\gamma)\alpha_s} \tag{30}$$

and

$$x_s \equiv \frac{\alpha_s G_\nu(\alpha_s)}{J_{\nu+1}(\alpha_s)}. \tag{31}$$

The system of equations ($s=1,2,3, \ldots \infty$) for continuity of $D_\xi V$ is

$$x_s - A_s\alpha_s \sum_{n=1}^{\infty} \frac{n\pi[\pi(in\pi/\gamma)H_\nu(in\pi/\gamma)]}{(n\pi)^2+(\gamma\alpha_s)^2} G_\nu\left(\frac{in\pi}{\gamma}\right) = \frac{A_s}{\gamma\alpha_s}. \tag{32a}$$

The additional condition, that $V(c,\xi)=1$ for $\xi>1$ is the equivalent of the identity in t in eq 10c, which becomes

$$G\left(\frac{in\pi}{\gamma}\right) = 2\gamma^2 J_\nu\left(\frac{in\pi}{\gamma}\right) \sum_{k=1}^{\infty} \frac{x_k}{(n\pi)^2+(\gamma\alpha_k)^2}. \tag{32b}$$

There is an infinite class of functions $G_\nu(t)$ that satisfy eq 32a making $D_\xi V$ continuous. There is another infinite class satisfying the identity (eq 10c) (or eq 32b in particular). These make $V(c,\xi)=1$ when $\rho>a$. The function common to both classes will be uniquely determined. The second condition (eq 10c or 32b) could be replaced by the statement that $G_\nu(t)$ is that solution of eq 32a such that $t^{-\nu} G_\nu(t)$ is an even integral function of t with asymptotic expansion (eq 23). For this property is all that was required to show that the potential of eq 24a and 24b satisfies all the external boundary conditions and is continuous at $x=c$ for $0\leq\xi\leq 1$. Hence if eq 32b is true, the potential is thereby determined and $D_\xi V$ is continuous. This potential is known to be unique.

Writing for brevity

$$X_{sk}^{(1)}(\gamma) = X_{ks}^{(1)}(\gamma) \equiv \sum_{n=1}^{\infty} \frac{2n\pi[\pi(in\pi/\gamma)H_\nu(in\pi/\gamma)J_\nu(in\pi/\gamma)]}{[(n\pi)^2+(\gamma\alpha_s)^2]\,[(n\pi)^2+(\gamma\alpha_k)^2]}, \tag{33}$$

the result of eliminating $G_\nu(in\pi/\gamma)$ between eq 32a and 32b is

$$x_s - \gamma^2 A_s\alpha_s \sum_{k=1}^{\infty} X_{sk}^{(1)} x_k = \frac{A_s}{\gamma\alpha_s}, \tag{34}$$

which was derived more briefly in the text.

If the s^{th} eq 34 is multiplied by $2J_\nu(\alpha_s\xi)/\alpha_s J_{\nu+1}(\alpha_s)$ and summed, this gives, by reference to eq 14b and 31

$$g_\nu(\xi) - \gamma^2 \sum_{k=1}^{\infty}\sum_{s=1}^{\infty} 2A_s\alpha_k X_{sk}^{(1)} \left[\frac{J_\nu(\alpha_s\xi)}{J_{\nu+1}(\alpha_s)}\right] \cdot \frac{G_\nu(\alpha_k)}{J_{\nu+1}(\alpha_k)} = \frac{2}{\gamma}\sum_{s=1}^{\infty} \frac{A_s J_\nu(\alpha_s\xi)}{\alpha_s^2 J_{\nu+1}(\alpha_s)}.$$

Since $G_\nu(\alpha_k) = \int_0^1 \xi_1 g_\nu(\xi_1) J_\nu(\alpha_k\xi_1)\,d\xi_1$ this is an integral equation to determine $g_\nu(\xi)$ for $0\leq\xi\leq 1$.

$$\left.\begin{aligned} g_\nu(\xi) - \gamma^2 \int_0^1 \xi_1 g_\nu(\xi_1) N(\xi,\xi_1)\,d\xi_1 &= \frac{2}{\gamma}\sum_{s=1}^{\infty} \frac{A_s J_\nu(\alpha_s\xi)}{\alpha_s^2 J_{\nu+1}(\alpha_s)} \\ \text{where} \qquad N(\xi,\xi_1) &= 2\sum_{s=1}^{\infty}\sum_{k=1}^{\infty} A_s\alpha_k X_{sk}^{(1)} \frac{J_\nu(\alpha_s\xi)J_\nu(\alpha_k\xi_1)}{J_{\nu+1}(\alpha_s)J_{\nu+1}(\alpha_k)}. \end{aligned}\right\} \tag{35}$$

It is known that the solution of this integral equation of Fredholm's type is given by the method of Neumann-Liouville, in a convergent series of iterated integrals, provided that γ^2 is less than $|\lambda_1|$ where λ_1 is the smallest characteristic constant, or root of the Fredholm determinant formed from N. The constants will of course be functions of β and γ. This suggested testing the Neumann-Liouville method, which in effect is the method of successive substitution that was proved in the text to give the solution of the system (eq 34) for all positive values of β and γ. Hence it may be concluded that λ_1 is a function of β and γ such that $|\lambda_1|$ is always greater than γ^2 (unless N is a kind of nucleus with no eigen-constants). It may be shown that this is not the case, and that N has an infinite number of constants λ_s all real.

For computation the system (eq 34) is disappointing, and, although it admits of a great variety of interesting transformations, these will probably all be unsatisfactory until someone discovers the appropriate normal functions for N or what amounts to an orthogonal transformation reducing the double series in eq 35 to diagonal terms only.

In view of the fact that the potential problem for the two-dimensional potential ($\nu=-1/2$) admits an exact (though implicit) solution by conformal mapping with theta-functions it does not seem improbable that someone might solve the problem here formulated for general values of ν or at least for $\nu=0$.

With this in view we add a few remarks and other integral equations, which so far have led nowhere.

In the series of eq 34 we may place

$$x_k \equiv \frac{\alpha_k G_\nu(\alpha_k)}{J_{\nu+1}(\alpha_k)} = \alpha_k^2 \int_0^\infty \frac{t_1 J_\nu(t_1) G_\nu(t_1)}{\alpha_s^2 - t_1^2}\,dt_1$$

$$= \frac{\alpha_k^2}{2} \int_p \frac{t_1 G_\nu(t_1) H_\nu(t_1)}{\alpha_k^2 - t_1^2}\, dt_1.$$

Hence if we multiply the s^{th} equation of the system (eq 34) by $2J_\nu(t)/(\alpha_s - t^2)$ and sum $s=1$ to ∞ this gives

$$G_\nu(t) - 2\gamma^2 \sum_{s=1}^{\infty} \sum_{k=1}^{\infty} \frac{A_s \alpha_s X_{sk}^{(1)} x_k J_\nu(t)}{\alpha_s^2 - t^2} = \frac{2J_\nu(t)}{\gamma} \sum_{s=1}^{\infty} \frac{A_s}{\alpha_s(\alpha_s^2 - t^2)}$$

Replacing x_k by the first integral above gives

$$\left.\begin{aligned} G_\nu(t) - \gamma^2 \int_0^\infty t_1 G_\nu(t_1) M(t, t_1)\, dt_1 &= \frac{2J_\nu(t)}{\gamma} \sum_{s=1}^{\infty} \frac{A_s}{\alpha_s(\alpha_s^2 - t^2)} \\ \text{where} \quad M(t, t_1) &= 2 \sum_{s=1}^{\infty} \sum_{k=1}^{\infty} A_s \alpha_k X_{sk}^{(1)} \left[\frac{\alpha_s J_\nu(t)}{\alpha_s^2 - t^2}\right] \cdot \left[\frac{\alpha_k J_\nu(t)}{\alpha_k^2 - t^2}\right]. \end{aligned}\right\} \quad (36)$$

This integral equation satisfied by $G_\nu(t)$ for $0 < t \infty$ is formally similar to its transform, the integral equation eq 35, which determines $g_\nu(\xi)$ for $0 < \xi < 1$. The nucleus $M(t, t_1)$ is formed from $N(\xi, \xi_1)$ by replacing the normal functions $J_\nu(\alpha_s \xi)/J_{\nu+1}(\alpha_s)$ in the double series by the normal function $\alpha_s J_\nu(t)/(\alpha_s^2 - t^2)$.

This set of normal functions is not closed, but this is compensated by the fact that the subsidiary relation (eq 10c) requires that the solution $G_\nu(t)$ be a function that is developable in terms of them.

The series in eq 32a may be put in the form of an integral, for

$$\frac{1}{2} \int_p t_1^2 \coth \gamma t_1 H_\nu(t_1) G_\nu(t_1) \frac{dt_1}{\alpha_s^2 - t_1^2} = \frac{1}{2} x_s \coth \gamma \alpha_s - \sum_{n=1}^{\infty} \frac{n\pi[\pi(in\pi/\gamma) H_\nu(in\pi/\gamma)]}{(n\pi)^2 + (\gamma\alpha_s)^2} G_\nu\left(\frac{in\pi}{\gamma}\right).$$

Hence the system of eq 32a is equivalent to

$$\gamma x_s + \frac{\alpha_s \tanh \beta\alpha_s}{2} \int_p t_1 G_\nu(t_1)(\gamma t_1) \coth (\gamma t_1) H_\nu(t_1) \frac{dt_1}{\alpha_s^2 - t_1^2} = \frac{\tanh \beta\alpha_s}{\alpha_s}. \quad (37)$$

Multiplying by $2J_\nu(t)/(\alpha_s^2 - t^2)$ and summing gives

$$\gamma G_\nu(t) + \frac{J_\nu(t)}{2} \int_p t_1 G_\nu(t_1) \frac{\gamma t_1 H_\nu(t_1)}{\tanh t_1 \gamma} \sum_{s=1}^{\infty} \frac{2\alpha_s \tanh \beta\alpha_s}{(\alpha^2 - t^2)(\alpha_s^2 - t_1^2)} dt_1 = 2J_\nu(t) \sum_{s=1}^{\infty} \frac{\tanh \beta\alpha_s}{\alpha_s(\alpha_s^2 - t^2)}, \quad (38a)$$

which may also be put in the form

$$\gamma G_\nu(t) + \int_0^\infty t_1 G_\nu(t_1) K(t, t_1) dt_1 = 2J_\nu(t) \sum_{s=1}^{\infty} \frac{\tanh \beta\alpha_s}{\alpha_s(\alpha_s^2 - t^2)}, \quad (38b)$$

where

$$K(t, t_1) = \gamma t_1 \coth \gamma t_1 \sum_{s=1}^{\infty} 2\alpha_s \tanh \beta\alpha_s \left[\frac{J_\nu(t)}{\alpha_s^2 - t^2}\right]\left[\frac{J_\nu(t_1)}{\alpha_s^2 - t_1^2}\right]. \quad (38c)$$

One method of avoiding the system (eq 34) consists in assuming such an expansion in series for $G_\nu(t)$ that the eq 10c becomes an identity in t without placing any reductions upon the constants or coefficients of the assumed series. In that case the set of eq 32a would be the only equations to be satisfied.

Such a form would be obtained for $G_\nu(t)$ if it is the Hankel's transformation of any suitable function $g_\nu(\xi)$ as in eq 14c.

Sonin's integral suggests a form for $g_\nu(\epsilon)$ that contains an arbitrary constant μ and arbitrary parameters σ.

If

$$g_\nu(\xi) = (i\mu)^{1-\sigma} \sum_m B_m \xi^\nu (1 - \xi^2)^{\frac{\sigma_m - 1}{2}} J_{\sigma_m - 1}(i\mu\sqrt{1 - \xi^2}) \quad (39a)$$

where $\sigma_m \geq 5/3$

Then Sonin's integral (eq 21) gives

$$G_\nu(t) = t^\nu \sum_m B_m \frac{J_{\nu+\sigma_m}(\sqrt{t^2 - \mu^2})}{(\sqrt{t^2 - \mu^2})^{\nu+\sigma_m}}. \quad (39b)$$

With this expression eq 10c would be an identity in t without placing restrictions upon the constants B_m (other than required for convergence). This may be verified directly by use of eq 9b in eq 14c.

If $G_\nu(t)$ is defined by a convergent series (eq 39b), then $t^{-\nu} G_\nu(t)$ is an even integral function of t. If the smallest value of σ_m is 5/3, then $G_\nu(t)$ has the asymptotic expansion of eq 23.

The set of equations (eq 32a) become the following set to determine B_m

$$\sum_m B_m \left\{ \frac{\alpha_s^\nu J_{\nu+\sigma_m}(\sqrt{\alpha_s^2 - \mu^2})}{A_s J_{\nu+1}(\alpha_s)(\sqrt{\alpha_s^2 - \mu^2})^{\nu+\sigma_m}} - \pi \sum_{n=1}^{\infty}$$

$$\left.\frac{n\pi(in\pi/\gamma)^{\nu+1}H_\nu(in\pi/\gamma)J_{\nu+\sigma_m}\left(i\sqrt{\left(\frac{n\pi}{\gamma}\right)^2+\mu^2}\right)}{[(n\pi)^2+(\gamma\alpha_s)^2]\left(i\sqrt{\left(\frac{n\pi}{\gamma}\right)^2+\mu^2}\right)^{\nu+\sigma_m}}\right\}=\frac{1}{\gamma\alpha_s^2}. \tag{39c}$$

$s=1, 2, 3 \ldots$

Taking $\mu=0$ and $\sigma_m=m/3$ $(m=5, 6, 7, \ldots$

$$g_\nu(\xi)=2\xi^\nu\sum_{m=5}^{\infty}\frac{B_m(1-\xi^2)^{\frac{m}{3}-1}}{2^{m/3}\Gamma(m/3)} \tag{40a}$$

$$G_\nu(t)=\sum_{m=5}^{\infty}B_m t^{-m/3}J_{\nu+m/3}(t) \tag{40b}$$

$$\sum_{m=5}^{\infty}B_m\left\{\frac{J_{\nu+m/3}(\alpha_s)}{A_s\alpha_s^{m/3}J_{\nu+1}(\alpha_s)}-\pi\sum_{n=1}^{\infty}\frac{n\pi H_\nu\left(\frac{in\pi}{\gamma}\right)J_{\nu+m/3}(in\pi/\gamma)}{\left(\frac{in\pi}{\gamma}\right)^{\frac{m}{3}-1}[(n\pi)^2+(\gamma\alpha_s)^2]}\right\}=\frac{1}{\gamma\alpha_s^2}. \tag{40c}$$

which might require less labor in computing B_m than is required to compute x_s from eq 34.

WASHINGTON, January 23, 1948.

U. S. Department of Commerce
National Bureau of Standards

Research Paper RP1971
Volume 42, March 1949

Part of the Journal of Research of the National Bureau of Standards

Properties of Aqueous Solutions of Perchloric Acid

By Langhorne H. Brickwedde

Several properties of the system $HClO_4$-H_2O for concentrations of $HClO_4$ varying from 0 to 70 percent by weight have been measured from −60° to +75°C. These properties include density, viscosity, electrical resistivity, and freezing temperatures of the solutions. An empirical relation between electrical resistivity, kinematic viscosity, and temperature has been found to be of the same form as the relation which Vinal and Craig found for sulfuric-acid solutions. The properties of perchloric-acid solutions of interest for battery work have been discussed. Some measurements of electrical resistivity of solutions containing the lead salt formed as a perchloric-acid battery discharges have been measured.

I. Some Properties of Aqueous Solutions of Perchloric Acid

1. Introduction

A study of several properties of the system $HClO_4$-H_2O for concentrations of $HClO_4$ varying from 0 to 70 percent by weight has been made. The density, viscosity, and electrical resistivity of the system have been measured from −60° to +75° C. The freezing temperatures of some of the solutions have also been determined. The work was done as part of the project on perchloric-acid and similar batteries for the Bureau of Ships, Navy Department. Four reports [1] were issued as the work progressed. These have since been declassified and made available for publication.

2. Density

(a) Apparatus

Two picnometers of 7.8- and 15.5-ml capacity were used in making the density measurements. Each picnometer consisted of a spherical bulb and a small-bore calibrated stem. The volumes in the stems were respectively 0.00995 and 0.00487 ml per division. Volumes read with a hand lens were estimated at 0.05 division and easily repeated to 0.1 division. Two observers read volumes for each determination. A precision of 0.1 division corresponded to 0.01 and 0.003 percent, respectively, of the total volume. Calibrated weights were used and all weighings were corrected to vacuum.

The temperature of the solution in the picnometer was controlled in a clear Dewar flask or a silvered Dewar with a clear strip. At +50° and +25° C water baths were used; at 0° C, an ice and water bath; and at −25° and −50° C, alcohol cooled by the addition of small pieces of solid CO_2. Except for the ice bath, a motor-driven horizontal stirrer and a hand-operated vertical stirrer were used. The baths were maintained at the desired temperature for 20 min before measurements were taken. A series of five or more temperature and volume measurements were then made over a period of 15 min or longer. Temperature variations of 0.2 deg C introduced uncertainties in the densities of only 0.01 percent. Except at −50° C, the temperature was easily controlled to 0.2 deg, and the mean of a series of measurements was probably affected less than 0.01 percent by temperature variations. At −50° C, the temperature variations were somewhat larger but probably affected the density values by less than 0.05 percent. Temperatures above −30° C were measured with calibrated mercury-in-glass thermometers with 0.1° or 0.2° divisions. At −50° C a calibrated toluene thermometer with

[1] (1) Resistivity of perchloric-acid solutions from +50° to −60° C. Langhorne H. Brickwedde (May 1943). (2) Resistivity of perchloroic-acid solutions containing lead perchlorate, from +75° to −40° C. Langhorne H. Brickwedde and Belen G. Pardo (August 1943). (3) Densities of perchloric-acid solutions from +50° to −50° C. Langhorne H. Brickwedde and Belen G. Pardo (January 1944). (4) Viscosity of perchloric-acid solutions from +50° to −60° C. Langhorne H. Brickwedde and Belen G. Pardo (August 1944).

1° divisions was used. Corrections for the ambient temperature of the emergent stem were applied.

The composition of the solutions, expressed as percentage of $HClO_4$ by weight, was determined by titrating two weighed portions of each solution, except for the 45-, 50-, and 55-percent-acid solutions. These three, together with the 40- and 60-percent solutions, were made from the 70-percent-acid solutions by carefully weighed successive dilutions. Since the composition of the 40- and 60-percent solutions determined by titration differed from the composition calculated for the dilution by only 0.05 and 0.03 percent, respectively, the calculated compositions for the three intermediate solutions have been used. As a check on the acid contents determined by titration, the densities of the 45-, 50-, 55-, 60-, and 70-percent solutions were measured. The average difference between the acid contents determined by titration and by density measurements, using the values of Markham [1][2] and Smith and Goehler [2], was less than 0.03 percent acid, except for one solution. The acid contents as determined by titration were used in expressing the results of the measurements.

Chemical analyses of these two samples of commercial perchloric acid used in the work showed them to be of very high purity. These analyses are given below:

Sample identification	70 to 72% of $HClO_4$	60% of $HClO_4$
Manufacturer	General Chemical Co.	Baker
	Percent	*Percent*
Assay	70.9	64
Nonvolatile matter	Not >0.000	Not >0.008
Chloride (Cl)	Not >.001	Not >.0006
Nitrogen compounds (as N)	Not >.004	Not >.002
Sulfate (SO_4)	Not >.005	Not >.005
Ammonia (NH_3)	Not >.001	Not >.0006
Heavy metals (limit 0.0005% of Pb)	Passed	.0005
Iron (Fe)	0.0002	.0002

Uncertainties in the composition may affect the density values by only 0.01 percent.

[2] Figures in brackets refer to literature references at the end of this paper.

(b) Measurements

The densities of perchloric-acid solutions containing 9.69, 19.72, 29.17, 40.01, 44.97, 49.95, 54.95, 60.00, and 70.02 percent of $HClO_4$, respectively, were measured at +50°, +25°, 0°, −25°, and −50° C., the range of measurements of some solutions being limited, however, by their freezing points. Adjustments of the observed density values for the small differences of temperature from the even values given above were calculated from the temperature coefficients at each point. For each temperature the densities, in grams per milliliter, were plotted on large scale against the content of $HClO_4$ (fig. 1). From these plots the densities for every 5 percent of $HClO_4$ were read and smoothed by plots of the differences. These density values are given in table 1. The values observed for the composition of the actual solutions are the points shown in figure 1.

TABLE 1. *Density of perchloric-acid solutions*

Percentage of $HClO_4$ (by weight)	[a] Density at —				
	+50° C	+25° C	0° C	−25° C	−50° C
	g/ml	*g/ml*	*g/ml*	*g/ml*	*g/ml*
0	[b] (0.9881)	[b] (0.9971)	[b] (0.9999)		
5	1.0150	1.0257	1.0308		
10	1.0437	1.0560	1.0637		
15	1.0744	1.0882	1.0986		
20	1.1075	1.1228	1.1356		
25	1.1433	1.1600	1.1749		
30	1.1821	1.2002	1.2168	1.2312	
35	1.2243	1.2436	1.2618	1.2779	
40	1.2703	1.2908	1.3111	1.3308	1.3515
45	1.3205	1.3428	1.3657	1.3893	1.4140
50	1.3752	1.3999	1.4255	1.4528	
55	1.4349	1.4615	1.4897	1.5203	1.5500
60	1.4994	1.5275	1.5580	1.5908	1.6300
65	1.5673	1.5963	1.6288	1.6620	(1.696)
70	1.6344	1.6644	1.6987	1.7306	

[a] The tabulated values are identical with those for the specific gravity referred to water at 4° C.

[b] Values for water are from the International Critical Tables.

Since for the viscosity measurements of the perchloric-acid solutions, densities were needed at several temperatures in addition to those at which the densities were measured, large-scale plots of the data of table 1 were made of density versus

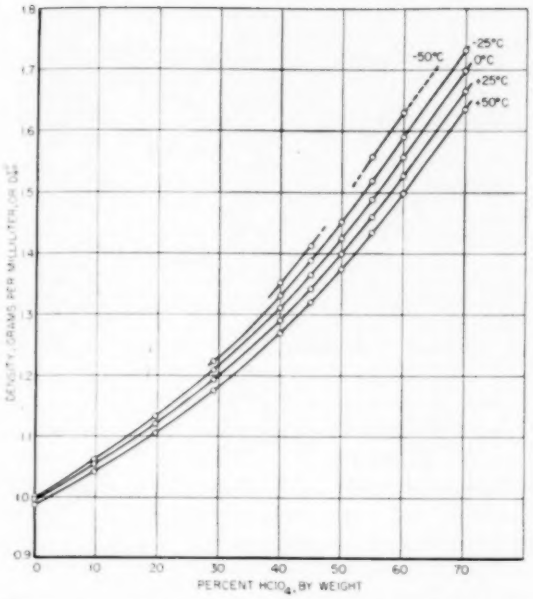

FIGURE 1. *Isotherms of the density of perchloric-acid solutions.*

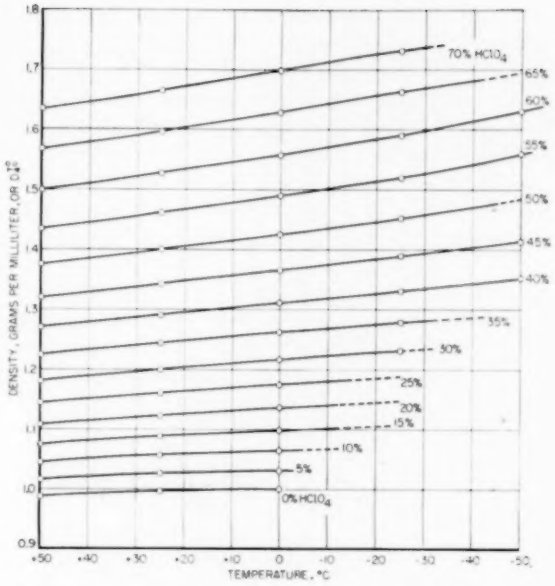

FIGURE 2. *Density of perchloric-acid solutions as a function of temperature.*

TABLE 2. *Enlarged table of densities*

(Values to more significant figures for certain temperatures are given in table 1)

Percentage of $HClO_4$	Density at—														
	+50° C	+40° C	+30° C	+25° C	+20° C	+15° C	+10° C	0° C	−10° C	−20° C	−25° C	−30° C	−40° C	−50° C	−60° C
	g/ml	*g/ml*	*g/ml*	*g/ml*	*g/ml*	*g/ml*	*g/ml*	*g/ml*	*g/ml*	*g/ml*	*g/ml*	*g/ml*	*g/ml*	*g/ml*	*g/ml*
0	0.988	0.992	0.996	0.997	0.998	0.999	1.000	1.000							
5	1.015	1.020	1.024	1.026	1.027	1.028	1.029	1.031							
10	1.044	1.050	1.054	1.056	1.058	1.060	1.061	1.064	(1.066)						
15	1.074	1.081	1.086	1.088	1.091	1.093	1.095	1.099	1.102	(1.105)					
20	1.107	1.114	1.120	1.123	1.125	1.128	1.131	1.136	1.140	(1.144)					
25	1.143	1.150$_5$	1.157	1.160	1.163	1.166	1.169	1.175	1.180	(1.185$_5$)	(1.189)				
30	1.182	1.189	1.196$_5$	1.200	1.204	1.207	1.210	1.217	1.223	1.228$_5$	1.231	(1.233)			
35	1.224	1.232	1.239$_5$	1.244	1.247	1.251	1.255	1.262	1.268	1.275	1.278	1.281	(1.286)		
40	1.270	1.278	1.286	1.291	1.294$_5$	1.298$_5$	1.303	1.311	1.318	1.326$_5$	1.331	1.335	1.343	1.352	
45	1.320	1.329	1.338	1.343	1.347	1.352	1.356	1.366	1.375	1.384	1.389	1.394	1.404	1.414	
50	1.375	1.385	1.395	1.400	1.405	1.410	1.415	1.425	1.436	1.447	1.453	1.459	1.472	(1.484)	
55	1.435	1.445	1.456$_5$	1.462	1.467	1.473	1.478	1.490	1.502	1.514	1.520	1.527	1.542	1.559	
60	1.499	1.510	1.521$_5$	1.527$_5$	1.533	1.539	1.545	1.558	1.571	1.584	1.591	1.598	1.613	1.630	(1.647)
65	1.567	1.578	1.590	1.596	1.603	1.609$_5$	1.616	1.629	1.643	1.656	1.662	1.669	(1.682)	(1.696)	
70	1.634	1.645	1.658	1.664	1.672	1.678$_5$	1.685$_5$	1.699	1.712$_5$	1.725	1.731	1.736			

* Values in parentheses are extrapolated and may represent solutions undercooled at the temperatures indicated.

temperature for each acid solution. From these plots, shown in figure 2, the densities at intermediate temperatures were read. These data are given in table 2.

(c) Discussion of Results

Some estimates of the uncertainties introduced into the measurements are discussed in section I, 2 (a) in connection with the description of the ap-

paratus. For values at the experimental temperatures of +50°, +25°, 0°, and −25° C, i. e., those values given in table 1 (except for the 65-percent solution), the uncertainties are about 0.01 percent. The uncertainties at −50° C may be as large as 0.05 percent. For the 65-percent solution the uncertainties in the interpolated densities may be as great as 0.1 percent at all temperatures. This is caused by the change in slope of the density-composition curves between 60- and 70-percent of $HClO_4$.

The smoothed values (table 1) are compared in table 3 with the observed values. The mean deviations between the smoothed and observed values are only 0.01 to 0.02 percent.

Density values at intermediate temperatures needed for the viscosity measurements are given in table 2. These values were read from curves (reproduced in fig. 2) which justified the recording of four significant figures. The values are probably reliable to about 0.1 percent. The permissible uncertainty in density values for the calculation of the viscosity data is greater than 0.1 percent.

Several workers have previously reported a few values for densities of perchloric acid solutions at several temperatures. Their data, or values interpolated from their data, are compared in table 4 with our measurements. The mean deviations between the our values and the more recent ones, those of Markham [1] and of Smith and Goehler [2] at +25° and +30° C, are 0.01 and 0.02 percent. The deviations of our data from the older values, those of van Emster [3] at +15° and van Wyk [4] at +50° C, are somewhat larger, 0.05 and 0.2 percent, respectively. Except for the data of van Wyk, the agreement of the values is satisfactory.

TABLE 3. *Differences between smoothed (table 1) and observed values of densities*

Percentage of $HClO_4$ (by weight)	(smoothed−observed) at−				
	+50° C	+25° C	0° C	−25° C	−50° C
	g/ml	g/ml	g/ml	g/ml	g/ml
10	−0.0001	0.0000	−0.0001	.....	.....
20	.0000	.0000	.0000	.....	.....
30	−.0001	−.0002	−.0004	−0.0002	.....
40	+.0005	+.0004	+.0002	−.0003	−0.0004
45	.0000	−.0001	−.0002	+.0002	+.0004
50	+.0003	−.0002	−.0005	−.0002	.....
55	−.0008	.0000	.0000	.0000	−.0001
60	+.0002	.0000	.0000	.0000	+.0002
70	.0000	.0000	.0000	+.0001	.....
Mean	0.0002[2]	0.0001[0]	0.0001[6]	0.0001[4]	0.0003
Deviation, %	0.01[7]	0.00[7]	0.01[2]	0.01[6]	0.01[9]

TABLE 4. *Comparison of NBS density values with previous determinations*

Percentage of $HClO_4$ (by weight)	+50° C			+30° C				+25° C				+15° C		
	NBS (1948)	van Wyk [4] (1906) [a]	NBS−van Wyk	NBS (1948)	Markham [1] (1941)	NBS−Markham	Smith and Goehler [2] (1931)	NBS (1948)	Markham [1] (1941)	NBS−Markham	Smith and Goehler [2] (1931)	NBS (1948)	van Emster [3] (1907) [a]	NBS−van Emster
	g/ml	g/ml	g/ml	g/ml	g/ml	g/ml	g/ml	g/ml	g/ml	g/ml	g/ml	g/ml	g/ml	g/ml
5	.....	.....	.....	.....	.....	.....	.....	1.0257	[a] 1.0257	0.0000	.....	1.028	1.028	0.000
10	.....	.....	.....	1.054	1.0539	+0.0001	.....	1.0560	1.0559	+.0001	.....	1.060	1.060	.000
15	.....	.....	.....	.....	.....	.....	.....	1.0882	[a] 1.0883	−.0001	.....	1.093	1.093	.000
20	.....	.....	.....	1.120	1.1200	.0000	.....	1.1228	1.1228	.0000	.....	1.128	1.128	.000
25	.....	.....	.....	.....	.....	.....	.....	1.1600	[a] 1.1599	+.0001	.....	1.166	1.166	.000
30	1.1821	1.180	+0.002	1.196[6]	1.1965	.0000	.....	1.2002	1.2000	+.0002	.....	1.207	1.206	+.001
35	.....	.....	.....	.....	.....	.....	.....	1.2436	[a] 1.2435	+.0001	.....	1.251	1.251	.000
40	1.2703	1.266	+.004	1.286	1.2866	−.0006	.....	1.2908	1.2907	+.0001	.....	1.299	1.299	.000
45	.....	.....	.....	.....	.....	.....	.....	1.3428	1.3425	+.0003	.....	1.352	1.352	.000
50	1.3732	1.373	+.002	1.395	1.3944	+.0006	.....	1.3999	1.3994	+.0005	.....	1.410	1.409	+.001
55	.....	.....	.....	.....	.....	.....	.....	1.4615	1.4613	+.0002	.....	1.473	1.472	+.001
60	1.4994	1.495	+.004	1.521[5]	1.5218	−.0003	.....	1.5275	1.5277	−.0002	.....	1.539	1.539	.000
65	.....	.....	.....	.....	.....	.....	.....	1.5963	1.5963	.0000	1.5966[5]	1.609	1.607	+.002
70	1.6344	1.631	+.003	1.658	.....	.....	1.6574	1.6644	.....	.....	1.6642	1.678	1.673	+.005
Mean deviation (algebraic)	.....	.....	+.003	.....	.....	−.0000[3]	.....	.....	.....	+.0001	.....	.....	.....	+.0007
Mean deviation (arithmetic)	.....	.....	.003	.....	.....	.0003	.....	.....	.....	.0001[5]	.....	.....	.....	.0007
Percent-arithmetic	.....	.....	.2	.....	.....	.02	.....	.....	.....	.01	.....	.....	.....	.05

[a] Values are interpolated from those given by authors.

(d) Summary

Values for the density of perchloric-acid solutions at intervals of 5-percent composition by weight from 0 to 70 percent (except for 65% acid) are given at +50°, +25°, 0°, and −25° C in table 1 with an uncertainty of about 0.01 percent. The values at −50° C and all values for 65-percent acid are given with an uncertainty of about 0.05 and 0.1%, respectively.

Densities arrived at by graphical interpolation for a number of additional temperatures are given in table 2 with an uncertainty of about 0.1 percent.

3. Viscosity

(a) Apparatus

The perchloric-acid solutions and the means of controling and measuring temperatures were the same as for the density work.

The viscometers were the Fenske modification of the Ostwald type, as shown in figure 3. Three different instruments (sizes 50, 100, and 200) were used because of the wide variation in viscosity of the perchloric-acid solutions between +50° and −60° C. The instruments were calibrated by members of the staff of the Lubrication Section of this Bureau. Because of the high precision of the perchloric-acid measurements made with viscometers 50/74 and 100/81, special attention was given to calibrating these instruments by flow tests with water and aqueous solutions of sulfuric acid. Viscometer 200/284 was calibrated by flow tests with oils of known viscosity. These calibrations were for:

1. Viscometer 50/74, a calibration curve relating η'/t to $1/t^2$.
2. Viscometer 100/81, $\eta'=0.01592t-0.638/t$.
3. Viscometer 200/284, $\eta'=0.09076t$.

η' is the kinematic viscosity of the liquid and t is the corrected time of flow in seconds.

In all cases corrections were made to the observed time of flow to compensate for the effect of the difference between the surface tension of the perchloric-acid solution and the calibrating liquid, and for the effect of thermal expansion for temperatures other than the calibration temperature. Since surface tensions for perchloric acid solutions are not known, values were estimated from sulfuric acid solutions. This was sufficiently accurate because the compensations for surface-tension differences are small.

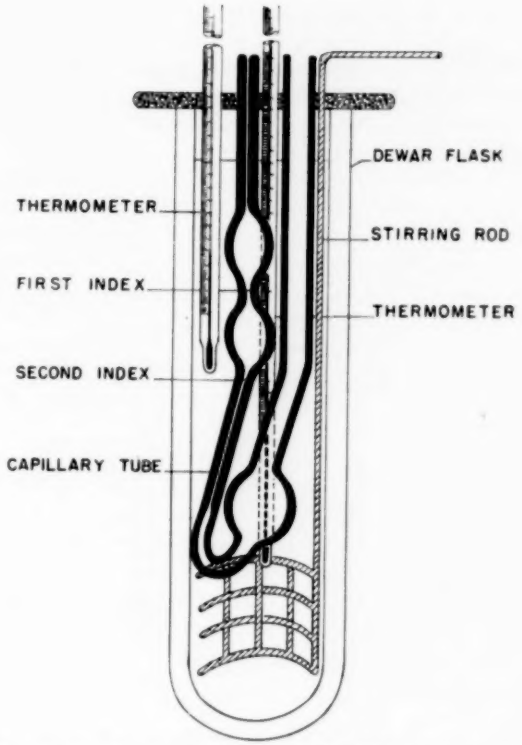

FIGURE 3. *Fenske modification of Ostwald type viscometer.*

Times of flow of the acid solutions through the viscometers were measured with a calibrated stopwatch. They ranged from 1.5 to 45 min.

All values of viscosity have been referred to the most probable value for the absolute viscosity of water at 20° C as given by Coe and Godfrey [5]. This value, $\eta_{H_2O \text{ at } 20^\circ C}$ is 1.002 centipoises.

(b) Measurements

Carefully standardized solutions, containing from 10 to 70 percent of $HClO_4$ (referred to in section I, 2, a) were investigated at +25° C and at 10-deg intervals from +50° C to the freezing point of the solution. The kinematic viscosities were calculated and large scale plots were used to get values for even temperatures and even compositions.

The absolute viscosities were calculated for each experimental point by using densities interpolated

from table 2. Large scale plots were again made to get values for even temperatures and compositions. The smoothed values from these plots and the absolute viscosities corresponding to the smoothed kinematic data were found to be in good agreement. The mean difference between the 138 pairs of values gotten from the two graphical treatments was less than 0.1 percent. The mean values are given in table 5 and the corresponding kinematic viscosities in table 6.

TABLE 5. *Absolute viscosity of perchloric-acid solutions*

Based on absolute viscosity of water at 20° C = 1.002 centipoises

Percentage of $HClO_4$ (by weight)	Absolute viscosity, centipoises, at—												
	+50° C	40° C	30° C	25° C	20° C	10° C	0° C	−10° C	−20° C	−30° C	−40° C	−50° C	−60° C
0	0.547	0.653	0.798	0.890	1.002	1.306	1.786	2.59	.....	.....	.....	.....	.....
5	.557	.662	.803	.894	1.004	1.287	1.743	2.47	.....	.....	.....	.....	.....
10	.569	.675	.813	.901	1.010	1.280	1.714	2.40	.....	.....	.....	.....	.....
15	.586	.692	.829	.913	1.022	1.286	1.701	2.347	.....	.....	.....	.....	.....
20	.610	.715	.853	.937	1.043	1.307	1.707	2.329	.....	.....	.....	.....	.....
25	.641	.750	.890	.974	1.080	1.347	1.745	2.353	.....	.....	.....	.....	.....
30	.684	.794	.940	1.031	1.139	1.413	1.815	2.434	3.415	.....	.....	.....	.....
35	.744	.859	1.013	1.108	1.223	1.514	1.925	2.572	3.581	.....	.....	.....	.....
40	.822	.950	1.118	1.224	1.345	1.670	2.113	2.814	3.928	5.887	9.670	18.21	.....
45	.940	1.080	1.274	1.395	1.534	1.900	2.426	3.244	4.582	7.139	11.96	23.13	.....
50	1.089	1.271	1.507	1.650	1.821	2.268	2.914	3.962	[a](5.732)	9.084	16.22	.....	.....
55	1.329	1.548	1.837	2.022	2.237	2.819	3.677	5.104	7.570	11.99	24.24	69.4	.....
60	1.646	1.928	2.296	2.532	2.813	3.560	4.713	6.700	9.962	16.25	34.70	90.9½	345
65	2.076	2.440	2.913	3.211	3.560	4.523	5.969	8.40	12.37	19.88	.....	.....	.....
70	2.639	3.094	3.692	4.060	4.504	5.675	7.333	9.92	14.19	22.19	.....	.....	.....

[a] Value interpolated from curve.

TABLE 6. *Kinematic viscosity of perchloric-acid solutions*

Percentage of $HClO_4$ (by weight)	Kinematic viscosity, centistokes, at—												
	+50° C	40° C	30° C	25° C	20° C	10° C	0° C	−10° C	−20° C	−30° C	−40° C	−50° C	−60° C
0	0.554	0.658	0.801	0.893	1.004	1.306	1.786	2.59	.....	.....	.....	.....	.....
5	.549	.649	.784	.871	0.978	1.251	1.691	2.40	.....	.....	.....	.....	.....
10	.545	.643	.771	.853	.955	1.206	1.611	2.25	.....	.....	.....	.....	.....
15	.546	.640	.763	.839½	.937	1.174	1.548	2.130	.....	.....	.....	.....	.....
20	.551	.642	.762	.834	.927	1.156	1.503	2.043	.....	.....	.....	.....	.....
25	.561	.652	.769	.840	.929	1.152	1.485	1.994	.....	.....	.....	.....	.....
30	.579	.668	.786	.859	.946	1.168	1.491	1.990	2.78	.....	.....	.....	.....
35	.608	.697	.817½	.891	.981	1.206½	1.525	2.028	2.809	.....	.....	.....	.....
40	.647	.743	.869	.948	1.039	1.282	1.612	2.135	2.961	4.410	7.20	13.47	.....
45	.712	.813	.932	1.039	1.139	1.401	1.776	2.359	3.311	5.121	8.52	16.36	.....
50	.799	.918	1.080	1.178½	1.296	1.603	2.045	2.759	[a](3.961)	6.226	11.02	.....	.....
55	.926	1.071	1.261	1.383	1.525	1.907	2.468	3.398	5.000	7.852	15.72	44.5	.....
60	1.098	1.277	1.509	1.657½	1.835	2.304	3.025	4.265	6.289	10.17	21.51	55.8	209
65	1.325	1.546	1.832	2.012	2.221	2.799	3.664	5.11	7.47	11.91	.....	.....	.....
70	1.615	1.881	2.227	2.440	2.694	3.367	4.316	5.79	8.227	12.78	.....	.....	.....

[a] Value interpolated from curve.

The relation of the viscosity to temperature is shown by graphs of the observed points for each solution in figure 4. The viscosity rises with decreasing temperature for all solutions. The rise is especially rapid at low temperatures for the solutions of higher $HClO_4$ content.

The isotherms relating viscosity to $HClO_4$ content are shown in figure 5. In general, the viscosity rises as the $HClO_4$ content of the solution increases. This rise is especially rapid at the lower temperatures and for the more concentrated solutions. At temperatures below +20° C, how-

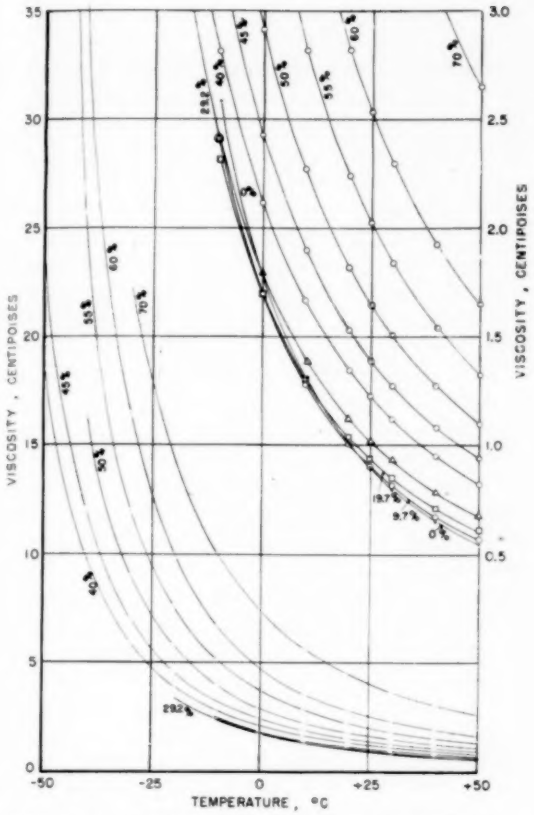

FIGURE 4. *Viscosity of perchloric-acid solutions as a function of temperature.*

ever, there are minima in the curves between 5 and 20 percent of $HClO_4$. A redetermination of some points, in some cases with a different viscometer, has definitely established the existence of minima in this region.

The inflections of the low-temperature isotherms at the higher acid compositions are interesting. The shapes of the curves suggest that the viscosities may go through maxima for solutions of compositions higher than those with which we worked. Even for a temperature as high as +50° C, van Wyk has reported a maximum in viscosity for a composition of about 80 percent of $HClO_4$ by weight. van Wyk's data showing the maximum are given in table 7 [6].

(c) Accuracy

The experimental determinations plotted in figure 4 are the averages of repeated measurements; usually from three to six discharges were made for each point. Smooth curves were passed through the 95 experimental points except for two cases (70-percent solution at +30° and −30° C), where the deviations of the plotted points from the curve are about 0.3 percent. Graphical treatments of the data both as kinematic viscosities and as absolute viscosities were carried out. The mean of the differences between the absolute viscosities arrived at in these two ways was less than 0.1 percent over the whole range of tem-

TABLE 7. *Comparison of NBS values with determination of van Wyk*

Percentage of $HClO_4$ (by weight)	Absolute viscosity, centipoises, at—					
	+50° C			+20° C		
	NBS (1948)	van Wyk (1906)	NBS−van Wyk	NBS (1948)	van Wyk (1906)	NBS−van Wyk
20	0.610	0.605	+0.005	1.043	1.042	+0.001
25	.641	.637	.004	1.080	1.082	−.002
30	.684	.680	.004	1.139	1.141	−.002
35	.744	.735	.009	1.223	1.226	−.003
40	.822	.810	.012	1.345	1.348	−.003
45	.940	.912	.028	1.534	1.522	+.012
50	1.099	1.064	.035	1.821	1.787	+.034
55	1.329	1.292	.037	2.237	2.188	+.049
60	1.646	1.605	.041	2.813	2.735	+.078
65	2.076	1.997	.079	3.560	3.435	+.125
70	2.639	2.550	.089	4.504	4.363	+.141
71.5		2.74				
76.3		3.54				
80.5		3.82				
84.1		3.51				
91.1		2.04				

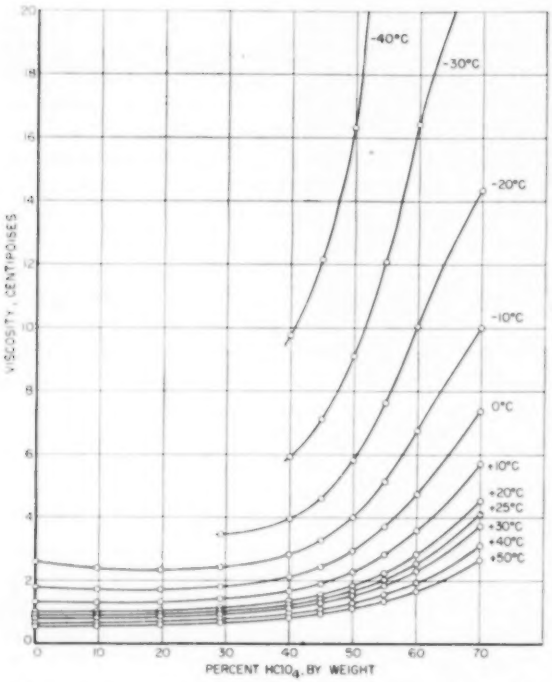

FIGURE 5. *Isotherms of the viscosity of perchloric-acid solutions.*

peratures and solutions. The maximum difference for any point was only 0.7 percent.

The measurements are subject to systematic errors from several sources. Attempts were made to eliminate systematic errors introduced by uncertainties in the constants of the viscometers. The No. 50 and No. 100 viscometers were calibrated with water and sulfuric-acid solutions. Three perchloric-acid solutions were measured at the ice point with each of these instruments. These measurements differed by less than 0.3 percent. Uncertainties in estimating the time compensations for differences in temperature and surface tension are less than 0.1 percent

Systematic errors in determining the composition of the solutions have been avoided as far as possible by checking the results of the weight titrations by measurements of the specific gravity. Except for one solution, differences in the composition as determined by the two methods would affect the viscosity by less than 0.1 percent. All the measurements have been calculated on the compositions determined by titration. Mean variations of duplicate titrations affect the viscosity by only 0.04 percent.

Accidental errors in measuring the temperature of the solutions were minimized by repetitions of the discharges. Usually from three to six repeated discharges were made at each temperature. From the higher temperatures through $-30°$ C, mercury-in-glass thermometers with 0.1° or 0.2° divisions were used. The estimated uncertainty is $\pm 0.02°$ or ± 0.07 percent or less above $-1°$ C; and somewhat larger at $-10°$, $-20°$, and $-30°$C, probably approaching $\pm 0.1°$ C or ± 0.5 percent in viscosity. At $-40°$, $-50°$, and $-60°$ C, spirit thermometers of 1° C divisions were used. In this range the uncertainty is probably ± 0.1 or $\pm 0.2°$ C, corresponding to an uncertainty of as much as 2 or 3 percent in viscosity.

Errors in timing the discharges were also minimized by repeating the experiments. Estimates of the magnitude of these errors can be gotten from the variations in measurements at the ice point where variations of the temperature are negligible. In only three of the nine measurements at 0° C was the variation as great as 0.1 sec for repeated runs. Therefore, we may say that accidental errors of timing even the fastest discharges were less than 0.1 percent. Instrumental errors introduced from the calibration of the watch were of the same order of magnitude.

The NBS density values used in computing the absolute viscosities were uncertain by about 0.1 percent or less.

In conclusion, the uncertainty of all values given in tables 5 and 6 is

1. For 0° to +50° C, less than 0.5 percent.
2. For $-10°$ to $-30°$ C, 0.5 to 1.0 percent.
3. At $-40°$ C, about 2 percent.
4. At $-50°$ and $-60°$ C, about 3 percent.

(d) Comparison with Previous Determinations

In the range of special interest for the present work, i. e. at the lower temperatures, no data were available in the literature. There were, however, some viscosity measurements at +50° and +20° C made in 1906 by van Wyk [6].

In table 7, values interpolated graphically from van Wyk's data are compared with our data. For the more dilute solutions, the data are in good agreement, but the differences increase as the concentration increases. At 70 percent of

$HClO_4$, our measurements differ from van Wyk's by 3 percent. This difference is greater than the estimated uncertainty, but probably not greater than the uncertainty of the earlier work.

In table 7 are also given some of van Wyk's measurements for solutions above 70 percent. These are included to show that the curves of viscosity versus composition go through maxima at high compositions. The present data, which cover the range up to 70 percent of $HClO_4$ show inflections at the lower temperatures and suggest the existence of maxima.

4. Electrical Resistivity

(a) Apparatus

The electrical bridge used was especially suited to measurements of electrolytic resistances. The authors are indebted to F. Wenner, formerly of this Bureau, for his assistance in planning the bridge. It consisted of two equal ratio arms having resistances of 10 ohms. The third arm was a decade resistance box with 0.1-ohm steps in the last dial. Between this and the fourth arm, i. e., the cell arm, there was a slide wire by means of which continuous resistance settings could be made. After each balance of the bridge with the cell, a high-precision noninductive decade resistor was substituted directly for the cell. This substitution method of determining the cell resistance eliminated errors from several sources. The potential applied to the bridge was 0.5 v at 1,000 cycles per second. The heating effect of the current was negligible, as shown by the fact that the change in resistance of the cell was less than 0.05 percent after a continuous flow of the current through the cell for ½ hr. Ordinarily a measurement was completed within a minute or two after the bridge circuit was closed.

The detector circuit consisted of a vacuum-tube booster amplifier and telephones. The telephone detector circuit was coupled to the bridge circuit by a small mutual inductor which permitted balancing any out-of-phase component of potential difference in the bridge. Resistance measurements could be repeated to 0.01 percent except for the highest values, where the precision was 0.04 percent.

Two conductivity cells having, respectively, cell-constants of 73.45_9 and 17.66_9 at 25° C were employed. A Parker solution of 76.627_6 g of purified potassium chloride per kilogram of distilled water was used for determining the constants. The difference in resistivity of several perchloric-acid solutions measured with both cells was in each case less than the estimated experimental error from other sources.

The temperature was controlled by immersing the cell in a Dewar flask containing an alcohol or water bath. The flask was covered with two layers of cork and was provided with a stirrer.

For each resistance measurement the temperature of the cell was measured by two liquid-in-glass thermometers with their bulbs placed close to the center of the conductivity cell. The temperatures were read through a telescope, and corrections for scale readings and for emergent-stem temperatures were applied to the readings. For temperatures above −38° C mercury thermometers graduated to 0.1° or 0.2° C were used. For temperatures below −38° C, toluene thermometers graduated in centigrade degrees, and mercury-thallium-alloy thermometers graduated to 0.5° F (about 0.3° C) were used. The solutions were the same as those for the density and viscosity measurements.

(b) Experimental Results

The resistance of each solution was measured at 10-deg intervals from +50° C down to the freezing temperature of the solution. Each solution was measured at each temperature from two to eight times. The individual observations were plotted on large scales, and the weighted mean values were determined. Resistivities, calculated from the mean resistances, were then plotted with respect to temperature for each solution. Resistivities at 10-deg intervals, with the addition of values for +15° and +25° C, were read from the curves. By using these resistivity values, isothermal curves for resistivity have been plotted against percentage composition of acid. These curves are shown in figure 6.

Table 8 gives the complete results of our measurements. The values of table 8 were read in part from the large scale plots of figure 6, in part from sectional plots made on a larger scale for low resistivities, and from semilogarithmic plots for resistivities above 20 ohm-cm.

TABLE 8. *Resistivity of perchloric-acid solutions*

Temperature	Percentage of perchloric acid—												
	10	15	20	25	30	35	40	45	50	55	60	65	70
°C	*Ohm-cm*	*Ohm-cm*	*Ohm-cm*	*Ohm-cm*	*Ohm-cm*	*Ohm-cm*	*Ohm-cm*	*Ohm-cm*	*Ohm-cm*	*Ohm-cm*	*Ohm-cm*	*Ohm-cm*	*Ohm-cm*
+50	2.297	1.580	1.272	1.106	1.028	0.990	1.001	1.056	1.154	1.313	1.540	1.903	2.401
+40	2.428	1.730	1.397	1.219	1.132	1.095	1.106	1.169	1.286	1.470	1.725	2.124	2.704
+30	2.715	1.933	1.562	1.362	1.262	1.222	1.240	1.314	1.452	1.668	1.961	2.417	3.084
+25	2.898	2.064	1.665	1.451	1.344	1.301	1.320	1.405	1.551	1.792	2.106	2.598	3.314
+20	3.100	2.200	1.776	1.551	1.436	1.393	1.414	1.502	1.670	1.928	2.275	2.776	3.575
+15	3.342	2.359	1.906	1.670	1.547	1.499	1.525	1.626	1.809	2.102	2.482	3.040	3.876
+10	3.628	2.532	2.072	1.809	1.665	1.616	1.647	1.757	1.964	2.286	2.705	3.372	4.227
0	4.420	3.095	2.488	2.169	1.992	1.920	1.968	2.111	2.376	2.792	3.320	4.120	5.129
−10	.....	(3.70)	3.102	2.681	2.464	2.384	2.436	2.622	2.982	3.551	4.242	5.24	6.418
−20	.....	.....	.....	.....	3.176	3.076	3.133	3.396	3.919	4.755	5.742	6.97	6.395
−30	.....	.....	.....	.....	.....	(4.25)	4.250	4.657	5.505	6.869	8.402	9.98	11.59
−40	.....	.....	.....	.....	.....	(6.17)	6.21	6.88	8.44	11.11	13.82	.....	.....
−50	.....	.....	.....	.....	.....	.....	10.41	12.02	.....	22.6	27.1	.....	.....
−60	.....	.....	.....	.....	.....	.....	.....	.....	.....	.....	76.8	.....	.....

[a] Values given in parentheses are extrapolated.

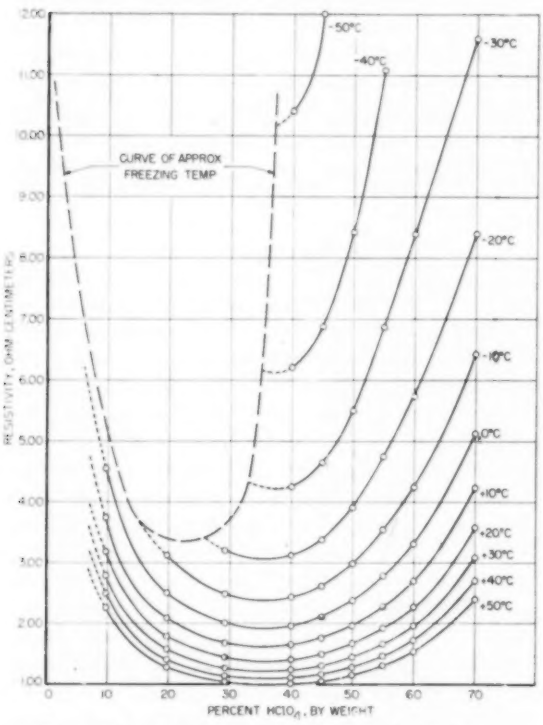

FIGURE 6. *Resistivity of perchloric-acid solutions.*

(c) Accuracy of Measurements

Several experimental errors were discussed in connection with the description of the apparatus in section I, 4 (a). These uncertainties in the measurements were less than 0.05 percent.

Uncertainties in the determination of the acid content of the solutions did not affect the resistivity values by more than 0.06 percent in any solution.

The greatest uncertainties were introduced by the variations and measurements of temperature. From −30° to +50° C uncertainties due to temperature were probably 0.1 percent or less. At −40° C the uncertainty introduced by the temperature was from 0.5 to 1 percent, and at −50° and −60° C it was probably between 1 and 2 percent.

Interpolated values read from carefully drawn curves for all observations above −30° C probably are not in error by more than 0.1 percent in the vicinity of the plotted points. Intermediate values read from the curves, however, may be subject to greater errors, but these are quite certainly less than 0.5 percent. In the following tabulation an estimate of the errors from all sources is given for the various parts of the work.

In conclusion, the uncertainty of values given in table 8 for points in the vicinity of the experimental values are

1. For −30° to +50° C, not more than 0.1 percent (except for the 10-percent solution at 0° C).
2. At −40° C, less than 1 percent.
3. At −50° and −60° C, less than 2 percent.

Values intermediate between the experimental values are probably not uncertain by more than 0.5 percent. These are the values given in table

s for +15° and +25° C and for 15-, 25-, 35-, and 65-percent-acid solutions.

5. Relation Between Resistivity, Kinematic Viscosity, and Temperature

Vinal and Craig [7] found in their work on the resistivity and viscosity of sulfuric-acid solutions an interesting empirical relation connecting these properties with the absolute temperature, T. They found that

$$\frac{\log\ (20\times\text{kinematic viscosity})}{\sqrt{T}\ \log\ (6\times\text{resistivity})}=K=0.100.$$

The constant K was found to be 0.100 (average deviation of only 1 percent) for 28- to 45-percent H_2SO_4 solutions, and extending over the temperature range of their work, −40° to +30° C.

The kinematic viscosity and resistivity of perchloric acid solutions are related by a function of the same form

$$\frac{\log\ (20\times\text{kinematic viscosity})}{\sqrt{T}\ \log\ (4\times\text{resistivity})}=K=0.100,$$

for solutions varying from 30 to 60 percent of $HClO_4$ and over the temperature range −50° to +50° C.

The values of K for each $HClO_4$ solution are given in table 9. From the table it can be seen that values of K for the 10-, 20-, and 70-percent $HClO_4$ solutions are not constant with respect to either temperature or concentration. Over the range of compositions where the relation does apply, i. e., 30 to 60 percent of acid, the average deviation is 1.8 percent. Over the entire range of the solutions, the average deviation is 6.7 percent.

It is interesting that the same type of function applies to concentrated solutions of sulfuric and perchloric acids and that the value of K is essentially 0.1 for both acids.

In table 9 are also given values for the log functions used in calculating K. These are included for convenience in finding intermediate values of resistivity and viscosity. The reciprocals of these log functions are nearly linear relations of the temperature and composition.

TABLE 9. *Relation between resistivity, kinematic viscosity, and absolute temperature*

$HClO_4$		Temperature		log (20×kinematic viscosity)	log (4×resistivity)	K
		T	$\sqrt{T}$			
Percent	° *C*	°*Abs*	$\sqrt{}$(°*Abs*)			
10	+50	323.16	17.98	1.0374	0.9459	0.0610
	40	313.16	17.70	1.1092	.9873	.0635
	30	303.16	17.41	1.1881	1.0358	.0659
	20	293.16	17.12	1.2810	1.0934	.0684
	10	283.16	16.83	1.3824	1.1617	.0707
	0	273.16	16.53	1.5081	1.2475	.0731
20	50	323.16	17.98	1.0422	0.7066	.0820
	40	313.16	17.70	1.1086	.7473	.0838
	30	303.16	17.41	1.1830	.7957	.0854
	20	293.16	17.12	1.2681	.8515	.0870
	10	283.16	16.83	1.3640	.9184	.0882
	0	273.16	16.53	1.4780	.9979	.0896
	−10	263.16	16.22	1.6113	1.0937	.0908
30	+50	323.16	17.98	1.0637	0.6140	.0963
	40	313.16	17.70	1.1258	.6559	.0970
	30	303.16	17.41	1.1964	.7031	.0977
	20	293.16	17.12	1.2769	.7592	.0982
	10	283.16	16.83	1.3685	.8235	.0987
	0	273.16	16.53	1.4745	.9014	.0990
	−10	263.16	16.22	1.5999	.9937	.0993
	−20	253.16	15.91	1.7451	1.1039	.0994
40	+50	323.16	17.98	1.1119	0.6025	.1026
	40	313.16	17.70	1.1720	.6458	.1025
	30	303.16	17.41	1.2400	.6955	.1024
	20	293.16	17.12	1.3176	.7525	.1023
	10	283.16	16.83	1.4089	.8188	.1022
	0	273.16	16.53	1.5084	.8961	.1018
	−10	263.16	16.22	1.6304	.9887	.1017
	−20	253.16	15.91	1.7725	1.0980	.1015
	−30	243.16	15.59	1.9455	1.2304	.1014
	−40	233.16	15.27	2.1584	1.3951	.1013
	−50	223.16	14.94	2.4304	1.6195	.1005
45	+50	323.16	17.98	1.1535	0.6257	.1025
	40	313.16	17.70	1.2111	.6699	.1021
	30	303.16	17.41	1.2797	.7206	.1020
	20	293.16	17.12	1.3576	.7787	.1018
	10	283.16	16.83	1.4475	.8468	.1016
	0	273.16	16.53	1.5505	.9266	.1012
	−10	263.16	16.22	1.6738	1.0207	.1011
	−20	253.16	15.91	1.8210	1.1330	.1010
	−30	243.16	15.59	2.0104	1.2702	.1015
	−40	233.16	15.27	2.2315	1.4396	.1015
	−50	223.16	14.94	2.5148	1.6820	.1001
50	+50	323.16	17.98	1.2036	0.6643	.1008
	40	313.16	17.70	1.2639	.7113	.1004
	30	303.16	17.41	1.3344	.7640	.1003
	20	293.16	17.12	1.4136	.8248	.1001
	10	283.16	16.83	1.5060	.8952	.1000
	0	273.16	16.53	1.6117	.9779	.0997
	−10	263.16	16.22	1.7418	1.0766	.0998
	−20	253.16	15.91	1.8988	1.1952	.0999
	−30	243.16	15.59	2.0952	1.3428	.1001
	−40	233.16	15.27	2.3432	1.5284	.1004

TABLE 9. *Relation between resistivity, kinematic viscosity, and absolute temperature*—Continued

$HClO_4$		Temperature		log (20×kinematic viscosity)	log (4×resistivity)	K
		T	$\sqrt{T}$			
Percent	° *C*	° *Abs*	(° *Abs*)½			
	+50	323.16	17.98	1.2676	0.7203	0.0979
	40	313.16	17.70	1.3308	.7694	.0977
	30	303.16	17.41	1.4018	.8243	.0977
	20	293.16	17.12	1.4843	.8872	.0977
	10	283.16	16.83	1.5814	.9611	.0978
55	0	273.16	16.53	1.6934	1.0480	.0978
	−10	263.16	16.22	1.8322	1.1524	.0980
	−20	253.16	15.91	2.0000	1.2792	.0983
	−30	243.16	15.59	2.1960	1.4390	.0979
	−40	233.16	15.27	2.4975	1.6478	.0993
	−50	223.16	14.94	2.9494	1.9562	.1009
	+50	323.16	17.98	1.3416	0.7806	.0945
	40	313.16	17.70	1.4072	.8388	.0948
	30	303.16	17.41	1.4797	.8945	.0950
	20	293.16	17.12	1.5647	.9590	.0953
	10	283.16	16.83	1.6635	1.0342	.0956
60	0	273.16	16.53	1.7818	1.1232	.0960
	−10	263.16	16.22	1.9310	1.2296	.0968
	−20	253.16	15.91	2.0996	1.3611	.0970
	−30	243.16	15.59	2.3084	1.5264	.0970
	−40	233.16	15.27	2.6337	1.7426	.0990
	−50	223.16	14.94	3.0477	2.0350	.1002
	−60	213.16	14.60	3.6212	2.4874	.0997
	+50	323.16	17.98	1.5092	0.9824	.0854
	40	313.16	17.70	1.5754	1.0341	.0861
	30	303.16	17.41	1.6488	1.0912	.0868
	20	293.16	17.12	1.7314	1.1553	.0875
70	10	282.16	16.83	1.8283	1.2281	.0885
	0	273.16	16.53	1.9361	1.3121	.0893
	−10	263.16	16.22	2.0637	1.4095	.0903
	−20	253.16	15.91	2.2163	1.5261	.0913
	−30	243.16	15.59	2.4076	1.6661	.0927
Average K (omitting 10-, 20-, and 70-percent solutions)						0.0995
Average deviation (omitting 10-, 20-, and 70-percent solutions)						±.0018
Average K (all observations)						.0950
Average deviation (all observations)						±.0067

6. Freezing Temperatures

The freezing temperatures of the various perchloric-acid solutions used in determining the other physical properties reported in this paper have been measured. On the more complicated parts of the curve, the freezing temperatures of some solutions of intermediate compositions were also measured. No attempt was made, however, to determine the complete phase diagram as had been done earlier by van Wyk [8]. Both van Wyk's data and ours are represented graphically in figure 10.

(a) Measurements

Freezing and melting temperatures were measured in an apparatus shown in figure 7. A 25-ml

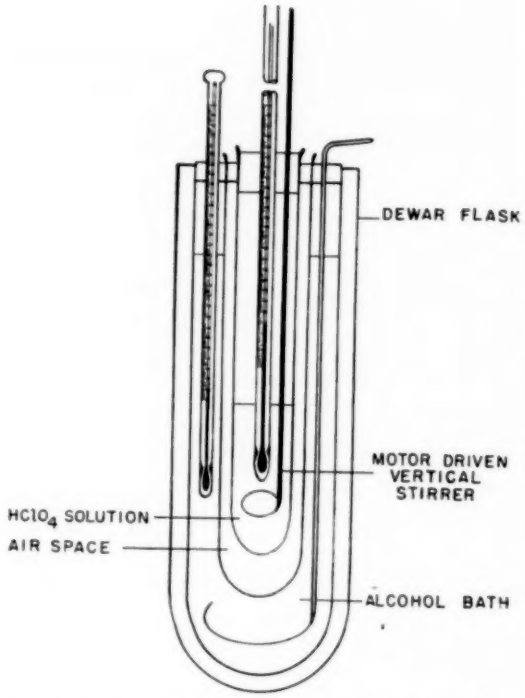

FIGURE 7. *Freezing and melting temperature apparatus.*

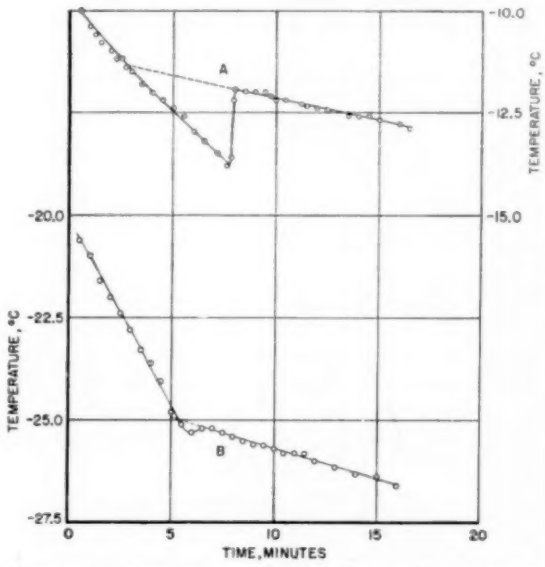

FIGURE 8. *Freezing curves for perchloric-acid solutions in region where ice separates as solid phase.*

A, 9.7 percent of $HClO_4$; B, 29.2 percent of $HClO_4$.

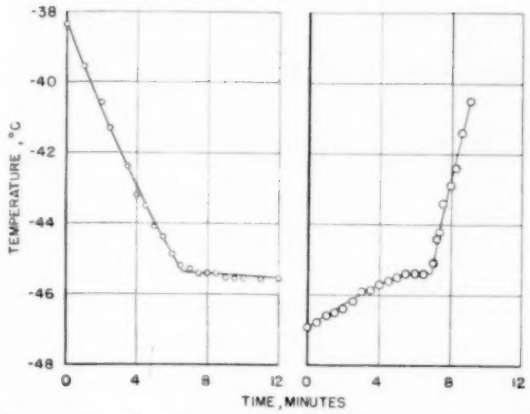

FIGURE 9. *Freezing and melting curves for 52-percent $HClO_4$ solution.*

sample was insulated from the bath by the air space between two concentric test tubes. A vertical shaft, motordriven stirrer of 100 to 150 strokes per minute was provided for stirring the sample. The alcohol cooling- or warming-bath was contained in a clear Dewar flask. Small amounts of solid carbon dioxide were added to keep the bath some 10 to 20 deg below or above the freezing or melting point of the solution.

The temperature of the solution, which was continually stirred, was read at 30-sec intervals. These temperatures, plotted with respect to time, gave typical freezing and melting curves. The intersection of the solid and liquid curves gave the freezing or melting points of the solution. Typical curves are shown in figures 8 and 9. Two or more freezing experiments were made for each solution. Supercooling was especially noticeable in the 60- and 70-percent solutions, where the solution sometimes supercooled as much as 35 deg C. To bring about crystallization close to the freezing temperature, crystals were introduced from a partially frozen auxiliary solution of the same composition. Melting experiments were also run for a number of solutions and the freezing and melting temperatures were found to be in good agreement. These data are given in table 10.

Mercury thermometers with 0.2° C divisions were used for solutions up to 30 percent of $HClO_4$.

TABLE 10. *Observed freezing and melting points of perchloric-acid solutions*

Percentage of $HClO_4$ (by weight)	Freezing temperature	Melting temperature	Estimated error of mean temperature	Percentage of $HClO_4$ (by weight)	Freezing temperature	Melting temperature	Estimated error of mean temperature
	°C	°C	°C		°C	°C	°C
9.69	−3.97	.....	±0.1	54.95	−52.8	.....	±0.5
9.69	−4.07	.....		54.95	−52.8	.....	
				54.95	−52.6	.....	
19.72	−11.33	.....	±.1	57.04	−53.7	.....	±.5
19.72	−11.50	.....		57.04	−54.0	−53.8	
29.17	−25.03	.....	±.1	58	−60.5	−59	Gelatinous mass.
29.17	−25.03	.....					
40.01	−56.8	.....	±.5	60.00	−46.3	−46.9	
40.01	−56.7	.....		60.00	−46.3	−46.8	
				60.00	−46.5	−46.7	
42.49	−55.8	−56.2	±.5	60.00	−52.4	−52.0	
42.49	−55.7	.....		60.00	[a]−65.6	.....	±0.5
				60.00	−60.6	.....	
44.97	−51.5	.....	±.5	60.00	−60.3	.....	
44.97	−51.6	.....		60.00	[b]−65.6	.....	
				60.00	−60.9	.....	
47.39	−47.2	−47.4	±.5	63.01	−42.0	−42.5	±.5
47.39	−47.0	.....		63.01	.....	−42.7	
49.97	−45.3	.....	±.5	65.0	−39.7	−39.6	±.5
49.97	−45.3	.....					
51.97	−45.3	−45.5	±.5	70.02	−30.0	−29.9	±.5
				70.02	.....	−29.8	

[a] This and the following two values were observed as flats on the same curve.
[b] This and the following value were observed as flats on the same curve.

For the solutions from 40 to 70 percent of $HClO_4$, spirit thermometers with 1° C divisions were used. All thermometers had been calibrated, and tabular and emergent-stem corrections were applied for all readings.

(b) Experimental Results

The experimental freezing and melting temperatures, table 10, plotted with respect to composition of the perchloric-acid solutions are shown in figure 10, together with van Wyk's more complete data. Freezing temperatures from the NBS curve are given in table 11.

TABLE 11. *Freezing temperatures of perchloric-acid solutions (from fig. 10)*

Percentage of $HClO_4$ (by weight)	Freezing temperature	Solid phase
	°C	
0	0	H_2O
5	−1.87	Do.
10	−4.25	Do.
15	−7.37	Do.
20	−11.75	Do.
25	−18.2	Do.
30	−26.5	Do.
35	−39.1	Do.
40	−56.8	Do.
40.7	−59.7	H_2O, $HClO_4.xH_2O$
42	−57.0	$HClO_4.xH_2O$
44	−53.2	Do.
46	−49.6	Do.
48	−46.8	Do.
50	−45.0	Do.
52	−45.4	Do.
54	−49.1	Do.
56	−56.6	Do.
56.1	−56.8	$HClO_4.xH_2O$, $HClO_4.yH_2O$
58	−51.4	$HClO_4.yH_2O$
60	−46.7	Do.
62	−43.2	Do.
64	−40.5	Do.
66	[−38.4]	Do.
70	−29.9	$HClO_4.zH_2O$

The first section of the curve, from 0 to 41 percent of $HClO_4$, is the region where ice separates on freezing. The solid phase separating from solutions above 41 percent consists of various hydrates of $HClO_4$. The eutectic point, determined by the intersection of the ice and hydrate curves, is at −59.7° C and 40.7 percent of $HClO_4$.

In the region from 41 to 70 percent of $HClO_4$, the curve becomes more complicated. Our data lie in general on curves that have the same shape as van Wyk's. A second eutectic was found for 56 percent of acid at −57° C.

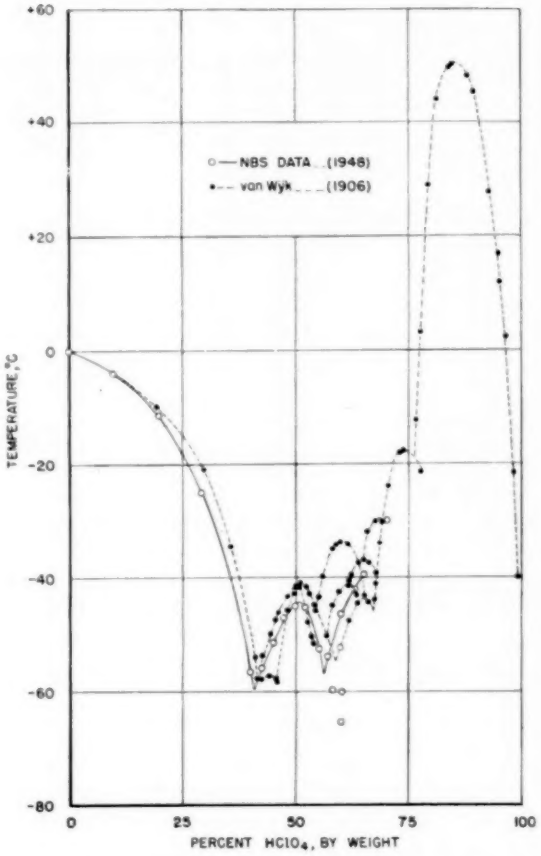

FIGURE 10. *Freezing curves of perchloric acid solutions.*
○——, NBS data (1948); ●– – –, van Wyk's data (1906).

The 60-percent-acid solution presented a very interesting problem. Over a range of 20 deg, from −46° to −66° C, four well-defined and reproducible "flats" were observed on the time-temperature curves. The temperatures of −46.5° and −52° C were determined both by freezing and by melting curves. The two lower temperatures, −60.5° and −65.6° C, were observed only on freezing curves. The solid nature of these solutions on freezing made stirring impossible and hence no reliable melting curves were obtainable.

van Wyk [8] made extensive measurements on the freezing of perchloric-acid solutions. His data, converted to weight percent, have been plotted in figure 10. The temperatures observed

by van Wyk are in many cases outside the experimental error of the NBS work. Since van Wyk gave no diagram of his freezing apparatus, used no stirrer except his thermometer, did not in general plot time-temperature curves, and gave no indication of having made corrections for emergent-stem temperatures for his alcohol thermometer, it is not possible to estimate the accuracy of his temperatures.

II. Properties of Perchloric-Acid Solutions Applied to Batteries

With the recent demands for more powerful batteries to operate at extreme low temperatures, the NBS perchloric-acid battery [9] was developed. The physical properties of the acid solutions reported in section I were measured to supplement meager data in the literature. Some comparisons of solutions of sulfuric and perchloric acids used in batteries are given here. Since during discharge of the lead-acid battery various concentrations of lead ions are in solution, resistivities of perchloric-acid solutions containing lead have been measured.

1. Comparison of Sulfuric- and Perchloric-Acid Solutions

(a) Viscosities

A comparison of perchloric and sulfuric acids ordinarily used in batteries is of interest. A 50-percent solution of perchloric acid is one that has been used in batteries designed for service over wide ranges of temperature, and 37 percent of sulfuric acid (sp gr 1.280) is the usual solution in the fully charged lead-acid storage battery. In table 12 the viscosities of these solutions are compared from +30° to −40° C. The perchloric acid is, in all cases, less viscous than the sulfuric. At room temperatures the viscosity of the perchloric is only three-fourths that of the sulfuric and at the lower temperatures it is only six-tenths as much.

In table 13 the viscosities of perchloric and sulfuric acids of the same equivalent strengths are compared. Acids containing 50 percent of $HClO_4$ and 28.41 percent of H_2SO_4 each contains 6.964 gram-equivalents per liter. At room temperature perchloric acid is slightly less viscous than the equivalent sulfuric acid, but at the lower temperatures it is only 80 percent as viscous.

TABLE 12. *Comparison of viscosities of perchloric- and sulfuric-acid solutions of concentrations commonly used in the respective types of batteries*

Temperature	50% $HClO_4$	Sulfuric acid, 1.280 sp gr [a] (37.4% H_2SO_4)	Ratio $\eta_{HClO_4}/\eta_{H_2SO_4}$
°C	*Centipoises*	*Centipoises*	
+50	1.10	.....	.....
+40	1.27	.....	.....
+30	1.51	1.94	0.78
+25	1.65	2.22	.74
+20	1.82	2.49	.73
+10	2.27	3.22	.70
0	2.91	4.35	.67
−10	3.96	6.15	.64
−20	5.73	9.15	.63
−30	9.08	14.9	.61
−40	16.2	26.9	.60
−50	.....	55.5	.....

[a] G. W. Vinal and D. N. Craig, BS J. Research **10**, 781 (1933) RP566.

TABLE 13. *Comparison of perchloric- and sulfuric-acid solutions containing the same number of equivalents of the respective acids per liter*

Temperature	50% HClO (6.964 gram-equivalents/liter)	28.41% H_2SO_4 [a] (6.964 gram-equivalents/liter)	Ratio $\eta_{HClO_4}/\eta_{H_2SO_4}$
°C	*Centipoises*	*Centipoises*	
+50	1.10	.....	.....
+40	1.27	.....	.....
+30	1.51	1.54	0.98
+25	1.65	1.71	.96
+20	1.82	1.93	.94
+10	2.27	2.49	.91
0	2.91	3.37	.86
−10	3.96	4.78	.83
−20	5.73	7.22	.79
−30	9.08	11.7	.78
−40	16.2	.....	.....

[a] G. W. Vinal and D. N. Craig, BS J. Research **10**, 781 (1933) RP566.

(b) Resistivities

For each temperature the concentration of $HClO_4$ having minimum resistivity is 36 percent (fig. 6 and table 14). Forty percent of acid, which is the lowest concentration commonly used in experimental batteries, has a resistivity only about 2 percent higher than the minimum resistivity at each temperature. As the concentration of acid is increased, the resistivity increases markedly. Ratios of the resistivities of 45- to 70-percent acid to the resistivity of 40 percent acid are given for various temperatures in table 15.

TABLE 14. *Comparison of minimum resistivities of perchloric- and sulfuric-acid solutions for the various temperatures* [a]

Temperature	Perchloric acid		Sulfuric acid		Ratio of col. 3 to col. 5
	Concentration	Resistivity	Concentration	Resistivity	
°C	*Percent*	*Ohm-cm*	*Percent*	*Ohm-cm*	
+50	36	0.988	----	-----	----
+40	36	1.093	-----	-----	----
+30	36	1.221	31.5	1.129	1.08
+25	36	1.300	31.1	1.213	1.07
+20	36	1.392	30.6	1.310	1.06
+15	36	1.499	30.2	1.425	1.05
+10	36	1.617	29.8	1.562	1.03
0	36	1.920	28.8	1.928	1.00
−10	36	2.38	27.9	2.48	0.96
−20	36	3.08	26.9	3.34	.92
−30	36	[b] (4.23)	----	-----	----
−40	36	[b] (6.14)	----	-----	----

[a] Isotherms for the resistivity of perchloric acid are shown in figure 6. For sulfuric acid, reference should be made to figure 1 of the paper by Vinal and Craig [7].

[b] Extrapolated value.

TABLE 15. *Ratio of resistivities to resistivity of 40-percent-$HClO_4$ solutions*

Temperature	Percentage of $HClO_4$—					
	45	50	55	60	65	70
°C						
+50	1.055	1.153	1.312	1.538	1.901	2.399
+40	1.057	1.163	1.329	1.560	1.920	2.445
+30	1.060	1.171	1.345	1.581	1.949	2.487
+25	1.064	1.175	1.358	1.596	1.968	2.511
+20	1.062	1.181	1.364	1.609	1.963	2.528
+15	1.066	1.186	1.378	1.627	1.993	2.541
+10	1.067	1.192	1.388	1.642	2.048	2.567
0	1.072	1.207	1.419	1.687	2.093	2.606
−10	1.076	1.224	1.458	1.741	2.151	2.635
−20	1.084	1.251	1.518	1.832	2.225	2.678
−30	1.096	1.297	1.617	1.977	2.348	2.727
−40	1.11	1.36	1.79	2.22	-----	-----
−50	1.16	-----	2.17	2.60	-----	-----

The choice of concentrations of perchloric acid for use in any particular application of a battery depends on a variety of conditions, such as the current drain, the lowest temperatures to which the batteries may be exposed, the materials employed in construction, and the permissible volume of the electrolyte. No acid stronger than 70 percent is used, and the lower limit is probably 40 percent. The tables therefore cover the entire range of concentrations and temperatures that may be needed for any application of the battery.

The minimum resistivities for perchloric- and sulfuric-acid solutions are given in table 14. Over the whole temperature range, from +50° to −40° C, the perchloric acid of minimum resistivity is very close to 36 percent by weight. The composition of sulfuric acid, on the other hand, shifts from 31.5 percent at +30° C to 26.9 percent at −20° C for minima in the resistivity curves. For temperatures above 0° C, sulfuric acid has lower minimum resistivities than perchloric acid, whereas for temperatures below 0° C, the sulfuric acid minima are higher than those of perchloric acid.

A comparison of the resistivities of perchloric- and sulfuric-acid solutions of concentrations commonly used in the respective types of batteries is given in table 16. Fifty percent of perchloric acid is compared with sulfuric acid of 1.280 sp gr 25°C/25°C (37.4% of H_2SO_4 by weight). For temperatures above −30° C, the resistivity of the sulfuric acid is less than that of the perchloric acid. At −40° C, however, the resistivity of perchloric acid is 3 percent less than that of the sulfuric.

TABLE 16. *Comparison of resistivities of perchloric- and sulfuric-acid solutions of concentrations commonly used in the respective types of batteries*

Temperature	Perchloric acid, 50 percent	Sulfuric acid, 1.280 sp gr 37.4 percent	Ratio, col. 2 to col. 3
°C	*Ohm-cm*	*Ohm-cm*	
+50	1.154	----------	---------
+40	1.286	----------	---------
+30	1.452	1.165	1.25
+25	1.551	1.258	1.23
+20	1.670	1.367	1.22
+15	1.809	1.493	1.21
+10	1.964	1.649	1.19
0	2.376	2.064	1.15
−10	2.98	2.69	1.11
−20	3.92	3.68	1.06
−30	5.51	5.41	1.02
−40	8.44	8.71	0.97

A further comparison between perchloric- and sulfuric-acid solutions can be made for acids that have the same number of equivalents per liter. Fifty percent of $HClO_4$ is equivalent to 28.41 percent of H_2SO_4; each solution contains 6.964 gram-equivalents per liter. The resitivities of

these acids are given in table 17. For each temperature the resistivity of perchloric is greater than that of sulfuric acid, but as the temperature is lowered the ratio of the resistivity of perchloric to the resistivity of sulfuric decreases.

TABLE 17. *Comparison of resistivities of perchloric- and sulfuric-acid solutions containing the same number of equivalents of the respective acids per liter*

Temperature	50 percent $HClO_4$, 6.964 gram-equivalents/liter	28.41 percent H_2SO_4, 6.964 gram-equivalents/liter	Ratio of col 2 to col 3
°C	*Ohm-cm*	*Ohm-cm*	
+50	1.154	.....	.....
+40	1.286	.....	.....
+30	1.452	1.139	1.274
+25	1.551	1.221	1.270
+20	1.670	1.317	1.268
+15	1.809	1.431	1.264
+10	1.964	1.566	1.254
0	2.376	1.928	1.232
−10	2.98	2.48	1.20
−20	3.92	3.36	1.17
−30	5.51	4.95	1.11
−40	8.44	.....	.....

Perchloric, like sulfuric, is a strong acid which provides solutions of low resistivity (high conductivity). On a practical basis, the comparison of solutions that would normally be employed in batteries shows an advantage for the perchloric acid solutions at the lower temperatures. The data given in these tables and graphically represented in figure 6 should enable one to select the best perchloric-acid electrolyte for any specified condition of operation.

2. Resistivity of Perchloric-Acid Solutions Containing Lead Perchlorate

(a) Apparatus

The apparatus and bridge used in making these measurements were the same as those used for the resistivities of perchloric-acid solutions described in section I, 4.

Solutions equivalent to the solution in a battery after different stages of discharge were prepared by adding basic lead carbonate $(PbCO_3)_2.Pb(OH)_2$ (assay 78.62% Pb) to various perchloric-acid solutions in amounts required to yield solutions containing 0, 5.0, 10.0, 20.0, and 30.0 percent of Pb. The initial solutions contained 30.1, 40.2, 50.0, 60.0, and 69.9 percent of $HClO_4$. The composition of the initial acids was determined by measuring the resistivity, and several solutions were checked by density determinations. The Pb content and the $HClO_4$ content of the various solutions after the addition of the salt $(PbCO_3)_2.Pb(OH)_2$ were calculated from the carefully weighed portions of this salt that were added to weighed portions of acid solutions. The free acid remaining in six of the solutions was determined by weight titrations. Since the calculated values did not differ by more than 0.2 percent from the titrated values, the calculated acid compositions of all the solutions were considered satisfactory.

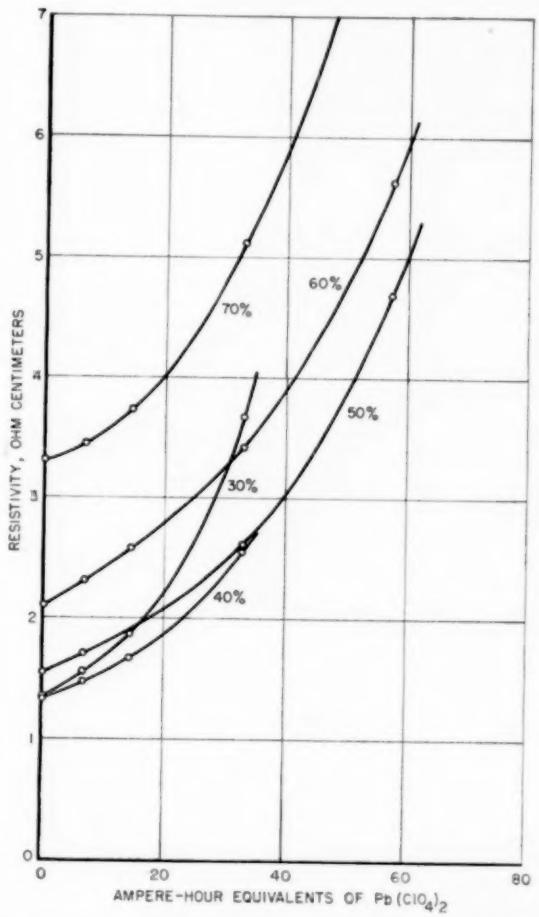

FIGURE 11. *Resistivities at 25° C of solutions containing initially 1,000 g of the specified concentrations of* $HClO_4$, *in which the indicated amounts of lead perchlorate have been formed.*

1 ampere hour=15.14 g of $Pb(ClO_4)_2$.

(b) Experimental Measurements

The resistance of each solution was measured at +50°, +25°, 0°, and −25°, and at −40° C if the solution did not freeze at that temperature. Some solutions were also measured at +75° C. Several measurements were made at each temperature and the mean value used in calculating the resistivity. Plots relating resistivity to temperature were used for interpolating the resistivities at even temperature values. For each temperature and for each lead content a curve relating resistivity to the percentage of $HClO_4$ was drawn. From these large-scale work-curves, values used in plotting the curves of figure 11 and similar curves for −40°, −25°, 0°, +50°, and +75° C were read.

The reaction in the NBS battery containing perchloric acid may be represented by the equation

$$Pb+PbO_2+4HClO_4=2Pb(ClO_4)_2+2H_2O.$$

By this reaction, 15.14 g of $Pb(ClO_4)_2$ is formed for each ampere-hour the battery is discharged. For cells containing initially 1,000 g of perchloric-acid solution, the number of ampere-hours and the final $HClO_4$ content were calculated for solutions containing 5, 10, 20, and 30 percent of Pb. The solutions calculated for the perchloric-acid battery after various discharges had the same Pb content but slightly different $HClO_4$ content from the experimental solutions formed by adding basic lead carbonate to the perchloric-acid solutions. The resistivity corresponding to the exact acid content of the battery solutions was read from the large-scale work-curves, described above, which related resistivity to percentage of $HClO_4$.

The curves of figure 11 relate the resistivity at

TABLE 18. *Resistivities of* $HClO_4$–$Pb(ClO_4)_2$–H_2O *solutions*

Initial $HClO_4$	Discharge in 1,000 g acid cell	Pb in solution	$HClO_4$ reacted	Resistivity at—					
				+75° C	+50° C	+25° C	0° C	−25° C	−40° C
Percent	*amp-hr*	*Percent*	*Percentage of initial acid*	*Ohm-cm*	*Ohm-cm*	*Ohm-cm*	*Ohm-cm*	*Ohm-cm*	*Ohm-cm*
70	0	0	0	.....	2.40	3.31	5.13	10.0	(a)
	10	7.14	5.35	1.92	2.54	3.55	5.61	11.6	23.5
	20	13.2	10.7	2.14	2.80	4.04	6.77	15.6	36.3
	30	18.6	16.1	2.44	3.24	4.82	8.67	23.0	58.1
	40	23.2	21.4	2.82	3.86	5.91	11.5	35.7	100
	50	27.3	26.8	3.30	4.71	7.39	15.6	56.7	191
	60	30.9	32.1	3.88	5.81	9.39	21.4	92.5	412
60	0	0	0	.....	1.54	2.11	3.32	6.8	13.8
	10	7.14	6.25	1.37	1.73	2.42	3.94	8.8	19.2
	20	13.2	12.5	1.50	1.96	2.78	4.75	11.3	26.5
	30	18.6	18.7	1.70	2.24	3.25	5.78	14.4	36.5
	40	23.2	25.0	1.95	2.59	3.90	7.14	18.5	49.7
	50	27.3	31.2	2.27	3.06	4.80	8.94	24.4	66.8
	60	30.9	37.5	2.71	3.73	6.00	11.4	33.7	89.0
50	0	0	0	.....	1.15	1.55	2.38	4.59	8.44
	10	7.14	7.50	1.05	1.30	1.79	2.75	5.45	10.3
	20	13.2	15.0	1.18	1.49	2.09	3.25	6.65	13.0
	30	18.6	22.5	1.38	1.76	2.48	3.95	8.45	17.1
	40	23.2	30.0	1.66	2.14	3.04	4.97	11.3	23.6
	50	27.3	37.5	2.04	2.68	3.88	6.50	15.6	33.9
	60	30.9	45.0	2.55	3.41	5.05	8.91	21.6	50.7
40	0	0	0	.....	1.00	1.32	1.97	3.61	6.21
	10	7.14	9.37	.....	1.17	1.55	2.34	4.40	7.59
	20	13.2	18.7	.....	1.38	1.86	2.87	5.49	8.83
	30	18.6	28.1	.....	1.70	2.35	3.66	7.19	(a)
	35	21.0	32.8	.....	1.94	2.69	4.19	8.46	(a)
30	0	0	0	.....	1.03	1.34	1.99	.....	(a)
	10	7.14	12.5	.....	1.28	1.68	2.51	4.69	(a)
	20	13.2	25.0	.....	1.66	2.21	3.44	.....	(a)
	30	18.6	37.5	.....	2.33	3.23	5.17	(a)	(a)
	35	21.0	43.7	.....	2.84	4.04	6.60	(a)	(a)

a Solution freezes.

+25° C of solutions, equivalent to those in a battery, to the ampere-hour discharge. The various curves represent the conditions in a battery that initially contained 1,000 g of 30-, 40-, 50-, 60-, or 70-percent $HClO_4$ solutions by weight. As the battery discharges, i. e., as H^+ ions are replaced by Pb^{++} ions, the resistivity of the solutions increases. The effect of temperature on resistivity is increasingly important as the battery discharges.

For every 5 ampere-hours, the resistivity values were read from each curve of figure 11 and similar curves for each experimental temperature. The differences between successive values were plotted and smoothed. These smoothed values are given for 10-ampere-hour intervals in table 18.

(c) Accuracy of Measurements

Errors introduced in the measurements from −40° to +25° C by uncertainties in the value of the cell constant, the heating effect of the current through the cell, and the measurement of resistance were less than 0.05 percent, as shown for the resistivity of perchloric-acid solutions (section I, 4). These uncertainties were the same for measurements at +50° and +75° C except for the cell constant, where the uncertainty was less than 0.5 percent and usually about 0.2 percent.

Uncertainties from other sources in the resistivity measurements of solutions containing Pb^{++} ions are somewhat larger than for solutions of the pure acid. The composition of the solutions was known to about 0.2 percent, and the corresponding uncertainty in resistivity was 0.2 percent. Temperatures were controlled and measured to about 0.05 to 0.1 deg C above −30° C, and to about 0.3 deg at −40° C. These uncertainties in the temperatures of the solution did not introduce uncertainties greater than 0.4 percent above −30° C

TABLE 19. *Relative resistivities*

Discharge [a] (amp-hr)		0	10	20	30	40	50	60
Percent Pb		0	7.14	13.2	18.6	23.2	27.3	30.9
Temperature	Initial $HClO_4$ content	Ratio of resistivities to resistivity of 70-percent solutions						
°C	*Percent*							
−40	70	----------	1.00	1.00	1.00	1.00	1.00	1.00
	60	----------	0.817	0.730	0.626	0.496	0.350	0.216
	50	----------	.438	.358	.294	.236	.177	.123
	40	----------	.323	.243	----------	----------	----------	----------
−25	70	1.00	1.00	1.00	1.00	1.00	1.00	1.00
	60	0.679	0.754	0.724	0.626	0.518	0.430	0.364
	50	.459	.470	.426	.367	.318	.274	.233
	40	.361	.379	.352	.313	----------	----------	----------
0	70	1.00	1.00	1.00	1.00	1.00	1.00	1.00
	60	0.647	0.702	0.701	0.666	0.620	0.573	0.533
	50	.493	.490	.480	.455	.432	.417	.417
	40	.384	.417	.424	.422	(.419)	----------	----------
	30	.388	.447	.508	.596	----------	----------	----------
+25	70	1.00	1.00	1.00	1.00	1.00	1.00	1.00
	60	0.635	0.682	0.688	0.674	0.660	0.649	0.639
	50	.468	.504	.517	.515	.514	.525	.538
	40	.398	.437	.460	.488	----------	----------	----------
	30	.406	.473	.547	.670	----------	----------	----------
+50	70	1.00	1.00	1.00	1.00	1.00	1.00	1.00
	60	0.642	0.682	0.700	0.692	0.670	0.650	0.642
	50	.481	.513	.532	.543	.554	.569	.587
	40	.417	.460	.491	.523	----------	----------	----------
	30	.428	.505	.593	.719	----------	----------	----------
+75	70	1.00	1.00	1.00	1.00	1.00	1.00	1.00
	60	----------	0.714	0.701	0.697	0.693	0.688	0.688
	50	----------	.547	.551	.566	.590	.618	.656

[a] Discharge for cell that initially contained 1,000 g of perchloric-acid solution.

UNIVERSITY OF MICHIGAN LIBRARIES

and 2.5 percent at −40° C. To summarize, the uncertainty of values in the vicinity of the experimental points is probably less than 1 percent above −30° C and 3 percent at −40° C.

Values intermediate between the experimentally determined values may be in error by several percent. The largest uncertainties are in the resistivities at −40° C for the more concentrated $Pb(ClO_4)_2-HClO_4$ solutions—solutions corresponding to those in batteries after 35 to 60-ampere-hour discharges. Here the uncertainty may be as much as 5 percent. For all other measurements the uncertainties probably do not exceed 3 percent and in most cases are less than 2 percent.

(d) Discussion of Results

A comparison of the relative resistivities of solutions during discharges of batteries which initially contained acids of different $HClO_4$ content is interesting. The ratios of the resistivity of the various solutions to the resistivity of a "70-percent-acid battery"[3] are given in table 19 for various discharges over the temperature range from −40° to +75° C.

From table 19 it can be seen that at room and higher temperatures the relative resistivities change very little as the battery discharges. Throughout the discharge at room temperature the resistivity of the 60-percent-acid battery is about two-thirds that of the 70-percent-acid battery solution, the 50-percent battery about one-half, and the 40-percent battery slightly less than one-half. The ratio of the 30-percent to the 70-percent battery solution does increase somewhat with the discharge.

The number of ampere-hours that a battery containing initially 1,000 grams of perchloric-acid solution may be discharged before the acid content has decreased to 10 percent is given in table 20. This is an indication of the low-rate-discharge capacity of batteries containing a given weight of solution of different perchloric-acid concentrations.

[3] The phrase "70-percent-acid battery" is used to refer to a solution in which the acid content is initially 70 percent. Only the solution at 0 ampere-hour is 70 percent, since $HClO_4$ reacts to form $Pb(ClO_4)_2$ as the battery discharges. A 70-percent battery at 20 ampere-hours therefore refers to a battery in which the solution contains only 47.2 percent of $HClO_4$ and 13.2 percent of Pb.

TABLE 20. *Theoretical capacity of battery before acid concentration falls to 10 percent*

Initial perchloric-acid solution, 1,000 g	Theoretical capacity
% $HClO_4$	*a-h*
70	72.1
60	60.1
50	48.1
40	36.1
30	24.0

(e) Summary

The resistivities of aqueous solutions of perchloric acid and lead perchlorate of the composition of solutions in the NBS battery during discharge have been measured for solutions from 30- to 70-percent initial $HClO_4$ content. These measurements extended from −40° to +75° C. In each of these solutions the resistivity increases as the battery discharges, i. e., as Pb^{++} ions replace H^+ ions in solution. At room temperature and above, the rate of change of the 40-, 50-, 60-, and 70-percent-acid battery solutions during discharge is constant. At lower temperatures, especially at −25° and −40° C, the 70-percent-acid battery solution increases much more rapidly during discharge than do the 50- and 60-percent-acid solutions.

The author acknowledges the contributions to this series of measurements made by Belen G. Pardo, now of Manila, P. I., whose care and patience in taking much of the data made possible the high precision obtained in the measurements. Acknowledgment is also made of the contribution of Elinor H. Ostrander in assisting in the observations of electrical resistivity of perchloric-acid solutions.

The author also expresses her grateful appreciation to G. W. Vinal, under whose supervision the work on the perchloric-acid battery and the measurements reported in this paper were carried out. Dr. Vinal's suggestion of the problem and his help in carrying out the various measurements are gratefully acknowledged.

III. References

[1] A. E. Markham, J. Am. Chem. Soc. **63,** 874 (1941).
[2] G. F. Smith and O. E. Goehler, Ind. Eng. Chem. Anal. Ed. **3,** 61 (1931).
[3] K. van Emster, Z. anorg. Chem. **52,** 278 (1907).
[4] H. J. van Wyk, Z. anorg. Chem. **48,** 41 to 45 (1906).
[5] J. R. Coe, Jr. and T. B. Godfrey, J. Applied Phys. **15,** 625 (1944).
[6] H. J. van Wyk, Z. anorg. Chem. **48,** 44 to 50 (1906).
[7] G. W. Vinal and D. N. Craig, J. Research NBS **13,** 695 (1934) RP738.
[8] H. J. van Wyk, Z. anorg. Chem. **48,** 6 to 29 (1906).
[9] J. P. Schrodt, W. J. Otting, Jr., J. O. Schoegler, and D. N. Craig, Trans. Electrochem. Soc. **90,** 449 (1946).

WASHINGTON, June 3, 1948.